



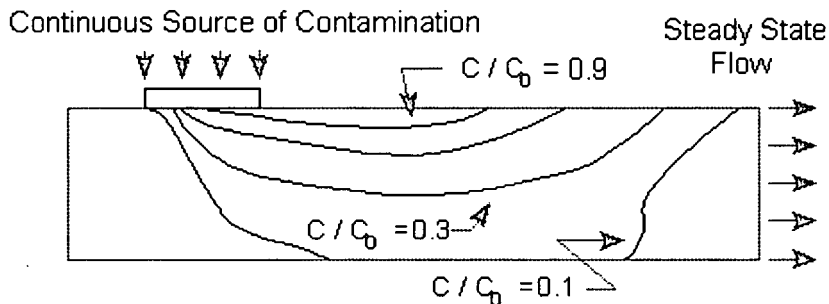
# UNDERSTANDING VARIATION IN PARTITION COEFFICIENT, $K_d$ , VALUES



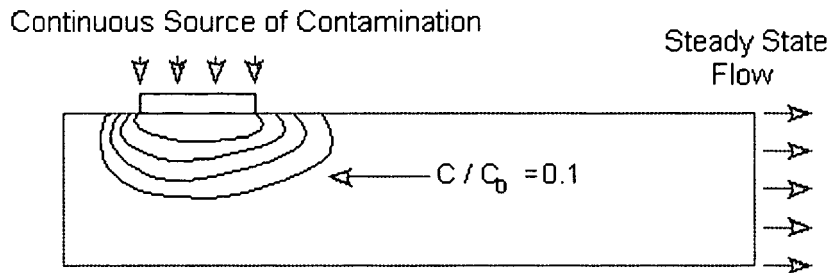
## Volume I:

### The $K_d$ Model, Methods of Measurement, and Application of Chemical Reaction Codes

Case I:  $K_d = 1$  ml/g



Case II:  $K_d = 10$  ml/g



Y212

**UNDERSTANDING VARIATION IN  
PARTITION COEFFICIENT,  $K_d$ , VALUES**

**Volume I:**

**The  $K_d$  Model, Methods of Measurement, and  
Application of Chemical Reaction Codes**

**August 1999**

**A Cooperative Effort By:**

**Office of Radiation and Indoor Air  
Office of Solid Waste and Emergency Response  
U.S. Environmental Protection Agency  
Washington, DC 20460**

**Office of Environmental Restoration  
U.S. Department of Energy  
Washington, DC 20585**

## NOTICE

The following two-volume report is intended solely as guidance to EPA and other environmental professionals. This document does not constitute rulemaking by the Agency, and cannot be relied on to create a substantive or procedural right enforceable by any party in litigation with the United States. EPA may take action that is at variance with the information, policies, and procedures in this document and may change them at any time without public notice.

Reference herein to any specific commercial products, process, or service by trade name, trademark, manufacturer, or otherwise, does not necessarily constitute or imply its endorsement, recommendation, or favoring by the United States Government.

## FOREWORD

Understanding the long-term behavior of contaminants in the subsurface is becoming increasingly more important as the nation addresses groundwater contamination. Groundwater contamination is a national concern as about 50 percent of the United States population receives its drinking water from groundwater. It is the goal of the Environmental Protection Agency (EPA) to prevent adverse effects to human health and the environment and to protect the environmental integrity of the nation's groundwater.

Once groundwater is contaminated, it is important to understand how the contaminant moves in the subsurface environment. Proper understanding of the contaminant fate and transport is necessary in order to characterize the risks associated with the contamination and to develop, when necessary, emergency or remedial action plans. The parameter known as the partition (or distribution) coefficient ( $K_d$ ) is one of the most important parameters used in estimating the migration potential of contaminants present in aqueous solutions in contact with surface, subsurface and suspended solids.

This two-volume report describes: (1) the conceptualization, measurement, and use of the partition coefficient parameter; and (2) the geochemical aqueous solution and sorbent properties that are most important in controlling adsorption/retardation behavior of selected contaminants. Volume I of this document focuses on providing EPA and other environmental remediation professionals with a reasoned and documented discussion of the major issues related to the selection and measurement of the partition coefficient for a select group of contaminants. The selected contaminants investigated in this two-volume document include: chromium, cadmium, cesium, lead, plutonium, radon, strontium, thorium, tritium ( $^3\text{H}$ ), and uranium. This two-volume report also addresses a void that has existed on this subject in both this Agency and in the user community.

It is important to note that soil scientists and geochemists knowledgeable of sorption processes in natural environments have long known that generic or default partition coefficient values found in the literature can result in significant errors when used to predict the absolute impacts of contaminant migration or site-remediation options. Accordingly, one of the major recommendations of this report is that for site-specific calculations, partition coefficient values measured at site-specific conditions are absolutely essential.

For those cases when the partition coefficient parameter is not or cannot be measured, Volume II of this document: (1) provides a "thumb-nail sketch" of the key geochemical processes affecting the sorption of the selected contaminants; (2) provides references to related key experimental and review articles for further reading; (3) identifies the important aqueous- and solid-phase parameters controlling the sorption of these contaminants in the subsurface environment under oxidizing conditions; and (4) identifies, when possible, minimum and maximum conservative partition coefficient values for each contaminant as a function of the key geochemical processes affecting their sorption.

This publication is the result of a cooperative effort between the EPA Office of Radiation and Indoor Air, Office of Solid Waste and Emergency Response, and the Department of Energy Office of Environmental Restoration (EM-40). In addition, this publication is produced as part of ORIA's long-term strategic plan to assist in the remediation of contaminated sites. It is published and made available to assist all environmental remediation professionals in the cleanup of groundwater sources all over the United States.

---

Stephen D. Page, Director  
Office of Radiation and Indoor Air

## ACKNOWLEDGMENTS

Ronald G. Wilhelm from ORIA's Center for Remediation Technology and Tools was the project lead and EPA Project Officer for this two-volume report. Paul Beam, Environmental Restoration Program (EM-40), was the project lead and sponsor for the Department of Energy (DOE). Project support was provided by both DOE/EM-40 and EPA's Office of Remedial and Emergency Response (OERR).

EPA/ORIA wishes to thank the following people for their assistance and technical review comments on various drafts of this report:

Patrick V. Brady, U.S. DOE, Sandia National Laboratories  
David S. Brown, U.S. EPA, National Exposure Research Laboratory  
Joe Eidelberg, U.S. EPA, Region 9  
Amy Gamedinger, Washington State University  
Richard Graham, U.S. EPA, Region 8  
John Griggs, U.S. EPA, National Air and Radiation Environmental Laboratory  
David M. Kargbo, U.S. EPA, Region 3  
Ralph Ludwig, U.S. EPA, National Risk Management Research Laboratory  
Irma McKnight, U.S. EPA, Office of Radiation and Indoor Air  
William N. O'Steen, U.S. EPA, Region 4  
David J. Reisman, U.S. EPA, National Risk Management Research Laboratory  
Kyle Rogers, U.S. EPA, Region 5  
Joe R. Williams, U.S. EPA, National Risk Management Research Laboratory  
OSWER Regional Groundwater Forum Members

In addition, special acknowledgment goes to Carey A. Johnston from ORIA's Center for Remediation Technology and Tools for his contributions in the development, production, and review of this document.

Principal authorship in production of this guide was provided by the Department of Energy's Pacific Northwest National Laboratory (PNNL) under the Interagency Agreement Number DW89937220-01-03. Lynnette Downing served as the Department of Energy's Project Officer for this Interagency Agreement. PNNL authors involved in this project include:

Kenneth M. Krupka  
Daniel I. Kaplan  
Gene Whelan  
R. Jeffrey Serne  
Shas V. Mattigod

**TO COMMENT ON THIS GUIDE OR PROVIDE INFORMATION FOR FUTURE  
UPDATES:**

Send all comments/updates to:

U.S. Environmental Protection Agency  
Office of Radiation and Indoor Air  
Attention: Understanding Variation in Partition ( $K_d$ ) Values  
401 M Street, SW (6602J)  
Washington, DC 20460

or

[webmaster.oria@epa.gov](mailto:webmaster.oria@epa.gov)

7

## ABSTRACT

This two-volume report describes the conceptualization, measurement, and use of the partition (or distribution) coefficient,  $K_d$ , parameter, and the geochemical aqueous solution and sorbent properties that are most important in controlling adsorption/retardation behavior of selected contaminants. The report is provided for technical staff from EPA and other organizations who are responsible for prioritizing site remediation and waste management decisions. Volume I discusses the technical issues associated with the measurement of  $K_d$  values and its use in formulating the retardation factor,  $R_f$ . The  $K_d$  concept and methods for measurement of  $K_d$  values are discussed in detail in Volume I. Particular attention is directed at providing an understanding of: (1) the use of  $K_d$  values in formulating  $R_f$ , (2) the difference between the original thermodynamic  $K_d$  parameter derived from ion-exchange literature and its "empiricized" use in contaminant transport codes, and (3) the explicit and implicit assumptions underlying the use of the  $K_d$  parameter in contaminant transport codes. A conceptual overview of chemical reaction models and their use in addressing technical defensibility issues associated with data from  $K_d$  studies is presented. The capabilities of EPA's geochemical reaction model MINTEQA2 and its different conceptual adsorption models are also reviewed. Volume II provides a "thumb-nail sketch" of the key geochemical processes affecting the sorption of selected inorganic contaminants, and a summary of  $K_d$  values given in the literature for these contaminants under oxidizing conditions. The contaminants chosen for the first phase of this project include chromium, cadmium, cesium, lead, plutonium, radon, strontium, thorium, tritium ( $^3\text{H}$ ), and uranium. Important aqueous speciation, (co)precipitation/dissolution, and adsorption reactions are discussed for each contaminant. References to related key experimental and review articles for further reading are also listed.

# CONTENTS

	<u>Page</u>
NOTICE .....	ii
FOREWORD .....	iii
ACKNOWLEDGMENTS .....	v
FUTURE UPDATES .....	vi
ABSTRACT .....	vii
LIST OF FIGURES .....	xii
LIST OF TABLES .....	xiv
1.0 Introduction .....	1.1
2.0 The $K_d$ Model And Its Use In Contaminant Transport Modeling .....	2.1
2.1 Introduction .....	2.1
2.2 Aqueous Geochemical Processes .....	2.3
2.2.1 Aqueous Complexation .....	2.3
2.2.2 Oxidation-Reduction (Redox) Chemistry .....	2.5
2.2.3 Sorption .....	2.8
2.2.3.1 Adsorption .....	2.10
2.2.3.1.1 Ion Exchange .....	2.13
2.2.3.2 Precipitation .....	2.13
2.3 Sorption Models .....	2.16
2.3.1 Constant Partition Coefficient ( $K_d$ ) Model .....	2.16
2.3.2 Parametric $K_d$ Model .....	2.19
2.3.3 Isotherm Adsorption Models .....	2.20
2.3.4 Mechanistic Adsorption Models .....	2.26
2.4 Effects of Unsaturated Conditions on Transport .....	2.27
2.5 Effects of Chemical Heterogeneity on Transport .....	2.33
2.5.1 Coupled Hydraulic and Chemical Heterogeneity .....	2.34
2.6 Diffusion .....	2.35
2.7 Subsurface Mobile Colloids .....	2.37
2.7.1 Concept of 3-Phase Solute Transport .....	2.37
2.7.2 Sources of Groundwater Mobile Colloids .....	2.38
2.7.3 Case Studies of Mobile-Colloid Enhanced Transport of	

Metals and Radionuclides .....	2.39
2.8 Anion Exclusion .....	2.39
2.9 Summary .....	2.40
3.0 Methods, Issues, and Criteria for Measuring $K_d$ Values .....	3.1
3.1 Introduction .....	3.1
3.2 Methods for Determining $K_d$ Values .....	3.2
3.2.1 Laboratory Batch Method .....	3.3
3.2.2 In-situ Batch Method .....	3.8
3.2.3 Laboratory Flow-Through Method .....	3.9
3.2.4 Field Modeling Method .....	3.14
3.2.5 $K_{oc}$ Method .....	3.14
3.3 Issues Regarding Measuring and Selecting $K_d$ Values .....	3.16
3.3.1 Using Simple Versus Complex Systems to Measure $K_d$ Values .....	3.16
3.3.2 Field Variability .....	3.18
3.3.3 The “Gravel Issue” .....	3.19
3.3.4 The “Colloid Issue” .....	3.21
3.3.5 Particle Concentration Effect .....	3.22
3.4 Methods of Acquiring $K_d$ Values from the Literature for Screening Calculations ...	3.23
3.4.1 $K_d$ Look-Up Table Approach: Issues Regarding Selection of $K_d$ Values from the Literature .....	3.23
3.4.2 Parametric $K_d$ Approach .....	3.26
3.4.3 Mechanistic Adsorption Models .....	3.28
3.5 Summary .....	3.28
4.0 Groundwater Calibration Assessment Based on Partition Coefficients: Derivation and Examples .....	4.1
4.1 Introduction .....	4.1
4.2 Calibration: Location, Arrival Time, and Concentration .....	4.1
4.3 Illustrative Calculations to Help Quantify $K_d$ Using Analytical Models .....	4.4
4.3.1 Governing Equations .....	4.4
4.3.2 Travel Time and the Partition Coefficient .....	4.7
4.3.3 Mass and the Partition Coefficient .....	4.8

10

4.3.4	Dispersion and the Partition Coefficient	4.10
4.4	Modeling Sensitivities to Variations in the Partition Coefficient	4.11
4.4.1	Relationship Between Partition Coefficients and Risk	4.11
4.4.2	Partition Coefficient as a Calibration Parameter in Transport Modeling	4.12
4.5	Summary	4.14
5.0	Application of Chemical Reaction Codes	5.1
5.1	Background	5.1
5.1.1	Definition of Chemical Reaction Modeling	5.2
5.1.2	Reviews of Chemical Reaction Models	5.3
5.1.3	Aqueous Speciation-Solubility Versus Reaction Path Codes	5.4
5.1.4	Adsorption Models in Chemical Reaction Codes	5.5
5.1.5	Output from Chemical Reaction Modeling	5.7
5.1.6	Assumptions and Data Needs	5.9
5.1.7	Symposiums on Chemical Reaction Modeling	5.10
5.2	MINTEQA2 Chemical Reaction Code	5.11
5.2.1	Background	5.11
5.2.2	Code Availability	5.11
5.2.3	Aqueous Speciation Submodel	5.12
5.2.3.1	Example of Modeling Study	5.13
5.2.3.2	Application to Evaluation of $K_d$ Values	5.15
5.2.4	Solubility Submodel	5.16
5.2.4.1	Example of Modeling Study	5.17
5.2.4.2	Application to Evaluation of $K_d$ Values	5.18
5.2.5	Precipitation/Dissolution Submodel	5.18
5.2.5.1	Example of Modeling Study	5.19
5.2.5.2	Application to Evaluation of $K_d$ Values	5.20
5.2.6	Adsorption Submodel	5.21
5.2.6.1	Examples of Modeling Studies	5.22
5.2.6.2	Application to Evaluation of $K_d$ Values	5.23
5.2.7	MINTEQA2 Databases	5.24
5.2.7.1	Thermodynamic Database	5.24
5.2.7.1.1	Basic Equations	5.25
5.2.7.1.2	Structure of Thermodynamic Database Files	5.26
5.2.7.1.3	Database Components	5.26
5.2.7.1.4	Status Relative to Project Scope	5.27
5.2.7.1.5	Issues Related to Database Modifications	5.32
5.2.7.2	Sorption Database	5.33

5.2.7.2.1 Status Relative to Project Scope .....	5.33
5.2.7.2.2 Published Database Sources .....	5.33
5.3 Adsorption Model Options in MINTEQA2 .....	5.35
5.3.1 Electrostatic Versus Non-Electrostatic Models .....	5.36
5.3.2 Activity Partition Coefficient ( $K_d$ ) Model .....	5.40
5.3.3 Activity Langmuir Model .....	5.42
5.3.4 Activity Freundlich Model .....	5.44
5.3.5 Ion Exchange Model .....	5.45
5.3.6 Diffuse Layer Model .....	5.45
5.3.7 Constant Capacitance Model .....	5.47
5.3.8 Triple Layer Model .....	5.48
5.4 Summary .....	5.50
6.0 References .....	6.1
Appendix A - Acronyms, Abbreviations, Symbols, and Notation .....	A.1
Appendix B - Definitions .....	B.1
Appendix C - Standard Method Used at Pacific Northwest National Laboratory for Measuring Laboratory Batch $K_d$ Values .....	C.1

12

## LIST OF FIGURES

	<u>Page</u>
Figure 2.1. Diffuse double layer and surface charge of a mineral surface . . . . .	2.11
Figure 2.2. Four types of adsorption isotherm curves shown schematically in parlance of Giles <i>et al.</i> (1973) . . . . .	2.22
Figure 2.3. Schematic diagram for conceptual model of water distribution in saturated (top two figures) and unsaturated soils (bottom two figures) suggesting differences in the unsaturated flow regime (indicated by arrows) for soils with varying texture . . . . .	2.30
Figure 2.4. Development of hydraulic heterogeneity (decreasing $\theta_m$ ) in unsaturated, non-aggregated soils with decreasing moisture saturation. . . . .	2.32
Figure 3.1. Procedure for measuring a batch $K_d$ value (EPA 1991) . . . . .	3.4
Figure 3.2. Demonstration calculation showing affect on overall $K_d$ by multiple species that have different individual $K_d$ values and are kinetically slow at interconverting between each composition state. . . . .	3.7
Figure 3.3. Procedure for measuring a column $K_d$ value . . . . .	3.9
Figure 3.4. Schematic diagram showing the relative concentrations of a constituent at the input source (figures on left) and in the effluent (figures on right) as a function of time for a pulse versus step input . . . . .	3.11
Figure 4.1. Relative relationships between input-data quality, output uncertainty, and types of problems addressed by each level of assessment . . . . .	4.2
Figure 4.2. Example illustrating a MEPAS $^{90}\text{Sr}$ calibration with $K_d$ equaling 0.8 ml/g and 1 monitored-data point . . . . .	4.13
Figure 4.3. Example illustrating MEPAS $^{90}\text{Sr}$ calibrations with $K_d$ equaling 0.4 and 0.8 ml/g and several monitored-data points . . . . .	4.14
Figure 5.1. Distribution of dominant U(VI) aqueous species for leachates buffered at pH 7.0 by local ground water (Figure 5.1a) and at pH 12.5 by cement pore fluids (Figure 5.1b) . . . . .	5.14
Figure 5.2. Saturation Indices calculated for rutherfordine ( $\text{UO}_2\text{CO}_3$ ) as a function of	

pH for solution analyses from Sergeyeva et al. (1972) .....	5.17
Figure 5.3. Maximum concentration limits calculated for total dissolved uranium as a function of pH based on the equilibrium solubilities of schoepite and uranophane .....	5.20
Figure 5.4. Schematic representation of the triple layer model showing surface species and surface charge-potential relationships .....	5.37
Figure 5.5. Schematic representation of the constant capacitance layer model showing surface species and surface charge-potential relationships .....	5.38

## LIST OF TABLES

	<u>Page</u>
Table 2.1. List of several redox-sensitive metals and their possible valence states in soil/groundwater systems .....	2.6
Table 2.2. Sequence of Principal Electron Acceptors in neutral pH aquatic systems (Sposito 1989) .....	2.7
Table 2.3. Zero-point-of-charge, $\text{pH}_{\text{zpc}}$ .....	2.9
Table 2.4. Cation exchange capacities (CEC) for several clay minerals (Grim 1968) .....	2.14
Table 2.5. Summary of chemical processes affecting attenuation and mobility of contaminants .....	2.41
Table 3.1. Representative chemical species in acidic and basic soil solutions (after Sposito 1989) . . . . .	3.17
Table 3.2. Example of a $K_d$ look-up table for uranium, uranium(VI), and uranium(IV) .....	3.25
Table 3.3. Advantages, disadvantages, and assumptions of $K_d$ determination methods and the assumptions in applying these $K_d$ values to contaminant transport models .....	3.30
Table 5.1. Chemical reaction models described in the literature .....	5.4
Table 5.2. Examples of technical symposiums held on development, applications, and data needs for chemical reaction modeling .....	5.10
Table 5.3. Component species in MINTEQA2 thermodynamic database .....	5.29
Table 5.4. Organic ligands in MINTEQA2 thermodynamic database .....	5.31

15

## 1.0 Introduction

The objective of this two volume report is to provide a reasoned and documented discussion on the technical issues associated with the measurement of partition (or distribution) coefficient,  $K_d$ ,<sup>1,2</sup> values and their use in formulating the contaminant retardation factor,  $R_f$ . Specifically, it describes the rate of contaminant transport relative to that of groundwater. The retardation factor is the empirical parameter commonly used in transport models to describe the chemical interaction between the contaminant and geological materials (*i.e.*, soils, sediments, and rocks). *Throughout this report, the term "soil" will be used as general term to refer to all unconsolidated geologic materials.*<sup>3</sup> The contaminant retardation factor includes processes such as surface adsorption, absorption into the soil structure, precipitation, and physical filtration of colloids. This report is provided for technical staff from EPA and other organizations who are responsible for prioritizing site remediation and waste management decisions.

Volume I contains a detailed discussion of the  $K_d$  concept, its use in fate and transport computer codes, and the methods for the measurement of  $K_d$  values. The focus of Chapter 2 is on providing an understanding of (1) the use of  $K_d$  values in formulating  $R_f$ , (2) the difference between the original thermodynamic  $K_d$  parameter derived from the ion-exchange literature and its "empiricized" use in contaminant transport codes, and (3) the explicit and implicit assumptions underlying the use of the  $K_d$  parameter in contaminant transport codes.

The  $K_d$  parameter is very important in estimating the potential for the adsorption of dissolved contaminants in contact with soil. As typically used in fate and contaminant transport calculations, the  $K_d$  is defined as the ratio of the contaminant concentration associated with the solid to the contaminant concentration in the surrounding aqueous solution when the system is at equilibrium. Soil and geochemists knowledgeable of sorption processes in natural environments have long known that generic or default  $K_d$  values can result in significant error when used to predict the absolute impacts of contaminant migration or site-remediation options. Therefore, for site-specific calculations,  $K_d$  values measured at site-specific conditions are absolutely essential.

---

<sup>1</sup> Throughout this report, the term "partition coefficient" will be used to refer to the  $K_d$  "linear isotherm" sorption model. It should be noted, however, that the terms "partition coefficient" and "distribution coefficient" are used interchangeably in the literature for the  $K_d$  model.

<sup>2</sup> A list of acronyms, abbreviations, symbols, and notation is given in Appendix A. A list of definitions is given in Appendix B

<sup>3</sup> The terms "sediment" and "soil" have particular meanings depending on one's technical discipline. For example, the term "sediment" is often reserved for transported and deposited particles derived from soil, rocks, or biological material. "Soil" is sometimes limited to referring to the top layer of the earth's surface, suitable for plant life. In this report, the term "soil" was selected as a general term to refer to all unconsolidated geologic materials.

16

To address some of this concern when using generic or default  $K_d$  values for screening calculations, modelers often incorporate a degree of conservatism into their calculations by selecting limiting or bounding conservative  $K_d$  values. For example, the most conservative estimate from an off-site risk perspective of contaminant migration through the subsurface natural soil is to assume that the soil has little or no ability to slow (retard) contaminant movement (*i.e.*, a minimum bounding  $K_d$  value). Consequently, the contaminant would migrate in the direction and, for a  $K_d$  value of  $\infty$ , travel at the rate of water. Such an assumption may in fact be appropriate for certain contaminants such as tritium, but may be too conservative for other contaminants, such as thorium or plutonium, which react strongly with soils and may migrate  $10^2$  to  $10^6$  times more slowly than the water. On the other hand, to estimate the maximum risks (and costs) associated with on-site remediation options, the bounding  $K_d$  value for a contaminant will be a maximum value (*i.e.*, maximize retardation).

The  $K_d$  value is usually a measured parameter that is obtained from laboratory experiments. The general methods used to measure  $K_d$  values (Chapters 3 and 4) include the laboratory batch method, *in-situ* batch method, laboratory flow-through (or column) method, field modeling method, and  $K_{oc}$  method. The ancillary information needed regarding the adsorbent (soil), solution (contaminated ground-water or process waste water), contaminant (concentration, valence state, speciation distribution), and laboratory details (spike addition methodology, phase separation techniques, contact times) are summarized. The advantages, disadvantages, and, perhaps more importantly, the underlying assumptions of each method are also presented.

A conceptual overview of geochemical modeling calculations and computer codes as they pertain to evaluating  $K_d$  values and modeling of adsorption processes is discussed in detail in Chapter 5. The use of geochemical codes in evaluating aqueous speciation, solubility, and adsorption processes associated with contaminant fate studies is reviewed. This approach is compared to the traditional calculations that rely on the constant  $K_d$  construct. The use of geochemical modeling to address quality assurance and technical defensibility issues concerning available  $K_d$  data and the measurement of  $K_d$  values is also discussed. The geochemical modeling review includes a brief description of the EPA's MINTEQA2 geochemical code and a summary of the types of conceptual models it contains to quantify adsorption reactions. The status of radionuclide thermodynamic and contaminant adsorption model databases for the MINTEQA2 code is also reviewed.

The main focus of Volume II is to: (1) provide a "thumb-nail sketch" of the key geochemical processes affecting the sorption of a selected set of contaminants; (2) provide references to related key experimental and review articles for further reading; (3) identify the important aqueous- and solid-phase parameters controlling the sorption of these contaminants in the subsurface environment under oxidizing conditions; and (4) identify, when possible, minimum and maximum conservative  $K_d$  values for each contaminant as a function key geochemical processes affecting their sorption. The contaminants chosen for the first phase of this project include chromium, cadmium, cesium, lead, plutonium, radon, strontium, thorium, tritium ( $^3\text{H}$ ), and uranium. The selection of these contaminants by EPA and PNNL project staff was based on two

criteria. First, the contaminant had to be of high priority to the site remediation or risk assessment activities of EPA. Second, due to budgetary constraints, a subset of the large number of contaminants that met the first criteria were selected to represent categories of contaminants based on their chemical behavior. The six nonexclusive categories are:

- Cations - cadmium, cesium, lead, plutonium, strontium, thorium, and uranium
- Anions - chromium(VI) (as chromate)
- Radionuclides - cesium, plutonium, radon, strontium, thorium, tritium ( $^3\text{H}$ ), and uranium
- Conservatively transported contaminants - tritium ( $^3\text{H}$ ) and radon
- Nonconservatively transported contaminants - other than tritium ( $^3\text{H}$ ) and radon
- Redox sensitive elements - chromium, lead, plutonium, and uranium

The general principles of geochemistry discussed in both volumes of this report can be used to estimate the geochemical interactions of similar elements for which data are not available. For example, contaminants present primarily in anionic form, such as Cr(VI), tend to adsorb to a limited extent to soils. Thus, one might generalize that other anions, such as nitrate, chloride, and U(VI)-anionic complexes, would also adsorb to a limited extent. Literature on the adsorption of these 3 solutes show no or very little adsorption.

The concentration of contaminants in groundwater is controlled primarily by the amount of contaminant present at the source; rate of release from the source; hydrologic factors such as dispersion, advection, and dilution; and a number of geochemical processes including aqueous geochemical processes, adsorption/desorption, precipitation, and diffusion. To accurately predict contaminant transport through the subsurface, it is essential that the important geochemical processes affecting contaminant transport be identified and, perhaps more importantly, accurately described in a mathematically defensible manner. Dissolution/precipitation and adsorption/desorption are usually the most important processes affecting contaminant interaction with soils. Dissolution/precipitation is more likely to be the key process where chemical nonequilibrium exists, such as at a point source, an area where high contaminant concentrations exist, or where steep pH or oxidation-reduction (redox) gradients exist. Adsorption/desorption will likely be the key process controlling inorganic contaminant migration in areas where the naturally-present constituents are already in equilibrium and only the anthropogenic constituents (contaminants) are out of equilibrium, such as in areas far from the point source. Diffusion flux spreads solute via a concentration gradient (*i.e.*, Fick's law). Diffusion is a dominant transport mechanism when advection is insignificant, and is usually a negligible transport mechanism when water is being advected in response to various forces.

## 2.0 The $K_d$ Model And Its Use In Contaminant Transport Modeling

### 2.1 Introduction

The concentration of contaminants in groundwater<sup>1</sup> is determined by the amount, concentration, and nature of contaminant present at the source, rate of release from the source, and a number of geochemical processes including aqueous and sorption geochemical processes (Section 2.2) and -diffusion (Section 2.6). Recently, attention has been directed at additional geochemical processes that can enhance the transport of certain contaminants: colloid-facilitated transport of contaminants (Section 2.7) and anion exclusion (Section 2.8). These latter processes are difficult to quantify, and the extent to which they occur has not been determined. To predict contaminant transport through the subsurface accurately, it is essential that the important geochemical processes affecting the contaminant transport be identified and, perhaps more importantly, accurately described in a mathematically defensible manner. Dissolution/precipitation and adsorption/desorption are considered the most important processes affecting contaminant interaction with soils. Dissolution/precipitation is more likely to be the key process where chemical nonequilibrium exists, such as at a waste disposal facility (*i.e.*, point source), an area where high contaminant concentrations exist, or where steep pH or oxidation-reduction (redox) gradients exist. Adsorption/desorption will likely be the key process controlling contaminant migration in areas where chemical equilibrium exists, such as in areas far from the disposal facilities or spill sites.

The simplest and most common method of estimating contaminant retardation (*i.e.*, the inverse of the relative transport rate of a contaminant compared to that of water) is based on partition (or distribution) coefficient,  $K_d$ ,<sup>2</sup> values (Section 2.3.1). In turn, the  $K_d$  value is a direct measure of the partitioning of a contaminant between the solid and aqueous phases. It is an empirical metric that attempts to account for various chemical and physical retardation mechanisms that are influenced by a myriad of variables. Ideally, site-specific  $K_d$  values would be available for the range of aqueous and geological conditions in the system to be modeled.

Values for  $K_d$  not only vary greatly between contaminants, but also vary as a function of aqueous and solid phase chemistry (Delegard and Barney, 1983; Kaplan and Serne, 1995; Kaplan *et al.*, 1994c). For example, uranium  $K_d$  values can vary over 6 orders of magnitude depending on the composition of the aqueous and solid phase chemistry (see Volume II, Appendix J). A more

---

<sup>1</sup> For information regarding the background concentration levels of macro and trace constituents, including elements of regulatory-interest such as arsenic, cadmium, chromium, lead, and mercury, in soils and groundwater systems, the reader is referred to Lindsay (1979), Hem (1985), Sposito (1989, 1994), Langmuir (1997), and other similar sources and the references cited therein.

<sup>2</sup> A list of acronyms, abbreviations, symbols, and notation is given in Appendix A. A list of definitions is given in Appendix B.

robust approach to describing the partitioning of contaminants between the aqueous and solid phases is the parametric  $K_d$  model, which varies the  $K_d$  value according to the chemistry and mineralogy of the system at the node<sup>1</sup> being modeled (Section 2.3.2). Though this approach is more accurate, it has not been used frequently. The added complexity in solving the transport equation with the parametric  $K_d$  adsorption model and its empirical nature may be why this technique has been used sparingly.

Inherent in the  $K_d$  “linear isotherm” adsorption model is the assumption that adsorption of the contaminant of interest is independent of its concentration in the aqueous phase. Partitioning of a contaminant on soil can often be described using the  $K_d$  model, but typically only for low contaminant concentrations as would exist some distance away (far field) from the source of contamination. It is common knowledge that contaminant adsorption on soils can deviate from the linear relationship required by the  $K_d$  construct. This is possible for conditions as might exist in leachates or groundwaters near waste sources where contaminant concentrations are large enough to affect the saturation of surface adsorption sites. Non-linear isotherm models (Section 2.3.3) are used to describe the case where sorption relationships deviate from linearity.

Mechanistic models explicitly accommodate the dependency of  $K_d$  values on contaminant concentration, competing ion concentration, variable surface charge on the absorbent, and solution species distribution. Incorporating mechanistic or semi-mechanistic adsorption concepts into transport models is desirable because the models become more robust and, perhaps more importantly from the standpoint of regulators and the public, scientifically defensible. However, less attention will be directed to mechanistic adsorption models because the focus of this project is on the  $K_d$  model which is currently the most common method for quantifying chemical interactions of dissolved contaminants with soils for performance assessment, risk assessment, and remedial investigation calculations. The complexity of installing these mechanistic adsorption models into existing computer codes used to model contaminant transport is difficult to accomplish. Additionally, these models also require a more intense and costly data collection effort than will likely be available to many contaminant transport modelers, license requestors, or responsible parties. A brief description of the state of the science and references to excellent review articles are presented (Section 2.3.4).

The purpose of this chapter is to provide a primer to modelers and site managers on the key geochemical processes affecting contaminant transport through soils. Attention is directed at describing how geochemical processes are accounted for in transport models by using the partition coefficient ( $K_d$ ) to describe the partitioning of aqueous phase constituents to a solid phase. Particular attention is directed at: (1) defining the application of the  $K_d$  parameter, (2) the explicit and implicit assumptions underlying its use in transport codes, and (3) the difference between the original thermodynamic  $K_d$  parameter derived from ion-exchange literature and its “empiricized” use in formulating the retardation factors used in contaminant transport

---

<sup>1</sup> A “node” is the center of a computation cell within a grid used to define the area or volume being modeled.

codes. In addition to geochemical processes, related issues pertaining to the effects of unsaturated conditions, chemical heterogeneity, diffusion, and subsurface mobile colloids on contaminant transport are also briefly discussed. These processes and their effects on contaminant mobility are summarized in a table at the end of this chapter.

## 2.2 Aqueous Geochemical Processes

Groundwater modelers are commonly provided with the total concentration of a number of dissolved substances in and around a contaminant plume. While total concentrations of these constituents indicate the extent of contamination, they give little insight into the forms in which the metals are present in the plume or their mobility and bioavailability. Contaminants can occur in a plume as soluble-free, soluble-complexed, adsorbed, organically complexed, precipitated, or coprecipitated species (Sposito, 1989). The geochemical processes that contribute to the formation of these species and their potential effect on contaminant transport are discussed in this chapter.

### 2.2.1 Aqueous Complexation

Sposito (1989) calculated that a typical soil solution will easily contain 100 to 200 different soluble species, many of them involving metal cations and organic ligands. A complex is said to form whenever a molecular unit, such as an ion, acts as a central group to attract and form a close association with other atoms or molecules. The aqueous species  $\text{Th}(\text{OH})_4$  (aq),  $(\text{UO}_2)_3(\text{OH})_5^+$ , and  $\text{HCO}_3^-$  are complexes with  $\text{Th}^{4+}$  (thorium),  $\text{UO}_2^{2+}$  (hexavalent uranium), and  $\text{CO}_3^{2-}$  (carbonate), respectively, acting as the central group. The associated ions,  $\text{OH}^-$  or  $\text{H}^+$ , in these complexes are termed ligands. If 2 or more bonds are formed between a single ligand and a metal cation, the complex is termed a chelate. The complex formed between  $\text{Al}^{3+}$  and citric acid  $[\text{Al}(\text{COO})_2\text{COH}(\text{CH}_2\text{COOH})]^+$ , in which 2  $\text{COO}^-$  groups and 1  $\text{COH}$  group of the citric acid molecule are coordinated to  $\text{Al}^{3+}$ , is an example of a chelate. If the central group and ligands in a complex are in direct contact, the complex is called inner-sphere. If one or more water molecules is interposed between the central group and a ligand, the complex is outer-sphere. If the ligands in a complex are water molecules [*e.g.*, as in  $\text{Ca}(\text{H}_2\text{O})_6^{2+}$ ], the unit is called a solvation complex or, more frequently, a free species. Inner-sphere complexes usually are much more stable than outer-sphere complexes, because the latter cannot easily involve ionic or covalent bonding between the central group.

Most of the complexes likely to form in groundwater are metal-ligand complexes, which may be either inner-sphere or outer-sphere. As an example, consider the formation of a neutral sulfate complex with a bivalent metal cation ( $\text{M}^{2+}$ ) as the central group:<sup>1</sup>

---

<sup>1</sup> Unless otherwise noted, all species listed in equations in this appendix refer to aqueous species.

21



where the metal M can be cadmium, chromium, lead, mercury, strontium, *etc.* The equilibrium (or stability) constant,  $K_{r,T}$ , corresponding to Equation 2.1 is:

$$K_{r,T} = \frac{\{MSO_4^{0}(\text{aq})\}}{\{M^{2+}\} \{SO_4^{2-}\}} \quad (2.2)$$

where quantities indicated by { } represent species activities. The equilibrium constant can describe the distribution of a given constituent among its possible chemical forms if complex formation and dissociation reactions are at equilibrium. The equilibrium constant is affected by a number of factors, including the ionic strength of the aqueous phase, presence of competing reactions, and temperature.

The most common complexing anions present in groundwater are  $HCO_3^-/CO_3^{2-}$ ,  $Cl^-$ ,  $SO_4^{2-}$ , and humic substances (*i.e.*, organic materials). Some synthetic organic ligands may also be present in groundwater at contaminated sites. Dissolved  $PO_4^{3-}$  can also be a strong inorganic complexant, but is generally not very soluble in natural groundwaters. The relative propensity of the inorganic ligands to form complexes with many metals is:  $CO_3^{2-} > SO_4^{2-} > PO_4^{3-} > Cl^-$  (Stumm and Morgan, 1981). Carbonate complexation may be equally important in carbonate systems, especially for tetravalent metals (Kim, 1986; Rai *et al.*, 1990). There can be a large number of dissolved, small-chain humic substances present in groundwater and their complexation properties with metals and radionuclides are not well understood. Complexes with humic substances are likely to be very important in systems containing appreciable amounts of humic substances (>1 mg/l). In shallow aquifers, organic ligands from humic materials can be present in significant concentration and dominate the metal chemistry (Freeze and Cherry, 1979). The chelate anion, EDTA,<sup>1</sup> which is a common industrial reagent, forms strong complexes with many cations, much stronger than carbonate and humic substances (Kim, 1986). Some metal-organic ligand complexes can be fairly stable and require low pH conditions (or high pH for some metal-organic complexes) to dissociate the complex.

Complexation usually results in lowering the solution concentration (*i.e.*, activity) of the central molecule (*i.e.*, uncomplexed free species). Possible outcomes of lowering the activity of the free species of the metal include lowering the potential for adsorption and increasing its solubility, both of which can enhance migration potential. On the other hand, some complexants (*e.g.*, certain humic acids) readily bond to soils and thus retard the migration of the complexed metals.

---

<sup>1</sup> EDTA is ethylene diamine triacetic acid.

### 2.2.2 Oxidation-Reduction (Redox) Chemistry

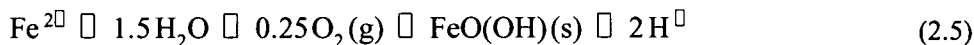
An oxidation-reduction (redox) reaction is a chemical reaction in which electrons are transferred completely from one species to another. The chemical species that loses electrons in this charge transfer process is described as oxidized, and the species receiving electrons is described as reduced. For example, in the reaction involving iron species:



the solid phase, goethite [FeO(OH) (s)], is the oxidized species, and Fe<sup>2+</sup> is the reduced species. Equation 2.3 is a reduction half-reaction in which an electron in aqueous solution, denoted e<sup>-</sup>, serves as one of the reactants. This species, like the proton in aqueous solution, is understood in a formal sense to participate in charge transfer processes. The overall redox reaction in a system must always be the combination of 2 half-reactions, an oxidation half-reaction and reduction half-reaction, such that the species e<sup>-</sup> does not exist explicitly. For example, to represent the oxidation of Fe<sup>2+</sup>, Equation 2.3 could be combined (or coupled) with the half-reaction involving the oxidation of H<sub>2</sub>O:



Combining Equation 2.3 with Equation 2.4 results in the cancellation of the aqueous electron and the oxidation of Fe<sup>2+</sup> via the reduction of O<sub>2</sub> (g) and subsequent precipitation of hydrous iron oxide. This is a possible reaction describing Fe<sup>2+</sup> leaching from a reduced environment in the near field to the oxidizing environment of the far field:



Equation 2.5 could represent a scenario in which Fe<sup>2+</sup> is leached from a reducing environment, where it is mobile, into an oxidized environment, where Fe<sup>3+</sup> precipitates as the mineral goethite.

The electron activity is a useful conceptual device for describing the redox status of aqueous systems, just as the aqueous proton activity is so useful for describing the acid-base status of soils. Similar to pH, the propensity of a system to be oxidized can be expressed by the negative common logarithm of the free-electron activity, pE:

$$\text{pE} = -\log \{e^-\} \quad (2.6)$$

The range of pE in the natural environment varies between approximately 7 and 17 in the vadose zone (Sposito, 1989). If anoxic conditions exist, say in a bog area, then the pE may get as low as -3. The most important chemical elements affected by redox reactions in ambient groundwater are carbon, nitrogen, oxygen, sulfur, manganese, and iron. In contaminated groundwater, this list

increases to include arsenic, cobalt, chromium, iodine, molybdenum, neptunium, plutonium, selenium, technetium, uranium, and others. Table 2.1 lists several redox-sensitive metals and the

**Table 2.1.** List of several redox-sensitive metals and their possible valence states in soil/groundwater systems.

Element	Valence States	Element	Valence States
Americium	+3, +4, +5, and +6	Neptunium	+3, +4, +5, and +6
Antimony	+3 and +5	Plutonium	+2, +3, +4, +5, and +6
Arsenic	+3 and +5	Ruthenium	+2, +3, +4, +6, and +7
Chromium	+2, +3, and +6	Selenium	-2, +4, and +6
Copper	+1 and +2	Technetium	+2, +3, +4, +5, +6, and +7
Iron	+2 and +3	Thallium	+1 and +3
Manganese	+2 and +3	Uranium	+3, +4, +5, and +6
Mercury	+1 and +2	Vanadium	+2, +3, +4, and +5

different valence states that they may be present as in soil/groundwater systems. The speciation of a metal in solution between its different valence states will depend on the site geochemistry, especially with respect to pH and redox conditions. Moreover, not all of the valence states for each metal are equally important from the standpoint of dominance in solution, adsorption behavior, solubility, and toxicity. For those redox-sensitive elements that are part of this project's scope (*i.e.*, chromium, plutonium, and uranium), these issues are discussed in detail in Volume II of this report.

There is a well defined sequence of reduction of inorganic elements (Table 2.2). When an oxidized system is reduced, the order that oxidized species disappear are  $O_2$ ,  $NO_3^-$ ,  $Mn^{2+}$ ,  $Fe^{2+}$ ,  $HS^-$ , and  $H_2$ . As the pE of the system drops below +11.0, enough electrons become available to reduce  $O_2$  (g) to  $H_2O$ . Below a pE of 5,  $O_2$  (g) is not stable in pH neutral systems. Above pE = 5,  $O_2$  (g) is consumed in the respiration processes of aerobic microorganisms. As the pE decreases below 8, electrons become available to reduce  $NO_3^-$  to  $NO_2^-$ . As the system pE value drops into the range of 7 to 5, electrons become plentiful enough to support the reduction of iron and manganese in solid phases. Iron reduction does not occur until  $O_2$  and  $NO_3^-$  are depleted, but manganese reduction can be initiated in the presence of  $NO_3^-$ . In the case of iron and manganese,

decreasing pE results in solid-phase dissolution, because the stable forms of Mn(IV) and Fe(III) are solid phases. Besides the increase in solution concentrations of iron and manganese expected from this effect of lowered pE, a marked increase is usually observed in the aqueous phase concentrations of metals such as cadmium, chromium, or lead, and of ligands such as  $\text{H}_2\text{PO}_4^-$  or

**Table 2.2.** Sequence of Principal Electron Acceptors in neutral pH aquatic systems (Sposito, 1989).

Reduction Half-Reactions	Range of Initial pE Values
$0.5 \text{ O}_2 (\text{g}) + 2 \text{ e}^- + 2 \text{ H}^+ = \text{H}_2\text{O}$	5.0 to 11.0
$\text{NO}_3^- + 2 \text{ e}^- + 2 \text{ H}^+ = \text{NO}_2^- + \text{H}_2\text{O}$	3.4 to 8.5
$\text{MnO}_2 (\text{s}) + 2 \text{ e}^- + 4 \text{ H}^+ = \text{Mn}^{2+} + 2 \text{ H}_2\text{O}$	3.4 to 6.8
$\text{FeOOH} (\text{s}) + \text{ e}^- + 3 \text{ H}^+ = \text{Fe}^{2+} + 2 \text{ H}_2\text{O}$	1.7 to 5.0
$\text{SO}_4^{2-} + 8 \text{ e}^- + 9 \text{ H}^+ = \text{HS}^- + 4 \text{ H}_2\text{O}$	0 to -2.5
$\text{H}^+ + \text{ e}^- = 0.5 \text{ H}_2 (\text{g})$	-2.5 to -3.7
$(\text{CN}_2\text{O})_n = n/2 \text{ CO}_2 (\text{g}) + n/2 \text{ CH}_4 (\text{g})$	-2.5 to -3.7

$\text{HMoO}_4^-$ , accompanying reduction of iron and manganese. The principal cause of this secondary phenomenon is the desorption of metals and ligands that occurs when the adsorbents (*i.e.*, mostly iron and manganese oxides) to which they are bound become unstable and dissolve. Typically, the metals released in this fashion, including iron and manganese, are soon reabsorbed by solids that are stable at low pE (*e.g.*, clay minerals or organic matter) and become exchangeable surface species.

These surface changes have an obvious influence on the availability (migration potential) of the chemical elements involved, particularly phosphorus. If a contaminant was involved in this dissolution/ exchange set of reactions, it would be expected that the contaminants would be less strongly associated with the solid phase.

As pE becomes negative, sulfur reduction can take place. If contaminant metals and radionuclides, such as Cr(VI), Pu (VI), or U(VI), are present in the aqueous phase at high enough concentrations, they can react with bisulfide ( $\text{HS}^-$ ) to form metal sulfides that are quite insoluble. Thus, anoxic conditions can diminish significantly the solubility of some redox-sensitive contaminants.

25

Redox chemistry may also have a direct affect on contaminant chemistry. It can directly affect the oxidation state of several contaminants, including, arsenic, cobalt, chromium, iodine, molybdenum, neptunium, lead, plutonium, selenium, technetium, and uranium. A change in oxidation in turn affects the potential of some contaminants to precipitate. For example, the reduction of Pu(IV),



makes plutonium appreciably less reactive in complexation [*i.e.*, Pu(III) stability constants are much less than those of Pu(IV)] and sorption/partitioning reactions (Kim, 1986). The reduction of U(VI) to U(III) or U(IV), has the opposite effect, *i.e.*, U(III) or U(IV) form stronger complexes and sorb more strongly to surfaces than U(VI). Reducing environments tend to make chromium, similar to uranium, less mobile, and arsenic more mobile.

Therefore, changes in redox may increase or decrease the tendency for reconcentration of contaminants, depending on the chemical composition of the aqueous phase and the contaminant in question. However, if the redox status is low enough to induce sulfide formation, reprecipitation of many metals and metal-like radionuclides can be expected. Redox-mediated reactions are incorporated into most geochemical codes and can be modeled conceptually. The resultant speciation distribution calculated by such a code is used to determine potential solubility controls and adsorption potential. Many redox reactions have been found to be kinetically slow in natural groundwater, and several elements may never reach redox equilibrium between their various oxidation states. Thus, it is more difficult to predict with accuracy the migration potential of redox-sensitive species.

### 2.2.3 Sorption

When a contaminant is associated with the solid phase, it is not known if it was adsorbed on to the surface of a solid, absorbed into the structure of a solid, precipitated as a 3-dimensional molecular structure on the surface of the solid, or partitioned into the organic matter (Sposito, 1989). Dissolution/precipitation and adsorption/desorption are considered the most important processes affecting metal and radionuclide interaction with soils and will be discussed at greater lengths than absorption and organic matter partitioning.

- Dissolution/precipitation is more likely to be the key process where chemical nonequilibrium exists, such as at a point source, an area where high contaminant concentrations exist, or where steep pH or redox gradients exist.
- Adsorption/desorption will likely be the key process controlling contaminant migration in areas where chemical equilibrium exists, such as in areas far from the point source.

A generic term devoid of mechanism and used to describe the partitioning of aqueous phase constituents to a solid phase is sorption. Sorption encompasses all of the above processes. It is frequently quantified by the partition coefficient,  $K_p$ , that will be discussed below (Section 2.3.1).

In many natural systems, the extent of sorption is controlled by the electrostatic surface charge of the mineral phase. Most soils have net negative charges. These surface charges originate from permanent and variable charges. The permanent charge results from the substitution of a lower valence cation for a higher valence cation in the mineral structure, where as the variable charge results from the presence of surface functional groups. Permanent charge is the dominant charge of 2:1 clays, such as biotite and montmorillonite. Permanent charge constitutes a majority of the charge in unweathered soils, such as exist in temperate zones in the United States, and it is not affected by solution pH. Permanent positive charge is essentially nonexistent in natural rock and soil systems. Variable charge is the dominant charge of aluminum, iron, and manganese oxide solids and organic matter. Soils dominated by variable charge surfaces are primarily located in semi-tropical regions, such as Florida, Georgia, and South Carolina, and tropical regions. The magnitude and polarity of the net surface charge changes with a number of factors, including pH. As the pH increases, the surface becomes increasingly more negatively charged. The pH where the surface has a zero net charge is referred to as the pH of zero-point-of-charge,  $\text{pH}_{\text{zpc}}$  (Table 2.3). At the pH of the majority of natural soils (pH 5.5 to 8.3), calcite, gibbsite, and goethite, if present, would be expected to have some, albeit little, positive charge and therefore some anion sorption capacity.

**Table 2.3.** pH of zero-point-of-charge,  $\text{pH}_{\text{zpc}}$ . [After Stumm and Morgan (1981) and Lehninger (1970)].

Material	$\text{pH}_{\text{zpc}}$
Gibbsite $[\text{Al}(\text{OH})_3]$	5.0
Hematite $(\square\text{-Fe}_2\text{O}_3)$	6.7
Goethite $(\square\text{-FeOOH})$	7.8
Silica $(\text{SiO}_2)$	2
Feldspars	2 to 2.4
Kaolinite $[\text{Al}_2\text{Si}_2\text{O}_5(\text{OH})_4]$	4.6
COOH	1.7 to 2.6 <sup>1</sup>
NH <sub>3</sub>	9.0 to 10.4 <sup>1</sup>

<sup>1</sup> These values represent the range of  $\text{pK}_a$  values for amino acids.

### 2.2.3.1 Adsorption

Adsorption, as discussed in this report, is the net accumulation of matter at the interface between a solid phase and an aqueous-solution phase. It differs from precipitation because it does not include the development of a 3-dimensional molecular structure. The matter that accumulates in 2-dimensional molecular arrangements at the interface is the adsorbate. The solid surface on which it accumulates is the adsorbent.

Adsorption on clay particle surfaces can take place via 3 mechanisms. In the first mechanism, an inner-sphere surface complex is in direct contact with the adsorbent surface and lies within the Stern Layer (Figure 2.1). As a rule, the relative affinity of a contaminant to sorb will increase with its tendency to form inner-sphere surface complexes. The tendency for a cation to form an inner-sphere complex in turn increases with increasing valence (*i.e.*, more specifically, ionic potential<sup>1</sup>) of a cation (Sposito, 1984).

The second mechanism creates an outer-sphere surface complex that has at least 1 water molecule between the cation and the adsorbent surface. If a solvated ion (*i.e.*, an ion with water molecules surrounding it) does not form a complex with a charged surface functional group but instead neutralizes surface charge only in a delocalized sense, the ion is said to be adsorbed in the diffuse-ion swarm, and these ions lie in a region called the diffuse sublayer (Figure 2.1). The diffuse-ion swarm and the outer-sphere surface complex mechanisms of adsorption involve exclusively ionic bonding, whereas inner-sphere complex mechanisms are likely to involve ionic, as well as covalent, bonding.

The mechanisms by which anions adsorb are inner-sphere surface complexation and diffuse-ion swarm association. Outer-sphere surface complexation of anions involves coordination to a protonated hydroxyl or amino group or to a surface metal cation (*e.g.*, water-bridging mechanisms) (Gu and Schulz, 1991). Almost always, the mechanism of this coordination is hydroxyl-ligand exchange (Sposito, 1984). In general, ligand exchange is favored at pH levels less than the zero-point-of-charge (Table 2.3). The anions  $\text{CrO}_4^{2-}$ ,  $\text{Cl}^-$ , and  $\text{NO}_3^-$ , and to lesser extent  $\text{HS}^-$ ,  $\text{SO}_4^{2-}$ , and  $\text{HCO}_3^-$ , are considered to adsorb mainly as diffuse-ion and outer-sphere-complex species.

---

<sup>1</sup> The ionic potential is the ratio of the valence to the ionic radius of an ion.

28

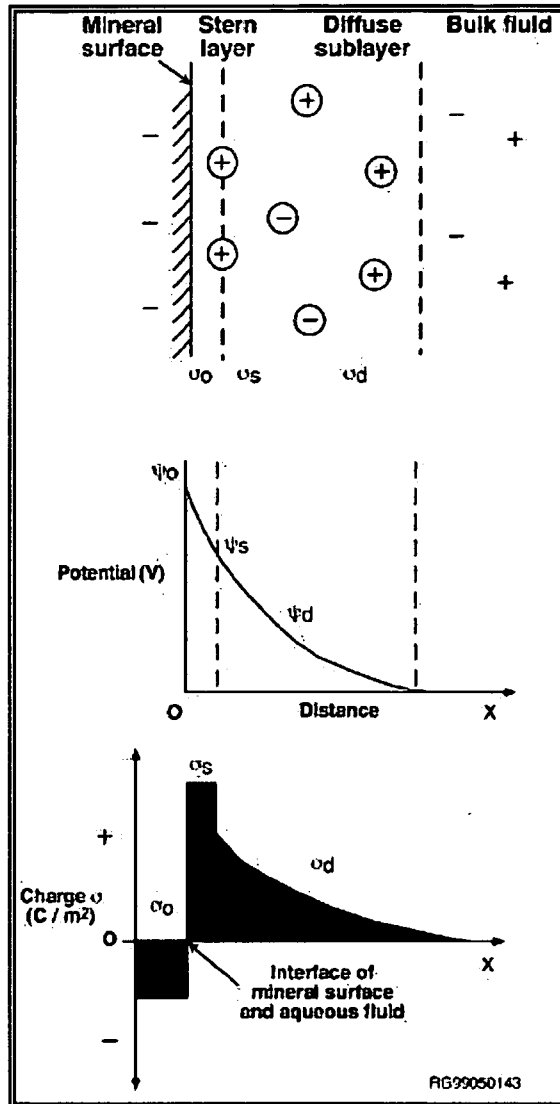


**Figure 2.1.** Diffuse double layer and surface charge of a mineral surface. ( $\sigma_0$ ,  $\sigma_s$ , and  $\sigma_d$  represent the surface charge at the surface, Stern layer, and diffuse layer, respectively;  $\psi_0$ ,  $\psi_s$ , and  $\psi_d$  represent the potential at the surface, Stern layer, and diffuse layer, respectively.)

29

As noted previously, the relative affinity of an adsorbent for a free-metal cation will generally increase with the tendency of a cation to form inner-sphere surface complexes, which in turn increases with higher ionic potential of a cation (Sposito, 1989). Based on these considerations and laboratory observations, the relative-adsorption affinity of metals has been described as follows (Sposito, 1989):



With respect to transition metal cations, however, ionic potential is not adequate as a single predictor of adsorption affinity, since electron configuration plays a very important role in the complexes of these cations. Their relative affinities tend to follow the Irving-Williams order:



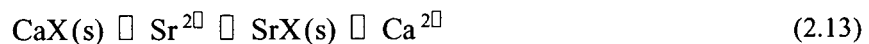
The molecular basis for this ordering is discussed in Cotton and Wilkinson (1972).

Adsorption of dissolved contaminants is very dependent on pH. As noted previously in the discussion of the pH of zero-point-of-charge,  $\text{pH}_{\text{zpc}}$  (Table 2.3), the magnitude and polarity of the net surface charge of a mineral changes with pH (Langmuir, 1997; Stumm and Morgan, 1981). At  $\text{pH}_{\text{zpc}}$ , the net charge of a surface changes from positive to negative. Mineral surfaces become increasingly more negatively charged as pH increases. At  $\text{pH} < \text{pH}_{\text{zpc}}$ , the surface becomes protonated, which results in a net positive charge and favors adsorption of contaminants present as dissolved anions. Because adsorption of anions is coupled with a release of  $\text{OH}^-$  ions, anion adsorption is greatest at low pH and decreases with increasing pH. At  $\text{pH} > \text{pH}_{\text{zpc}}$ , acidic dissociation of surface hydroxyl groups results in a net negative-charge which favors adsorption of contaminants present as dissolved cations. Because adsorption of cations is coupled with a release of  $\text{H}^+$  ions, cation adsorption is greatest at high pH and decreases with decreasing pH. It should be noted that some contaminants may be present as dissolved cations or anions depending on geochemical conditions. In soil/groundwater systems containing dissolved carbonate, U(VI) may be present as dissolved cations (e.g.,  $\text{UO}_2^{2+}$ ) at low to near-neutral pH values or as anions [e.g.,  $\text{UO}_2(\text{CO}_3)_3^{4-}$ ] at near neutral to high pH values. The adsorption of U(VI) on iron oxide minerals (Waite *et al.*, 1994) is essentially 0 percent at pH values less than approximately 3, increases rapidly to 100 percent in the pH range from 5 to 8, and rapidly decreases to 0 percent at pH values greater than 9. This adsorption behavior for U(VI) (see Volume II) is reflected in the  $K_d$  values reported in the literature for U(VI) at various pH values.

It should also be noted that the adsorption of contaminants to soil may be totally to partially reversible. As the concentration of a dissolved contaminant declines in groundwater in response to some change in geochemistry, such as pH, some of the adsorbed contaminant will be desorbed and released to the groundwater.

### 2.2.3.1.1 Ion Exchange

One of the most common adsorption reactions in soils is ion exchange. In its most general meaning, an ion-exchange reaction involves the replacement of 1 ionic species on a solid phase by another ionic species from an aqueous solution in contact with the solid. As such, a previously sorbed ion of weaker affinity is exchanged by the soil for an ion in aqueous solution. Most metals in aqueous solution occur as charged ions and thus metal species adsorb primarily in response to electrostatic attraction. In the cation-exchange reaction:



$\text{Sr}^{2+}$  replaces  $\text{Ca}^{2+}$  from the exchange site, X. The equilibrium constant ( $K_{\text{ex}}$ ) for this exchange reaction is defined by the equation:

$$K_{\text{ex}} \rightleftharpoons \frac{\{\text{SrX(s)}\} \{\text{Ca}^{2\oplus}\}}{\{\text{CaX(s)}\} \{\text{Sr}^{2\oplus}\}} \quad (2.14)$$

There are numerous ion-exchange models and they are described by Sposito (1984) and Stumm and Morgan (1981). The original usage of  $K_d$ , often referred to as the thermodynamic  $K_d$ , is a special case of Equation 2.14. When one of the cations, such as Sr as the  $^{90}\text{Sr}$  contaminant, is present at trace concentrations, the amount of Ca on the exchange sites  $\text{CaX(s)}$  remains essentially constant, as does  $\text{Ca}^{2+}$  in solution. These two terms in Equation 2.14 can thus be replaced by a constant and

$$K_d \rightleftharpoons \frac{\{\text{SrX(s)}\}}{\{\text{Sr}^{2\oplus}\}} \quad (2.15)$$

The ranges of cation exchange capacity (CEC, in milliequivalents/100 g) exhibited by several clay minerals are listed in Table 2.4 based on values tabulated in Grim (1968).

### 2.2.3.2 Precipitation

The precipitation reaction of dissolved species is a special case of the complexation reaction in which the complex formed by 2 or more aqueous species is a solid. Precipitation is particularly important to the behavior of heavy metals (*e.g.*, nickel and lead) in soil/groundwater systems. As an example, consider the formation of a sulfide precipitate with a bivalent radionuclide cation ( $\text{M}^{2+}$ ):



**Table 2.4.** Cation exchange capacities (CEC) for several clay minerals (Grim, 1968).

Mineral	CEC (milliequivalents/100 g)
Chlorite	10 - 40
Halloysite · 2H <sub>2</sub> O	5 - 10
Halloysite · 4H <sub>2</sub> O	40 - 50
Illite	10 - 40
Kaolinite	3 - 15
Sepiolite-Attapulgite-Palygorskite	3 - 15
Smectite	80 - 150
Vermiculite	100 - 150

The equilibrium constant,  $K_{r,T}$ , corresponding to Equation 2.16 is:

$$K_{r,T} \square \frac{\{M(HS)_2(s)\}}{\{M^{2\oplus}\} \{HS^{\ominus}\}^2} \square \frac{1}{\{M^{2\oplus}\} \{HS^{\ominus}\}^2} \quad (2.17)$$

By convention, the activity of a pure solid phase is set equal to unity (Stumm and Morgan, 1981). The solubility product,  $K_{sp,T}$ , corresponding to dissolution form of Equation 2.16 is thus:

$$K_{sp,T} \square \{M^{2\oplus}\} \{HS^{\ominus}\}^2 . \quad (2.18)$$

Precipitation of radionuclides is not likely to be a dominant reaction in far-field (*i.e.*, a distance away from a point source) or non-point source plumes because the contaminant concentrations are not likely to be high enough to push the equilibrium towards the right side of Equation 2.16. Precipitation or coprecipitation is more likely to occur in the near field as a result of high salt concentrations in the leachate and large pH or pE gradients in the environment. Coprecipitation is the simultaneous precipitation of a chemical element with other elements by any mechanism (Sposito, 1984). The 3 broad types of coprecipitation are inclusion, absorption, and solid solution formation.

32

Solubility-controlled models assume that a known solid is present or rapidly forms and controls the solution concentration in the aqueous phase of the constituents being released. Solubility models are thermodynamic equilibrium models and typically do not consider the time (*i.e.*, kinetics) required to dissolve or completely precipitate. When identification of the likely controlling solid is difficult or when kinetic constraints are suspected, empirical solubility experiments are often performed to gather data that can be used to generate an empirical solubility release model.<sup>1</sup> A solubility limit is not a constant value in a chemically dynamic system. That is, the solubility limit is determined by the product of the thermodynamic activities of species that constitute the solid (see Equation 2.18). If the system chemistry changes, especially in terms of pH and/or redox state, then the individual species activities likely change. For example, if the controlling solid for plutonium is the hydrous oxide  $\text{Pu}(\text{OH})_4$ , the solubility product,  $K_{sp}$ , (as in Equation 2.18) is the plutonium activity multiplied by the hydroxide activity taken to the fourth power, *i.e.*,  $\{\text{Pu}\}\{\text{OH}\}^4 = \text{solubility product}$ . The solubility product is fixed, but the value of  $\{\text{Pu}\}$  and  $\{\text{OH}\}$  can vary. In fact, if the pH decreases 1 unit ( $\{\text{OH}\}$  decreases by 10), then for  $K_{sp}$  to remain constant,  $\{\text{Pu}\}$  must increase by  $10^4$ , all else held constant. A true solubility model must consider the total system and does not reduce to a fixed value for the concentration of a constituent under all conditions. Numerous constant concentration (*i.e.*, empirical solubility) models are used in performance assessment activities that assume a controlling solid and fix the chemistry of all constituents to derive a fixed value for the concentration of specific contaminants. The value obtained is only valid for the specific conditions assumed.

When the front of a contaminant plume comes in contact with uncontaminated groundwater, the system enters into nonequilibrium conditions. These conditions may result in the formation of insoluble precipitates which are best modeled using the thermodynamic construct,  $K_{sp}$  (*i.e.*, the solubility product described in Equation 2.18). Precipitation is especially common in groundwater systems where the pH sharply increases. Additionally, soluble polymeric hydroxo solids of metallic cations tend to form as the pH increases above 5 (Morel and Hering, 1993). At pH values greater than 10, many transition metals and transuranic hydroxide species become increasingly more soluble. The increase in solubility results from the formation of anionic species, such as  $\text{Fe}(\text{OH})_4^-$ ,  $\text{UO}_2(\text{CO}_3)_2^{2-}$ , or  $\text{UO}_2(\text{CO}_3)_3^{4-}$ . A demonstration calculation of the solubility of U(VI) as a function of pH is given in Chapter 5. As the pH of the plume decreases from values greater than 11 to ambient levels below approximately pH 8, some metal hydroxo solids, such as  $\text{NpO}_2(\text{s})$  and  $\text{Fe}(\text{OH})_3(\text{s})$ , may precipitate. The solubility behaviors of the contaminants included in the first phase of this project are discussed in detail in the geochemistry background sections in Volume II of this report.

---

<sup>1</sup> An empirical solubility release model is a model that is mathematically similar to solubility, but has no identified thermodynamically acceptable controlling solid.

## 2.3 Sorption Models

### 2.3.1 Constant Partition Coefficient ( $K_d$ ) Model

The constant partition coefficient,  $K_d$ , is a measure of sorption and is defined as the ratio of the quantity of the adsorbate (*i.e.*, metal or radionuclide) adsorbed per unit mass of solid to the quantity of the adsorbate remaining in solution at equilibrium. For the reaction



the mass action expression for  $K_d$  (typically in units of ml/g) is

$$K_d \rightleftharpoons \frac{A_i}{C_i} \quad (2.20)$$

where  $A$  = free or unoccupied surface adsorption sites,  
 $C_i$  = total dissolved adsorbate remaining in solution at equilibrium ( $\mu\text{g/ml}$ ), and  
 $A_i$  = adsorbate on the solid at equilibrium ( $\mu\text{g/g}$ ).

Describing the  $K_d$  in terms of this simple reaction assumes that  $A$  is in great excess with respect to  $C_i$  and that the activity of  $A_i$  is equal to 1. The  $K_d$  term is valid only for a particular adsorbent and applies only to those aqueous chemical conditions (*e.g.*, adsorbate concentration, solution/electrolyte matrix, temperature) in which it was measured. Also inherent in the  $K_d$  term are the assumptions that the system is reversible and is independent of the adsorbate concentration in the aqueous phase.

Essentially all of the assumptions associated with the thermodynamically defined  $K_d$  value (Equation 2.20) are violated in the common protocols used to measure  $K_d$  values for use in contaminant transport codes. Typically, the  $K_d$  for a given adsorbent is determined in the laboratory using soil from the study area and actual or simulated groundwater to which an adsorbate is added at some trace concentration. The values of  $C_i$  and  $A_i$  are operationally defined as the adsorbate concentrations measured in the fractions that passed through or were retained by, respectively, filtration by some known filter pore size, such as 0.45- $\mu\text{m}$  diameter. An important practical limitation of the measurement of  $K_d$  values is that the total concentration or radioactivity of the adsorbate is measured, thereby treating the adsorbate as a single species. This assumption is not an inherent requirement, but it is generally applied for convenience. A hypothetical example of the species measured in a neptunium  $K_d$  experiment are presented in Equation 2.21:

$$K_d \rightleftharpoons \frac{\sum_{i=1}^n \{ \text{NpO}_2\text{X}(s) \} \rightleftharpoons \{ \text{NpO}_2\text{Y}(s) \} \rightleftharpoons \{ \text{NaNpO}_2(\text{CO}_3)(s) \} \rightleftharpoons \{ \text{Na}_3\text{NpO}_2(\text{CO}_3)_2(s) \} \rightleftharpoons \dots}{\sum_{i=1}^n \{ \text{NpO}_2^{\square} \} \rightleftharpoons \{ \text{NpO}_2(\text{OH})_2^{\square} \} \rightleftharpoons \{ \text{NpO}_2(\text{OH})^{\square}(\text{aq}) \} \rightleftharpoons \{ \text{NpO}_2(\text{CO}_3)_2^{2\square} \} \rightleftharpoons \dots} \quad (2.21)$$

where { } indicate activity, and X and Y are 2 different mineral species. The solid phase in this example contains 4 solid neptunium species, including the species adsorbed to species X and Y and the species precipitated as  $\text{NaNpO}_2(\text{CO}_3)$  and  $\text{Na}_3\text{NpO}_2(\text{CO}_3)_2$ . The dissolved phase in this example contains 4 neptunium species including  $\text{NpO}_2^+$ ,  $\text{NpO}_2(\text{OH})_2^-$ ,  $\text{NpO}_2(\text{OH})^-$  (aq), and  $\text{NpO}_2(\text{CO}_3)_2^{2-}$ . Using common laboratory techniques, experimentalist would not be able to measure the concentrations of each of these dissolved and solid phases. Consequently, the experimentalist can not distinguish between adsorbed and precipitated species. In this example, there are more than just 1 dissolved and sorbed species, thereby violating an important assumption underlying the  $K_d$  value. Furthermore, many solutes have been observed to sorb more readily than desorb from mineral or organic surfaces, a phenomena referred to as hysteresis.

In chemistry, the term conditional  $K_d$  is often used (Jenne, 1977) to identify experimentally derived partition coefficients that may not necessarily denote an equilibrium value or require some of the other assumptions inherent in the more rigorous use of the  $K_d$  term. The definition of conditional  $K_d$  is given in Equation 2.22:

$$\text{Conditional } K_d = \frac{\sum A_i}{\sum C_i} \quad (2.22)$$

where  $A_i$  = sorbed species  
 $C_i$  = dissolved species.

Compared to Equation 2.20, Equation 2.22 more clearly represents the example represented by Equation 2.21. No attempt will be made in this text to distinguish between the true thermodynamic and the conditional  $K_d$ .

An important limitation of the constant  $K_d$  model is that it does not address sensitivity to changing conditions. If the groundwater properties (e.g., pH and solution ionic strength) change, a different  $K_d$  value should be used in the model. This limitation will be discussed further in Section 2.2.3.2.

Chemical retardation,  $R_r$ , is defined as,

$$R_r = \frac{v_p}{v_c} \quad (2.23)$$

where  $v_p$  = velocity of the water through a control volume  
 $v_c$  = velocity of contaminant through a control volume.

The chemical retardation term does not equal unity when the solute interacts with the soil; almost always the retardation term is greater than 1 due to solute sorption to soils. In rare cases, the retardation factor is actually less than 1, and such circumstances are thought to be caused by anion exclusion (Section 2.8). To predict the effects of retardation, sorption processes must be described in quantitative terms. The  $K_d$  provides such a quantitative estimate. Knowledge of the  $K_d$  and of media bulk density and porosity for porous flow, or of media fracture surface area, fracture opening width, and matrix diffusion attributes for fracture flow, allows calculation of the retardation factor. For porous flow with saturated moisture conditions, the  $R_f$  is defined as

$$R_f = 1 + \frac{\rho_b}{n_e} K_d \quad (2.24)$$

where  $\rho_b$  = porous media bulk density (mass/length<sup>3</sup>)  
 $n_e$  = effective porosity of the media at saturation.

For 1-dimensional advection-dispersion flow with chemical retardation, the transport equation can be written as

$$\frac{\partial C_i}{\partial t} = \frac{1}{R_f(i)} \left[ D_x \frac{\partial^2 C_i}{\partial x^2} - v_x \frac{\partial C_i}{\partial x} \right] \quad (2.25)$$

where  $C_i$  = concentration of contaminant species I in solution (mass/length<sup>3</sup>),  
 $D_x$  = dispersion coefficient of species I (length<sup>2</sup>/time),  
 $v_x$  = pore velocity of groundwater (length/time), and  
 $R_f(i)$  = retardation factor for species i.

For simplicity, radioactive decay has been omitted from Equation 2.25.

When the  $K_d$  term is incorporated into the retardation factor,  $R_f$ , as in Equation 2.24, the  $R_f$  term is also devoid of sorption mechanism, *i.e.*, adsorption, absorption, or precipitation can not be distinguished from one another as the mechanism by which the contaminants partitioned to the solid phase. Furthermore, incorporating the  $K_d$  term into the  $R_f$  term assumes implicitly that the reactions go to equilibrium and are reversible and that the chemical environment along the solute flow path does not vary in either space or time (Muller *et al.*, 1983). Although these assumptions rarely hold true in the natural environment, single-value model parameters are generally employed, with the justification that the approach builds conservatism into the analysis. Additionally, the paucity of geochemical data at most sites precludes a more rigorous conceptual model (Section 2.3.3).

### 2.3.2 Parametric $K_d$ Model

Clearly, the greatest limitation of using  $K_d$  values to calculate retardation terms (Equation 2.24) is that it describes solute partitioning between the aqueous and solid phases for only 1 set of environmental conditions. Such homogeneity does not exist in nature and therefore greatly compromises the usefulness of the constant. For example, when the aqueous phase chemistry was varied, americium  $K_d$  values in a Hanford sediment ranged from 0.2 to 53 ml/g, roughly a 200-fold range (Delegard and Barney, 1983). Additional variability in the americium  $K_d$  values, albeit less, were observed when slightly different Hanford sediments were used: 4.0 to 28.6 ml/g (Delegard and Barney, 1983: Solution 1). Using similar aqueous phases but diverse soils, Sheppard *et al.* (1976) measured americium  $K_d$  values ranging from 125 to 43,500 ml/g.

Another practical conceptual model for adsorption is called the parametric  $K_d$  model. The  $K_d$  value in this model varies as a function of empirically derived relationships with aqueous and solid phase independent parameters. Thus, it has the distinct advantage of being more robust and removes the burden of determining new  $K_d$  values for each environmental condition. Because the value of a  $K_d$  term is a function of a large number of variables, it is common to systematically vary several parameters simultaneously in 1 experimental study. Factorial design strategies are most often invoked to determine the systematic change resulting from varying the independent variables on the dependent variables, typically the partition coefficient (Box and Behnken, 1960; Cochran and Cox, 1957; Davies, 1954; Plackett and Burman, 1946). Statistical methods commonly used to derive quantitative predictor equations include standard linear or nonlinear regression (Snedecor and Cochran, 1967), stepwise regression (Hollander and Wolfe, 1973), and adaptive-learning networks (Mucciardi *et al.*, 1979, 1980). All these techniques have been used to develop empirical relationships describing  $K_d$  values in terms of other variables (Routson and Serne, 1972; Serne *et al.*, 1973; Routson *et al.*, 1981; Delegard and Barney, 1983).

The empirical predictor equations commonly take the form of a nonlinear polynomial expression. For example, after evaluating solutions consisting of several sodium salts, organic chelates, and acids, Delegard and Barney (1983) derived with the following expression for an americium  $K_d$  value:

$$\text{Log } K_d (\text{Americium}) = 2.0 + 0.1[\text{NaOH}] + 26.8[\text{HEDTA}] + 153.4[\text{HEDTA}]^2 \quad (2.26)$$

Numerous salts were found to have no significant effect on americium  $K_d$  values and therefore were not included in the expression. Delegard and Barney (1983) also evaluated higher exponential and logarithmic terms and determined that these terms did not improve the predictive capabilities of the expression (*i.e.*, the regression coefficients were not significant at  $P \leq 0.05$ ).

It is critical that parametric  $K_d$  equations, such as Equation 2.26, be used to calculate  $K_d$  values for systems only within the range of the independent variables used to create the equation. In the case of Equation 2.26, the range of independent variables used to generate the model were selected to simulate a plume emanating from a steel-lined concrete tank that contained strong

caustic and high sodium contents. Using Equation 2.26 to generate americium  $K_d$  values for a plume low in pH and sodium concentrations would not be appropriate.

These types of statistical relationships are devoid of causality and therefore provide no certain information on the mechanism by which the radionuclide partitioned to the solid phase, whether it be by adsorption, absorption, or precipitation. For example, the statistical analyses may suggest a very strong relationship between pH and the  $K_d$  term, when the actual sorption process may be controlled by iron oxide adsorption. Because pH and the surface charge of iron oxides are covariants, a statistical relationship could be calculated, suggesting that sorption is solely caused by pH.

The parametric  $K_d$  model can be used in the retardation factor term (Equation 2.24) and the transport equation (Equation 2.25). When used in the transport equation, the code must also keep track of the current value of the independent variables (*e.g.*, [NaOH] and [HEDTA])<sup>1</sup> for the examples described in Equation 2.26) at each point in space and time to continually update the concentration of the independent variables affecting the  $K_d$  value. Thus, the code must track many more parameters, and some numerical solving techniques (*e.g.*, closed-form analytical solutions) can no longer be used to perform the integration necessary to solve for contaminant concentration. Generally, computer codes that can accommodate the parametric  $K_d$  model use a chemical subroutine to update the  $K_d$  value used to determine the  $R_f$ , when called by the main transport code. The added complexity in solving the transport equation with the parametric  $K_d$  sorption model and its empirical nature may be the reasons this approach has been used sparingly.

### 2.3.3 Isotherm Adsorption Models

Some adsorption studies are conducted in a systematic fashion to evaluate the effects of various parameters on  $K_d$ . The results of a suite of experiments evaluating the effect of contaminant concentration on adsorption, while other parameters are held constant, are called an "adsorption isotherm." For soils, it is common knowledge that contaminant adsorption can deviate from the linear relationship required by the  $K_d$  construct discussed in Section 2.3.1. If it was possible to keep increasing the amount of contaminant in solution contacting soil, all adsorption sites would become saturated at some contaminant concentration and the linear relationship between contaminant adsorbed to contaminant in solution would no longer hold. Isotherm models are used to describe the case where sorption relationships deviate from linearity. For many short-lived radionuclides, the mass present never reaches quantities large enough to start loading surface adsorption sites to the point that the linear  $K_d$  relationship is not accurate. However, long-lived radionuclides and stable elements, such as RCRA-regulated metals, can be found in leachates and groundwaters near waste sources at concentrations large enough to affect the saturation of surface adsorption sites.

---

<sup>1</sup> HEDTA is N-(2-hydroxyethyl) ethylenediaminetetraacetic acid.

In situations where the amount of contaminant loaded on the available adsorption sites is large enough to impact the linear adsorption construct, isotherm models are often invoked. Three adsorption isotherm models used frequently are the Langmuir, Freundlich, and Dubinin-Radushkevich models.

The Langmuir model was originally proposed to describe adsorption of gas molecules onto homogeneous solid surfaces (crystalline materials) that exhibit one type of adsorption site (Langmuir, 1918). Many investigators have tacitly extended the Langmuir adsorption model to describe adsorption of solution species onto solid adsorbents including heterogeneous solids such as soils. The Langmuir model for adsorption is

$$A_i = \frac{K_L A_m C_i}{1 + K_L C_i} \quad (2.27)$$

where  $A_i$  = amount of adsorbate adsorbed per unit mass of solid  
 $K_L$  = Langmuir adsorption constant related to the energy of adsorption  
 $A_m$  = maximum adsorption capacity of the solid  
 $C_i$  = equilibrium solution concentration of the adsorbate.

Substituting  $1/B$  for  $K_L$ , one obtains

$$A_i = \frac{A_m C_i}{B + C_i} \quad (2.28)$$

A plot of values for  $A_i$  (y-axis) versus values of  $C_i$  (x-axis) passes through the origin and is nearly linear at low values of  $C_i$ . As  $C_i$  increases,  $A_i$  should approach  $A_m$ . Taking the reciprocal of Equation 2.28 and multiplying both sides of the equation by  $A_i A_m$  yields

$$A_i = \frac{A_i}{A_m} = B \frac{A_i}{C_i} + A_m \quad (2.29)$$

Then, by plotting  $A_i$  on the y-axis and  $(A_i/C_i)$  on the x-axis, one can determine the value of  $-B$  from the slope of the best fit line and the value of  $A_m$  from the intercept. Sposito (1984) and Salter *et al.* (1981a) cite several instances where the Langmuir isotherm has successfully fit trace adsorption by natural substrates. Further Sposito (1984) and Salter *et al.* (1981b) discuss modifications of the Langmuir model to accommodate 2 distinct sites and competition of 2 adsorbates (the nuclide and the ion it replaces on the adsorbent) which further extend this conceptual model's usefulness on natural substrates. In the parlance of Giles *et al.* (1974) [also see Sposito (1984)], the Langmuir adsorption isotherm is the L-curve. For L-curve isotherms, the initial slope of  $A_i$  (amount of solute adsorbed per unit mass of solid) [plotted on the y-axis] versus  $C_i$  (equilibrium solution concentration of the adsorbate) [plotted on the x-axis] is large, but the slope decreases as  $C_i$  increases. This forms the concave shaped curve shown in Figure 2.2. The various curves depicted in Figure 2.2 are discussed in greater detail later in this section.

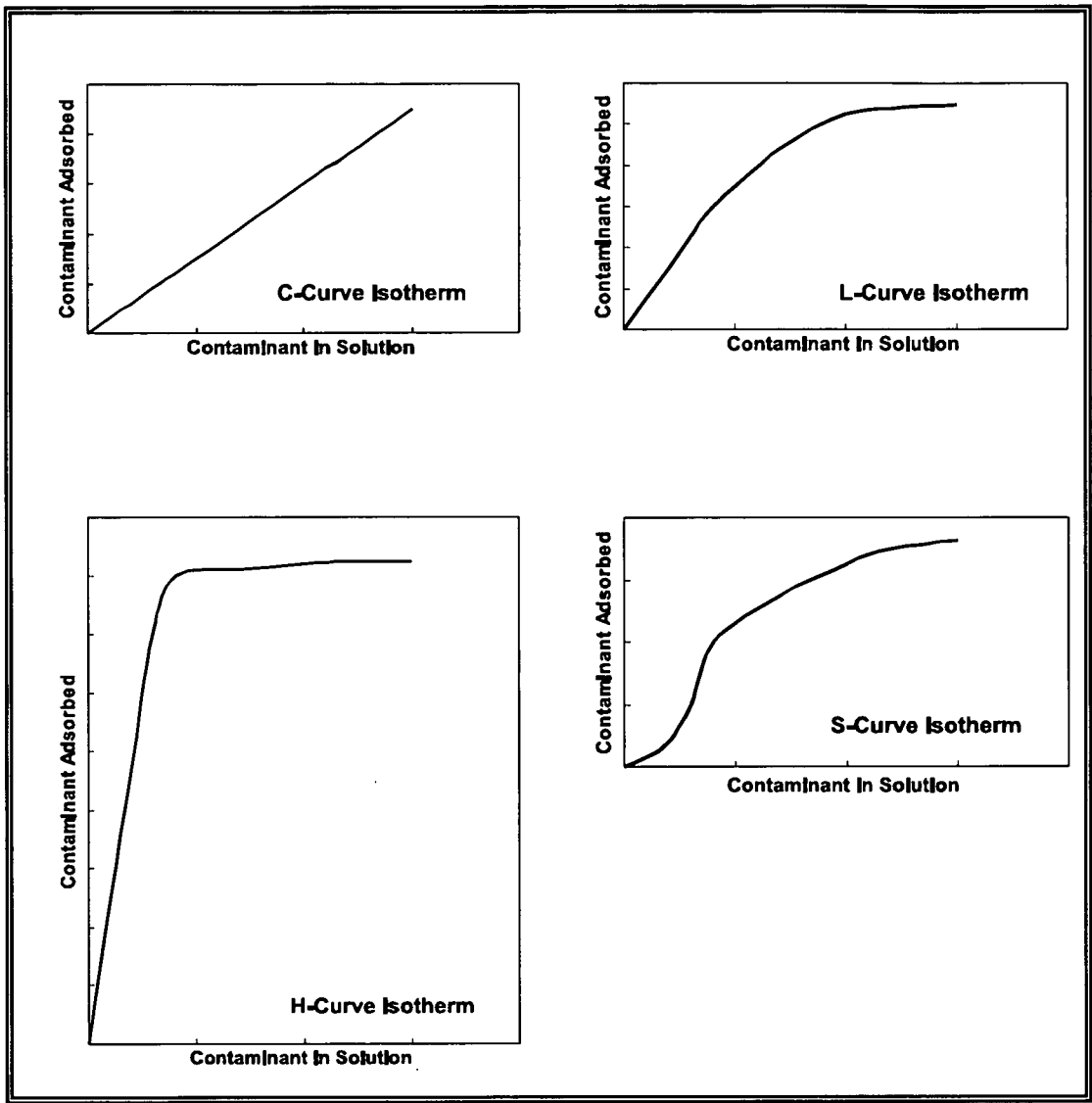


Figure 2.2. Four types of adsorption isotherm curves shown schematically in parlance of Giles *et al.* (1974).

40

The Freundlich isotherm model (Freundlich, 1926) is defined as:

$$A_i = K_F C_i^N \quad (2.30)$$

where  $A_i$  = amount of adsorbate adsorbed per unit mass of solid  
 $C_i$  = equilibrium solution concentration of the adsorbate  
 $K_F$  = Freundlich adsorption constant  
 $N$  = constant.

The Freundlich equation is sometimes written with the exponent in Equation 2.30 being  $1/N$  instead of  $N$ . The Freundlich model does not account for finite adsorption capacity at high concentrations of solute, but when considering trace constituent adsorption, ignoring such physical constraints is usually not critical. The Freundlich isotherm can be transformed to a linear equation by taking the logarithms of both sides of Equation 2.30:

$$\log A_i = \log K_F + N \log C_i \quad (2.31)$$

When  $\log A_i$  is plotted on the y-axis and  $\log C_i$  on the x-axis, the best-fit straight line has a slope of  $N$ , and  $\log K_F$  is its intercept. When  $N=1$ , the Freundlich isotherm, represented by Equation 2.31 reduces to a linear relationship. Because  $A_i/C_i$  is the ratio of the amount of solute adsorbed to the equilibrium solution concentration (the definition of  $K_d$ ), the Freundlich  $K_F$  is equivalent to the value of  $K_d$ .

Because adsorption isotherms at very low solute concentrations are often linear, either the Freundlich isotherm with  $N$  equaling 1 or the Langmuir isotherm with  $K_L \cdot C_i$  much greater than 1 fits the data. The value of  $N$  for the adsorption of many radionuclides is often significantly different from 1, such that nonlinear isotherms are observed. In such cases, the Freundlich model is a better predictor than the Langmuir model. Sposito (1984) shows how the Freundlich isotherm is equivalent to the Langmuir isotherm where the parameter  $K_F$  is log normally distributed. Sposito (1984) also stresses that the Freundlich isotherm only applies to data obtained at low values of  $C_i$  (concentration of contaminant in the equilibrium solution).

A third adsorption model that has been used recently in nuclide studies is the Dubinin-Radushkevich isotherm (Dubinin and Radushkevich, 1947). This model is applicable for the adsorption of trace constituents. Should the adsorbent surface become saturated or the solute exceed its solubility product, the model is inappropriate. The Dubinin-Radushkevich model is more general than the Langmuir model, because it does not require either homogeneous adsorption sites or constant adsorption potential. Its mathematical form is

$$A_i = A_m e^{-K_{DR} Q^2} \quad (2.32)$$

where  $A_i$  = observed amount of adsorbate adsorbed per unit mass  
 $A_m$  = sorption capacity of adsorbent per unit mass

- $K_{DR}$  = Dubinin-Radushkevich adsorption constant  
 $\beta$  =  $RT \ln(1 + 1/C_i)$   
 $R$  = gas constant  
 $T$  = temperature (in Kelvin)  
 $C_i$  = equilibrium solution concentration of the adsorbate.

The Dubinin-Radushkevich equation can be transformed to

$$\ln A_i - \beta \ln A_m = K_{DR} \beta^2 \quad (2.33)$$

A plot of  $\ln A_i$  (y-axis) versus  $\beta^2$  (x-axis) allows the estimation of  $\ln A_m$  as the intercept and  $-K_{DR}$  as the slope of the resultant straight line. Ames *et al.* (1982) successfully used this model to describe adsorption of uranium and cesium onto basalt and its weathering products.

All 3 isotherm models can be compared against data from experiments that systematically vary the mass of a trace constituent or radionuclide while holding all other parameters as constant as possible. It is important to consider the total mass of the element present, including all stable and other radioactive isotopes, when evaluating isotherms. It is incorrect to calculate isotherms based on only one isotope if the system includes several (both stable and radioactive) for a particular element. For convenience, isotherm experiments tend to consider only the total concentration or radioactivity content and thus lumps all species for a given isotope.

It can be argued that all 3 isotherm models are based on physicochemical processes or mechanisms. If the experiments are performed and characterized rigorously to assure equilibrium conditions and constancy of variables aside from the trace constituent concentration, then the resultant isotherm constants undoubtedly have some relationship to adsorption capacities and to site adsorption energies. On the other hand, any suite of experiments that can be plotted as amount adsorbed versus amount in solution at the time of measurement can also be analyzed using these models to see whether predictive equations can be determined. The latter empirical approach is a step up in sophistication over the constant  $K_d$  model.

Giles *et al.* (1974) state that isotherm shapes are largely determined by the adsorption mechanism, and thus can be used to explain the nature of adsorption. The S-curve (Figure 2.2) is explained by Giles *et al.* (1974) as adsorption where the presence of the individual solute molecules bound to the solid interact with each other. This increases the strength of the individual solute bonds to the solid surface when the solid has low contaminant loading. Thus, for a brief period during adsorption, the first bound molecules enhance adsorption of the next molecules that bind to the solid. The slope of the isotherm increases from the lowest concentration of contaminant where surface coverage is so sparse that adsorbed molecules cannot interact. At some point, the sites become laden with contaminant and the slope of the adsorption isotherm starts decreasing again. Sposito (1984) gives another plausible explanation for the S-curve, wherein complexing solution ligands compete with the surface sites for the contaminant until the complexing ligands are

complexed with the contaminant and additional contaminant is free to adsorb with less or no complexant competition.

The L-curve (Figure 2.2) is the classical Langmuir curve where the loading of contaminant on the solid starts to decrease the adsorption slope as sites become saturated. The adsorption of many RCRA-regulated metals and long-lived radionuclides on soils have been successfully described by Langmuir isotherms. Giles *et al.* (1974) shows that the L-shaped curve is found for systems where the activation energy for the adsorption/desorption of each adsorbate is unaffected by the other adsorbates and solvent (water) in the systems. Rai and Zachara (1984) include one compilation of Langmuir isotherms for RCRA-regulated metals.

The H-curve (Figure 2.2) is an extreme version of the L-curve isotherm. The H-curve describes adsorption of "high-affinity" adsorbates onto solid adsorbents. The activation energy of the desorption of the analyte of interest is much larger than other species in the solution.

The C-curve (constant slope) (Figure 2.2) suggests that the number of available sorption sites remains constant throughout the whole range of solute concentrations (whereas the  $K_d$  model applies to low solute concentrations) or the available surface expands proportionally with the amount of material adsorbed up to the point where all adsorption sites are filled. Giles *et al.* (1974) discuss two conceptual models on how the available sorption sites can expand in proportion to the adsorbed mass. The model where the adsorbent is microporous and the adsorbate has a much higher affinity for the adsorbent surfaces than the water is most germane for soils. The adsorbates enter the microporous solid and act like a molecular wedge to open up more sorption sites through continued penetration.

It is difficult to assess whether one should put much weight on isotherm shape constructs discussed by Giles *et al.* (1974) as a vehicle to elaborate on adsorption mechanisms. The number of discrete crystalline minerals and amorphous phases and coatings present in soils as well as the multitude of inorganic and organic ligands found or expected in soil solutions combine to make a quantitative description of contaminant adsorption and the controlling mechanisms a formidable activity. To quote Sposito (1984, pg. 122), "The adherence of experimental sorption data to an adsorption isotherm provides no evidence as to the actual mechanism of the sorption process in soils and sediments." We value this statement and suggest that isotherms are just one step more sophisticated than the constant  $K_d$  construct in delineating or quantifying adsorption of contaminants.

It must be stressed that isotherm models, as expressed by Equations 2.27, 2.30, and 2.32, explicitly consider dependency of the partition coefficient on only the solution concentration of the contaminant of interest. Isotherm models do not consider dependence on other solid and solution parameters that can influence adsorption, such as those discussed in Volume II for each contaminant of interest.

The incorporation of adsorption isotherm models into transport codes is relatively easy. Each of the aforementioned isotherm equations can be rearranged to calculate a partition coefficient,  $K_d$ , that is a function of  $C$ , the solution concentration of the radionuclide, and 1 or 2 constants. As the transport model solves for  $C$ , substitution of an equation that depends only upon  $C$  (and derivable constants) for the  $K_d$  in the retardation factor (see Equations 2.23 and 2.24) should be straightforward. For simple cases, analytical closed-formed solutions are possible, or numerous numerical approximation schemes can be used. Thus, with little additional work or increases in computer storage requirements, most transport codes can be formulated to predict radionuclide migration with an adsorption isotherm model. It should be repeated, however, that this approach accounts for the dependency of  $K_d$  on only one parameter, the concentration of the radionuclide. If the mass of contaminant in the environment is low, and complicating factors such as complexing agents and type S sorption behavior are not expected, all 3 adsorption isotherms discussed above are readily simplified to the constant  $K_d$  model.

### *2.3.4 Mechanistic Adsorption Models*

Mechanistic models explicitly accommodate for the dependency of  $K_d$  values on contaminant concentration, competing ion concentration, variable surface charge on the adsorbent, and solute species solution distribution. Incorporating mechanistic, or semi-mechanistic, adsorption concepts into transport models is attempted because the models become more robust and, perhaps more importantly from the standpoint of regulators and the public, scientifically defensible. However, less attention will be directed to these adsorption models because we judge them of little practical use for the majority of site-screening applications. The complexity of installing these mechanistic adsorption models into existing transport codes is difficult to accomplish. Additionally, mechanistic adsorption models also require a more intense and costly data collection effort than will likely be available to the majority of EPA, DOE, and NRC contaminant transport modelers and site remediation managers. A brief description of the state of the science is presented below. References to excellent review articles have been included in the discussion to provide the interested reader with additional information.

Experimental data on interactions at the mineral-electrolyte interface can be represented mathematically through 2 different approaches: (1) empirical models and (2) mechanistic models. An empirical model can be defined as a mathematical description of the experimental data without any particular theoretical basis. For example, the  $K_d$ , Freundlich isotherm, Langmuir isotherm, Langmuir Two-Surface Isotherm, and Competitive Langmuir construct are considered empirical models by this definition (Sposito, 1984). Mechanistic models refer to models based on thermodynamic concepts such as reactions described by mass action laws and material balance equations. Four of the most commonly used mechanistic models include the Helmholtz, Gouy-Chapman, Stern, and Triple Layer models (Sposito, 1984). The empirical models are often mathematically simpler than mechanistic models and are suitable for characterizing sets of experimental data with a few adjustable parameters, or for interpolating between data points. On the other hand, mechanistic models contribute to an understanding of the chemistry at the interface and are often useful for describing data from complex multicomponent systems for

which the mathematical formulation (*i.e.*, functional relationships) for an empirical model might not be obvious. Mechanistic models can also be used for interpolation and characterization of data sets in terms of a few adjustable parameters (Westall, 1986). However, it is important to realize that adjustable parameters are required for both mechanistic and empirical models, except the  $K_d$  model. The need to include adjustable parameters in order to apply/solve mechanistic models compromises their universal application.

Any complete mechanistic description of chemical reactions at the mineral-electrolyte interface must include a description of the electrical double layer (Figure 2.1). While this fact has been recognized for years, a satisfactory description of the double layer at the mineral-electrolyte interface still does not exist. Most electrical double layer models were written for specific conditions and are only accurate under limited environmental conditions. For instance, the Stern model is a better model for describing adsorption of inner-sphere complexes, whereas the Gouy-Chapman model is a better model for describing outer-sphere or diffuse swarm adsorption (Sposito, 1984; Westall, 1986) (Figure 2.1).

Truly mechanistic models are rarely, if ever, applied to complex natural soils (Schindler and Sposito, 1991; Sposito, 1984; Westall and Hohl, 1980; Westall, 1986; Westall, 1994). The primary reason for this is because the surfaces of natural mineral are very irregular and difficult to characterize. These surfaces consist of different microcrystalline structures and/or coatings of amorphous phases that exhibit quite different and complex chemical properties when exposed to solutions. Thus, examination of the surface by virtually any experimental method yields only averaged characteristics of the surface and the interface. Parsons (1982) discussed the surface chemistry of single crystals of pure metals and showed that the potential of zero charge of different crystal faces of the same pure metal can differ by over 400 mV. For an oxide surface, this difference was calculated by Westall (1986) to be energetically equivalent to a variation in the pH of zero-point-of-charge ( $\text{pH}_{\text{zpc}}$ ) of more than 6 pH units. This example indicated that an observable macroscopic property of a polycrystalline surface might be the result of a combination of widely different microscopic properties and that characterizations of these surfaces will remain somewhat operational in nature.

Another fundamental problem encountered in characterizing reactions at the mineral-electrolyte interface is the coupling between electrostatic and chemical interactions, which makes it difficult to distinguish the effects of one from the effects of the other. Westall and Hohl (1980) have shown that many models for reactions at the mineral-electrolyte interface are indeterminate in this regard.

#### ***2.4 Effects of Unsaturated Conditions on Transport***

The major pathway for contaminant transport in arid areas is through unsaturated soils. Although considerable effort has been expended over the past few years to quantify the mobility of contaminants and determine factors that influence contaminant mobility, little work has been done to investigate the transport of radionuclides under conditions of partial saturation.

45

At unsaturated moisture conditions, the pores are partially filled with air and water. The water in the pores is partly held in place by attractive forces of capillarity. A key hydrologic measurement in unsaturated (vadose zone) soils is the soil-water matric potential (or suction). Matric potential is defined as, the amount of work that must be done per unit of soil solution in order to transport, reversibly and isothermally, an infinitesimal quantity of water from a pool of soil solution at a given elevation above the water table (and at atmospheric pressure) to the soil pores at the same elevation and pressure (SSSA, 1997). When the work (or energy) is expressed on a weight basis, the matric potential is expressed in units of length (*i.e.*, m or cm). Matric potential is always negative (*i.e.*, energy is gained in going from a saturated solution to unsaturated soil pores, because of adsorptive forces and capillarity of porous material). Matric suction is the absolute value of matric potential and is used for convenience to express the matric forces (potentials) as positive values. By definition, at the water table, both the matric potential and matric suction are zero.

Unsaturated flow properties include the unsaturated hydraulic conductivity and the water retention characteristics (relationship between water content and matric suction values). Analogous to saturated flow where the advective flux<sup>1</sup> is the product of the saturated hydraulic conductivity and the gradient of the hydrostatic head,<sup>2</sup> the advective flow in unsaturated sediments is the product of the unsaturated conductivity and the matric potential (or suction) gradient. The suction gradient defines the direction of flow (from areas of low to high suction). At most vadose zone sites there have been no direct measurements of either the unsaturated conductivity or water retention characteristics for sediments. Generally only water contents have been measured (often by neutron logging) in boreholes or from split-spoon samples.

When the soil is saturated, nearly all pores are filled and hydraulic conductivity is at a maximum. As the soil becomes unsaturated, some of the pores become air-filled and the conductive cross-sectional areas are decreased. In addition, the first pores to empty are the largest and most conductive and tortuosity is increased for any water molecule that is still actively advecting through the porous media (*i.e.*, the water must find less direct pathways around these empty pores). In unsorted soils, the large pores that resulted in high conductivity at saturation become barriers to liquid flow between smaller pores during unsaturated flow. Hence, the transition from saturated to unsaturated flow may result in a steep drop in hydraulic conductivity of several orders of magnitude as the tension increase from 0 to 1 bar. At higher tensions (*i.e.*, more unsaturation), conductivity may be so low that steep pressure gradients are required for any appreciable soil water flow to occur. An interesting corollary of the pore size-conductivity relationship is that at, or near, saturation, a sandy soil conducts water more rapidly than a clay soil with many micropores. When the soils are unsaturated, however, many of the micropores in the clay soil remain filled, and consequently, the hydraulic conductivity in the clay soil does not decrease nearly as sharply as it does in sandy soil under the same tension. If the soil water does

---

<sup>1</sup> The flux density is the volume of water flowing through a cross-section area per unit time.

<sup>2</sup> The hydraulic gradient is the head drop per unit distance in the flow direction.

2/10

not move, then the contaminant in, or contacted by, the soil water does not move except by diffusion (Section 2.6), which is a relatively slow process (Rancon, 1973).

In modeling contaminant transport in unsaturated conditions, Equation 2.24 takes the form:

$$R_f = 1 + \frac{\theta}{\theta_b} K_d \quad (2.34)$$

where  $\theta$ , the volumetric water content of the soil ( $\text{cm}^3$  water/ $\text{cm}^3$  total), replaces  $n$  ( $\text{cm}^3$  void space/ $\text{cm}^3$  total), soil porosity, in Equation 2.24. Equation 2.27 explicitly assumes that the extent to which contaminants sorb to soils, the  $K_d$  value, is constant as a function of the volumetric water content. This relationship is convenient for modeling; however, its validity is not certain. There have been experiments to test this assumption, and the results have been mixed (Gee and Campbell, 1980; Knoll, 1960; Lindenmeier *et al.*, 1995; Nielsen and Biggar, 1961; Nielsen and Biggar, 1962; Routson and Serne, 1972).

There are theoretical reasons for believing that  $K_d$  values vary as a function of volumetric water content. First, as the soil becomes increasingly unsaturated there will be a smaller percentage of the total exchange sites in contact with the aqueous phase. For example, if only half of the exchange sites of a soil come into contact with the aqueous phase, then the effective exchange capacity of the soil is only half of that, had all the available exchange sites come into contact with the aqueous phase. Therefore, as less mineral surface is exposed to the aqueous phase, the lower the effective exchange capacity becomes because less of the surface is exposed to the solute of interest. On the other hand, the clay fraction of the soil constitutes the largest exchange capacity and smallest pore sizes. Because the smaller pores are involved in unsaturated flow, there may be little measurable effect on the exchange capacity of the soil in unsaturated conditions. Another reason for believing that  $K_d$  values would vary with degree of saturation is because in the unsaturated systems the aqueous phase is in closer contact with the soil surfaces. Solutes in the middle of large pores have less interaction with soil surfaces than solutes nearer to the soil surfaces. In unsaturated conditions, the middle of large pores tend to be empty, resulting in a greater percentage of pore water being in close contact with the soil surface. Finally, the ionic strength of the aqueous phase tends to increase closer to the clay surfaces. Thus, as a soil dehydrates, the system tends to have a higher ionic strength. The  $K_d$  value for many cations tends to decrease with increases in ionic strength.

The average size of individual pores is larger for coarse- versus fine-textured soils, despite the finer-grained soils having a larger total porosity. In saturated soil, all of the pore space is water-filled; the pores are continuous or "connected," and generally water conducting. As a saturated soil is desaturated, the larger pores drain first, and air becomes a barrier to water flow. Water flow in unsaturated soils may occur as film flow along the particle surface, or as "matrix flow" through smaller, water-filled pores. The unsaturated flow regime is expected to differ in unsaturated coarse- versus fine-textured soils, with film flow dominating the former, and matrix flow the latter. This conceptualizations is illustrated in Figure 2.3. Recent improvements in

imaging technologies [*i.e.*, magnetic resonance imaging (MRI) and X-ray microtomography] have increased our ability to directly distinguish the distribution of water, such as films at the particle surface, pendular water forming a meniscus at the intersection of two particles, and water held in small pores. Improved imaging of the water distribution in unsaturated soils is increasing fundamental understanding of the unsaturated flow regime.

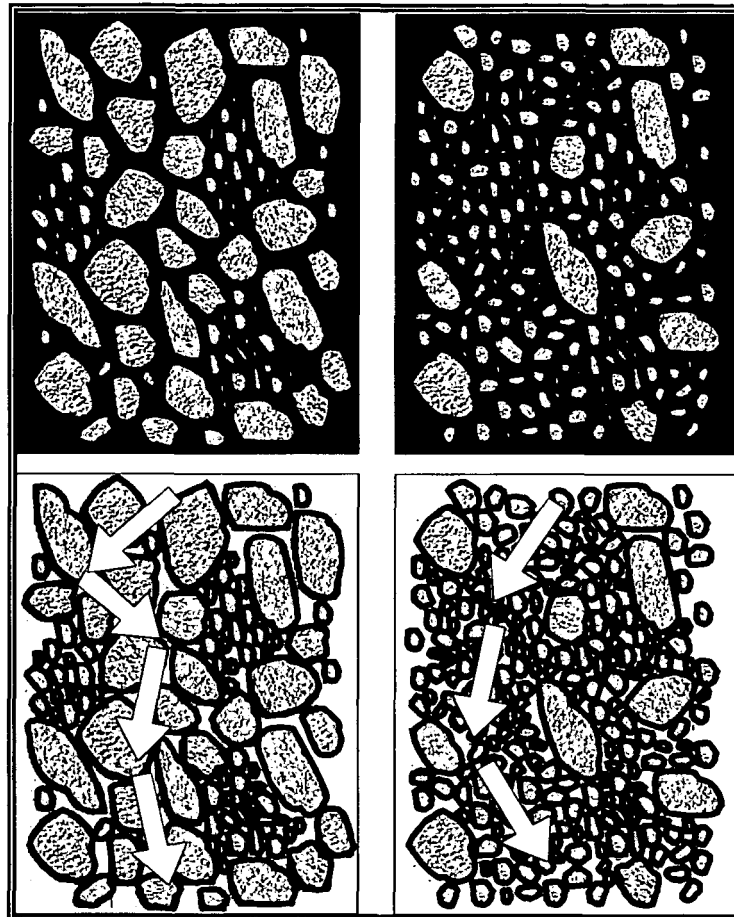


**Figure 2.3.** Schematic diagram for conceptual model of water distribution in saturated (top two figures) and unsaturated soils (bottom two figures) suggesting differences in the unsaturated flow regime (indicated by arrows) for soils with varying texture. [The two figures on left represent coarse-textured soils, whereas the two figures on the right represent fine-textured soils. Soil particles, air, and water are shown, respectively, in stippled gray, white, and black.]

As a soil is progressively desaturated, retained water is held with increasingly greater "suction," expressed as the matric or negative pressure potential. Hydraulic conductivity,  $K_h$  (m/sec) reflects the ease of water flow through the media and decreases with decreasing moisture saturation (*i.e.*, greater resistance to flow at lower water contents). Hydraulic conductivity is also highly dependent on soil texture. Relationships between hydraulic conductivity, matric potential, and water content are well-established (Hillel, 1998; Jury *et al.*, 1991). The spatial variability of hydraulic conductivity and the effect on solute transport in saturated soils have been the subject of modeling investigations (*e.g.*, Dagan, 1984; Gelhar and Axness, 1983; Tompson and Gelhar, 1990). Various modeling approaches are reviewed by Koltermann and Gorelick (1996) and compared to field data by Sudicky (1986). For unsaturated soils, research has focussed on scaling, and the effect of spatially variable hydraulic conductivity on water flow, infiltration, and drainage (Hopmans *et al.*, 1988; Nielsen *et al.*, 1973; Peck *et al.*, 1977; Warrick and Amoozegar-Fard, 1979).

In unsaturated soils, the pathway for water flow can become more tortuous, and water held in films and in small pores can be "disconnected" with respect to the flow regime. In reviewing water flow and transport in the vadose zone, Nielsen *et al.* (1986) noted that in addition to water held within aggregates, immobile water may exist in thin liquid films around soil particles, in dead-end pores, or as relatively isolated regions associated with unsaturated flow. Immobile water is also apparent in saturated systems. Most investigations that consider mass transfer between mobile and immobile water regions have been conducted in saturated systems.

Immobile water is manifest as hydraulic heterogeneity, and is typically characterized with a "dual porosity" or "two-region" model (Coats and Smith, 1964; Haggerty and Gorelick, 1995; van Genuchten and Wierenga, 1976). The liquid phase is partitioned into mobile and immobile (stagnant or micro-porosity) regions, where advective solute transport is limited to the mobile water phase. The mobile water fraction,  $\theta_m$ , is defined as the volume fraction of water associated with the mobile domain,  $\theta_m$ , relative to the total water content,  $\theta_v$  (*i.e.*,  $\theta_m = \theta_m / \theta_v$ ). Transport in and out of the immobile water domain is diffusion-limited. A small degree of hydraulic heterogeneity can be characterized by increased hydrodynamic dispersion (Pickens *et al.*, 1981).

However, a 2-region flow regime is required as the fraction of stagnant water increases. The importance of particle scale properties (Ball *et al.*, 1990), specifically mass transfer between mobile and immobile water regions (Haggerty and Gorelick, 1995), in affecting larger-scale transport has been noted. Compared to the standard advection-dispersion model with sorption, physical models accounting for mobile-immobile water described better reactive solute transport in a field-scale natural gradient tracer study (Goltz and Roberts, 1986), although other factors contributing to non-ideal behavior may also be important (Brusseau, 1994).

The development of heterogeneous unsaturated flow, in non-aggregated porous media was suggested in several studies comparing the transport of non-sorptive tracers at various degrees of moisture saturation (Biggar and Nielsen, 1962; Bond and Wierenga, 1990; Nielsen and Biggar, 1961). The fraction of immobile water increased from 4 to 40 percent when water content was

49

decreased from 71 to 55 percent moisture saturation in a disturbed sand column (Gaudet *et al.*, 1977). It is important to note one study with contrasting results where a decrease in dispersion (heterogeneity) was observed when moisture content was reduced from 100 to 97 and 93 percent (Jardine *et al.*, 1993). This was observed in undisturbed cores and the effect was attributed to the elimination of macropore flow for the slightly unsaturated conditions. Changes in hydraulic heterogeneity at lower water contents were not evaluated.

Recent studies of unsaturated sands (Gamerdinger *et al.*, 1998, Gamerdinger and Kaplan, 1999) confirmed the findings of Gaudet *et al.* (1977). The development of an increasing fraction of immobile water (*i.e.*, decreasing  $\theta_m$ ) is illustrated in Figure 2.4 for sandy soils (filled diamond and square symbols). Data for a fine-textured soil (loamy fine sand, represented by the filled triangle in Figure 2.4) with a high  $\theta_m$  is consistent with the conceptual model (above) that water held in the smaller pores of unsaturated fine-texture soils remains conductive.

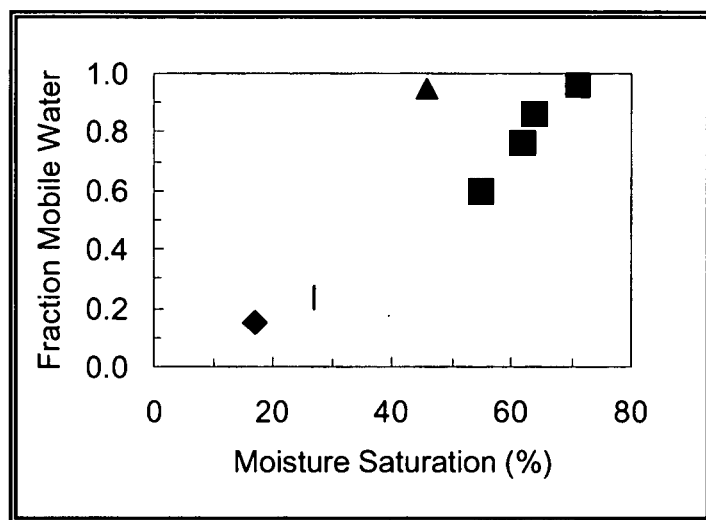


**Figure 2.4.** Development of hydraulic heterogeneity (decreasing  $\theta_m$ ) in unsaturated, non-aggregated soils with decreasing moisture saturation. [Filled diamond and square symbols represent data for sandy soils from Gamerdinger and Kaplan (1999) and Gaudet *et al.* (1977), respectively. The filled triangle symbol is data for finer-textured loamy fine sand from Bond and Wierenga (1990).]

50

The unsaturated flow regime is expected to differ in soils dominated by coarse-textured particles in contrast to those with fine-textured particles. As shown schematically in Figure 2.3, the flow regime will consist of film flow along the surfaces of large particles, versus matrix flow through small pores formed by fine particles. Hydraulic conductivity varies with soil texture and decreases with decreasing moisture saturation. Hydraulic heterogeneity resulting from a 2-region, mobile-immobile water, flow domain, increases in unsaturated soils. Limited data suggest a dependence on soil texture for non-aggregated soils where the heterogeneity is not apparent for saturated conditions.

In summary, the development of hydraulic heterogeneity in non-aggregated unsaturated soils has long been identified. However, the implications for the sorptive and transport behavior of contaminants are unknown. Current transport models account for lower, and spatially variable, hydraulic conductivity in unsaturated soils. Hydraulic heterogeneity resulting from mobile-immobile water domains has been considered when modeling transport in saturated systems. Fewer investigations have considered unsaturated systems.

### ***2.5 Effects of Chemical Heterogeneity on Transport***

In context of contaminant adsorption and transport, chemical heterogeneity refers in this report to the variability in particle surface reactivity. Iron oxide minerals are abundant in the subsurface environment and mineral coatings consisting of Fe(III)-oxides can be a significant source of reactivity for contaminant adsorption in a variety of soil systems [*e.g.*, Smith and Jenne (1991) as summarized by Tompson *et al.* (1996)]. The effect of chemical heterogeneity arising from spatially variable Fe(III)-oxide abundance has been considered in modeling the transport of cobalt (Brusseau and Zachara, 1993) and reactive transport of uranyl-citrate (Tompson *et al.*, 1996) and Co-EDTA (Szecsody *et al.*, 1998a, 1998b) complexes. Modeling studies of reactive solute transport in saturated systems have shown that chemical heterogeneities result in non-ideal transport behavior (Bosma *et al.*, 1993, Sugita *et al.*, 1995).

Different approaches for representing chemical heterogeneity (*i.e.*, spatial distribution of sorption sites) have been considered when combining processes in reactive flow and transport models for saturated systems (Szecsody *et al.*, 1998a, 1998b; Tompson *et al.*, 1996). The effect of a homogeneous versus a heterogeneous (spatially variable) distribution of reactive sites was compared in simulations of reactivity in batch (non-flowing) and column systems (Szecsody *et al.*, 1998b). While reactive site heterogeneity had a small effect in batch systems, it was highly significant in columns. A major conclusion was that particle-scale heterogeneities significantly influenced the interactions of sorptive (and reactive) solutes during advective flow (Szecsody *et al.*, 1998b).

51

### 2.5.1 Coupled Hydraulic and Chemical Heterogeneity

The absence of well-controlled laboratory investigations of contaminant transport in physically and chemically heterogeneous porous media has been noted (Brusseau and Zachara, 1993). The increased importance of particle scale heterogeneity in flowing versus non-flowing systems has implications for the advance from saturated to unsaturated solute transport. Variability in accessibility to reactive sites by mobile solutes is expected to increase with increased tortuosity. Predictive models that incorporate heterogeneity usually focus on reactive site abundance (Szecsody *et al.*, 1998a; Thompson *et al.*, 1996), although the length of Fe(III)-oxide inclusions has been considered (Szecsody *et al.*, 1998a). In an unsaturated soil, the distribution and abundance of reactive sites is considered to be the same as when the soil is saturated. However, the observed increase in hydraulic heterogeneity with decreased moisture saturation suggests greater variability in access to reactive sites, and thus an even greater significance of particle scale chemical heterogeneity during transport in unsaturated soils. Models which consider spatially variable reaction capacity and accessibility have been developed for saturated porous media flow (Reichle *et al.*, 1998).

Unsaturated systems have received less attention, with few investigations considering the combined effects of hydraulic and chemical heterogeneity. Russo (1989a,b) evaluated spatially variable hydraulic conductivity from a different perspective, considering the effect of solution properties on soil properties which included hydraulic conductivity and water content. The spatial variability of pesticide transport and sorption in unsaturated soil was evaluated in field, laboratory column, and batch experiments (Elabd *et al.*, 1986; Jury *et al.*, 1986). Although average  $K_d$  values from batch and column experiments were similar, there was no correlation between values measured in batch (non-flowing) and column systems (Jury *et al.*, 1986). For 18 of the 36 samples, retardation in laboratory columns with undisturbed field cores was greater than predicted from the batch  $K_d$  value (Elabd *et al.*, 1986). Non-sorptive tracer (*e.g.*, chloride) transport did not show the same degree of heterogeneity as the pesticides, suggesting sorption variability in addition to flow heterogeneity (Jury *et al.*, 1986). This research indicates that sorption during unsaturated transport is not accurately predicted from measurements in batch systems.

An important issue for modeling transport in a chemically heterogeneous system is the correlation between reactivity and other parameters that are used to characterize the medium. Correlations between reactivity and permeability (or hydraulic conductivity) are often used, but the appropriate form of the correlation for specific systems can be debated (Tompson *et al.*, 1996). Data to support specific correlations between particle size and particle surface reactivity are sparse. Consequently, approximate negative correlations are often used (Burr *et al.*, 1994; Tompson, 1993; Tompson *et al.*, 1996), or alternative possibilities of negative, positive, or no correlation are evaluated (Bosma *et al.*, 1993, 1996; Tompson, 1993;).

Experimental evidence for a negative correlation between particle size and the sorption of organic chemicals has been demonstrated (Barber *et al.*, 1992; Karickhoff *et al.*, 1979; Schwarzenbach and Westall, 1981). However, the findings of Ball *et al.* (1990) for the Canadian Forces Base

Borden Aquifer soils do not support this trend. A significant, but weak, correlation between strontium sorption and “ln  $K_h$ ” was observed for the Borden Aquifer soils (Robin *et al.*, 1991). Preferential sorption of strontium to the fine-textured soil fraction and with micaceous minerals of the coarsest fraction of Chalk River aquifer soils from Ontario, Canada was observed by Pickens *et al.* (1981).

The importance of grain scale properties in determining the sorption and transport of reactive solutes and the need for systematic study of factors that affect correlation for specific porous media and reactions is evident. Due to the increasing complexity of unsaturated systems, the success of simply extending relationships that are developed in saturated systems is questionable. Fundamental research in unsaturated systems with measurement of relevant parameters relating media properties to chemical heterogeneity and reactive transport is needed.

In summary, the relationships between soil texture, porosity, moisture saturation, hydraulic heterogeneity and sorption are complex. Hydraulic heterogeneity in unsaturated soils results from disconnectivity of pore water which can be caused by thin liquid films around soil particles, dead-end pores, or relatively isolated regions associated with unsaturated flow. The proportion of disconnected or immobile water increases with decreasing moisture saturation (Figure 2.4). The unsaturated flow regime is thought to depend on the soil texture, where film flow is more likely to dominate in unsaturated coarse-textured soils, and matrix flow through small pores prevailing in fine-textured soils.

## 2.6 Diffusion

The transport of matter in the absence of bulk flow is referred to as diffusion. The flux of matter due to diffusion is proportional to the concentration gradient and is a molecular process. In general terms, the flux,  $J_{ix}$ , of component I in the x direction is

$$J_{ix} = -D \frac{dC_i}{dx} \quad (2.35)$$

where  $D$  = proportionality constant or diffusion coefficient with the dimensions of length<sup>2</sup>/time  
 $C_i$  = concentration of constituent i.

The  $J_{ix}$  has the dimensions of moles/length<sup>2</sup>/time, and the negative sign indicates that flow of constituent I in the x direction is also in the direction of lower I concentration. In an infinitely dilute aqueous solution, the movement is quantified by the diffusion coefficient,  $D$ . For most simple aqueous species,  $D$  is about  $10^{-9}$  m<sup>2</sup>/s or  $10^{-5}$  cm<sup>2</sup>/s.

Atkinson (1983), Atkinson *et al.* (1986), and Atkinson and Nickerson (1988) present a useful conceptual model for describing the transport of contaminants through a porous media such as soil. The authors consider that the transport is a combination of both physical processes, such as diffusion, and chemical processes, such as precipitation/solubility and adsorption/desorption. In

the constrained geometry of a porous media, such as soil, the  $D$  is reduced compared to the  $D$  in free aqueous solution. The  $D$  for a species within a porous media is defined as  $D_p$  and is equal to

$$D_p = \frac{D}{\tau^2} \quad (2.36)$$

where  $\tau$  = constrictivity of the porous media  
 $\tau$  = tortuosity of the porous media.

For experimentalists, it is convenient to measure the average flux of a contaminant per unit area of the porous media in relation to the concentration gradient of the contaminant in the aqueous phase. The concentration gradient in the aqueous phase is influenced by the volume fraction of the void space in the porous media (the porosity,  $n_e$ ). This leads to another equation that defines the "intrinsic" diffusion coefficient,  $D_i$ :

$$D_i = D_p n_e = \frac{D n_e}{\tau^2} \quad (2.37)$$

A key assumption herein is that all the porosity in the porous media is interconnected and thus can contribute to diffusion of the contaminant. All three parameters, porosity ( $n_e$ ), constrictivity ( $\tau$ ), and tortuosity ( $\tau$ ), characterize the physical contribution to diffusion through the porous media.

The chemical contributions to diffusion can potentially be quite varied, such as ion exchange, specific adsorption, precipitation, and lattice substitution. If a very simple chemical process is assumed, reversible surface adsorption having fast kinetics and a linear isotherm (*i.e.*,  $K_d$ ), then diffusion of a reactive contaminant can be characterized by an apparent diffusion coefficient,  $D_a$ :

$$D_a = \frac{D_i}{\rho'} = \frac{D_p n_e}{\rho'} = \frac{D n_e}{\tau^2 \rho'} \quad (2.38)$$

where  $\rho'$  = capacity factor or ratio of the moles per unit volume of water-saturated solid,  $C_s$ , to the moles per unit volume of liquid,  $C_l$ .

The capacity factor is related to the  $K_d$  by the equation

$$\rho' = n_e \rho_b K_d \quad (2.39)$$

where  $\rho_b$  = dry bulk density of the porous media.

Also note that  $\rho'/n_e$  is the familiar retardation factor used in transport modeling:

$$\frac{\rho'}{n_e} = R_r = 1 + \frac{\rho_b K_d}{n_e} \quad (2.40)$$

It should be noted that these simple relationships are strictly only valid for reversible, linear adsorption reactions with fast kinetics. This point is often overlooked and should not be. Nevertheless, such simplifying assumptions allow for some interesting analysis of common laboratory data and experiments.

Equation 2.40 has been incorporated into the transport equation:

$$\frac{\partial C}{\partial t} = \frac{D}{R_f} \frac{\partial^2 C}{\partial x^2} \quad (2.41)$$

where  $R_f$  = retardation factor, as defined in Equations 2.23 or 2.24  
 $t$  = time.

Note that Equation 2.41, which is strictly for transport by diffusion, is similar to Equation 2.25, which describes contaminant migration due to advective flow.

Therefore, the apparent diffusion coefficients,  $D_a$ , for reactive constituents account for the chemical retardation as well as the physical hindrance to contaminant mobility caused by the small pore sizes and tortuosity of the soil.

## 2.7 Subsurface Mobile Colloids

### 2.7.1 Concept of 3-Phase Solute Transport

Contaminant transport models generally treat the subsurface environment as a 2-phase system in which contaminants are distributed between a mobile aqueous phase and an immobile solid phase (e.g., soil). Contaminants with a high affinity for sorbing to rock or vadose zone soils are assumed to be retarded relative to the rate of groundwater flow. However, an increasing body of evidence indicates that under some subsurface conditions, components of the solid phase may exist as colloids<sup>1</sup> that may be transported with the flowing water. Association of contaminants with this additional mobile phase may enhance not only the amount of contaminant that is transported, but also the rate of contaminant transport. Most current approaches to predicting contaminant transport ignore this mechanism not because it is obscure or because the mathematical algorithms have not been developed (Corapcioglu and Kim, 1995; Mills *et al.*, 1991), but because little information is available on the occurrence, the mineralogical properties, the physicochemical properties, or the conditions conducive to the generation of mobile colloids.

---

<sup>1</sup> A colloid is any fine-grained material, sometimes limited to the particle-size range of <0.00024 mm (*i.e.*, smaller than clay size), that can be easily suspended (Bates and Jackson, 1979). In its original sense, the definition of a colloid included any fine-grained material that does not occur in crystalline form. The geochemistry of colloid systems is discussed in detail in sources such as Yariv and Cross (1979) and the references therein.

There are 2 primary problems associated with studying colloid-facilitated transport of contaminants under natural conditions. First, it is difficult to collect colloids from the subsurface in a manner which minimizes or eliminates sampling artifacts. Sampling artifacts can arise when groundwater is pumped too rapidly, yielding particles that would otherwise remain immobile in the aquifer (Backhus *et al.*, 1993; McCarthy and Degueldre, 1993; Powell and Puls, 1993). Colloids may also be generated during sampling by exposing groundwater containing readily oxidizable metals, such as Fe(II), to atmospheric conditions and causing the precipitation of fine grain-sized hydrous oxide colloids (Backhus *et al.*, 1993; McCarthy and Degueldre, 1993; Ryan and Gschwend, 1990). Secondly, it is difficult to unambiguously delineate between the contaminants in the mobile-aqueous and mobile-solid phases (Buffle *et al.*, 1992; Degueldre *et al.*, 1989; McCarthy and Degueldre, 1993; Puls, 1990). Using ultrafiltration techniques to accomplish this goal is not entirely satisfactory because it provides only indirect evidence, is subject to a number of artifacts, and usually requires high analytical precision at very low contaminant concentrations (Buffle *et al.*, 1992; Danielsson, 1982; Degueldre *et al.*, 1989; McCarthy and Degueldre, 1993).

### 2.7.2 Sources of Groundwater Mobile Colloids

Subsurface mobile colloids originate from (1) the dispersion of surface or subsurface soils, (2) decementation of secondary mineral phases, and (3) homogeneous precipitation of groundwater constituents (McCarthy and Degueldre, 1993). First, colloidal particles can be dispersed and become mobile in aquifers as a result of changes in the groundwater chemistry, such as a decrease in ionic strength or changes in ionic composition from a calcium- to a sodium-dominated chemistry. The effect of sodium and ionic strength on colloid suspension stability is interactive such that the dispersive quality of sodium is enhanced at low salt levels (Kaplan *et al.*, 1996).

Geochemical or microbiological changes that result in dissolution of cementing phases, such as iron oxides and calcium carbonate can result in release of colloids. For example, Gschwend *et al.* (1990) observed 10 to 100 mg/l of silica colloids in groundwater receiving recharge from evaporation ponds and a fly ash basin. The infiltrate was enriched in carbon dioxide that dissolved the soil-cementing carbonate mineral, thus releasing the silica colloids. The third source of groundwater mobile colloids is homogeneous precipitation. Changes in groundwater geochemical conditions such as pH, major element composition, redox potential, or partial pressures of CO<sub>2</sub> can induce supersaturation and coprecipitation of colloidal particles. The precipitates can include major elements such as oxides of iron and manganese, calcium carbonates, and iron sulfides, as well as minor elements such as carbonates and sulfides of metals and radionuclides. Mobile colloid precipitates may form when soluble contaminants are introduced into a system resulting in their exceeding the solubility product. For example, Gschwend and Reynolds (1987) observed precipitation of ferrous phosphate colloids (1 to 10 mg/l of 100 nm-sized particles) down gradient of a sewage infiltration site. Solubility calculations suggested that the dissolved phosphate ions from the sewage and reduced iron in the aquifer exceeded the solubility product of ferrous phosphate, resulting in the formation of insoluble colloids. Other studies have documented the formation of iron oxide colloids in groundwater as a result of changes in pH and oxygenation that

56

caused the solubility limit of Fe(III) oxides to be exceeded (Liang *et al.*, 1993). Many strongly hydrolyzing radionuclides also form submicron-sized particles. Increases in solution pH have been shown to induce the formation of plutonium-, uranium-, and americium-oxide colloids in carbonate systems (Ho and Miller, 1986; Kim, 1986).

### 2.7.3 Case Studies of Mobile-Colloid Enhanced Transport of Metals and Radionuclides

Although the concept of colloid-facilitated transport is often invoked to account for anomalies between predicted and observed transport of contaminants, little field or experimental verification of this potentially important phenomenon is available (McCarthy and Degueldre, 1993). There have been a few field studies describing colloid-facilitated transport and these studies have provided only circumstantial evidence that this is in fact the actual mechanism responsible for the enhanced transport of contaminants (Buddemeier and Hunt, 1988; Degueldre *et al.*, 1989; Kaplan *et al.*, 1994a; Kaplan *et al.*, 1995a; Penrose *et al.*, 1990).

Although laboratory studies at Los Alamos National Laboratory (LANL) predicted that the movement of actinides in subsurface environments would be limited to less than a few meters, both americium and plutonium were detectable in monitoring wells as far as 3,390 m down gradient from the point source (Penrose *et al.*, 1990). Almost all of the americium and plutonium in the groundwater at the 3,390 m well were associated with colloids 0.025 to 0.45  $\mu\text{m}$  in diameter. Similarly, based on laboratory measurements using site-specific soils and a 2-phase solute transport code, americium, curium, plutonium, and uranium were expected to travel less than 10 m in the F-Area of the Savannah River Site; the contaminants were found associated with groundwater colloids 1,200 m away from the point source (Kaplan *et al.*, 1994a). To a lesser extent, chromium, copper, nickel, and lead were also detected directly on suspended groundwater particles collected from the F-Area study site (Kaplan, 1994b, 1995a). The reader is cautioned that, because most transport predictions do not account for preferred flow paths, the interpretation that colloid-facilitated migration is the best explanation for such enhanced migration is still being debated.

### 2.8 Anion Exclusion

Dissolved chloride, bromide, and nitrate are usually reported to travel through natural systems or soil columns at the same rate as, or faster than, water (James and Rubin, 1986; McMahon and Thomas, 1974). Anion exclusion, the mechanism by which anions move faster than water, occurs when the diffuse double layer, an extension of a particle's negative surface charge into the surrounding solution, repulses anions (Sposito, 1984). By excluding anions from the diffuse double layer, where water is relatively immobile, the system restricts anions to the faster moving pore water, resulting in an average rate of anion transport that is greater than the average pore water velocity defined by Darcy's Law (James and Rubin, 1986; McMahon and Thomas, 1974). Anion exclusion is more pronounced with higher cation exchange capacity (*i.e.*, negative charge) of the soil or rock. For example, smectites (CEC  $\approx$  3 meq/g) exhibit anion exclusion to a greater degree than do the kaolinite (CEC  $\approx$  0.2 meq/g) minerals (McMahon and Thomas, 1974).

The implication of anion exclusion for anionic contaminants (*e.g.*, nitrates, chloride, chromate, pertechnetate) and anionic complexes [*e.g.*,  $\text{UO}_2(\text{CO}_3)_2^-$ ] is that they may be able to travel through the subsurface at a rate greater than water. There is some indirect evidence that anion exclusion may exist for pertechnetate. In an unsaturated column study, pertechnetate breakthrough ( $C/C_0$ , 0.5) occurred at 0.95 pore volumes, whereas for tritium, a conservative tracer, breakthrough occurred at 1.02 pore volumes; that is, pertechnetate may have traveled 5 percent faster than tritium (Gee and Campbell, 1980). Chloride breakthrough in these columns occurred at 0.80 pore volumes, or 22 percent faster than tritium, providing evidence that the transport of chloride may be affected by anion exclusion.

## 2.9 Summary

The objective of this chapter is to present a primer on the key geochemical processes affecting contaminant transport in subsurface environments. References to important review articles and books are included for each of the major subject areas: aqueous geochemical processes, sorption, diffusion, subsurface mobile colloids, and anion exclusion. These processes are summarized in Table 2.5.

Particular attention is directed at describing the geochemical processes affecting chemical retardation. A brief discussion of mechanistic and semi-empirical adsorption models. Incorporating mechanistic and semi-mechanistic adsorption concepts into transport models is desirable because the models become more robust and scientifically defensible. However, mechanistic models are rarely, if ever, applied to field-scale problems. The reasons for this are the following: (1) mechanistic models require a more intense data collection effort than will likely be available to the majority of transport modelers, licensee requestors, or responsible parties; (2) installing these mechanistic adsorption models into existing transport codes is quite complex; and (3) mechanistic adsorption models require full characterization of the mineral surfaces, information that is impossible to obtain in natural heterogeneous soils. Importantly, these models provide a paradigm for using simpler models, such as the conditional  $K_d$  model.

Conditional  $K_d$  values can be derived from laboratory or field experiments. Unlike the thermodynamic  $K_d$  term, they are less rigorously defined in that the conditional  $K_d$  values are not necessarily limited to a single aqueous species and single solid phase. This broader definition lends itself more readily to natural systems, while at the same time resulting in several technical issues and complexities. The understanding of the important geochemical factors affecting the transport of the contaminants of interest is critical for site-specific calculations.

**Table 2.5.** Summary of chemical processes affecting attenuation and mobility of contaminants.

Process	Mechanism	Enhancement of Attenuation or Mobility of Contaminant?	Key Facts
Aqueous Complexation	Reaction where an aqueous molecular unit (ion) acts as a central group to attract and form a close association with other atoms or molecules	May enhance attenuation or mobility, depending on contaminant and geochemical conditions	<ul style="list-style-type: none"> <li><input type="checkbox"/> Function of pH and redox</li> <li><input type="checkbox"/> Complexation may lower the potential for adsorption and/or increase solubility, both of which can enhance potential for mobility</li> <li><input type="checkbox"/> Complexes may more readily bond to soils and thus retard migration</li> <li><input type="checkbox"/> Organic ligands from humic materials can be present in significant concentrations and dominate contaminant complexation in some systems</li> </ul>
Redox Reactions	Reaction where electrons are transferred completely from one species to another	May enhance attenuation or mobility, depending on contaminant and geochemical conditions	<ul style="list-style-type: none"> <li><input type="checkbox"/> Change in redox status changes aqueous speciation which may increase or decrease adsorption and solubility</li> <li><input type="checkbox"/> If redox status is sufficiently low to induce precipitation of sulfide minerals, reprecipitation of some contaminants may be expected</li> <li><input type="checkbox"/> More difficult to predict mobility of redox-sensitive species because many redox reactions are kinetically slow in natural groundwater, and several elements may never reach equilibrium between their various valence states</li> </ul>

Table 2.5. Continued.

Process	Mechanism	Enhancement of Attenuation or Mobility of Contaminant?	Key Facts
Adsorption and Ion Exchange	Special case of a complexation reaction where there is a net accumulation of a contaminant at the interface between a solid phase and an aqueous-solution phase; does not include the development of a 3-dimensional molecular structure	Enhances Attenuation	<ul style="list-style-type: none"> <li><input type="checkbox"/> Occurs primarily in response to electrostatic attraction</li> <li><input type="checkbox"/> Very dependent on pH and mineralogy</li> <li><input type="checkbox"/> Anion adsorption is greatest at low pH and decreases with increasing pH</li> <li><input type="checkbox"/> Cation adsorption is greatest at high pH and decreases with decreasing pH.</li> <li><input type="checkbox"/> Some contaminants may be present as cations or anions depending pH</li> <li><input type="checkbox"/> Totally-to-partially reversible; decline in contaminant concentration in groundwater may result in desorption and release of adsorbed contaminant to groundwater</li> <li><input type="checkbox"/> Likely key process controlling contaminant mobility in areas where chemical equilibrium exists</li> </ul>
Precipitation	Special case of a complexation reaction in which the complex formed by 2 or more aqueous species is a solid with 3-dimensional molecular structure	Enhances Attenuation	<ul style="list-style-type: none"> <li><input type="checkbox"/> Very dependent on pH and redox</li> <li><input type="checkbox"/> Totally-to-partially reversible; decline in contaminant concentration in groundwater may result in dissolution of precipitated contaminant to groundwater</li> <li><input type="checkbox"/> Likely process where chemical nonequilibrium exists, an area where high contaminant concentrations exist, or where steep pH and/or redox gradients exist</li> </ul>

60

Table 2.5. Continued.

Process	Mechanism	Enhancement of Attenuation or Mobility of Contaminant?	Key Facts
Diffusion	Molecular process of transport of matter in the absence of bulk flow	Enhances Mobility	<ul style="list-style-type: none"> <li><input type="checkbox"/> Flux of matter due to diffusion is proportional to concentration gradient</li> </ul>
Subsurface Colloids	Contaminants associated with suspended fine-grained material (smaller than clay size) that may be transported with flowing groundwater	Enhances Mobility	<ul style="list-style-type: none"> <li><input type="checkbox"/> Little information on occurrence, mineralogical and physicochemical properties, or conditions conducive to the generation of mobile colloids</li> <li><input type="checkbox"/> May originate from the dispersion of soils, decementation of secondary mineral phases, and/or precipitation of groundwater constituents</li> <li><input type="checkbox"/> Difficult to collect colloids from subsurface in a manner that minimizes or eliminates sampling artifacts</li> <li><input type="checkbox"/> Difficult to unambiguously delineate between the contaminants in the mobile-aqueous and mobile-solid phases</li> </ul>
Anion Exclusion	Occurs when the diffuse double layer, an extension of a particle's negative surface charge into the surrounding solution, repulses anions	Enhances Mobility	<ul style="list-style-type: none"> <li><input type="checkbox"/> By excluding anions from the diffuse double layer, where water is relatively immobile, anions restricted to the faster moving pore water, resulting in an average rate of anion transport greater than the average pore water velocity defined by Darcy's Law</li> <li><input type="checkbox"/> more pronounced with higher cation exchange capacity (<i>i.e.</i>, negative charge) of the soil or rock</li> </ul>

61

### 3.0 Methods, Issues, and Criteria for Measuring $K_d$ Values

#### 3.1 Introduction

The partition (or distribution) coefficient,  $K_d$ ,<sup>1</sup> is a measure of sorption of contaminants to soils and is defined as the ratio of the quantity of the adsorbate adsorbed per unit mass of solid to the amount of the adsorbate remaining in solution at equilibrium. It is the simplest, yet least robust model available. There are 5 general methods used to measure  $K_d$  values: laboratory batch method, *in-situ* batch method, laboratory flow-through (or column) method, field modeling method, and  $K_{oc}$  method. Each method has advantages and disadvantages, and perhaps more importantly, each method has its own set of assumptions for calculating  $K_d$  values from experimental data. Consequently, it is not only common, but expected that  $K_d$  values measured by different methods will produce different values.

A number of issues exist concerning the measurement of  $K_d$  values and the selection of  $K_d$  values from the literature. These issues include: using simple versus complex natural geologic materials as adsorbents, field variability, the "gravel issue," the "colloid issue," and the particle concentration effect. Soils are a complex mixture containing solid, gaseous, and liquid phases. Each phase contains several different constituents. The use of simplified systems containing single mineral phases and aqueous phases with 1 or 2 dissolved species have provided valuable paradigms for understanding sorption processes in more complex, natural systems. However, the  $K_d$  values generated from these simple systems are generally of little value for importing directly into transport models. Values for transport models should be generated from materials from or similar to the study site. The "gravel issue" is the problem that transport modelers face when converting laboratory-derived  $K_d$  values based on experiments using the less than 2-mm fraction into values that can be used in systems containing particles greater than 2 mm in size. No standard methods exist to address this issue. The "colloid issue" was discussed previously in Section 2.7. Some investigators have observed that  $K_d$  values determined in the laboratory often decrease as the ratio of solid to solution used in the measurements increases. This particle concentration effect is puzzling, because a  $K_d$  value should not depend from a theoretical perspective on the solid-to-solution ratio. Investigators have offered several explanations involving physical/chemical processes and/or experimental artifacts for the observed dependency.

Spatial variability provides additional complexity to understanding and modeling contaminant retention to subsurface soils. The extent to which contaminants partition to soils often changes as field mineralogy and chemistry changes. Thus, a single  $K_d$  value is often not sufficient for an entire study site and should change as important environmental conditions change. It is therefore important to be able to identify and measure the effect of ancillary environmental parameters that influence contaminant sorption. Three approaches used to vary  $K_d$  values in transport codes are the  $K_d$  look-up table approach, the parametric  $K_d$  approach, and the mechanistic  $K_d$  approach.

---

<sup>1</sup> A list of acronyms, abbreviations, symbols, and notation is given in Appendix A. A list of definitions is given in Appendix B

67

The extent to which these approaches are presently used and the ease of incorporating them into flow models varies greatly.

The objective of this chapter is to provide an overview of the different methods of measuring and determining  $K_d$  values used in site-specific contaminant transport and risk assessment calculations. Issues regarding the selection of  $K_d$  values from the literature for use in screening calculations are discussed.

### 3.2 Methods for Determining $K_d$ Values

There are 5 methods of determining  $K_d$  values: (1) laboratory batch method, (2) *in-situ* batch method, (3) laboratory flow-through (or column) method, (4) field modeling method, and (5)  $K_{oc}$  method (EPA, 1991; Ivanovich *et al.*, 1992; Jackson and Inch, 1989; Johnson *et al.*, 1995; Karickhoff *et al.*, 1979; Landstrom *et al.*, 1982; Lyman *et al.*, 1982; Roy *et al.*, 1991; Serkiz *et al.*, 1994; Sposito, 1984; van Genuchten and Wierenga, 1986). Each method provides an estimate of the propensity of a contaminant to sorb to the solid phase. However, the techniques used and the assumptions underlying each method are quite different. Consequently,  $K_d$  values for a given system that were measured by different methods commonly have values ranging over an order of magnitude (Gee and Campbell, 1980; Relyea, 1982). This subsection will describe the different methods and compare their implicit and explicit assumptions.

The  $K_d$  model originates from thermodynamic chemistry (see detailed discussion in Chapter 2) (Alberty, 1987). It is a measure of sorption and is defined as the ratio of the quantity of the adsorbate adsorbed per gram of solid to the amount of the adsorbate remaining in solution at equilibrium. For the reaction



the mass action expression is the partition coefficient ( $K_d$ , ml/g):

$$K_d \rightleftharpoons \frac{A_i}{C_i} \quad (3.2)$$

- where  $A$  = concentration of free or unoccupied surface adsorption site on a solid phase (mol/ml),  
 $C_i$  = total dissolved adsorbate concentration remaining in solution at equilibrium (mol/ml or  $\mu\text{g/ml}$ ), and  
 $A_i$  = concentration of adsorbate on the solid at equilibrium (mol/g or  $\mu\text{g/g}$ ).

Equation 3.2 is valid only when  $A$  is in great excess with respect to  $C_i$  and the activity of  $A_i$  is equal to unity. For saturated conditions and non-polar organic constituents, sorption from the aqueous phase to the porous media of the subsurface can be treated as an equilibrium-partitioning

63

process when solute concentrations are low (*e.g.*, either  $\leq 10^{-5}$  molar, or less than half the solubility, whichever is lower) (EPA, 1989). Partitioning often can be described using the above linear isotherm.

Also inherent in the thermodynamic definition of the  $K_d$  term are the assumptions that the reaction is independent of the contaminant concentration in the aqueous phase and that the system is reversible, *i.e.*, that the desorption rate is equal to the adsorption rate. The thermodynamic  $K_d$  term describes a precisely defined system, including fixed pH and temperature, with one type of adsorption site,  $A$ , and one type of dissolved aqueous species,  $C_i$ . Although the thermodynamic  $K_d$  term is overly restrictive for use in natural heterogeneous systems, it provides an important paradigm to base empiricised  $K_d$  terms. The assumptions that need to be made to empiricise this construct vary between analytical methods.

### 3.2.1 Laboratory Batch Method

Batch studies represent the most common laboratory method for determining  $K_d$  values (ASTM, 1987; EPA, 1991; Roy *et al.*, 1991). Figure 3.1 illustrates an EPA (1991) procedure for measuring a batch  $K_d$  value. A well characterized soil of known mass ( $M_{sed}$ ) is added to a beaker. A known volume ( $V_w$ ) and concentration ( $C_0$ ) of an aqueous contaminant solution is added to the soil in the beaker. The beaker is sealed and mixed until sorption is estimated to be complete, typically 1 to 7 days. When possible, the person conducting the study should ascertain the actual time required to reach sorption equilibrium. The solutions are centrifuged or filtered, and the remaining concentration of the contaminant ( $C_i$ ) in the supernatant is measured. The concentration of adsorbate sorbed on the solid phase ( $A_i$ , sometimes noted as  $q_i$ ) is then calculated by Equation 3.3:

$$A_i \text{ or } q_i = \frac{V_w (C_0 - C_i)}{M_{sed}} \quad (3.3)$$

Equation 3.3 is used to calculate the numerator of the  $K_d$  term (Equation 3.2) and the denominator,  $C_i$ , of the  $K_d$  term is measured directly in the laboratory. Thus,

$$K_d = \frac{V_w (C_0 - C_i)}{M_{sed} C_i} \quad (3.4)$$

For organic compounds that can degrade into other compounds, it should be noted that the difference in solution concentrations in Equation 3.3 represents both adsorption and degradation. Therefore, the calculated  $K_d$  for organic compounds of this type can overestimate the amount of true adsorption. If container blanks are not included in the batch test matrix, adsorption of a contaminant to the container is included in the calculated  $K_d$ . Care must be taken when interpreting batch  $K_d$  test results.

64

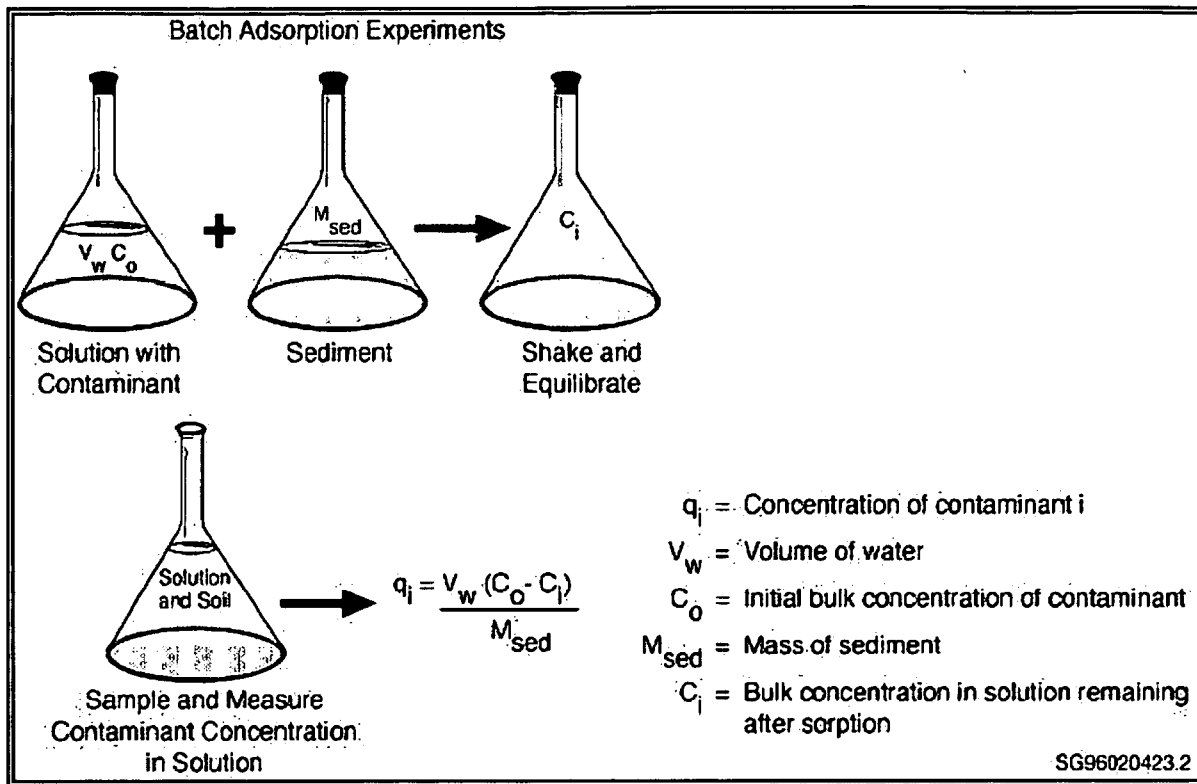


**Figure 3.1.** Procedure for measuring a batch  $K_d$  value (EPA, 1991).

It is important to note that the interpretation of results from batch  $K_d$  sorption tests generally allow no distinction to be made on how the sorbate (*i.e.*, contaminant) is associated with the sorbent (*i.e.*, soil). The sorbate may be truly adsorbed by ion exchange, chemisorption, bound to complexes that are themselves sorbed on the solid, and /or precipitated. If the  $K_d$  values are going to be used in transport calculations that already account for precipitation processes, it is imperative that the  $K_d$  values only include the decrease in dissolved concentrations of the sorbate due to adsorption. That is, the user must be certain that the experiments were performed correctly to prevent significant removal of the sorbate by precipitation reactions. Otherwise, the estimated retardation can be significantly overestimated.

There are several variations of this general procedure, each variation addressing the specific needs of the system. It is necessary to have some latitude in the method because of limits due to analytical chemistry considerations. For instance, for contaminants in which very low sorption is expected, a larger ratio of solid to liquid may increase the small difference in the term  $(C_0 - C_i)$ . Conversely, for contaminants in which high sorption is expected, a lower ratio of solid to liquid may be desirable. For gamma-ray emitting contaminants, it is possible to directly count the

65

activity on the equilibrated solid and in the solution, such that the  $K_d$  can be directly determined as opposed to relying on the difference in activity (*i.e.*, concentration) in the solution phase only.

One of the most common variations of the EPA method is to conduct a series of batch tests that are identical except for varying of the concentration of the dissolved contaminant,  $C_i$ . The  $K_d$  for the resulting isotherm is typically calculated from the slope of a  $C_i$  versus  $A_i$  plot. As discussed in Section 2.3.3, adsorption isotherm experiments are often conducted to evaluate the effect of contaminant concentration on adsorption, while other parameters are held constant. For soils, it is common knowledge that contaminant adsorption can deviate from the linear relationship required by the  $K_d$  construct. This approach obviously requires more work, but can provide a more accurate estimate.

Other variations of the batch  $K_d$  procedure deal with the ratio of solids to liquid, liquid composition, and contaminant concentration. A detailed description of a batch  $K_d$  procedure is included in Appendix C.

Contaminant transport modelers are often interested in the  $K_d$  value of a contaminant in a specific groundwater plume (*e.g.*, an acidic plume) in contact with a specific soil. In such a case, an experimenter would spike the contaminant into a representative groundwater, as opposed to pure water. Additionally, the experimenter would attempt to equilibrate the soils with the background aqueous solution (*e.g.*, the acidified groundwater) before bringing the soil in contact with the contaminant of interest. The reason for this latter step is to isolate the adsorption/desorption reaction of interest between the contaminant and soil. By pre-equilibrating the soil first with the acidic plume water (without the contaminants present), all the extraneous chemical reactions should be near equilibrium. Then, when the contaminant is added, its reaction is isolated.

The batch method is popular because the equipment, cost, and time requirements are low and the methodology is quite simple. However, the seemingly elementary operations mask numerous subtleties resulting in variability of data (EPA, 1991; Roy *et al.*, 1991; Serne and Relyea, 1981). One of the most comprehensive exercises to evaluate interlaboratory precision and identify important procedural details was conducted by 9 laboratories (Serne and Relyea, 1981). General guidelines on groundwater compositions, radionuclides, and procedural details were given to participants in this exercise. The measured  $K_d$  values were surprisingly varied for 2 of 3 contaminants investigated. As much as 3 orders of magnitude difference were determined in cesium ( $1.3 \pm 0.4$  to  $880 \pm 160$  ml/g) and plutonium ( $70 \pm 36$  to  $63,000 \pm 19,000$  ml/g). Conversely, the strontium  $K_d$  values measured in the 9 laboratories were within an order of magnitude of each other,  $1.4 \pm 0.2$  to  $14.9 \pm 4.6$  ml/g. Serne and Relyea (1981) concluded that the cause of the variability of the plutonium and cesium  $K_d$  values was due to: (1) method of tracer addition to solution, (2) solution-to-solid ratio, (3) initial tracer concentration in influent solution, (4) particle size distribution, (5) solid-solution separation method, (6) sample containers, and (7) temperature. The authors discussed in detail each of these parameters that are generally not controlled in batch  $K_d$  methods.

lele

Essentially all of the assumptions associated with the thermodynamic  $K_d$  value (Equation 3.2) are violated in the common batch  $K_d$  value. The natural soils used in these studies are not completely defined or quantified with respect to their mineralogy and organic phases. The background aqueous phases that are spiked with the adsorbate are typically not pure water and are rarely completely characterized, especially in the case when natural groundwater are used as the background aqueous phase. The background aqueous phases often contain the dominant electrolytes of the study site or actual uncontaminated groundwater from the study site, consisting of several dissolved and perhaps colloidal species. Furthermore, the sorption/desorption process of adsorbates from soils is typically not reversible, *i.e.*, hysteresis is observed, such that desorption occurs at a slower rate than sorption (Sposito, 1994). However, the batch  $K_d$  term can be of much greater value to the contaminant transport modeler than the thermodynamic value if the soil and the aqueous phase closely represent the natural system being modeled. Importantly, such a complex system, though not completely characterized, provides the best available estimate of the extent to which a sorbate partitions to a given soil in the presence of the electrolytes present in the experiment. This issue of measuring  $K_d$  values in complex- versus simple-systems is further discussed in Section 3.3.1.

One significant limitation inherent in the batch method is that commonly used analytical instruments can not differentiate between species of a given contaminant. For example, the atomic absorption (AA) spectrophotometer can measure total cadmium in the aqueous phase but can not identify each of its species [*e.g.*,  $\text{Cd}^{2+}$ ,  $\text{CdSO}_4^{\text{aq}}$ ,  $\text{CdCl}^-$ , *etc.*]. Multiple species typically exist in groundwater and the effect of their individual  $K_d$  values have a profound effect on the overall  $K_d$  value. For example, consider a system that consists of a contaminant or radionuclide with 2 equal concentration species that are kinetically slow at converting between each composition state; one with a  $K_d$  of 0 ml/g and the second with a  $K_d$  of 1,000 ml/g. The laboratory batch method would yield an intermediate  $K_d$  of about 30 ml/g in an experiment with a solution-to-solid ratio of 30. A demonstration calculation illustrating this issue is given in Figure 3.2. Using the  $K_d$  value 30 ml/g in subsequent mass transport calculations would not be conservative because 50 percent of the radionuclide would move at the speed of the carrier solution. For this reason, when there is any suspicion that multiple species with significantly differing  $K_d$  values may be present, a second sorption methodology, such as the flow-through method (Section 3.2.3), should be run to search for early breakthrough.

67

### Assumptions:

- Total concentration,  $C_0$ , of contaminant I in the original solution is 1,000 mg/ml.
- Batch test is performed with 1 g of clay soil contacting 30 ml of the original solution.
- The total concentration  $C_0$  is equally divided between two species, A and B, of contaminant I.
- The true  $K_d$  values for species A and B are 0 and 1,000 ml/g, respectively.
- Kinetic barriers exist that affect their interconversion between these two composition states over the time period of the test.

### Equations and Calculation:

Rearranging the equation

$$K_d \square \frac{V_w (C_0 \square C_i)}{M_{\text{sed}} C_i}$$

to solve for the concentration of species X of contaminant I ( $C_{Xi}$ ) (i.e.,  $C_{Ai}$  and  $C_{Bi}$ , where  $C_A$  and  $C_B$  at end of test), one gets

$$C_{Xi} \square \frac{C_{0,X} V_w}{K_{d,X} M_{\text{sed}} \square V_w}$$

For  $C_{Ai}$ , we know that there is no adsorption. Therefore,  $C_{Ai} = C_{0,A} = 0.5 \cdot C_0 = 500$  mg/ml.

For  $C_{Bi}$ , we calculate from the above equation for  $C_{Xi}$ :

$$C_{Bi} \square \frac{500 \times 30}{(1,000 \times 1) \square 30} \square \frac{15,000}{1,030} \square 14.56$$

$C_i$  for total solution is

$$C_{Ai} \square C_{Bi} \square 500 \square 14.56 \square 514.56$$

Therefore, if one does not realize that multiple contaminant species are present which do not rapidly interconvert, the overall  $K_d$  for the total contaminant would be

$$K_d \square \left( \frac{1,000 \square 514.56}{514.56} \right) \frac{30}{1} \square 28.30 \square 28$$

**Figure 3.2.** Demonstration calculation showing affect on overall  $K_d$  by multiple species that have different individual  $K_d$  values and are kinetically slow at interconverting between each composition state.

### 3.2.2 *In-situ* Batch Method

A method developed out of the desire to produce an *in-situ*  $K_d$  value has been used to a limited extent (Jackson and Inch, 1989; Johnson *et al.*, 1995; Landstrom *et al.*, 1982; McKinley and Alexander, 1993; Read *et al.*, 1991). The procedure used in this method is somewhat similar to that of the laboratory batch  $K_d$  method described in Section 3.2.1. A core sample containing a paired solid and aqueous phase is removed directly from an aquifer. The aqueous phase is separated from the solid phase by centrifugation or filtration and then analyzed for the solute concentration,  $C_i$ . The solid is then analyzed for the concentration of the contaminant associated with the solid phase,  $A_i$ .

Clearly, the advantage of this approach compared to the laboratory  $K_d$  method is that the precise solution chemistry and solid phase mineralogy is used for the modeling. Furthermore, the pore water removed from the core material may have had sufficient time to equilibrate and therefore true equilibrium may be attained. The disadvantages are somewhat less apparent but none the less appreciable. The concentration of most metal contaminants on the soil surfaces is typically quite low, in the mg/kg range. It should be noted moreover that the minimum detection limit for radionuclides on solid surfaces is even lower. The most common instruments available to measure metal concentrations on surfaces, energy dispersive x-ray analysis (EDX), or x-ray fluorescence, typically has detection limits in the order of 10,000 and 100 mg/kg, respectively. Another method of measuring  $A_i$  is to dissolve the solid phase with acid and then measure the resulting solution by inductively coupled plasma spectroscopy (ICP), inductively coupled plasma/mass spectroscopy (ICP/MS), and/or atomic adsorption spectroscopy (AA) techniques. This latter technique may provide a lower (*i.e.*, better) detection limit. In addition to the detection limit problem, it is not possible by any of these methods to distinguish between sorption and precipitation - processes which are treated quite differently in transport models. Furthermore, some trace metals are present in crystalline lattice sites of minerals present in soils. These molecules are not readily controlled by adsorption/desorption and should not be included in the  $q_i$  term. An in-depth discussion of the limitations of the *in-situ* batch method is presented by McKinley and Alexander (1993). For anthropogenic radionuclides present at trace levels, it is possible to assume that precipitation and lattice site contributions are nil and that the total mass/activity measured on the solid does represent adsorption/desorption-controlled molecules. In this scenario, a field *in-situ*  $K_d$  may be accurate.

One rather successful application of this technique was recently reported by Johnson *et al.* (1995). They compared laboratory and field batch  $K_d$  values of uranium along a transect through a pH gradient of pH 3.0 to 5.6. The field results yielded  $K_d$  values that ranged from 0.4 to greater than 15,000 ml/g for approximately 36 samples. The  $K_d$  values generated by the laboratory batch technique were generally lower, ranging from 0.08 to greater than 10,000 ml/g. The  $K_d$  values determined by both methods varied as a function of soil pH at the study site. When both sets of values were incorporated into a transport code, the results were not significantly different, *i.e.*, both methods were essentially equally good at predicting contaminant retardation in the study site.

### 3.2.3 Laboratory Flow-Through Method

The laboratory flow-through (or column) method of determining  $K_d$  values is the second most commonly used method (EPA, 1991; Relyea, 1982; Van Genuchten and Wierenga, 1986). A solution containing known amounts of a contaminant is introduced into a column of packed soil of known bulk density (*i.e.*, mass of soil per unit volume of column, g/ml) and porosity (*i.e.*, volume of pore space per unit volume of column, ml/ml) (Figure 3.3). The effluent concentration is monitored as a function of time. A known amount of a nonadsorbing tracer may also be introduced into the column and its time-varying concentration provides information about the pore-water velocity. The resulting data is plotted as a break-through curve (Figure 3.3). The velocity of each constituent (*i.e.*, tracer and contaminant) is calculated as the length of the column divided by the constituent's mean residence time.

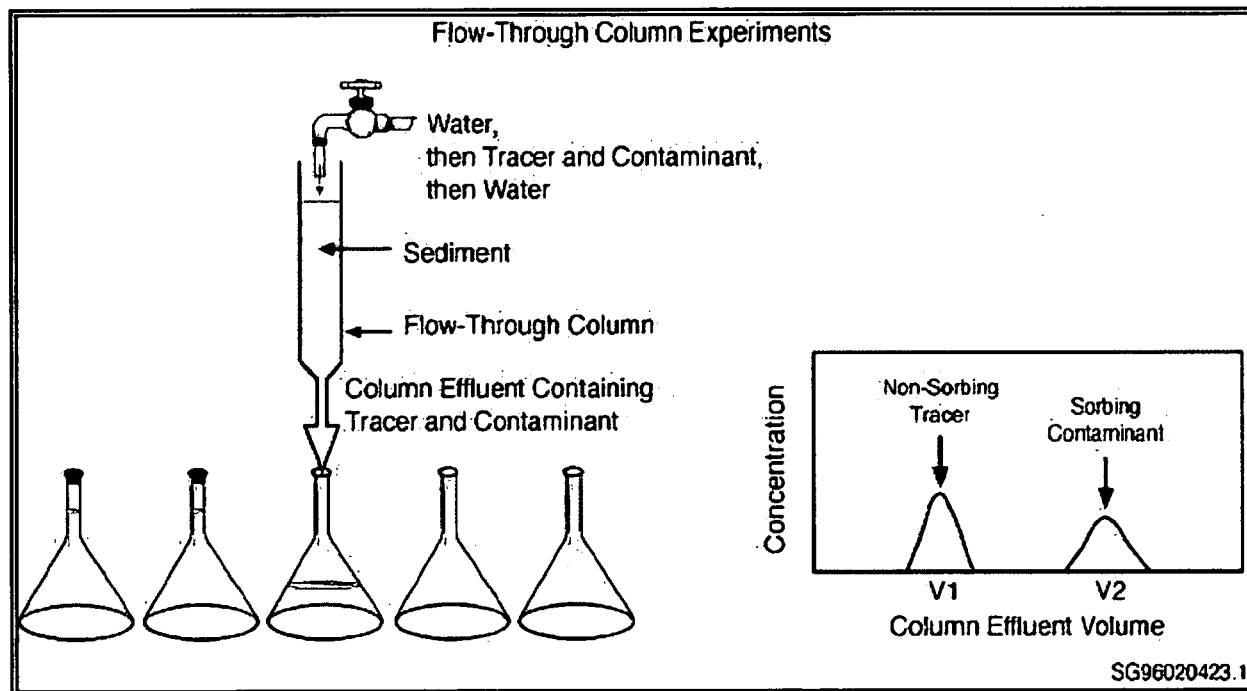


Figure 3.3. Procedure for measuring a column  $K_d$  value.

70

The mean residence time for a pulse input is calculated as follows (Relyea, 1982):

$$t_{\text{pulse}} = \frac{\int_{t_{\text{min}}}^{t_{\text{max}}} t C_i dt}{\int_{t_{\text{min}}}^{t_{\text{max}}} C_i dt} \quad (3.5)$$

where  $t_{\text{pulse}}$  = mean residence time for a pulse input (hr),  $t_{\text{max}}$  is the end of the break-through curve (hr),  
 $t_{\text{min}}$  = beginning of the break-through curve (hr),  
 $C_i$  = constituent concentration [(g or curies)/ml], and  
 $t$  = time (hr).

The relative concentrations of a constituent at the input source and in the effluent based on a pulse input are shown schematically in the top left and right of Figure 3.4. The mean residence time for a step (continual steady-state) input is calculated as follows:

$$t_{\text{step}} = \frac{\int_{C_{\text{min}}}^{C_{\text{max}}} t dC}{\int_{C_{\text{min}}}^{C_{\text{max}}} C_i dt} \quad (3.6)$$

where  $t_{\text{step}}$  = mean residence time for a step input/release (hr),  
 $C_{\text{max}}$  = maximum concentration measured in the effluent [(g or curies)/ml], and  
 $C_{\text{min}}$  = minimum concentration measured at the beginning of breakthrough [(g or curies)/ml].

When the effluent curve is ideal,  $t_{\text{step}}$  equals the time when the breakthrough curve reaches 0.5 or 50 percent breakthrough (*i.e.*,  $C/C_0=0.5$ ). The relative concentrations of a constituent at the input source and in the effluent based on a step input are shown schematically in the bottom left and right of Figure 3.4.

71

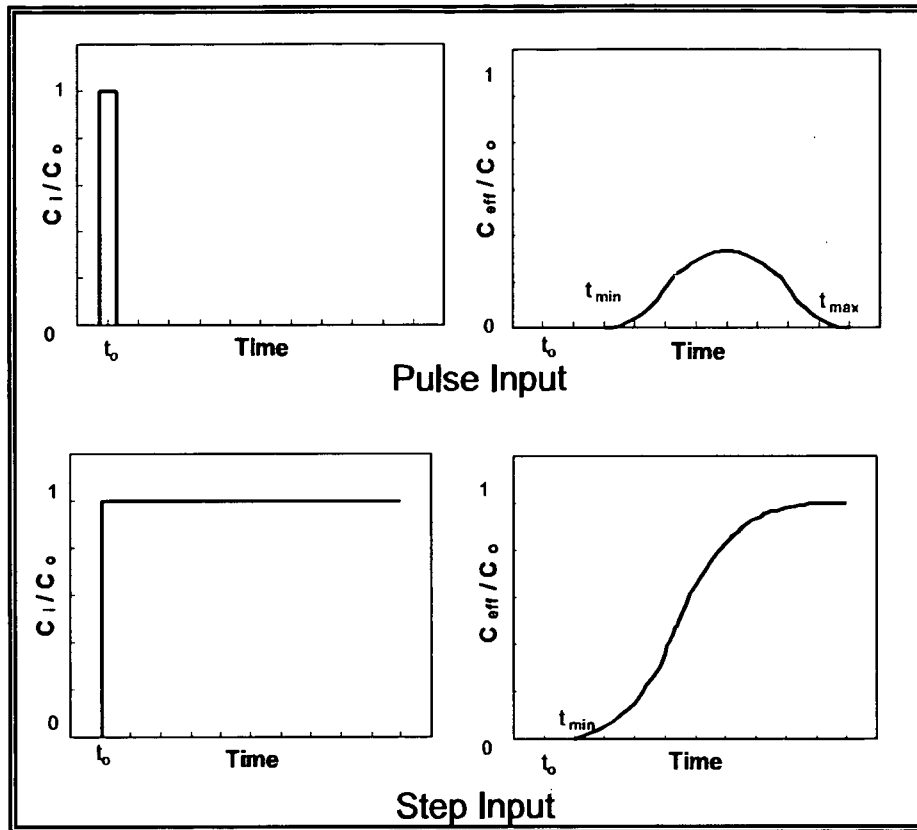


**Figure 3.4.** Schematic diagram showing the relative concentrations of a constituent at the input source (figures on left) and in the effluent (figures on right) as a function of time for a pulse versus step input. [ $C_o$ ,  $C_i$ , and  $C_{eff}$  refer, respectively, to the concentration of the constituent at  $t_0$  and the concentrations of the constituents in the input and effluent.]

The retardation factor ( $R_r$ ) is the ratio of the pore-water velocity ( $v_p$ , cm/hr) to the contaminant velocity ( $v_c$ , cm/hr):

$$R_r = \frac{v_p}{v_c} \quad (3.7)$$

The pore-water velocity is operationally defined as the velocity of the nonadsorbing tracer.

72

The  $K_d$  value can be calculated directly from the retardation factor ( $R_f$ ) and soil properties. Depending upon the environmental conditions in which the contaminant moves and interacts with the soil, the retardation factor can be correlated to the partition coefficient in a number of different ways. At least 4 formulations of the retardation factor have been proposed [see reviews in Bouwer (1991) and Whelan *et al.* (1987, 1996)]. These include the following:

$$R_f = \frac{n}{n_e} = \frac{K_d \rho_b}{n_e} \quad (3.8)$$

$$R_f = 1 + \frac{K_d \rho_b}{n_e} \quad (3.9)$$

$$R_f = 1 + \frac{K_d \rho_b}{n} \quad (3.10)$$

$$R_f = 1 + \frac{K_d \rho_b}{\rho} \quad (3.11)$$

where  $n$  = total porosity ( $\text{cm}^3$  pore/ $\text{cm}^3$  total volume),  
 $n_e$  = effective porosity ( $\text{cm}^3$  pore/ $\text{cm}^3$  total volume),  
 $\rho$  = volumetric water content in the vadose zone ( $\text{cm}^3$  water/ $\text{cm}^3$  total volume), and  
 $\rho_b$  = bulk density (g soil/ $\text{cm}^3$  total volume).

Total porosity is the ratio of the air/water volume to the total soil. The effective porosity differs from the total porosity in that the numerator is the volume of only those pore spaces that water can travel through, excluding such void volumes as exist within aggregates or dead-end pore spaces. Equation 3.10 was the original equation relating  $K_d$  to  $R_f$ . It was developed on an empirical basis for use in chemical engineering and was first applied to groundwater situations by Higgins (1959) and Baetslé (1967). Equations 3.8-3.11 were derived from the general transport equation, which is the differential equation describing solute concentration changes in relation to time, distance, dispersion coefficient, water velocity, soil bulk density, porosity, mass of solute per unit dry mass of soil, and degradation of solute (Bouwer, 1991).

Equation 3.8 assumes that the soil has 2 types of pore spaces, those that permit flow to occur ( $n_e$ ), and those pore spaces that do not permit flow to occur ( $n - n_e$ ). The contaminant in Equation 3.8 is assumed to migrate through the interconnected pore spaces, diffuse into dead-end pore spaces, and instantaneously adsorb to or desorb from the soil matrix where fluid is and is not flowing. Equation 3.8 also assumes that the solute concentration in the dead-end pore spaces is equivalent to the solute concentration in the free-flowing spaces. Equation 3.8 has the appearance of being more comprehensive than the other equations, but it does not allow the contaminant to travel with the same speed as the fluid (*i.e.*, nonadsorbing case), unless the total and effective porosities are equal. Experience has shown that Equation 3.8 does not adequately reflect real-world phenomena, suggesting deficiencies in our understanding of the geohydrochemical processes

impacting contaminant movement in the subsurface environment (Whelan *et al.*, 1987). Furthermore, in field studies, total porosity ( $n$ ) can be measured directly, whereas effective porosity ( $n_e$ ) can only be calculated from equations based on assumptions that are difficult to defend (Freeze and Cherry, 1979).

Equation 3.9 includes the same processes as Equation 3.8, except that the contaminant does not diffuse into the dead-end pore spaces. Many models use Equation 3.9 in their formulations. van Genuchten and Wierenga (1986) suggest the use of Equation 3.10. Equation 3.10 includes the same phenomena as Equation 3.9 except that the porous medium contains no dead-end pore spaces. Again, the merit of its use over Equation 3.9 is that the measurable parameter  $n$  is included in the formulation and not the calculated parameter  $n_e$ . Equation 3.8, 3.9, and 3.10 describe chemical retardation in the saturated zone, whereas Equation 3.11 describes chemical retardation in the unsaturated, or vadose, zone. As with Equation 3.10, contaminant transport and retardation in Equation 3.11 occurs only in the free-flowing pore space. Bouwer (1991) promotes the use of Equation 3.11 but defines the  $\theta$  term more generally as the water that is moving, whether in unsaturated or saturated conditions. In his derivation of Equation 3.11, Bouwer suggests that the  $\theta$  term also be used to quantify the mobile phases of water. Along with van Genuchten and Wierenga (1986), he also contends that the use of Equation 3.11 allows better distinction between retardation effects due to sorption and acceleration effects due to preferential flow or anion exclusion.

Flow-through column experiments are appealing in that they allow observation of contaminant migration rates in the presence of hydrodynamic effects (*e.g.*, dispersion, colloidal transport, *etc.*), and chemical phenomena (*e.g.*, multiple species, reversibility, *etc.*). Ideally, flow-through column experiments would be used exclusively for determining  $K_d$  values, but equipment costs, time constraints, experimental complexity, and data reduction uncertainties discourage widespread use. One common problem in using column studies to measure  $K_d$  values is that the breakthrough curves are asymmetric. Such curves cannot be interpreted using Equations 3.8, 3.9, 3.10, or 3.11. They require more complicated equations for solving for  $K_d$  (Brusseau and Rao, 1989; van Genuchten and Alves, 1982; van Genuchten and Wierenga, 1986).

One of the unique characteristics of measuring  $K_d$  values from column experiments is that nonequilibrium conditions can be imposed. Especially under conditions in which the solute has slow adsorption kinetics [*e.g.*, those that may occur with uranium (Sposito, 1994)] or when groundwater flow is fast, a measure of adsorption at equilibrium may over-estimate the extent to which sorption occurs under actual field conditions. When either of these conditions are known to exist in a study site, researchers should conduct column experiments at the flow rate existing in the field, thereby creating realistic conditions.

Relyea (1982) provided an excellent review on the theoretical and experimental application of the laboratory flow-through method of determining  $K_d$  values. He reported that retardation factors measured in column experiments depended on the water velocity and column dimension. For short columns and slow water velocities, diffusion can become a major transport mechanism

resulting in lower retardation factors and lower  $K_d$  values. At high velocities the effective pore volume of a sample can decrease for short columns. High water velocities can also result in lower retardation factors as a result of the solute not having sufficient time to adsorb to the soil, *i.e.*, chemical equilibrium was not obtained. The effects of column length, mass of solute added to column, diameter ratio of particle to column, and ratio of column diameter to column width on the measured  $K_d$  value were also presented by Relyea (1982).

### 3.2.4 Field Modeling Method

Field studies can provide accurate indications of the time of travel of the contaminant because the concentrations of a dissolved contaminant are measured directly from samples taken from monitoring wells. The field modeling method of estimating a  $K_d$  value, also called the field calibration method, uses a transport model and existing groundwater monitoring data. This process, which is referred to as calibrating a groundwater transport model to  $K_d$  values, involves treating the  $K_d$  value as an adjustable parameter (or dependent variable) while simulating contaminant concentrations determined at monitoring wells. Groundwater calibration captures the essence of the problem in the field. This is an iterative process that frequently requires the adjusting the values for several other input parameters, such as effective porosity, dispersion, and flow rate, to yield meaningful  $K_d$  values. The minimum information that is needed for such a calculation is the contaminant concentration at the source term, date of release, groundwater flow path, groundwater flow rate, contaminant concentration at a monitoring well, distance between source-release and monitoring well, dispersion coefficient, and source term. The retardation of the chemical is then estimated as the ratio of the pore-water velocity to the contaminant velocity (Equation 3.7). The pore-water velocity,  $v_p$ , can be based on Darcy's law (Freeze and Cherry, 1979) where

$$v_p = \frac{v_d}{n_e} \quad (3.12)$$

where  $v_d$  = Darcy velocity  
 $n_e$  = effective porosity

However, 2 key drawbacks to this technique is that it is highly site specific and very model dependent. Additionally, many assumptions have to be made about the water flow in the study site including uniform flow and flow path. Not obvious, is that the  $K_d$  value calculated by this method greatly improves with more data. A detailed description of the theory of calculating  $K_d$  values by this method and some examples of this approach are presented in Chapter 4.

### 3.2.5 $K_{oc}$ Method

The extent to which an organic contaminant partitions between the solid and solution phases is determined by several physical and chemical properties of the contaminant and soil (Lyman *et al.*, 1982). Since most sorption of hydrophobic organic substances is to the natural organic matter present in sediments or soils, the usual approach is to assume that all sorption is to that matter and

75

to invoke a partition coefficient between organic carbon ( $K_{oc}$ ) or organic matter ( $K_{om}$ ) and water (Seth *et al.*, 1999). Hydrophobic solutes appear to bind readily and rapidly with the outer surface region in a few hours to a few days and then diffuse slowly into (and out of) the hydrophobic interior region and narrow cavities in the sediment or soil organic matter during time periods of weeks (Seth *et al.*, 1999). An empirical approach that has had wide acceptance in the scientific community is the organic-carbon partitioning coefficient ( $K_{oc}$ ) method introduced by Karickhoff *et al.* (1979).

For this method, sorption of an organic contaminant, such as polynuclear aromatic hydrocarbon (PAH), is assumed to occur only to the organic material in the soil. The partitioning between the solid and solution phases is expressed as:

$$K_d \approx K_{oc} f_{oc} \quad (3.13)$$

where  $K_{oc}$  = ratio of the contaminant concentration on the organic matter on a dry weight basis to its dissolved concentration in the surrounding fluid (ml/g) and  
 $f_{oc}$  = fraction of organic carbon in the soil (mg/mg).

Importantly, the  $K_{oc}$  method is only applicable for estimating organic compound partitioning. Gschwend and Wu (1985) report that if precautions are taken to eliminate or account for nonsettling microparticles or organic macromolecules which remain in the aqueous phase during laboratory sorption tests, the observed organic-carbon partitioning coefficient have been found to remain constant over a wide range of environmental and experimental conditions. However, recent studies by Chiou *et al.* (1998) and Seth *et al.* (1999) indicate that for any given chemical, an inherent variability in  $K_{oc}$  values is expected as a result of different environmental conditions and equilibrium times. Dragnon (1988) identified the following conditions when this approach is less accurate:

- When the organic fraction,  $f_{oc}$ , is less than 1.0 percent<sup>1</sup> (LaGrega, 1994) or greater than 20 percent (EPA, 1988)
- When there are large amounts of swelling clays present (*e.g.*, montmorillonite)
- When the partitioning organic compound is polar
- When mechanisms other than simple partitioning contribute to adsorption (*e.g.*, cation-exchange, anion-exchange)
- When a substantial time is required to reach equilibrium

The organic content of most soils falls in the range of 0.2 to 3.0% (LaGrega, 1994).

---

<sup>1</sup> Other limits have been suggested for the minimum organic fraction,  $f_{oc}$ , such as less than 0.1 percent (EPA, 1989) or less than a few tenths of a percent (Pignatello, 1989).

76

The commonest correlation for  $K_{oc}$  is with the octanol-water partition coefficient ( $K_{ow}$ ) for which extensive databases and reliable estimation methods exist (Seth *et al.*, 1999). A simplified relationship between these two parameters is given by Equation 3.14.

$$K_{oc} = \rho K_{ow} \quad (3.14)$$

where  $\rho$  = correlation coefficient (unitless).

LaGrega (1994) reports a value of ( $\rho = 0.63$ ) as a commonly used value while Seth *et al.* (1999) calculate a value of ( $\rho = 0.35$ ) with a variation in  $\rho$  by a factor of 2.5 in either direction. Seth *et al.* (1999) also suggested that  $K_{oc}$  estimates be viewed as a distribution, which includes uncertainties about attainment of equilibrium and the variability in the composition of organic matter present in soils and sediments, rather than as a single point value.

Streng and Peterson (1989) applied the principle of the  $K_{oc}$  model to estimating the partition coefficients for organic compounds on soils. They defined the  $K_d$  for organic compounds through the combination of the  $K_{oc}$  model and a parametric model (discussed in Section 3.4.2) based on the concentrations of organic material ( $C_{om}$ , percent w/w), clay ( $C_{clay}$ , percent w/w), silt ( $C_{silt}$ , percent w/w) and sand ( $C_{sand}$ , percent w/w) as dependent variables:

$$K_d = 10^{0.4} K_{oc} [57.735(C_{om}) + 2.0(C_{clay}) + 0.4(C_{silt}) + 0.005(C_{sand})] \quad (3.15)$$

Equation 3.15 has the disadvantage of requiring more input parameters than Equations 3.13 and 3.14, but it provides an innovative approach for estimating the  $K_d$  of organic compounds.

### 3.3 Issues Regarding Measuring and Selecting $K_d$ Values

#### 3.3.1 Using Simple Versus Complex Systems to Measure $K_d$ Values

Soils are a complex mixture of solid, gaseous, and liquid phases. Each phase contains several different constituents. Sposito (1989) estimated that the aqueous phase of a typical soil easily contains between 100 and 200 different soluble complexes, many of them involving metal cations and organic ligands (Table 3.1). The main effect of pH on these complexes, as is evident in Table 3.1, is to favor free metal cations and protonated anions at low pH and carbonate or hydroxyl complexes at high pH. The number of soluble complexes are also likely to be greater in systems with elevated pH and organic matter concentrations. The solid phase in natural soils typically contains more than 10 different constituents, including minerals, microbes, oxides, naturally occurring organic matter, and organic, carbonate and/or oxide (e.g., iron, aluminum, and manganese) coatings. The gas phase is quite different from that of above ground air as a result of its interaction with the other phases and effects of pressure, temperatures, and microbial activity (Sposito, 1989). For instance, the carbon dioxide levels is commonly several orders of magnitude greater in soils than in above ground air (Wood and Petratis, 1984).

**Table 3.1.** Representative chemical species in acidic and basic soil solutions (after Sposito, 1989).

Cation	Principal Species <sup>1</sup>	
	Acid Soils	Alkaline Soils
Aluminum	Al-org, <sup>2</sup> AlF <sup>2+</sup> , AlOH <sup>2+</sup>	Al(OH) <sub>4</sub> <sup>-</sup> , Al-org
Cadmium	Cd <sup>2+</sup> , CdSO <sub>4</sub> <sup>0</sup> (aq), CdCl <sup>+</sup>	Cd <sup>2+</sup> , CdCl <sup>+</sup> , Cd SO <sub>4</sub> <sup>0</sup> (aq), CdHCO <sub>3</sub> <sup>+</sup>
Calcium	Ca <sup>2+</sup> , CaSO <sub>4</sub> <sup>0</sup> (aq), Ca-org	Ca <sup>2+</sup> , Ca SO <sub>4</sub> <sup>0</sup> (aq), CaHCO <sub>3</sub> <sup>+</sup>
Chromium(III)	CrOH <sup>2+</sup>	Cr(OH) <sub>4</sub> <sup>-</sup>
Chromium(VI)	CrO <sub>4</sub> <sup>2-</sup>	CrO <sub>4</sub> <sup>2-</sup>
Copper(II)	Cu-org, Cu <sup>2+</sup>	CuCO <sub>3</sub> <sup>0</sup> (aq), Cu-org, CuB(OH) <sub>4</sub> <sup>+</sup> , Cu[B(OH) <sub>4</sub> ] <sub>4</sub> <sup>0</sup> (aq)
Iron(II)	Fe <sup>2+</sup> , FeSO <sub>4</sub> <sup>0</sup> (aq), FeH <sub>2</sub> PO <sub>4</sub> <sup>+</sup>	FeCO <sub>3</sub> <sup>0</sup> (aq), Fe <sup>2+</sup> , FeHCO <sub>3</sub> <sup>+</sup> , FeSO <sub>4</sub> <sup>0</sup> (aq)
Iron(III)	FeOH <sup>2+</sup> , Fe(OH) <sub>3</sub> <sup>0</sup> (aq), Fe-org	Fe(OH) <sub>3</sub> <sup>0</sup> (aq), Fe-org
Lead	Pb <sup>2+</sup> , Pb-org, PbSO <sub>4</sub> <sup>0</sup> (aq), PbHCO <sub>3</sub> <sup>+</sup>	Pb <sup>2+</sup> , PbHCO <sub>3</sub> <sup>+</sup> , Pb-org, Pb(CO <sub>3</sub> ) <sub>2</sub> <sup>2-</sup> , PbOH <sup>+</sup>
Magnesium	Mg <sup>2+</sup> , MgSO <sub>4</sub> <sup>0</sup> (aq), Mg-org	Mg <sup>2+</sup> , MgSO <sub>4</sub> <sup>0</sup> (aq), MgCO <sub>3</sub> <sup>0</sup> (aq)
Manganese(II)	Mn <sup>2+</sup> , MnSO <sub>4</sub> <sup>0</sup> (aq), Mn-org	Mn <sup>2+</sup> , MnSO <sub>4</sub> <sup>0</sup> (aq), MnCO <sub>3</sub> <sup>0</sup> (aq), MnHCO <sub>3</sub> <sup>+</sup> , MnB(OH) <sub>4</sub> <sup>+</sup>
Molybdenum(VI)	H <sub>2</sub> MoO <sub>4</sub> <sup>0</sup> (aq), HMoO <sub>4</sub> <sup>-</sup>	HMoO <sub>4</sub> <sup>-</sup> , MoO <sub>4</sub> <sup>2-</sup>
Nickel	Ni <sup>2+</sup> , NiSO <sub>4</sub> <sup>0</sup> (aq), NiHCO <sub>3</sub> <sup>+</sup> , Ni-org	NiCO <sub>3</sub> <sup>0</sup> (aq), NiHCO <sub>3</sub> <sup>+</sup> , Ni <sup>2+</sup> , NiB(OH) <sub>4</sub> <sup>+</sup>
Potassium	K <sup>+</sup>	K <sup>+</sup> , KSO <sub>4</sub> <sup>-</sup>
Silicon	H <sub>4</sub> SiO <sub>4</sub> <sup>0</sup> (aq)	H <sub>4</sub> SiO <sub>4</sub> <sup>0</sup> (aq)
Sodium	Na <sup>+</sup>	Na <sup>+</sup> , NaHCO <sub>3</sub> <sup>0</sup> (aq), NaSO <sub>4</sub> <sup>-</sup>
Zinc	Zn <sup>2+</sup> , ZnSO <sub>4</sub> <sup>0</sup> (aq), Zn-org	ZnHCO <sub>3</sub> <sup>+</sup> , ZnCO <sub>3</sub> <sup>0</sup> (aq), Zn-org, Zn <sup>2+</sup> , ZnSO <sub>4</sub> <sup>0</sup> (aq), ZnB(OH) <sub>4</sub> <sup>+</sup>

<sup>1</sup> Complexes for each cation are listed in the order of their relative concentrations from greatest to lowest concentration.  
<sup>2</sup> Org □ Organic complexes (e.g., fulvic acid complexes).

Scientists will conduct geochemical studies with pure phases, such as goethite, quartz, or montmorillonite to work in well-defined systems. They may also choose not to work with actual groundwater, but instead work with a "synthesized groundwater," such as a calcium chloride solution or a calcium chloride/sodium chloride solution. Again, the intent is to work in a chemically well-defined system with as few constituents as possible. Experiments conducted under simplified systems have provided information about the mechanisms by which solutes interact with solid surfaces (Sposito, 1984; Sposito, 1989), information that otherwise would not be possible to obtain from experiments conducted with natural heterogeneous soils and groundwater.

Ideally, for site-specific calculations, the transport modeler should use sorption values determined for site-specific materials at site-specific conditions. In the absence of such data, the modeler often selects a  $K_d$  value taken from the literature that was measured under similar conditions as existing at the study site. However, as discussed in Chapter 2 (Section 2.2.3), very subtle properties of the solid and aqueous phases can have a profound affect on a contaminants  $K_d$ . For example, only 1 percent (w/w) organic matter existing as surface coatings in a South Carolina surface soil completely masked the surface properties of the underlying minerals (Kaplan *et al.*, 1993). The organic coatings imposed a much greater sorption potential than would have been expected based on mineralogical considerations. Similarly, the surface properties of the soils just below these soils were entirely dominated by iron-oxide coatings (Seaman *et al.*, 1995). The effect of the iron-oxide coatings was to create a solid phase that was dominated by pH dependent charge surfaces. These subsurface soils adsorbed large amounts of anions because the pH was below the zero-point-of-charge [discussed in Chapter 2 (Section 2.2.3)] of the iron oxides, pH  $\sim$ 8. Subtle changes in the aqueous composition in a batch  $K_d$  test may also have a profound affect on the measured  $K_d$  value (Delegard and Barney, 1983). Thus, it is essential for the modeler selecting  $K_d$  values to recognize which solid and aqueous phase components have a strong affect on the sorption of the contaminant of interest. Identifying these important components is the subject of Volume II.

### 3.3.2 Field Variability

The purpose of any soil sample is to obtain information about a particular soil. The sample itself is seldom, if ever, the entire soil mass in which one is interested. In statistics, this larger aggregate of material, in which we are ultimately interested, is called the "population." Information from the sample is of interest only insofar as it yields information about the population, and the information may or may not be representative, depending on how the sample is selected.

The population itself may be large or small, or even a part of what the modeler considers a larger population. For contaminant transport modeling, the population is commonly defined by either stratigraphic units or soil texture. The justification supporting the use of these definitions is based both on practical and scientific considerations. Soil texture and stratigraphy can be easily and inexpensively determined from well-log data and the close correlation of a number of hydrological and chemical properties with soil textures is well documented (Petersen *et al.*, 1996). A some-

what better definition of soil populations would be the cation- or anion-exchange capacity of the soils. However, this option is appreciably more expensive and is valuable only for defining  $K_d$  populations. The soil texture data are also used for defining water flow populations.

The intensity with which a soil must be sampled to estimate with given accuracy some characteristic, such as  $K_d$  value, will depend on the magnitude of the variation within the soil population under consideration. The more heterogeneous the population, the more intense must be the sampling rate to attain a given precision. In general, although differences have been found to exist among lithographic units, considerable variation may be expected within the units for such characteristics as pH, phosphorous, potassium, sodium, conductivity, volume weight, permeability and porosity (Peterson and Calvin, 1986). In some instances, the variation within contiguous units is so great that it is not feasible to estimate differences between the units with any satisfactory degree of precision. For most characteristics, the variation, both within and among units, decreases, with increasing depth in the profile (Peterson and Calvin, 1986). Hence, subsurface environments generally need to be sampled less than surface soils to attain comparable accuracy (Mackay *et al.*, 1986; Warrick and Nielsen, 1980). Mackay *et al.* (1986) reported that a number of soil properties, including  $K_d$  values, changed more vertically than laterally.

### 3.3.3 The "Gravel Issue"

Because most  $K_d$  values are measured in laboratory studies, the sample size has an upper mass limit of about 100 g soil (and often 10 g with the increased emphasis of waste minimization and high disposal costs for laboratory wastes) in batch  $K_d$  measurements and several kilograms of soil in column studies. Both tests also have particle size limitations. The batch  $K_d$  is typically limited to the less than 2-mm size fraction (Appendix C, ASTM, 1987; EPA, 1991; Roy *et al.*, 1991). This size fraction was selected for a number of reasons that are both practical and scientific in nature. The less than 2-mm fraction has historically been defined as the soil fraction and the greater than 2-mm fraction as the rock fraction. The less than 2-mm fraction is also convenient for most standard glassware used in batch  $K_d$  tests (Figure 3.1). Another practical consideration is that greater uniformity of the soil sample and therefore of the measured  $K_d$  value can be achieved if the range of particle sizes used in the test is limited. Finally, the smallest fraction is the most chemically reactive fraction due to its high specific surface area ( $m^2/g$ ). The particle size used in column studies is also commonly limited to the less than 2-mm fraction. This size fraction was selected for similar reasons as for the batch studies and to compare results between the 2 common methods. However, Relyea (1982) indicated that the less than 2-mm size fraction should only be used in columns greater than 80 mm in diameter. He indicates that to avoid local velocity effects (*e.g.*, channeling or a radial velocity gradient), the column diameter should be at least 30 to 40 times the particle diameter of the solids used to pack the column.

The "gravel issue" is the problem that transport modelers face when converting laboratory-derived  $K_d$  values based on experiments conducted with the less than 2-mm fraction into values that can be used in systems containing particles greater than 2 mm in size. As mentioned above, the less than 2-mm fraction is the more chemically reactive fraction due primarily to its large

surface area. There are many subsurface soils dominated by cobbles, gravel, or boulders. To base the  $K_d$  values on the less than 2-mm size fraction, which may constitute less than 1 percent of the soil volume, would grossly overestimate the actual  $K_d$  of the aquifer. Including large soil particles in a  $K_d$  determination will increase the cost of laboratory equipment and perhaps more importantly will result in  $K_d$  values with large error terms because of the great variability of the particle size distribution in subsamples of a single soil.

Two general approaches have been proposed to address the "gravel issue." The first is to assume that all particles greater than 2 mm have a  $K_d = 0$  ml/g. As an example, if 75 percent (w/w) of a formation is composed of particles greater than 2 mm and the  $K_d$  value of the less than 2-mm size fraction was 100 ml/g, then the  $K_d$  value used in the model would be 25 ml/g. Although the assumption underlying this approach is incorrect, the extent to which sorption occurs on these larger particles may be small. This approach is likely to yield a more accurate value in systems dominated by cobbles, gravel, and boulders.

The second approach is to normalize laboratory-derived  $K_d$  values by surface area. Thus, instead of having units of

$$\frac{\frac{\mu\text{g metal}}{\text{g sediment}}}{\frac{\mu\text{g metal}}{\text{ml solution}}} \square \frac{\text{ml}}{\text{g}}, \quad (3.16)$$

the laboratory  $K_d$  value would have units of

$$\frac{\frac{\text{g metal}}{\text{m}^2 \text{ sediment}}}{\frac{\mu\text{g metal}}{\text{ml solution}}} \square \frac{\text{ml}}{\text{m}^2}, \quad (3.17)$$

(Kaplan *et al.*, 1995b). Theoretically, this latter approach is more satisfying because it permits some sorption to occur on the >2-mm fraction and the extent of the sorption is proportional to the surface area. The underlying assumption in this approach is that the mineralogy is similar in the less than 2- and greater than 2-mm fractions and that the sorption processes occurring in the smaller fraction are similar to those that occur in the larger fraction. Because sorption is a surface area phenomena (Equation 3.16), as opposed to a weight phenomena (Equation 3.17), normalizing the data to surface area has logic, and is commonly done in soil (Sposito, 1989) and colloid chemistry (Alberty, 1987). The drawback to this approach is that an additional measurement is needed to calculate the newly defined  $K_d$  value in the laboratory. Specific surface area measurement is a rather common and simple procedure (Carter *et al.*, 1986). This approach

to the "gravel issue" also requires a means to convert available soil texture data, which are often available from well-hole logs or outcroppings of the formation, into surface area data.

### 3.3.4 The "Colloid Issue"

The "colloid issue," as it pertains to measuring  $K_d$  values, is the problem experimentalists have in separating the aqueous from the solid phases during a laboratory batch  $K_d$  measurement (see Chapter 2). Typically centrifugation or filtration are used to accomplish this. If contaminants are sorbed to tiny particles that remain in suspension after the separation step, the experimenter will incorrectly assign the sorbed contaminant to the dissolved phase,  $C_i$  (Equation 3.2). This will result in underestimating the true  $K_d$  value. This is an especially important problem for contaminants that sorb strongly to solids, especially organic matter. Organic matter has a much lower density than clay (*i.e.*,  $\sim 1.05 \text{ g/cm}^3$  for organic matter versus  $\sim 2.6 \text{ g/cm}^3$  clays) and therefore the common centrifugation protocol may not be sufficient to separate the phases. Also, organic matter may exist as extremely small particles, or molecules,  $\sim 0.005 \mu\text{m}$  in diameter. Thus, when a great deal of organic matter is present in a soil, or when only a trace amount of organic matter has a profound affect on the measured  $K_d$ , additional precautions must be followed (Gschwend and Wu, 1985). For example, Gschwend and Wu (1985) reported that they were able to increase the partitioning coefficient, which is related to the  $K_d$  term (see Section 3.2.3), of polychlorinated biphenyl by 3 orders of magnitude by very carefully removing unsettled organic particles from suspension.

Using a centrifuge to make the solid and solution phase separations can also result in the formation of a very thin zone at the liquid surface where surface tension holds fine-grained particles at the top of the solution. The experimentalist should look for such problems and avoid sampling the surface of the clarified liquid. When pipets are used to remove supernatant solution, the pipet should be inserted sufficient distance below the surface to avoid drawing in suspended particles, but to a distance where the pipet tip is above the settled solids-liquid interface to avoid drawing in previously settled fines.

For these reasons, many experimentalists prefer to filter the supernatant solution after centrifugation. Filtration does have its problems, however. Filtering a small volume of supernatant solution can bias the contaminant's concentration if the filter membrane adsorbs solute species. The type of filter membrane used effects the potential for adsorption. In our experience polyethylene or other plastic-based filter membranes are more inert than cellulosic-based membranes. Filter membranes can also be "pre-treated" with the supernatant solution by discarding the first aliquot and filtering a second aliquot that is saved for analysis. If the filter membrane does adsorb the analyte of interest, the amount adsorbed usually rapidly diminishes as the volume of solution filtered increases. Thus discarding the first aliquot of filtered solution and using subsequent aliquots for analysis lowers the chances of biasing final  $K_d$  values.

Another problem associated with colloids, is that the traditional 2-phase solute transport model does not account for contaminants moving in association with mobile colloids. This subject is

discussed in Chapter 2 (Section 2.5.1). Briefly, contaminants with a high affinity for sorbing to rock or vadose zone soils are assumed to be retarded relative to the rate of groundwater flow. However, an increasing body of evidence indicates that under some subsurface conditions, components of the solid phase may exist as colloids that may be transported with the flowing water. Association of contaminants with this additional mobile phase may enhance not only the amount of the contaminant that is transported, but also the rate of contaminant transport. Most current approaches to predicting contaminant transport ignore this mechanism not because it is obscure or the mathematical algorithms have not been developed (Corapcioglu and Kim, 1995; Mills *et al.*, 1991), but because little information is available on the occurrence, the mineralogical properties, the physicochemical properties, or the conditions conducive to the generation of mobile colloids. There have been numerous examples in which mobile colloids have been implicated as the vector responsible for enhanced transport (Kaplan *et al.*, 1994a,b; Kaplan *et al.*, 1995a; reviewed by McCarthy and Degueudre, 1993).

### 3.3.5 Particle Concentration Effect

Many investigators have observed that  $K_d$  values determined in the laboratory often exhibit a dependence with respect to the ratio of solid to solution used in the measurements. As recently discussed by Oscarson and Hume (1998), this dependence is puzzling. From a theoretical perspective, the  $K_d$  value should not depend on the solid-to-solution ratio, because the definition of the  $K_d$  model (see Equation 2.20) normalizes the ratio of the solute sorbed to the solid to the solute concentration left in solution based on the mass of solid and solution used for the measurement. Thus the  $K_d$  has units of volume/mass, such as typically ml/g.

Investigators have often found that  $K_d$  values measured for many contaminants for a given soil-groundwater system decrease as the solid-to-solution ratio increases. For example, this particle concentration effect on  $K_d$  values has been observed by O'Conner and Connolly (1980), Oscarson and Hume (1998), Honeyman and Santschi (1988), Meier *et al.* (1987), and others. The same trend with respect to particle concentration has also been observed for  $K_d$  values for organic contaminants [*e.g.*, see Gschwend and Wu (1985) and Voice *et al.* (1983)].

Investigators have offered several explanations for the observed dependency. These explanations can be categorized into two groups: (1) "real" physical/chemical processes, and (2) experimental artifacts. One rationalization offered in the "real" category is that the particle concentration effect is thought to be caused by particle-particle interactions. In systems with higher solids content, these interactions are perhaps physically blocking some adsorption sites from the adsorbing solutes and thus causing decreased adsorption, or creating electrostatic interferences such that the electrical surface charges on the closely packed particles diminish attractions between the adsorbing solutes and surfaces of individual grains. In terms of physical effects, individual particles in a slurry having a high solid-to-solution ratio may have a greater tendency to coagulate and flocculate into larger particles that have less available surface adsorption sites than individual grains and thus can adsorb less adsorbate. This phenomenon is likely exacerbated by diffusion processes that in short-term laboratory measurements, do not allow sufficient time for

the adsorbate to diffuse to the internal surface adsorption sites. The net effect is a  $K_d$  measurement with a lower value when a high solid-to-solution ratio is present, because not enough time was allocated for the water/soil system to reach a final equilibrium state. Thus there are possible experimental artifacts even within the context of this "real" process explanation.

Plausible experimental artifacts also include less efficient separation of the solid phase from high solids-content slurries, such that more colloidal size particles laden with adsorbate remain in the solution phase and the associated adsorbate gets included in the analysis of the solution phase. Complexing agents may desorb and/or dissolve from the solids, and in turn compete with the adsorbate for the available sorption surface sites. Soluble organic carbon is a common example of this process. Such effects increase when higher solid contents are used. Other artifacts include changes in the aqueous system that are caused by mass transfer from the larger quantity of solids but are not recorded during these measurements. Another consideration in the category of possible experimental artifacts for the solid-to-solution effect is improper data reduction. McKinley and Jenne (1991) suggest that the so-called particle concentration effect often goes away when adsorption data are replotted as adsorption isotherms, where the mass of solute adsorbed per mass of solid and the concentration of solute in the equilibrium solution are plotted on the y- and x-axes, respectively.

The explanations for the particle concentration (solid-to-solution ratio) effect are numerous and still rather perplexing [see summaries by Oscarson and Hume (1998) and Jenne (1998a)]. Jenne (1998a,b) includes valuable discussion on this "solids concentration effect." He also presents some recommendations that should be followed when performing adsorption experiments and identifies several key issues that should be addressed by future adsorption research. One practical position that has been supported by EPRI (1991) is to conduct adsorption experiments as close as possible to the conditions that exist at the site where contaminant mobility is being simulated and assessed. In most cases, this recommendation would require that  $K_d$  values determined by flow-through column testing would be preferred over batch measurements conducted at low solid-to-solution ratios.

As noted above, it has been suggested that  $K_d$  values may decrease with increasing solid-to-solution ratios. If this is a real effect, application of  $K_d$  values based on a batch experiment conducted with a solid-to-solution ratio significantly less than those that would exist in the field would therefore overestimate the magnitude of contaminant sorption and underestimate the extent of contaminant migration.

### **3.4 Methods of Acquiring $K_d$ Values from the Literature for Screening Calculations**

#### ***3.4.1 $K_d$ Look-Up Table Approach: Issues Regarding Selection of $K_d$ Values from the Literature***

Clearly, the greatest limitation of using a  $K_d$  value to calculate a retardation term (Equations 3.8, 3.9, 3.10, and 3.11) is that it describes solute partitioning between the aqueous and solid phases

for only 1 set of environmental conditions.  $K_d$  values are known to vary greatly with only slight changes in the composition of the solid and aqueous phases and these conditions often vary greatly in 1 study site. For example, when the aqueous chemistry for a batch  $K_d$  measurement was varied, americium  $K_d$  values in a Hanford sediment ranged from 0.2 to 53 ml/g, greater than a 200-fold difference (Delegard and Barney, 1983). Additional variability in the americium  $K_d$  values were observed when slightly different Hanford sediments were used: 4.0 to 28.6 ml/g (Delegard and Barney, 1983). Similarly, Sheppard *et al.* (1976) measured americium  $K_d$  values ranging from 125 to 43,500 ml/g using identical aqueous phases but different soils.

An alternative approach to a constant  $K_d$  model is one in which the  $K_d$  value varies as a function of a select group of environmental conditions (Delegard and Barney, 1983; Routson and Serne, 1972; Streng and Peterson, 1989). The easiest variable  $K_d$  model to interface with a transport code is one based on a look-up table. For look-up tables, separate  $K_d$  values are assigned to a matrix of discrete categories defined by chemically important environmental parameters (Streng and Peterson, 1989; Whelan *et al.*, 1992). Streng and Peterson (1989) used 9 categories defined by soil pH and texture in the Multimedia Environmental Pollutant Assessment System (MEPAS) code. The 3 soil texture classes were <10 percent, 10 to 30 percent, >30 percent clay/organic matter/oxide content. The 3 pH classes were >9, 5 to 9, and <5. The 9 cells defined by the pH and soil texture classes contained literature-derived  $K_d$  values and where data was not available, estimated values were included in the table. The inorganic contaminants in the  $K_d$  look-up table were actinium, aluminum, americium, antimony, arsenic, asbestos, barium, beryllium, borate, cadmium, calcium hypochlorite, calcium oxide, carbon, cerium, chlorate, chromium (III), chromium (VI), cobalt, copper, curium, europium, fluoride, hydrogen fluoride, iodine, iron, krypton, lead, lead oxide, lithium hydroxide, lithium ion, magnesium, manganese, mercury, molybdenum, neptunium, nickel, niobium, nitrate, nitric acid, nitrogen dioxide, palladium, phosphate ion, phosphorus, plutonium, polonium, potassium hydroxide, potassium ion, protactinium, radium, ruthenium, samarium, selenium, silicate ion, silver, sodium ion, strontium, sulfate, sulphur, thallium, thorium, tin, tritium, uranium, vanadium, yttrium, zinc compounds, zinc, and zirconium.

For any literature-derived  $K_d$  value, it is essential to clearly understand the selection criteria and the logic used to estimate  $K_d$  values not found in the literature. For instance, Streng and Peterson (1989) reported a wide range of literature  $K_d$  values for several cells, typically greater than 10-fold and sometimes greater than a 100-fold difference between minimum and maximum values. The values included in the MEPAS look-up table were the minimum values found in the literature. They justified this criteria because they wanted to build conservatism into the code. Conservatism is traditional when addressing the extent of contaminant migration and associated health effects, but may be erroneous if the modeling calculations are being used to address remediation options, such as pump-and-treat remediation. Conservatism for remediation calculations would tend to error on the side of under estimating the extent of contaminant desorption that would occur in the aquifer once pump-and-treat of soil flushing treatments commenced. Such an estimate would provide an upper limit to time, money, and work required to extract a contaminant from a soil. This would be accomplished by selecting a  $K_d$  from the

upper range of literature  $K_d$  values. Thus, the  $K_d$  values in MEPAS would not provide a conservative estimate for clean-up efforts .

Other important issues regarding the use of literature-derived  $K_d$  values are illustrated in Table 3.2. In any  $K_d$  look-up table, a small number of ancillary parameters must be selected to define the cells. pH and soil texture were the ancillary parameters used in the MEPAS code. These are excellent general categories for a large number of contaminants, however, they are of only secondary importance to a large number of other contaminants. For example, the amount of vermiculite, which is a 2:1 layer silicate mineral common in the United States, especially in the west and mid-west, is arguable the single most important ancillary parameter affecting cesium sorption (Douglas, 1989). Redox state is another example of an ancillary parameter that is extremely important relative to affecting the removal from redox-sensitive contaminants solution [this is actually a precipitation process and not an adsorption phenomena (Ames and Rai, 1978; Rai and Zachara, 1984; Sposito, 1989)]. Some important redox sensitive contaminants include arsenic, chromium, molybdenum, neptunium, plutonium, selenium, technetium, and uranium. The  $K_d$  values of uranium in the 9 MEPAS categories range from 0 to 500 ml/g (Table 3.2).

**Table 3.2.** Example of a  $K_d$  (ml/g) look-up table for uranium, uranium(VI), and uranium(IV).

Material	pH								
	□ 9			5 - 9			□ 5		
Fines <sup>1</sup> (%)	<10	10-30	>30	<10	10-30	>30	<10	10-30	>30
U <sup>2</sup>	0	5	50	0	50	500	0	5	50
U(IV) <sup>3</sup>	200	500	1,000	100	250	500	20	30	50
U(VI) <sup>3</sup>	0	1	2	1	2	5	2	5	20

<sup>1</sup> Fines (%) = sum of percentages of clay, organic matter, and hydrous-oxide in soil  
<sup>2</sup> Reference: Streng and Peterson (1989)  
<sup>3</sup> Authors' opinion based on values reported in Ames and Rai (1978), Ames and McGarrah (1980), Cloninger *et al.* (1980), Cloninger and Cole (1981), Serne and Relyea (1981), and Rai and Zachara. (1984).

By including an additional ancillary parameter of oxidation state, appreciably greater accuracy can be assigned to  $K_d$  values. For U(VI), the 9 categories may be assigned  $K_d$  values in the range of 0 to 20 ml/g, whereas, as for U(IV), the 9 categories may be assigned  $K_d$  values in the range of 20 to 1,000 ml/g. In this example, oxidation state is obviously a more important ancillary parameter than soil texture and in systems with pH values greater than 5, oxidation state is more important

86

than pH. The reduced form of U, U(IV), has a much greater  $K_d$  value than U(VI) because the former is known to precipitate from solution. The rather low uranium  $K_d$  values reported by Streng and Peterson (1989) are somewhat misleading in that they represent, as mentioned above, minimum values identified in the literature. These values would be entirely inappropriate for modeling U(IV) transport. Thus, an important point to this discussion is that no single set of ancillary parameters, such as pH and soil texture, is universally appropriate for defining categories in  $K_d$  look-up tables for all contaminants. Instead, the ancillary parameters used in look-up tables must be based on the unique chemical properties of each contaminant.

An apparent inconsistency in Table 3.2 is that the minimum values selected by Streng and Peterson (1989) for the uranium data are greater than those for U(VI). This inconsistency is not due to differences in literature used to estimate these values. Instead it arises from differences in how  $K_d$  values are estimated for cells in which no data are available.<sup>1</sup> This illustrates another important reason for clearly understanding the criteria and process used in selecting data incorporated into a look-up table. Clearly, differences in the criteria and process used to select  $K_d$  values can result in appreciable different values included in a look-up table; in this example, as much as 3 orders of magnitude.

### 3.4.2 Parametric $K_d$ Approach

The parametric  $K_d$  approach is similar to that of the  $K_d$  look-up table approach in that it varies  $K_d$  values used in a transport model as a function of important ancillary parameters. It differs from the  $K_d$  look-up table in that it uses a regression equation to define the  $K_d$  values instead of using discrete categories. The  $K_d$  value in this model varies as a function of empirically derived relationships with aqueous and solid phase independent parameters. Thus, it has the distinct advantage over look-up tables of having a continuum of  $K_d$  values.

Factorial design experiments are most often used to determine the systematic change resulting from varying the independent variables (*e.g.*, pH, soil texture, and redox status) on the dependent variables (uranium  $K_d$ ) (Box and Behnken, 1960; Cochran and Cox, 1957; Davies, 1954; Plackett and Burman 1946). Statistical methods commonly used to derive quantitative predictor equations include standard linear or nonlinear regression (Snedecor and Cochran, 1967), stepwise regression

---

<sup>1</sup> Streng and Peterson (1989) generated most of the values in the pH>9 categories by multiplying the  $K_d$  values from the pH 5 to 9 category by 0.1. A significant quantity of  $K_d$  values exist in the literature for the latter pH category. The "0.1 factor" was based on consistent, but flawed logic that metal contaminants are less likely to sorb because their cationic valence decreases by  $[M^{a+}(OH)_x]^{a-x}$ . It is now known that hydrolysis species adsorb as well as or better than free cations ( $M^{a+}$ ). Also many contaminants precipitate at higher pH values, giving the appearance of increased  $K_d$  values. There are a few exceptions in pH >9 systems:  $Zr(OH)_5$  species that may not adsorb as well as  $Zr^{4+}$ , and  $UO_2(CO_3)_2^{2-}$  and  $UO_2(CO_3)_3^{4-}$  species do not adsorb as well as the  $UO_2^{2+}$  and  $UO_2OH^+$  species. The  $CO_3^{2-}$  activity increases as pH increases so complexes get more important at elevated pH levels.

(Hollander and Wolfe, 1973), and adaptive-learning networks (Mucciardi *et al.*, 1979, 1980). All these techniques have been used to develop empirical relationships describing  $K_d$  values in terms of other variables (Delegard and Barney, 1983; Routson and Serne, 1972; Serne *et al.*, 1973; Routson *et al.*, 1981).

The empirical predictor equations commonly take the form of a nonlinear polynomial expression. For example, after evaluating solutions consisting of several sodium salts, organic chelates, and acids, Delegard and Barney (1983) came up with the following expression for an americium  $K_d$  value:

$$\text{Log } K_d (\text{Americium}) = 2.0 + 0.1[\text{NaOH}] + 26.8[\text{HEDTA}] + 153.4[\text{HEDTA}]^2 \quad (3.18)$$

where HEDTA is N-(2-hydroxyethyl) ethylenediaminetetraacetic acid. Numerous salts were found to have no significant effect on americium  $K_d$  values and therefore were not included in the expression. Delegard and Barney (1983) also evaluated higher exponential and logarithmic terms and determined that these terms did not improve the predictive capabilities of the expression (*i.e.*, the regression coefficients were not significant at  $P < 0.05$ ).

It is critical that parametric  $K_d$  equations, such as Equation 3.18, be used to calculate  $K_d$  values for systems within the range of the independent variables used to create the equation. In the case of Equation 3.18, the range of independent variables used to generate the model were selected to simulate a plume beneath the Hanford Site in Richland, Washington. Using Equation 3.18 to generate americium  $K_d$  values for a plume low in pH and Na concentrations would not be appropriate.

These types of statistical relationships are devoid of causality and therefore provide no certain information regarding the mechanism by which the contaminant partitioned to the solid phase, whether it be by adsorption, absorption, or precipitation. For example, the statistical analyses may suggest a very strong relationship between pH and the  $K_d$  term, when the actual sorption process may be controlled by iron oxide adsorption. Because pH and iron-oxide charge are covariants, a statistical relationship may suggest that sorption is due to pH, when in fact, suggesting that sorption is solely caused by pH.

The parametric  $K_d$  model is used in the transport equation, the code must also keep track of the current value of the independent variables (*e.g.*, [NaOH] and [HEDTA]) for the examples described in Equation 3.18) at each point in space and time to continually update the concentration of the independent variables affecting the  $K_d$  value. Thus, the code must track many more parameters, and some numerical solving techniques (*e.g.*, closed-form analytical solutions) can no longer be used to perform the integration necessary to solve for concentration. Generally, computer codes that can accommodate the parametric  $K_d$  model use a chemical subroutine to update the  $K_d$  value used to determine the  $R_f$ , when called by the main transport code. The added complexity in solving the transport equation with the parametric  $K_d$  sorption model and its empirical nature may be the reasons this approach has been used sparingly.

### 3.4.3 Mechanistic Adsorption Models

Mechanistic models explicitly accommodate for the dependency of  $K_d$  values on contaminant concentration, competing ion concentration, variable surface charge on the adsorbent, and solute species solution distribution. Incorporating mechanistic, or semi-mechanistic, concepts into models is attempted because the models become more robust and, perhaps more importantly from the standpoint of regulators and the public, scientifically defensible. The complexity of installing these mechanistic adsorption models into existing transport codes is difficult to accomplish. Additionally, these models also require a more intense and costly data collection effort than will likely be available to the majority of contaminant transport modelers who are conducting screening calculations. Descriptions of the state of this science, with references to excellent review articles, are presented in Chapter 2 and 5. A review of the methodology associated with the determination of the constants for use in these mechanistic models, however, is beyond the scope of this project. A review of the mechanistic adsorption models contained in EPA's MINTEQA2 geochemical reaction code is also presented in Chapter 5.

### 3.5 Summary

The objective of this chapter is to describe methods used to measure  $K_d$  values. The advantages and disadvantages and the assumptions underlying each method were discussed, and are summarized in Table 3.3. A number of issues regarding the selection of  $K_d$  values from the literature for screening calculations are also addressed in this chapter. Specific issues discussed included the use of simple versus complex systems to measure  $K_d$  values, field variability, the "gravel issue," and the "colloid issue."

Clearly, the greatest limitation of using a  $K_d$  value to calculate a retardation term is that it is only applicable to a single set of environmental conditions. Consequently, researchers have generated  $K_d$  values that varies as a function of ancillary environmental parameters. They include the look-up table  $K_d$ , the parametric  $K_d$ , and the mechanistic  $K_d$ . Models generated for parametric  $K_d$  values have typically been for rather limited environmental conditions. Mechanistic  $K_d$  values are limited to uniform solid and aqueous systems with little application to the heterogenous soils that exist in the natural environment. The easiest and the most common variable  $K_d$  model to interface with a transport code is the look-up table. No single set of ancillary parameters, such as pH and soil texture, is universally appropriate for defining categories in  $K_d$  look-up tables. Instead, the ancillary parameters must vary in accordance to the geochemistry of the contaminant. It is essential that the modeler fully understand the criteria and process used for selecting the values incorporated in such a table. Just as important is to understand the logic used to estimate  $K_d$  values not found in the literature. Differences in the criteria and process used to select  $K_d$  values can result in appreciable different  $K_d$  values.

It is incumbent upon the transport modeler to understand the strengths and weaknesses of the different  $K_d$  methods and perhaps more importantly the underlying assumption of the methods in order to properly select  $K_d$  values from the literature. The  $K_d$  values reported in the literature for

any given contaminant may vary by as much as *6 orders of magnitude*. An understanding of the important geochemical processes and knowledge of the important ancillary parameters affecting the sorption chemistry of the contaminant of interest is necessary for selecting appropriate  $K_d$  value(s) for contaminant transport modeling.

**Table 3.3.** Advantages, disadvantages, and assumptions of different methods used to determine  $K_d$  and the assumptions in applying these  $K_d$  values to contaminant transport models.

Methods for Determining $K_d$				
Batch <sup>1</sup>	<i>In-Situ</i> Field Batch	Flow-Through	Field Modeling	$K_{oc}$ <sup>2</sup>
<b>Minimum Input Data<sup>3</sup></b>				
<input type="checkbox"/> $M_{sed}$ <input type="checkbox"/> $C_i$ <input type="checkbox"/> $C_0$ <input type="checkbox"/> $V_w$	<input type="checkbox"/> $C_i$ <input type="checkbox"/> $A_i$ (or $q_i$ )	<input type="checkbox"/> $C_o$ <input type="checkbox"/> $n, \theta,$ or $n_e$ <input type="checkbox"/> $\theta_{particle}^4$ <input type="checkbox"/> $>10 C_{effluent}$ data points <input type="checkbox"/> $C_o$ tracer <input type="checkbox"/> Time	<input type="checkbox"/> $C_{release}$ <input type="checkbox"/> $C_{well}$ <input type="checkbox"/> Time <input type="checkbox"/> Distance <input type="checkbox"/> $v_w$ <input type="checkbox"/> $n, \theta,$ or $n_e$ <input type="checkbox"/> Diffusion or dispersion coefficients	<input type="checkbox"/> $K_{oc}$ <input type="checkbox"/> $f_{oc}$
<b>Advantages</b>				
<input type="checkbox"/> Inexpensive <input type="checkbox"/> Quick	<input type="checkbox"/> <i>In-situ</i> measurements <input type="checkbox"/> Equilibrium conditions <input type="checkbox"/> Aqueous and solid phases are precisely those of the modeled system	<input type="checkbox"/> Can measure sorption at field flow rates, <i>i.e.</i> , at non-steady state conditions <input type="checkbox"/> Can measure hydrodynamic effects ( <i>e.g.</i> , dispersion, colloidal transport, <i>etc.</i> ) on $R_f$ , and subsequently incorporate into $K_d$ value <input type="checkbox"/> Can measure effects of chemical phenomena ( <i>e.g.</i> , multiple species, reversibility, <i>etc.</i> ) on $R_f$ and $K_d$ values.	<input type="checkbox"/> Derived $K_d$ has the precise geochemical conditions and flow conditions of the study site	<input type="checkbox"/> Fairly accurate indirect method <input type="checkbox"/> Often can use look-up tables to get $K_{oc}$ value <input type="checkbox"/> $f_{oc}$ is an easy measurement <input type="checkbox"/> $K_{oc}$ can be correlated with $K_{ow}$ which has been measured for many different chemicals

91

Table 3.3. Continued.

Methods for Determining $K_d$				
Batch <sup>1</sup>	<i>In-Situ</i> Field Batch	Flow-Through	Field Modeling	$K_{oc}$ <sup>2</sup>
<b>Disadvantages</b>				
<ul style="list-style-type: none"> <li><input type="checkbox"/> Provides estimate of chemical processes at equilibrium; flow conditions are not always at equilibrium</li> <li><input type="checkbox"/> Physics involved not considered</li> <li><input type="checkbox"/> Better mixing in batch than in nature</li> <li><input type="checkbox"/> Typically uses larger ratio of solution/soil than exist in nature</li> <li><input type="checkbox"/> Experiments measure adsorption instead of desorption, the dominant process in transport; desorption is typically much slower than adsorption</li> <li><input type="checkbox"/> Speciation of different forms not considered</li> </ul>	<ul style="list-style-type: none"> <li><input type="checkbox"/> Expensive to collect samples</li> <li><input type="checkbox"/> Commonly have high detection limits (undesirable) for measuring contaminant on solid phase (<math>A_s, q_s</math>)</li> <li><input type="checkbox"/> Site-specific data</li> <li><input type="checkbox"/> Cannot unequivocally differentiate between, adsorbed, precipitated, and structural constituents</li> </ul>	<ul style="list-style-type: none"> <li><input type="checkbox"/> Commonly flow-through system is not at equilibrium and therefore results cannot be applied to other flow conditions</li> <li><input type="checkbox"/> Directly measure <math>R_f</math>, then back out <math>K_d</math>; therefore must make assumptions about relation between <math>K_d</math> and <math>R_f</math><sup>5</sup></li> <li><input type="checkbox"/> Measured <math>K_d</math> values commonly vary with water velocity and column dimensions</li> <li><input type="checkbox"/> Requires relatively expensive equipment</li> <li><input type="checkbox"/> Requires a lot of time</li> <li><input type="checkbox"/> Complex experiment to conduct</li> <li><input type="checkbox"/> Data are commonly not well behaved, <i>i.e.</i>, asymmetric or peakless breakthrough curves</li> <li><input type="checkbox"/> Can investigate some secondary processes affecting contaminant transport, such as effects of unsaturated flow, colloid-facilitated contaminant transport, mobile vs immobile water phases</li> </ul>	<ul style="list-style-type: none"> <li><input type="checkbox"/> <math>K_d</math> is truly site specific</li> <li><input type="checkbox"/> <math>K_d</math> is transport model specific</li> <li><input type="checkbox"/> Need to make many assumptions about the water flow including uniform flow, direction, and path length that affect the calculated <math>K_d</math> value</li> <li><input type="checkbox"/> Measure <math>R_f</math>, then back out <math>K_d</math>; many assumptions go into relating <math>K_d</math> to <math>R_f</math></li> <li><input type="checkbox"/> May or may not be in equilibrium, therefore not a thermodynamic <math>K_d</math></li> <li><input type="checkbox"/> <math>K_d</math> value greatly improves with more field data collected</li> <li><input type="checkbox"/> Calculations can be quite involved</li> </ul>	<ul style="list-style-type: none"> <li><input type="checkbox"/> For organic compounds only</li> <li><input type="checkbox"/> More hydrophobic the contaminant compound, more accurate the <math>K_d</math>; vice versa with hydrophilic compounds</li> </ul>

92

Table 3.3. Continued.

Methods for Determining $K_d$				
Batch <sup>1</sup>	<i>In-Situ</i> Field Batch	Flow-Through	Field Modeling	$K_{oc}$ <sup>2</sup>
Assumptions in Calculating $K_d$				
<ul style="list-style-type: none"> <li><input type="checkbox"/> Adsorption rate = desorption rate</li> <li><input type="checkbox"/> Only 1 type of surface adsorption site, A</li> <li><input type="checkbox"/> Only 1 type of aqueous dissolved species, <math>C_i</math></li> <li><input type="checkbox"/> <math>A \gg A_i</math></li> <li><input type="checkbox"/> Activity of <math>A_i = 1</math></li> <li><input type="checkbox"/> Equilibrium has been achieved during mixing period</li> <li><input type="checkbox"/> No adsorbate on suspended colloids</li> <li><input type="checkbox"/> No precipitation of adsorbate due to <math>C_0</math> concentration exceeding solubility</li> </ul>	<ul style="list-style-type: none"> <li><input type="checkbox"/> Same as for batch <math>K_d</math></li> <li><input type="checkbox"/> Measurement of adsorbed contaminant, <math>A_i</math> (<math>q_i</math>), can differentiate between adsorbed, precipitated, and structural constituents</li> </ul>	<ul style="list-style-type: none"> <li><input type="checkbox"/> Must assume a relationship between <math>R_f</math> and <math>K_d</math><sup>5</sup></li> <li><input type="checkbox"/> Water flow and dispersion coefficient is constant</li> </ul>	<ul style="list-style-type: none"> <li><input type="checkbox"/> Must assume a relationship between <math>R_f</math> and <math>K_d</math></li> <li><input type="checkbox"/> Know <math>n_e</math> or <math>n</math></li> <li><input type="checkbox"/> Must know the flow path and velocity of plume</li> <li><input type="checkbox"/> Sorption is uniform in the study size</li> </ul>	<ul style="list-style-type: none"> <li><input type="checkbox"/> Same as for laboratory batch <math>K_d</math></li> <li><input type="checkbox"/> Organic contaminant sorbs (partition) only to organic matter in soil, no sorption occurs to inorganic phases</li> </ul>

93

Table 3.3. Continued.

Methods for Determining $K_d$				
Batch <sup>1</sup>	<i>In-Situ</i> Field Batch	Flow-Through	Field Modeling	$K_{oc}$ <sup>2</sup>
Assumptions in Applying Measured $K_d$ to Transport Model				
<ul style="list-style-type: none"> <li><input type="checkbox"/> Adsorption of solute is linear, <i>i.e.</i>, it is independent of <math>C_i</math></li> <li><input type="checkbox"/> Adsorption of solute is reversible</li> <li><input type="checkbox"/> Solute movement is slow enough that equilibrium conditions exist between the solute and soil</li> <li><input type="checkbox"/> Geochemical conditions (presence and concentration of background electrolytes and solid phases) of batch experiment are identical to those in aquifer</li> <li><input type="checkbox"/> Temperature and pressure conditions of batch experiment are identical to those in the aquifer</li> <li><input type="checkbox"/> Mixing in aquifer is as thorough as in batch experiment</li> <li><input type="checkbox"/> Difference between the soil/water ratio in the aquifer and batch experiment is not important to <math>K_d</math> value</li> </ul>	<ul style="list-style-type: none"> <li><input type="checkbox"/> Same as for laboratory batch <math>K_d</math> (except fourth point not relevant to <i>in-situ</i> batch method)</li> </ul>	<ul style="list-style-type: none"> <li><input type="checkbox"/> It is more common to enter the <math>R_f</math> value derived from experiment than the <math>K_d</math> value into transport code; consequently, do not need to make any assumptions about the relationship between <math>R_f</math> and <math>K_d</math></li> <li><input type="checkbox"/> If <math>R_f</math> value from column experiment is entered into transport code and the flow conditions of the experiment are similar to those in the site being modeled, then no assumptions need to be made regarding affect of nonequilibrium conditions</li> </ul>	<ul style="list-style-type: none"> <li><input type="checkbox"/> None</li> </ul>	<ul style="list-style-type: none"> <li><input type="checkbox"/> Same as for laboratory batch <math>K_d</math></li> </ul>
<p><sup>1</sup> See Equation 3.4</p> <p><sup>2</sup> See Equation 3.13</p> <p><sup>3</sup> <math>A</math> = Concentration of free or unoccupied surface adsorption site on a solid phase; <math>C_i</math> = the total dissolved adsorbate concentration remaining in solution at equilibrium; <math>f_{oc}</math> = fraction of soil that is organic carbon; <math>C_{release}</math> = concentration of solute at time of release; <math>C_{well}</math> = concentration of solute in monitoring well; <math>M_s</math> = soil mass; <math>A_s</math> = the concentration of adsorbate on the solid at equilibrium; <math>n</math> = total porosity; <math>n_e</math> = effective porosity; <math>V_w</math> = solution volume; <math>\rho_b</math> = bulk density; <math>\rho_{particle}</math> = particle density; <math>\theta</math> = water saturation.</p> <p><sup>4</sup> <math>\rho_{particle}</math> is used to calculate bulk density (<math>\rho_b</math>); <math>\rho_b = [\rho_{particle} (1 - n)]</math>.</p> <p><sup>5</sup> See Equations 3.8, 3.9, 3.10, and 3.11.</p>				

94

## 4.0 Groundwater Calibration Assessment Based on Partition Coefficients: Derivation and Examples

### 4.1 Introduction

Partition (or distribution) coefficient,  $K_d$ ,<sup>1</sup> values are utilized in transport and risk assessment modeling because of their simplicity in (1) understanding, (2) measuring, and (3) providing closed-form, explicit, analytical solutions to the advective-dispersive equations. Whelan (1996) presented a discussion that illustrates the inherent difficulties associated with utilizing partition coefficients as the sole parameter to define the geochemical properties of a solute as it migrates through a subsurface environment. Multiple definitions for  $K_d$  values have been identified, including those based on thermodynamics (*e.g.*, Gibbs free energy of formation), experiments (*e.g.*, batch and flow-through tests), and theory (*e.g.*, isotherms). Each of these procedures identifies a different value for the same parameter, which is supposed to describe the same phenomena. Although  $K_d$  values can be thermodynamically defined, their meaning becomes less clear in the real world. As such,  $K_d$  values can be estimated using transport models. This process, called calibrating a groundwater transport model to  $K_d$  values, involves treating the  $K_d$  value as the adjustable parameter (or dependent variable) while simulating known monitored contaminant data. Groundwater calibration captures the essence of the problem in the field. This is an iterative process that frequently requires that the magnitude of a number of other input parameters, such as effective porosity, dispersion, and flow rate, be adjusted to yield meaningful  $K_d$  values. A  $K_d$  value represents one of the calibration parameters because its magnitude is subject to not only the laboratory analyses but also to the heterogeneity in the field and different ways it is used in the mathematical constructs of different models.

### 4.2 Calibration: Location, Arrival Time, and Concentration

When calibrating a groundwater model to monitored information (*e.g.*, concentrations at a monitoring well), the model must predict the correct arrival time at the correct location, matching the magnitude of the monitored concentration. Therefore, time, location and magnitude are 3 crucial elements associated with any calibration exercise, and  $K_d$  impacts two of them (*i.e.*, travel time and magnitude). Location is predetermined by the user with respect to monitoring wells, receptor locations, *etc.* Once the distances have been defined, the calibration requires modifications to parameters that govern travel times and concentration levels. Parameters, which influence water and contaminant movement, are varied within acceptable ranges in an attempt to recreate conditions in the field. As the model complexity increases, the number of parameters that the analyst can vary increases, and the calibration process becomes increasingly more complicated. Figure 4.1 illustrates the relative relationships between input-data quality, output uncertainty, and types of problems addressed by each level of assessment. As Figure 4.1 indi-

---

<sup>1</sup> A list of acronyms, abbreviations, symbols, and notation is given in Appendix A. A list of definitions is given in Appendix B

95

cates, the computational requirements tend to be less at the earlier stages of an assessment when available data are less, and, correspondingly, the uncertainty with the output results tends to be greater. As the assessment progresses, improved site-characterization data and conceptualization of the problem increase, thereby reducing the overall uncertainty in risk estimates.

Figure 4.1 also illustrates some of the characteristics and relationships between screening-level (ranking), “analytical” (prioritization and preliminary assessments), and numerical (detailed) models.

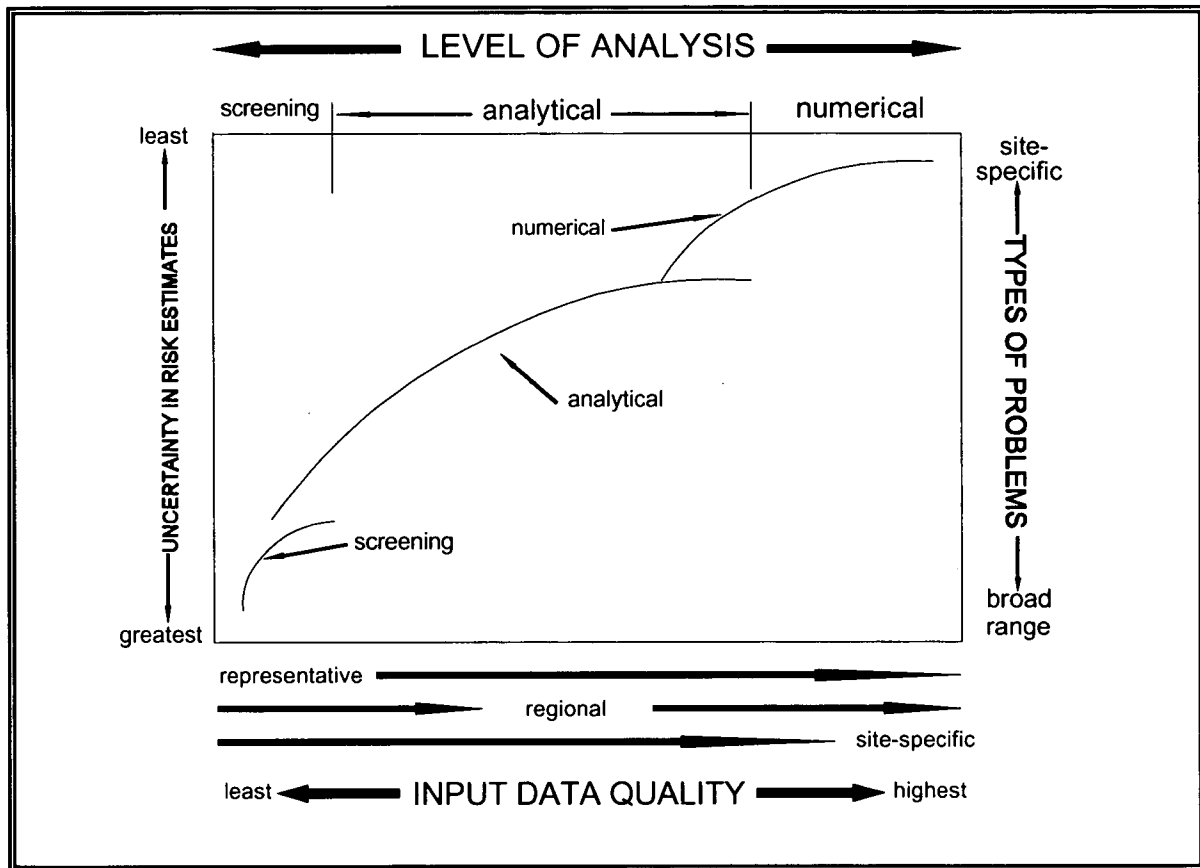


**Figure 4.1.** Relative relationships between input-data quality, output uncertainty, and types of problems addressed by each level of assessment.

96

Screening models are used to identify environmental concerns. These models, often based on a structured-value approach, are designed to be used with regional/representative information. Models such as the Hazard Ranking System (HRS) (EPA, 1984, 1992b) divide site and release characteristics into predetermined categories that are assigned a point value based on answers to questions. The score from such systems is useful to determine if a situation requires further analysis, but not to provide a method for estimating actual concentrations or impacts in the environment.

Detailed analyses require a highly specialized assessment of potential impacts. Detailed analyses are usually reserved for the most complex models, are data intensive, and are based on the expertise of the analyst. These detailed assessment models are used to address complex problems and concerns that are relatively well-defined. Models for detailed analyses tend to focus on special sets of problems and special types of situations. Although detailed assessment tools are appropriate for their intended application, extension beyond the site-specific application is often difficult or cost prohibitive. Typical models include MODFLOW (McDonald and Harbaugh, 1988) and CFEST (Cole *et al.*, 1988).

Analytically/semianalytically/empirically based models (designated as “analytical” models in Figure 4.1) can be utilized for prioritization or preliminary assessments and exist between initial-screening and highly specialized numerical models. These physics-based models are the most versatile as they do not have the data constraints associated with the numerical models. The analytical models may contain some numerical computations, hence the semianalytical designation. As Figure 4.1 illustrates, the analytical models are designed to provide environmental evaluations over a wide range of applications. Groundwater models that fall into this category include AT123D (Yeh, 1981), GROUND and GRDFLX (Codell *et al.*, 1982), and MEPAS (Buck *et al.*, 1995; Whelan *et al.*, 1992). The analytical-assessment models are codes with physics-based algorithms whose components can be utilized in a detailed (*i.e.*, numerical) or an initial-screening (*i.e.*, ranking/prioritization) assessment, where data and circumstances warrant.

The calibration process is an interactive one. Because data tend to be limiting, there are generally multiple ways in which parameters can be combined so the simulation results match monitored information. With increasing number of monitored data available, less combinations of the modeling parameters are possible to match the monitored information. In addition, many of these “matches” can assign unrealistic values to parameters; therefore, the number of acceptable possible combinations becomes even more limited. When calibrating, parameters can only be varied within ranges that physically make sense for the site and its conditions. If unrealistic output is a result of the analysis, then the (1) conceptual site model has to be re-evaluated, (2) input data must be re-examined, and/or (3) model must be re-evaluated to ensure that the assessment does not violate the assumptions, limitations, and constraints associated with the mathematical constructs of the code.

Each code has its own mathematical equations upon which it is based. A calibration exercise is performed to meet the constructs of these equations. Analytical models tend to be easier to work

with because of their closed-form, explicit solutions. With an analytical model, some initial calculations can be made that can provide an initial starting point for the calibration process; this process also illustrates how retardation factors (and ultimately  $K_d$ ) influence the calibration process. As noted earlier, the intent of the calibration process is to get a contaminant from a source to the monitored location (e.g., monitoring well) at the proper time with the appropriate concentration. In addition, the amount of mass monitored in the environment must be conserved, that is, the amount of mass predicted by the model to be in the environment should match the amount of mass monitored in the environment.

Travel times are influenced by the retardation factor, pore-water velocity, and dispersivity, although other parameters can also influence the outcomes. The retardation factor can be directly impacted by  $K_d$ . In the vadose zone, soil type and moisture content influence pore-water velocity, and in the saturated zone, soil type and effective porosity influence pore-water velocity. Longitudinal dispersivity normally influences the time to peak but by no more than 10 percent, although more is possible. Concentrations are generally influenced by the contaminant flux rate (or total mass released into the environment), mixing distances (dilution), pore-water velocity (dilution), retardation factor ( $K_d$ ), and dispersivity (dispersion). If the size of the source is not well known, the areal extent of contamination influences concentration levels for spatially near-field problems. In any modeling exercise, the analyst will know some of the general characteristics of the parameters. Typically, the parameters that are used to calibrate the model are not known exactly; therefore, they can be modified within an appropriate range to help the analyst capture the essence of the problem.

### 4.3 Illustrative Calculations to Help Quantify $K_d$ Using Analytical Models

If  $K_d$  forms the basic premise for retarding the movement of contaminants in a subsurface environment in the mathematical algorithms of a groundwater transport code, then the  $K_d$  permeates all of the contaminant transport calculations. Different computer codes may use different mathematical constructs, but the influence of  $K_d$  is usually very pronounced. The  $K_d$  value influences the calculations for determining the (1) contaminant travel time, (2) mass of contamination at the source or in a plume, and (3) distribution of the concentration in the environment. As an illustration of the impact that the  $K_d$  parameter can have in transport calculations, the influences of  $K_d$  on an analytical solution to the advective-dispersive equation are explored.

#### 4.3.1 Governing Equations

The 1-dimensional advective, 3-dimensional dispersive equation with first-order degradation/decay can be expressed as follows:

$$\frac{\partial C_i}{\partial t} + v \frac{\partial C_i}{\partial x} = D_x \frac{\partial^2 C_i}{\partial x^2} + D_y \frac{\partial^2 C_i}{\partial y^2} + D_z \frac{\partial^2 C_i}{\partial z^2} - \lambda C_i \quad (4.1)$$

in which

$$v^* = \frac{v_p}{R_f} \quad (4.2)$$

$$v_p = \frac{v_d}{n_e} \quad (4.3)$$

$$R_f = 1 + \frac{\rho_b K_d}{n_e} \quad \text{saturated} \quad (4.4)$$

$$R_f = 1 + \frac{\rho_b K_d}{\theta_{vz}} \quad \text{vadose} \quad (4.5)$$

$$K_d = \frac{A_i}{C_i} \quad (4.6)$$

$$D^* = \frac{D_{mech} + D_{mol}}{R_f} \quad (4.7)$$

$$D_{mech} = \theta v_p \quad (4.8)$$

- where
- $C_i$  = dissolved concentration
  - $v^*$  = contaminant velocity
  - $D^*$  = dispersion coefficient in the x, y, and z directions adjusted for retardation with the retardation factor
  - $\lambda$  = first-order degradation/decay coefficient
  - $v_p$  = pore-water velocity
  - $v_d$  = Darcy velocity
  - $R_f$  = retardation factor
  - $n_e$  = effective porosity
  - $\rho_b$  = bulk density
  - $\theta_{vz}$  = moisture content in the vadose zone
  - $K_d$  = partition (distribution) coefficient
  - $A_i$  = adsorbed contaminant concentration on the soil particles
  - $D_{mech}$  = mechanical dispersion
  - $D_{mol}$  = molecular diffusion coefficient

$\alpha$  = dispersivity in the x, y, or z direction

The solution of advective-dispersive equation for an instantaneous release through a point source in a saturated zone, which is uniformly mixed in the vertical direction, at a distance (x) down gradient from the center of the source is as follows (Codell *et al.*, 1982; Fischer *et al.*, 1979; Whelan *et al.*, 1996; Yeh and Tsai, 1976; Yeh 1981):

$$C_i = \alpha' X_{Gf} Y_{Gf} Z_{Gf} \quad (4.9)$$

where  $\alpha'$  = mass-related constant  
 $X_{Gf}$ ,  $Y_{Gf}$  and  $Z_{Gf}$  = Green's functions (which are orthogonal) in the x, y, and z directions, respectively  
 $X_{Gf}$  = Green's function corresponding to flow direction

in which

$$\alpha' = \frac{M_{rel}}{R_f n_e} \quad (4.10)$$

$$X_{Gf} = \left( \frac{1}{4 \alpha D_x t} \right)^{1/2} \exp(-\alpha x t) \exp \left[ - \left( \frac{(x - v_p t)^2}{4 D_x t} \right) \right] \quad (4.11)$$

$$Y_{Gf} = \left( \frac{1}{4 \alpha D_y t} \right)^{1/2} \exp \left[ - \left( \frac{y^2}{4 D_y t} \right) \right] \quad (4.12)$$

$$Z_{Gf} = \frac{1}{h_m} \quad (4.13)$$

where  $M_{rel}$  = released mass  
 $y$  = off-centerline distance  
 $h_m$  = mixing-zone thickness

and all other parameters retain their previous definitions.

The impact that the retardation factor and, hence,  $K_d$  has on the calculated value of the concentration at the receptor location can be profound, as illustrated by the number of locations that these terms appear in the governing equations.

100

### 4.3.2 Travel Time and the Partition Coefficient

As previously noted, it is very important to ensure that the contaminant arrives at the monitoring location at the appropriate time, and  $K_d$  can have a profound impact on the travel time. The advective travel time of the contaminant is defined as the distance  $x$  traveled divided by the contaminant velocity:

$$t_T = \frac{x}{v} \quad (4.14)$$

where  $t_T$  = total advective travel time of the contaminant

If a contaminant is traveling from a contaminated source through a vadose zone, through a saturated zone to a monitoring location, the total advective travel time is the summation of the travel times through the vadose ( $t_{vz}$ ) and saturated ( $t_{sat}$ ) zones:

$$t_T = t_{vz} + t_{sz} = \left( \frac{H_1 R_{f1}}{v_{p1}} \right) + \left( \frac{x_2 R_{f2}}{v_{p2}} \right) \quad (4.15)$$

where  $H_1$  = thickness of the vadose zone  
subscripts 1 and 2 = vadose and saturated zones, respectively

Substituting the definitions for retardation factor gives a slightly modified equation:

$$t_T = \frac{(H_1) \left( 1 + \frac{b_1 K_{d1}}{n_{vz}} \right)}{v_{p1}} + \frac{(x_2) \left( 1 + \frac{b_2 K_{d2}}{n_2} \right)}{v_{p2}} \quad (4.16)$$

This equation demonstrates the potential impact that  $K_d$  has on the travel time. Because  $K_d$  is assumed to be constant over the distance traveled, a constant,  $\alpha$ , can be defined, which represents the ratio of the partition coefficients between the vadose and saturated zones:

$$\alpha = \frac{K_{d1}}{K_{d2}} \quad (4.17)$$

Substituting  $\alpha$  into the total travel time equation gives the travel time as a function of the saturated zone's partition coefficient:

$$t_T = \left( \frac{H_1}{v_{p1}} \right) \left( 1 + \left( \frac{b_1}{n_{vz}} \right) \alpha K_{d2} \right) + \left( \frac{x_2}{v_{p2}} \right) \left( 1 + \left( \frac{b_2}{n_{e2}} \right) K_{d2} \right) \quad (4.18)$$

(10)

Rearranging this equation and solving for  $K_{d2}$  gives:

$$t_T \left( \frac{H_1}{v_{p1}} \right) \left( \frac{H_1 \theta_{b1}}{v_{p1} \theta_{vz}} \frac{x_2 \theta_{b2}}{v_{p2} n_{e2}} \right) (K_{d2}) \left( \frac{x_2}{v_{p2}} \right) \quad (4.19)$$

$$K_{d2} = \frac{t_T \left( \frac{H_1}{v_{p1}} \right) \left( \frac{x_2}{v_{p2}} \right)}{\left( \frac{H_1 \theta_{b1}}{v_{p1} \theta_{vz}} \right) \left( \frac{x_2 \theta_{b2}}{v_{p2} n_{e2}} \right)} \quad (4.20)$$

This equation can be used to estimate initial values for the partition coefficients in the vadose and saturated zones, which will help ensure that the contaminant reaches the monitoring location at the appropriate time. These values can also be compared to literature or experimental values to see if they are consistent. If not, then the conceptual site model must be re-analyzed to ensure that the proper problem has been captured or that the appropriate data are being utilized.

### 4.3.3 Mass and the Partition Coefficient

The partition coefficient can be used to help estimate the mass of contamination that exists at the source or in a plume. The reported soil contamination in the vadose zone is usually expressed as the adsorbed concentration ( $A_i$ ) and typically has units of mg/kg, which is also expressed as ppm (parts per  $10^6$ ). The aqueous concentration ( $C_i$ ), using  $K_d$  as a conversion factor, can be calculated as follows:

$$C_i = \frac{A_i}{K_d} \quad (4.21)$$

The mass associated with the adsorbed phase in the vadose zone can be estimated as:

$$M_{ads} = V_{source} A_i (1 - n) \rho_{particle} \quad (4.22)$$

where  $M_{ads}$  = mass associated with the adsorbed phase in the vadose zone  
 $V_{source}$  = volume associated with the contaminated source  
 $n$  = total porosity  
 $\rho_{particle}$  = particle density

The mass associated with the aqueous phase in the vadose zone can be estimated as:

$$M_{aq} = \frac{V_{source} A_i \theta_{vz}}{K_d} \quad (4.23)$$

102

where  $M_{aq}$  = mass associated with the aqueous phase in the vadose zone

The total mass associated with the vadose zone represents the summation of the mass associated with the adsorbed and aqueous phases, assuming no free product:

$$M_{\text{vadose}} = (M_{\text{ads}} + M_{\text{aq}})_{\text{vadose}} \quad (4.24)$$

where  $M_{\text{vadose}}$  = total mass associated with the vadose zone

The reported aqueous contamination in the saturated zone is usually expressed as the dissolved concentration  $C_i$  and typically has units of mg/l, which is also expressed as ppm (parts per  $10^6$ ). The mass associated with the aqueous phase in the saturated zone can be estimated as:

$$M_{\text{aq}} = V_{\text{source}} C_i n \quad (4.25)$$

The mass associated with the adsorbed phase in the saturated zone can be estimated as:

$$M_{\text{ads}} = V_{\text{source}} C_i K_d (1 - n) \rho_{\text{particle}} \quad (4.26)$$

The total mass in the vadose zone represents the summation of the mass associated with the adsorbed and aqueous phases, assuming no free product:

$$M_{\text{saturated}} = (M_{\text{ads}} + M_{\text{aq}})_{\text{saturated}} \quad (4.27)$$

where  $M_{\text{saturated}}$  = total mass associated with the saturated zone

The total mass in the system is the summation of the masses in the vadose and saturated zones:

$$M_{\text{Total}} = M_{\text{vadose}} + M_{\text{saturated}} \quad (4.28)$$

If the environmental contamination in the vadose zone is expressed as a total mass in the waste site (or layer) per dry weight of soil, the dissolved and adsorbed concentrations can be calculated as follows (Whelan *et al.*, 1987):

$$C_i = \frac{C_{Tp} \rho_b}{\rho_{\text{vz}} \rho_b K_d} \quad (4.29)$$

$$A_i = \frac{C_{Tp} \rho_b K_d}{\rho_{\text{vz}} \rho_b K_d} \quad (4.30)$$

where  $C_{Tp}$  = total mass at the site per dry weight of soil

If the environmental contamination is expressed as a total mass per total volume of the waste site (or soil layer), the dissolved and adsorbed concentrations can be calculated as follows (Whelan *et al.*, 1987):

$$C_i = \frac{C_T}{\nu_z + \nu_b K_d} \quad (4.31)$$

$$A_i = \frac{C_T K_d}{\nu_z + \nu_b K_d} \quad (4.32)$$

where  $C_T$  = total mass at the site per total site volume

#### 4.3.4 Dispersion and the Partition Coefficient

The 1-dimensional, dispersive equation in the lateral direction can be expressed as

$$\frac{\partial C_i}{\partial t} = D_y \frac{\partial^2 C_i}{\partial y^2} \quad (4.33)$$

where all of the terms are as previously defined. For an instantaneous release from a unit area in an aquifer of infinite lateral extent, the time-varying concentration as a function of lateral distance off the center line can be expressed as follows:

$$C_i = \left( \frac{M_A}{\sigma_{sd} (2\pi)^{1/2}} \right) \exp \left[ - \left( \frac{y^2}{2\sigma_{sd}^2} \right) \right] \quad (4.34)$$

in which

$$\sigma_{sd} = (2 D_y t)^{1/2} = \left( \frac{2 D_y t}{R_f} \right)^{1/2} \quad (4.35)$$

$$D_y = \nu_y v_p \quad (4.36)$$

where  $M_A$  = instantaneous mass released per unit area (*i.e.*, instantaneous point-source release)  
 $\sigma_{sd}$  = standard deviation associated with the Gaussian solution

Note that the standard deviation (*i.e.*, the degree of lateral spreading) is a function of the retardation factor and, hence,  $K_d$ .

104

To gain an understanding of the impact of the retardation factor (and  $K_d$ ) on simple advective-dispersive systems, the impact of retardation at a location,  $x$ , can be discerned by substituting the time,  $t$ , with the advective travel time, as follows:

$$t = \frac{x R_r}{v_p} \quad (4.37)$$

$$\sigma_{sd} = (2 \sigma_y x)^{1/2} \quad (4.38)$$

The standard deviation that indicates the degree of spread at location  $x$  is independent of the retardation factor and  $K_d$ . This phenomenon is expected because when combined with flow in the longitudinal direction, advection impacts the effects of dispersion in the lateral direction. In effect, advection transports the contaminant in the longitudinal direction, so there is no infinite dispersion at any location in the lateral direction. Hence, Gaussian plumes grow as they migrate down gradient. Unlike the contaminant travel time, the dispersive phenomenon is not closely tied to  $K_d$ .

#### **4.4 Modeling Sensitivities to Variations in the Partition Coefficient**

Because the retardation factor and partition coefficient permeate many aspects associated with the mathematical algorithms for contaminant transport in the subsurface environment,  $K_d$  can have a significant impact on the outcome of any modeling exercise. Under certain circumstances though,  $K_d$  can have very little impact on the outcome. The next 2 sections discuss the conditions under which partition coefficients influence the outcome.

1. Relationship Between Partition Coefficients and Risk -- This section explores the situations under which variations in  $K_d$  can have a significant influence on simulated groundwater concentrations and, hence, risk.
2. Partition Coefficient as a Calibration Parameter in Transport Modeling -- This section presents an illustrative example of a calibration exercise where the calibration parameter is the partition coefficient.

##### **4.4.1 Relationship Between Partition Coefficients and Risk**

The  $K_d$  parameter potentially has a very large impact on the mobility of constituents in a subsurface environment. When combined with other phenomena (*e.g.*, degradation/decay, dispersion, pore-water velocity),  $K_d$  can have a significant impact by redistributing the contaminant both spatially and temporally.

For example, when the  $K_d$  parameter is sufficiently large, the contaminant moves slowly from the source to the receptor. Because significant levels of contaminant have not reached the receptor

within the receptor's lifetime, the risks over the lifetime are low. If the value of the  $K_d$  parameter is increased (*i.e.*, its mobility decreased even further), the risks are still low because the contaminant still has not reached the receptor. However, if the  $K_d$  parameter is sufficiently small, the contaminants arrive very quickly, and the receptors are exposed within their lifetime.

Different methods were presented in the previous section for determining  $K_d$ , and 4 different retardation factors were presented, which were based on  $K_d$ . Because different models use different formulations for the retardation factor, pore-water velocity, or contaminant velocity, the same  $K_d$  will produce different simulation results by the different models. As one can imagine, there are no accurate generalizations that can be made with regard to defining  $K_d$ ; as such, it tends to represent a calibration parameter in computer models. Because any modeling exercise (conceptually, physically, and mathematically) represents a simplification of the real world, many phenomena unknown or misunderstood are lumped into the parameters upon which modeling is based.  $K_d$  represents one of those parameters, where known and many unknown phenomena are lumped; as such,  $K_d$  tends to lose some of its meaning in the modeling world, although it retains its full meaning in the laboratory.

In the laboratory,  $K_d$  is determined under carefully controlled conditions; all aspects of the experiments are controlled to ensure accuracy in the experimental exercise. The real world does not afford the luxury of controlling the environment; therefore, the conditions surrounding the sorption phenomenon must be estimated. Unfortunately, site conditions may not be adequately described by sampling. Moreover, the identification of a single representative  $K_d$  value for a site may be impossible due to the large heterogeneities of the site's subsurface system.

#### ***4.4.2 Partition Coefficient as a Calibration Parameter in Transport Modeling***

Calibrations do not necessarily ensure that the simulated results capture the essence of the transport phenomena. For example, Figures 4.2 and 4.3 present the results of a calibration using the MEPAS model to monitored data.<sup>1</sup> Each figure presents time-varying <sup>90</sup>Sr concentrations. Figure 4.2 presents MEPAS simulation with a  $K_d$  equaling 0.4 ml/g (*i.e.*, solid line and no symbols) and a simulation with  $K_d$  equaling 0.8 ml/g (*i.e.*, solid line with open triangles). The solid triangle represents the monitored data, identifying in a concentration of 220 pCi/l at year 27. As Figure 4.2 shows, the "0.8" calibration is precise and passes directly through the monitored data (*i.e.*, an exact match). The "0.4" simulation does not appear to capture the essence of the problem, as it predicts a concentration of 55,600 pCi/l at year 27. The "0.4" simulation seems to have over predicted the concentration by over 2 orders of magnitude. The significant difference in the peak concentration between the 2 simulations were the result of a minor change in  $K_d$  (*i.e.*, changes in the tenths place).

---

<sup>1</sup> The MEPAS simulations were based on actual site data published in Lewis *et al.* (1994) for the CERCLA hazardous waste site ST-19. Only the contaminant information was changed. Radionuclides were never present at the site; they are only used here as an illustrative example.

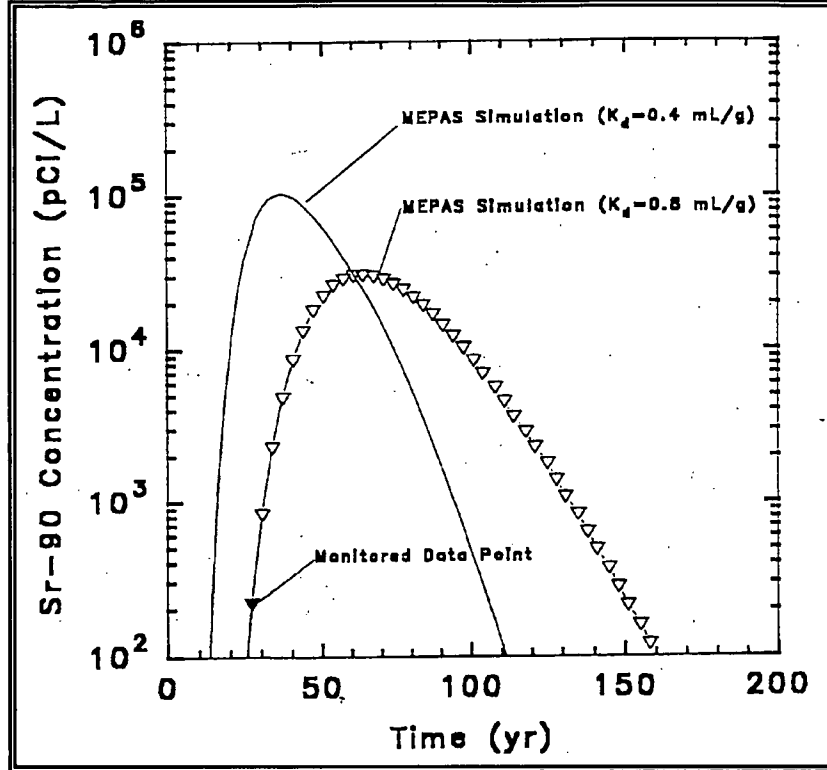
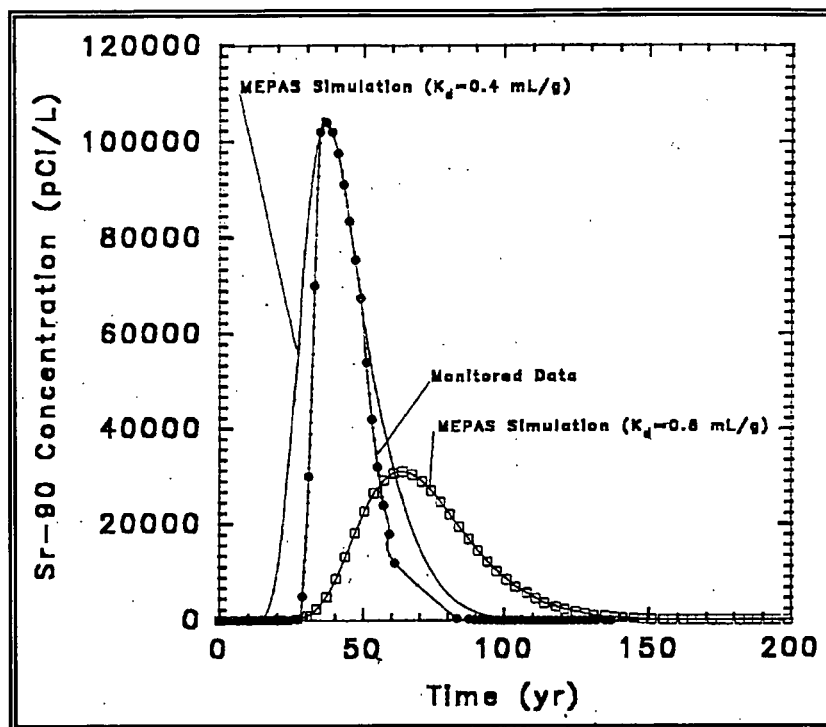


Figure 4.2. Example illustrating a MEPAS <sup>90</sup>Sr calibration with  $K_d$  equaling 0.8 ml/g and 1 monitored-data point.

Figure 4.3 presents the entire curve that is defined by monitored data, which includes the single data point from Figure 4.2. The monitored data in Figure 4.3 are presented as solid circular symbols. When all of the time-varying monitored data are considered in the assessment, the MEPAS simulation with a  $K_d$  equaling 0.4 ml/g appears to have captured the essence of the shape of the monitored data more accurately than the results associated with the 0.8 ml/g simulation. Although the “0.4” simulation does not precisely capture the entire shape of the monitored-data curve, it has captured the peak information, which usually is considered to be most important. Figure 4.3 illustrates the difficulty of calibrating a groundwater model to a single data point or a set of points that are not well distributed in time. Although the “0.8” simulation captured the single data point, it completely missed the peak concentrations and the time to peak. Because only 1 monitored data point is used in the calibration, an unlimited number of curves could have been simulated to pass through the monitored data point.



**Figure 4.3.** Example illustrating MEPAS  $^{90}\text{Sr}$  calibrations with  $K_d$  equaling 0.4 and 0.8 ml/g and several monitored-data points.

Figure 4.3 illustrates that minor changes in  $K_d$  (*i.e.*, in the tenths place) can result in significant changes in simulation results. The concentrations between simulations at year 27 varied by over 2 orders of magnitude. The peak concentration decreased from 104,000 pCi/l to 31,000 pCi/l by increasing the  $K_d$  by only 0.4 ml/g. One simulation is over 5 times the drinking water limit of 20,000 pCi/l, while the other simulation is nearly equal to this limit. If the "0.8" results were assumed to be correct, the assessment would have underestimated the impacts by a factor of 3.4. Although the difference between 0.4 and 0.8 mg/l does not appear to be large, these results do illustrate the difficulties in using  $K_d$  and other parameters in the calibration process. These results also suggest that the discrepancy between "calibrated" simulations and limited data could be much larger (*i.e.*, orders of magnitude).

#### 4.5 Summary

Various sections in this report have illustrated that there are many definitions for  $K_d$  (*e.g.*, theoretical, analytical, experimental, thermodynamic, *etc.*), all resulting with different values. The results presented in Figures 4.2 and 4.3 should represent a sobering reminder of the difficulties associated with groundwater assessments using partition coefficients. In many instances, a groundwater simulation is performed with no calibration at a site using  $K_d$  values that

have been obtained from "peer-reviewed" literature. The analyst tries to match soil types and environmental conditions with their site when "selecting" an appropriate  $K_d$ . It must be emphasized that these  $K_d$  values are unrelated to the actual site and only represent the laboratory conditions reported in the literature; they do not represent actual conditions at the site under investigation. The peer-reviewed values only provided an idea as to the possible magnitude associated with the  $K_d$  value. Different geochemical conditions, some known and unknown, exist between the actual site and those reported in the literature. The difficulty in using existing literature numbers is that the phrase "peer-reviewed literature" tends to lend too much credibility to these potentially inappropriate  $K_d$  values.

## 5.0 Application of Chemical Reaction Codes

### 5.1. Background

Determination of species distributions for dissolved major and trace constituents, including radionuclides, is necessary to understand the processes that control the chemistry of soil-water systems. Several processes will control the thermodynamic activities of dissolved species and, to some extent, their mobility in surface and ground waters and bioavailability to man. These processes are described in detail in Chapter 2 and references cited therein. The processes include the following:

- Aqueous complexation
- Oxidation/reduction
- Adsorption/desorption
- Mineral precipitation/dissolution

The distribution of aqueous species in a multi-component chemical system, such as those in soil-water environments, can only be reliably calculated from a combination of accurate analyses of water compositions and a competent chemical reaction model. Computerized chemical reaction models based on thermodynamic principles may be used to calculate these processes depending on the capabilities of the computer code and the availability of thermodynamic and/or adsorption data for aqueous and mineral constituents of interest. Use of thermodynamic principles to calculate geochemical equilibria in soil-water systems is well established and described in detail in many reference books, such as Bolt and Bruggenwert (1978), Garrels and Christ (1965), Langmuir (1997), Lindsay (1979), Morel (1983), Nordstrom and Munoz (1985), Sposito (1989, 1994), Stumm and Morgan (1981), and others. The reader is referred to these sources for detailed discussions and examples of specific applications relative to the thermodynamic principles and equations that govern these calculations.

Because of the great importance of the aqueous speciation, adsorption, and solubility processes relative to the concentrations and mobility of contaminants that may leach from waste, an understanding of the capabilities and application of chemical reaction models is essential. This understanding is additionally important because these models are used for both the scientific and legal aspects of risk and performance assessment studies of waste disposal and mitigation of environmental contamination.

The purpose of this chapter is to provide a brief conceptual overview of chemical reaction codes and their use in addressing technical defensibility issues associated with data from  $K_d$  studies. Particular attention is given to the capabilities of EPA's MINTEQA2 code, including the types of conceptual models the code contains to quantify adsorption. Issues pertaining to the availability of databases for these adsorption models and the status of the MINTEQA2 aqueous speciation and solubility database for radionuclides are also discussed.

### 5.1.1 Definition of Chemical Reaction Modeling

Chemical reaction models/codes are referred to by several terms in the literature. The term may include either of the adjectives "chemical" or "geochemical," often depending on the technical field of expertise of the author and/or anticipated audience. Additionally, the models/codes can be referred to as reaction, equilibrium, speciation, or mass transfer<sup>1</sup> (and others) models/codes, although some of these terms refer to submodel capabilities. Throughout this report, the terms "chemical reaction models" and "chemical reaction codes" will be used as collective terms for all variations of these models and codes.

A chemical reaction model is defined here as the integration of mathematical expressions describing theoretical concepts and thermodynamic relationships on which the aqueous speciation, oxidation/reduction, precipitation/dissolution, and adsorption/desorption calculations are based. A chemical reaction code refers to the translation of a chemical reaction model into a sequence of statements in a particular computer language. We define a competent chemical reaction model as a model that contains all the necessary submodels and important aqueous complexes, solids and gases for the important elements of interest required to adequately interpret a given data set.

Most chemical reaction models are based on equilibrium conditions, and contain limited or no kinetic equations in any of their submodels. Some processes, such as aqueous speciation and cation or anion exchange, are closely approximated by equilibrium conditions over short time frames of hours to days. On the other hand, kinetic factors may limit other processes, such as some precipitation/dissolution and redox-sensitive reactions, from reaching equilibrium over reaction periods of tens of years or more. Moreover, without information or assumptions regarding the rate of release of the contaminant of interest from its source term, such as contaminated soils or a decommissioning site, modeling calculations cannot provide an estimate of the total mass (*i.e.*, mass present in aqueous solution plus associated mineral phases) of a contaminant released in the environment under review. At best, chemical modeling based on equilibrium conditions may provide estimates of bounding limits for some processes depending on the reactions being considered. Because of the limited availability of kinetic data and incorporation of kinetic algorithms into chemical reaction codes, this is an important area for future experimental studies and development of chemical reaction models. Readers are referred to references on reviews of chemical reaction models cited later in this chapter for more details on this issue.

Because thermodynamic data typically do not have the resolution to distinguish among different isotopic forms of contaminant-containing aqueous species or solids, geochemical modeling

---

<sup>1</sup> *Mass transfer* is the transfer of mass between 2 or more phases that includes an aqueous solution, such as the mass change resulting from the precipitation of a mineral or adsorption of a metal on a mineral surface. In contrast, *mass transport* is the time-dependent movement of one or more solutes during fluid flow.

calculations do not provide any information on the distribution of the different contaminant isotopes present in the aqueous, gaseous, or associated solid phases. However, in most situations, radionuclide isotopes will react the same as natural (stable) isotopes of the element. By assuming ideal isotopic mixing or exchange, one can estimate the distribution of any selected isotopes among the bulk elemental distribution.

### 5.1.2 Reviews of Chemical Reaction Models

Numerous reviews of chemical reaction codes have been published. Some of the more extensive reviews include those by Jenne (1981), Kincaid *et al.* (1984), Mercer *et al.* (1981), Nordstrom *et al.* (1979), Nordstrom and Ball (1984), Nordstrom and Munoz (1985), Potter (1979), and others. These reviews have been briefly described in Serne *et al.* (1990). The reviews discuss issues such as:

- Basic mathematical and thermodynamic approaches that are required to formulate the problem of solving geochemical equilibria in aqueous solutions
- Applications for which these codes have been developed and used, such as the modeling of adsorption equilibria, complexation and solubility of trace metals, equilibria in brine solutions and high-temperature geothermal fluids, mass transfer, fluid flow and mass transport, and redox balance of aqueous solutions
- Selection of thermodynamic data and development of thermodynamic databases
- Limitations of chemical reaction codes, such as the testing of the equilibrium assumption, application of these models to high-ionic strength aqueous solutions (*e.g.*, the ion association versus ion interaction conceptual models), the reliability of thermodynamic databases, and the use of validation to identify inadequacies in the conceptual models developed with chemical codes.

Table 5.1 provides a sampling of some chemical reaction codes that have been described in the literature and mentioned in published proceedings, such as Erdal (1985), Jackson and Bourcier (1986), Jacobs and Whatley (1985), Jenne (1979), Loeppert *et al.* (1995), Melchior and Bassett (1990), and the reviews cited above. The reader is directed to these published proceedings and reviews for the appropriate reference to the documentation of each code. Although this list of chemical reaction models is not meant to be complete and continues to expand each year, it demonstrates the diversity of codes that exist, and, in some cases, the evolution of some codes.

**Table 5.1.** Chemical reaction models described in the literature.

ADSORP	EQUIL	MINTEQ	SOILCHEM
AION	EQUILIB	MINTEQA1	SOLGASWATE
ALCHEMI	EVAPOR	MINTEQA2	R
AQ/SALT	FASTCALC	MIRE	SOLMNEQ
ASAME	FASTPATH	MIX2	SOLMNEQ.88
BALANCE	GEOCHEM	NOPAIR	SOLVEQ
C-Salt	GEOCHEM-PC	PATH	SYSTAB
CHEMIST	GIBBS	PATHCALC	THERMAL
CHEMTRN	GMIN	PATHI	WATCH1
CHES	HALTAFALL	PHREEQE	WATCHEM
COMICS	HARPHRQ	PHRQPITZ	WATEQ
DISSOL	HITEQ	REDEQL	WATEQ2
ECES	HYDRAQL	REDEQL.EPAK	WATEQ3
ECHEM	IONPAIR	REDEQL2	WATEQ4F
EHMSYS	KATKHE	RIVEQL	WATEQF
EQ3	KATKLE1	SEAWAT	WATEQFC
EQ3NR	MICROQL	SENECA	WATSPEC
EQ6	MINEQL	SENECA2	
EQBRAT	MINEQL2	SIAS	

Nordstrom and Ball (1984) discuss the issue of why so many chemical reaction codes exist. They attribute this diversity of codes to (1) the lack of availability, (2) inadequate documentation, (3) difficulty of use of some chemical codes, and (4) the wide variety of calculational requirements that include aqueous speciation, solubility, and/or adsorption calculations for aqueous systems that range from simple, chemical systems associated with laboratory experiments to complex, multi-component systems associated with natural environments. No single code can do all of the desired calculations in a perfectly general way. Typically the more general and comprehensive a geochemical code is, the more difficult and costly it is to use. Another factor may be that scientists are inherently reluctant to use any computer code that they and their immediate coworkers have not written.

### *5.1.3 Speciation-Solubility Versus Reaction Path Codes*

Jenne (1981) divides chemical reaction codes into 2 general categories: aqueous speciation-solubility codes and reaction path codes. All of the aqueous speciation-solubility codes may be

used to calculate aqueous speciation/complexation,<sup>1</sup> and the degree of saturation (*i.e.*, saturation index) of the speciated composition of the aqueous solution with respect to the solids in the code's thermodynamic database. Some aqueous speciation-solubility codes also include the capabilities to calculate mass transfer between a single initial and final state, that results from mineral precipitation/dissolution and/or adsorption/desorption reactions. Chemical reaction codes, such as WATEQ, REDEQL, GEOCHEM, MINEQL, MINTEQ, and their later versions, are examples of codes of this type.

Reaction path codes include the capabilities to calculate aqueous speciation and the degree of saturation of aqueous solutions, but also permit the simulation of mass transfer due to mineral precipitation/dissolution or adsorption onto adsorbents as a function of reaction progress. Typical applications include the modeling of chemical changes associated with the interaction of a mineral assemblage and ground water (*e.g.*, INTERA, 1983, and Delany, 1985) or the release of radionuclides from a proposed glass waste form (*e.g.*, Bourcier, 1990) as a function of time. Computationally, 1 unit of reaction progress means that 1 unit of gaseous or solid reactant (*e.g.*, radioactive waste source term) has reacted with an aqueous solution in contact with solid phases with which the solution is already in equilibrium. At each step of reaction progress, the code calculates the changes or path of mineral and gaseous solubility equilibria that are constraining the composition of the aqueous solution, the masses of minerals precipitated and/or dissolved to attain equilibrium, and the resulting composition of the aqueous solution. Examples of reaction path codes include the PHREEQE, PATHCALC, and the EQ3/EQ6 series of codes.

#### ***5.1.4 Adsorption Models in Chemical Reaction Codes***

Various adsorption models have been incorporated into a small number of chemical reaction codes to calculate the mass of a dissolved component adsorbing on a user-specified mineral phase, such as iron hydroxide that coat mineral grains in soil. The adsorption modeling capabilities in these codes have been briefly reviewed by others (*e.g.*, Goldberg, 1995, and Davis and Kent, 1990) and will not be duplicated here. The options vary from code to code. Adsorption models incorporated into chemical reaction codes include non-electrostatic, empirical models as well as the more mechanistic and data intensive, electrostatic, surface complexation models. Examples of non-electrostatic models include the partition (or distribution) coefficient ( $K_d$ ), Langmuir isotherm, Freundlich isotherm, and ion exchange models. The electrostatic, surface complexation models (SCMs) incorporated into chemical reaction codes include the diffuse layer model (DLM)

---

<sup>1</sup> *Complexation* (*i.e.*, complex formation) is any combination of dissolved cations with molecules or anions containing free pairs of electrons. *Species* refers to actual form in which a dissolved molecule or ion is present in solution. Definitions are taken from Stumm and Morgan (1981).

A list of acronyms, abbreviations, symbols, and notation is given in Appendix A. A list of definitions is given in Appendix B

174

[or diffuse double layer model (DDLDM)], constant capacitance model (CCM), Basic Stern model, and triple layer model (TLM).

Some of the chemical reaction codes identified in the reviews by Goldberg (1995) and Davis and Kent (1990) as having adsorption models include HARPHRE (Brown *et al.*, 1991), HYDRAQL (Papelis *et al.*, 1988), SOILCHEM (Sposito and Coves, 1988), and the MINTEQA series of chemical reaction codes, including MINTEQA2 (Allison *et al.*, 1991) developed for the U.S. Environmental Protection Agency (EPA). Compared to other codes, MINTEQA2 contains some of the most extensive options for modeling adsorption, including all of the models listed above, except for the Basic Stern model. The MINTEQA2 adsorption model options are discussed further in Section 5.2, and their associated equation and reaction formulations as coded within MINTEQA2 are described in Section 5.3. It should be noted that the partition coefficient ( $K_d$ ), Langmuir, and Freundlich models incorporated into MINTEQA2 are formulated in terms of species activities,<sup>1</sup> and not the more traditional approach of total concentrations of dissolved metal. This variation in modeling approach and the rationale for its use are discussed in Section 5.2.

Some of these models are briefly described in Chapter 2. The reader is also referred to reference texts by Langmuir (1997), Morel (1983), Sposito (1984), and Stumm and Morgan (1981) for more detailed background descriptions, associated equations and data needs, and model comparisons pertaining to these adsorption models.

As noted in Chapter 2, the electrostatic, surface complexation models, although robust, are not expected to have a significant impact on contaminant transport and risk assessment modeling due to their significant data needs and more complex equation formulations. Detailed descriptions, comparisons, and derivations of the relevant equations and reactions associated with these models are described in Westall and Hohl (1980), Morel *et al.* (1981), Barrow and Bowden (1987), Davis and Kent (1990), and others. The data needs and associated derivation (*i.e.*, parameterization) of model constants are discussed by Morel *et al.* (1981), Turner (1991), and Goldberg (1995). The electrostatic models were developed to provide a mechanistic description of adsorption reactions in systems containing a pure single phase of an amorphous or crystalline metal oxide. Numerous studies have demonstrated their success in predicting adsorption of trace metals in such simplified systems (*e.g.*, Turner, 1993). Application of such adsorption models to natural systems where the reactive surfaces include a combination of impure phases, clays, and humic materials are limited. The adsorption behavior of such systems unfortunately cannot be modeled assuming that the

---

<sup>1</sup> In general terms, the *activity* of an ion is its effective concentration that determines its behavior to other ions with which it might react. The activity of an ion is equal to its concentration only in infinitely dilute solutions, and is related to its analytical concentration by an activity coefficient,  $\gamma$ . Activities, activity coefficients, and associated thermodynamic relationships are discussed in detail in texts such as Glasstone (1972), Lewis and Randall (1961), Morel (1983), Sposito (1984), and Stumm and Morgan (1981).

adsorptive properties of a phase mixture, such as soil, can be readily predicted by adding the adsorption constants for the individual solid phases in some normalized fashion.

Numerous papers have been published relative to the application of non-electrostatic and electrostatic adsorption models to modeling the migration of radionuclides released from high (HLW) and low level (LLW) radioactive waste disposal facilities. These include reviews and references cited therein by Serne and Muller (1987) and Turner (1993,1995) for application to HLW disposal and Serne *et al.* (1990) for application to LLW disposal issues. The reader should also be aware of an extensive literature review by Berry (1992a,b,c) of adsorption studies conducted in the United Kingdom and the international community on sorption relative to the release and transport of radionuclides in the near<sup>1</sup> and far field. The literature review is published as 3 reports. The first report summarizes studies funded by the United Kingdom (UK) Nirex and Department of the Environment (UK DoE). The second report contains an extensive bibliography, including reference citations and complete abstracts, of United Kingdom and international publications on the subject area. The third report compares the objectives and approaches used in studies funded by Nirex and UK DoE to those in related studies undertaken by the international community.

### ***5.1.5 Output from Chemical Reaction Modeling***

The results from chemical reaction codes vary depending on the capabilities, design of the output report, and user-selected options for each code. The output may be in the form of a report directed to a printer, and/or a total or partial report stored as an ASCII (American Standard Code for Information Interchange)-formatted file for future use in word processing or spreadsheet software or as input for other scientific application software. The output can be extensive depending on the options used for the modeling calculations and the level of output report requested by the user.

The output report from MINTEQA2 chemical reaction code (Allison *et al.*, 1991) will be used as a typical example. The MINTEQA2 code was developed by EPA and is described in greater detail in Section 5.2. For each modeling calculation, the output can include the following:

- Documentation and constraints applied to the calculation
  - Name of the data file and the date and time of modeling calculations
  - Documentation to describe modeling calculation
  - Listing of the model parameters used to control the calculations (*e.g.*, maximum number of permitted iterations, method for calculating activity coefficients, alkalinity option, units used for input of water composition, temperature), level of output report (*e.g.*, short versus long report), and type of selected adsorption algorithm

---

<sup>1</sup> The "near field" is that portion of a contaminant plume that is near the point source and whose chemical composition is significantly different from that of the uncontaminated portion of the aquifer. The "far field" refers to that which is not the "near field."

116

- Listing of the input water composition
  - Listing of any controls (*e.g.*, pH, Eh, redox equilibria) applied to the calculation
  - Listing of any additions or modifications made as part of the input file to the code's thermodynamic database
  - Listing of any adsorption reactions and associated constants used for adsorption reaction calculations
  - Listing of any solid phases and associated masses considered for mass transfer calculations
  - Listing of any gases whose solubility will control the concentration of a dissolved constituent (*e.g.*, solubility of CO<sub>2</sub> gas to fix the total concentration of dissolved carbonate)
- Results of aqueous speciation calculations
- Number of iterations required for the aqueous speciation calculation to converge
  - Calculated concentrations, activities, activity coefficients, equilibrium constants as modified for ionic strength and temperature for each aqueous species extracted from the code's thermodynamic database and included in the calculation
  - Charge imbalance before and after calculation of aqueous speciation
  - Listing of the distribution of important (*i.e.*, greater than 1 percent of the total concentration of a dissolved component) uncomplexed and complexed aqueous species for each valence form of each dissolved component (See "Glossary" for technical definition of "component.")
- Results of solubility calculations
- Degree of saturation of the starting water composition relative to equilibrium solubility of every solid in the code's thermodynamic database containing the components included in that water analysis
  - Listing of the reaction stoichiometries and associated temperature-corrected equilibrium constants for each solid phase included in the calculation
- Results of mass transfer calculations at each stage of calculations where a solubility and/or adsorption equilibrium condition is reached
- Repeat of all speciation results for new calculated water composition
  - Repeat of the solubility results for new calculated water composition
  - Calculated mass of each element in dissolved, precipitated, and/or adsorbed states for new calculated water composition

Parts of example output reports from MINTEQ are listed and explained in detail in Allison *et al.* (1991) and Peterson *et al.* (1987a).

### 5.1.6 Assumptions and Data Needs

Chemical reaction models may be used to predict the concentrations of elements, such as uranium, that may be present in an aqueous solution. This type of modeling calculation requires the user to select either a solubility or an adsorption reaction to constrain the maximum concentration limit of a contaminant or any other dissolved constituent. The modeling process is based on the following assumptions and data needs for the environment of interest:

- For a solution-concentration limit based on a solubility reaction, the mineral phase selected as the solubility control for the contaminant of interest must have known thermodynamic data (*e.g.*, solubility constant). The selection of the solid phase must be technically defensible in that the phase is known to exist in analogous aqueous environments and have rates of precipitation and dissolution that are not limited by kinetics.
- For a solution-concentration limit based on an adsorption reaction,<sup>1</sup> the substrate (*e.g.*, an iron-oxyhydroxide coating) selected as the adsorption control for the contaminant of interest must be technically defensible relative to the soil or sediment being modeled. The adsorption parameters must be known for the contaminant of interest and its major competing ions for the substrate and the range of appropriate environmental conditions.
- The reactions or conditions that control the pH, redox conditions, and concentrations of complexing ligands (*e.g.*, dissolved carbonate) for the derived aqueous solution must be assumed and technically defensible.
- The model must have an adequate thermodynamic database that includes all the necessary aqueous species, redox reactions, minerals, and sorption substrates for the contaminant of interest and for the other constituents of environmental importance.
- The composition of water (in particular, pH, Eh, and alkalinity) contacting the contaminant-containing phases must be known.
- Most chemical modeling calculations will be limited to equilibrium conditions, because of the general absence of kinetic rate values for the aqueous speciation, solubility, and/or sorption reactions involving the contaminant of interest and other constituents of environmental importance. Equilibrium (actually steady state) conditions are likely in the far field, but are less likely in the near-field environment or at the boundaries of contaminant plumes.

---

<sup>1</sup> When using the partition coefficient ( $K_d$ ) or Freundlich adsorption models, the predicted solution-concentration limits are only valid when modeling trace concentrations of a contaminant of interest.

### 5.1.7 Symposiums on Chemical Reaction Modeling

Both the diversity and interdependency of research efforts associated with chemical reaction modeling are effectively demonstrated by the papers presented at several symposiums held on this subject. Some of these conferences are listed in Table 5.2.

The symposiums typically include papers on a range of subjects, such as theoretical advancements; model and code development, including documentation; application studies of equilibrium and mass transfer codes, transport and coupled codes, and surface processes; database development, including thermodynamic data, kinetic data, and data on organic compounds; modeling sensitivities; and model validation.<sup>1</sup>

The reader is encouraged to peruse these proceedings. The proceedings' papers show that the development of chemical reaction models is concurrent with the expansion and improvement of thermodynamic databases for aqueous species and solids and for adsorption, as well as with application studies that test the validity of these models and their associated databases.

**Table 5.2.** Examples of technical symposiums held on development, applications, and data needs for chemical reaction modeling.

Published Proceedings	Date of Symposium	Location	Sponsorship
Jenne (1979)	Sept. 11-13, 1978	Miami Beach, Florida	Amer. Chem. Soc.
Erdal (1985)	June 20-22, 1984	Los Alamos, New Mexico	U.S. Department of Energy (DOE) and U.S. Nuclear Regulatory Commission (NRC)
Jacobs and Whatley (1985)	Oct. 2-5, 1984	Oak Ridge, Tennessee	NRC
Jackson and Bourcier (1986)	Sept. 14-17, 1986	Fallen Leaf Lake, California	DOE and LLNL
Melchior and Bassett (1990)	Sept. 25-30, 1988	Los Angeles, California	Amer. Chem. Soc.
Loeppert <i>et al.</i> (1995)	Oct. 23-24, 1990	San Antonio, Texas	Soil Sci. Soc. Amer. and Amer. Soc. Agron.

---

<sup>1</sup> *Model validation* is the integrated test of the accuracy with which a geochemical model and its thermodynamic database simulate actual chemical processes. In contrast, *code verification* is the test of the accuracy with which the subroutines of the computer code perform the numerical calculations.

## 5.2 MINTEQA2 Chemical Reaction Code

### 5.2.1 Background

The MINTEQA2 computer code and its predecessor versions are described by Allison *et al.* (1991, MINTEQA2), Brown and Allison (1987, MINTEQA1), Peterson *et al.* (1987a, MINTEQ), and Felmy *et al.* (1984, MINTEQ). The MINTEQ code was developed with EPA funding. It was originally constructed by combining the mathematical structure of the MINEQL code (Westall *et al.*, 1976) with the thermodynamic database and geochemical attributes of the WATEQ3 code (Ball *et al.*, 1981a).

The MINTEQA2 code is used in conjunction with a thermodynamic database to calculate complex chemical equilibria among aqueous species, gases, and solids, and between dissolved and adsorbed states. Conceptually, the code can be considered as having the following 4 submodels: (1) aqueous speciation, (2) solubility, (3) precipitation/dissolution, and (4) adsorption. These submodels include calculations of aqueous speciation/complexation, oxidation-reduction, gas-phase equilibria, solubility and saturation state (*i.e.*, saturation index), precipitation/dissolution of solid phases, and adsorption. The MINTEQA2 code incorporates a Newton-Raphson iteration scheme to solve the set of mass-action and mass-balance expressions.

The reader is referred to the references and user guides listed above for details regarding the use of the MINTEQ code, types and examples of geochemical equilibria calculations possible with this code, the basic equations on which the model is based, and examples of input and output files.

### 5.2.2 Code Availability

MINTEQA2 (Version 3.11) is the most current version of MINTEQ available from EPA. It is compiled to execute on a personal computer (PC) using the MS-DOS computer operating system. The MINTEQA2 software package distributed by EPA also includes PRODEFA2, which is a user-interactive code used to create and modify input files for MINTEQA2.<sup>1</sup> The user is referred to the description of PRODEFA2 in Allison *et al.* (1991).

Copies of the files containing the source and executable codes for MINTEQA2 and PRODEFA2, thermodynamic databases, example input data sets, and documentation are available by mail from

---

<sup>1</sup> Versions of MINTEQ modified to operate on DOS and Macintosh personal computer systems are also available from commercial sources.

Center for Exposure Assessment Modeling (CEAM)  
U.S. Environmental Protection Agency  
Office of Research and Development  
Environmental Research Laboratory  
960 College Station Road  
Athens, Georgia 30605-2720

These files may also be downloaded using the Internet by accessing CEAM's home page. The address of the CEAM home page is

*ftp://ftp.epa.gov/epa\_ceam/wwwhtml/ceamhome.htm*

The MINTEQA2 code and documentation are located under "software products" in "...CEAM software products and related *descriptive information* is..." The CEAM home page may also be accessed via EPA's home page at

*http://www.epa.gov*

by selecting "software" in "EPA Data Systems and Software," and then "Center for Exposure Assessment Modeling."

Training courses are commonly held on the use of chemical reaction modeling techniques and the application of the MINTEQA2 code. In the past, MINTEQ training has been provided to EPA and NRC by their supporting national laboratory and private contractors. Allison Geoscience Consultants, Inc.<sup>1</sup> have, for example, conducted several MINTEQA2 modeling workshops. The Pacific Northwest National Laboratory (Peterson *et al.*, 1987a) has provided MINTEQA2 training to the NRC. Short course announcements from the Environmental Education Enterprises, Inc. (E<sup>3</sup>)<sup>2</sup> for environmental science and engineering training also included MINTEQ workshops.

### **5.2.3 Aqueous Speciation Submodel**

The MINTEQA2 code can be considered as having the following 4 parts: (1) an aqueous speciation submodel, (2) solubility submodel, (3) precipitation/dissolution submodel, and

---

<sup>1</sup> The use of commercial business and product names is for descriptive purposes only, and does not imply endorsement by EPA or PNNL.

Allison Geoscience Consultants, Inc., 3920 Perry Lane, Flowery Branch, Georgia 30542.

<sup>2</sup> Environmental Education Enterprises, Inc. (E<sup>3</sup>), 2764 Sawbury Boulevard, Columbus, Ohio 43235-4580.

(4) adsorption submodel. The aqueous speciation submodel is fundamental to all other submodels. It first uses the MINTEQA2 thermodynamic database to calculate the activities of the uncomplexed and complexed aqueous species for an initial water composition. The activities of individual aqueous species are corrected for ionic strength using the Davies or extended Debye-Hückel equations.

The aqueous speciation of a dissolved contaminant can only be determined using thermodynamic calculations such as those formulated in the aqueous speciation submodel of chemical reaction codes. Except for pH, which is the negative of the logarithm of the activity of the uncomplexed  $H^+$  aqueous ion, the user typically supplies the total concentrations of a chemical constituent in an input file for a chemical reaction code. Most common analytical techniques measure the total concentrations of a dissolved constituent such as uranium, and not the concentration of any of its many individual species such as  $UO_2^{2+}$ ,  $UO_2OH^+$ ,  $UO_2(CO_3)_2^{2-}$ ,  $UO_2SO_4^{(aq)}$ , or  $UO_2PO_4^-$ .

Aqueous speciation, and hence the testing of solubility hypotheses in the solubility submodel, is only reliable if the quality of the chemical analysis of the water is adequate. The description of the water composition is usually obtained by direct measurement of major cations and anions, pH, Eh, and trace constituents. As a quality check of the water chemical analysis, the MINTEQA2 code calculates the cation/anion balance for each speciated water composition. The cation/anion balance is calculated using the equation

$$\text{Cation/Anion Balance (\%)} = \frac{[\text{Anions (equiv./l)}] - [\text{Cations (equiv./l)}]}{[\text{Anions (equiv./l)}] + [\text{Cations (equiv./l)}]} \times 100. \quad (5.1)$$

For simple groundwater compositions and accurate analytical work, the cation/anion balance should not exceed a few percent (Hem, 1985).

The importance of complexation is discussed in Chapter 2 and elsewhere, such as Langmuir (1997), Lindsay (1979), Morel (1983), and Stumm and Morgan (1981). Complexation of dissolved metals with ligands, such as carbonate, will increase the total concentration of a dissolved metal in a soil-water system, and affect its availability for sorption and migration in geochemical systems. The output from the MINTEQA2 aqueous speciation submodel identifies, based on the data in the code's thermodynamic database, the distribution (*i.e.*, dissolved masses) of uncomplexed and complexed aqueous species for the constituents included in the input water composition.

### 5.2.3.1 Example of Modeling Study

Krupka and Serne (1998) used the MINTEQA2 code to analyze solubility limits for contaminants that may be released from a hypothetical low-level radioactive waste (LLW) disposal facility being considered in a NRC performance assessment test case analysis. The species distributions plotted for dissolved U(VI) in Figure 5.1 were taken from the MINTEQA2 calculations by Krupka and Serne. They provide a good example of the type of information

122

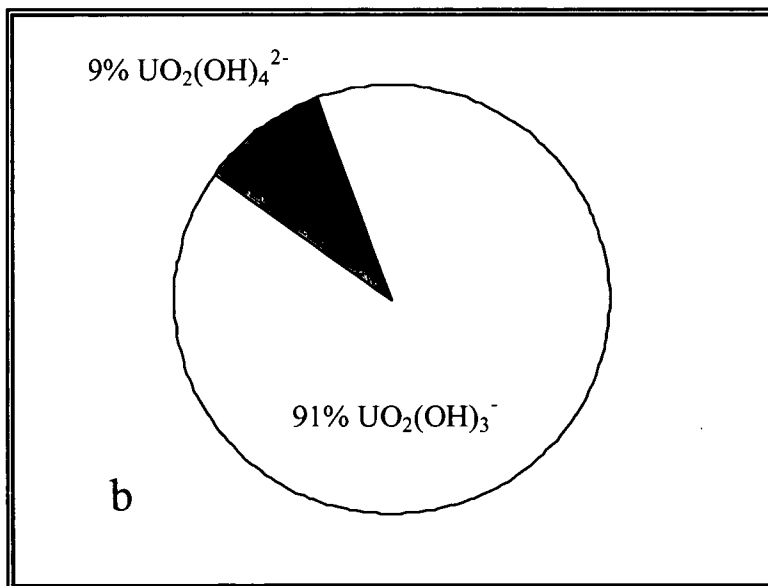
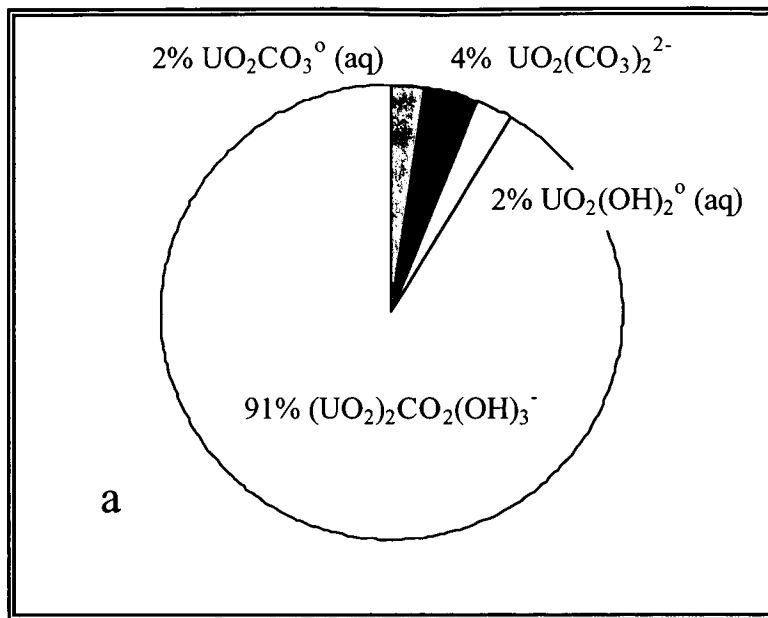


**Figure 5.1.** Distribution of dominant U(VI) aqueous species for leachates buffered at pH 7.0 by local ground water (Figure 5.1a) and at pH 12.5 by cement pore fluids (Figure 5.1b). [Adapted from MINTEQA2 modeling results of Krupka and Serne (1998).]

provided by the aqueous speciation submodel. Figure 5.1a shows the distribution of dominant species (*i.e.*, greater than 1 percent of total dissolved mass) of dissolved U(VI), respectively, for leachates buffered at pH 7.0 by the local ground water. This distribution can be contrasted to that in Figure 5.1b which shows the distribution of dominant U(VI) species at pH 12.5 by pore fluids derived from ground-water interactions with cementitious materials in the hypothetical LLW disposal facility. At pH 7.0, the speciation of dissolved U(VI) is dominated by uranyl carbonate complexes. At very basic pH conditions, the anionic uranyl hydrolysis species dominate the chemistry of dissolved U(VI). The speciation results clearly demonstrate that major differences can occur in the speciation of a dissolved metal as a function of different solution chemistries, such as pH.

#### 5.2.3.2 Application to Evaluation of $K_d$ Values

As noted in Chapter 2 and published references, such as Morel (1983), Sposito (1989, 1994), Stumm and Morgan (1981), and others, the ionic nature and composition of the dominant aqueous species for a contaminant are important factors relative to its adsorption behavior on reactive mineral surfaces. Moreover, as demonstrated in the example given above, the ionic nature and composition of the dominant aqueous species are dependent on the composition, pH, and redox conditions of a surface or ground water.

If thermodynamic data exist for the important aqueous species of a contaminant of interest, chemical reaction models *provide the most cost and time effective means of predicting the dominant aqueous species* that could exist for practically any water composition. The rate at which these calculations can be done is limited only by the rate at which a user can enter the input data, given the fast speeds of processors used in modern personal computers. The user can rapidly evaluate whether the dominant species is(are) cationic or anionic, as well as how their compositions might be affected by complexation with dissolved ligands such as carbonate and phosphate. If there is uncertainty relative to the pH evolution or ligand content of a water, the user may then quickly modify the input value(s) and complete a series of sensitivity analyses to determine how the ionic charges and compositions of the dominant aqueous species change.

This information can then be used to substantiate the conceptual model that is being used for adsorption for a particular contaminant. For example, if 90 percent of the mass of a dissolved contaminant is present in anionic form, is this consistent with low or high  $K_d$  values that one might find reported in the literature? If the calculations indicate strong complexation with dissolved sulfate, are the default  $K_d$  values in transport or risk assessment models, such as MEPAS, conservative estimates relative to this specific site chemistry? If toxicology studies indicate that an uncomplexed species, such as  $\text{Cu}^{2+}$ , is the important actor relative to bioavailability, how does this affect the predicted risk when the aqueous speciation calculations indicate that 99 percent of the mass of dissolved copper is present as a carbonate complex in a given water? Chemical reaction models provide an effective tool for calculating the responses in aqueous speciation to different conceptual models that one might consider for soil-water systems.

For example, Kaplan *et al.* (1998) conducted laboratory batch  $K_d$  experiments to study the effects of background geochemistry on the sorption of U(VI) on natural sediments. The MINTEQA2 code was used to calculate the aqueous speciation of U(VI) in a groundwater before and after equilibrium with sediments. The modeling results indicated dissolved U(VI) was present as essentially all aqueous anionic U(VI)-carbonate complexes [*e.g.*,  $\text{UO}_2(\text{CO}_3)_3^{4-}$ ] at high pH conditions. Studies by Waite *et al.* (1994) and others have shown that these complexes, due to their anionic nature, tend to sorb appreciably less to sediments than cationic U(VI) complexes which are present at lower pH conditions.

#### 5.2.4 Solubility Submodel

After calculating the aqueous speciation for a given water composition, solubility-equilibria hypotheses are tested. Ion activity products (IAP) are calculated from the activities of the component (or basis) species,<sup>1</sup> using the stoichiometries of the solubility reactions for minerals and other solids in the thermodynamic database. These activity products are then compared to the equilibrium constants ( $K_{r,T}$ )<sup>2</sup> stored in the database for the solubilities for the same solids, to test the assumption that certain of the dissolved constituents in the aqueous solution are in equilibrium with particular solid phases. Saturation indices, [ $\log (\text{IAP}/K_{r,T})$ ], are calculated to determine if the water is at

$$\text{Equilibrium: } \quad \text{Log} (\text{IAP}/K_{r,T}) \approx 0 , \quad (5.2)$$

$$\text{Oversaturated: } \quad \text{Log} (\text{IAP}/K_{r,T}) > 0 , \quad (5.3)$$

or

$$\text{Undersaturated: } \quad \text{Log} (\text{IAP}/K_{r,T}) < 0 , \quad (5.4)$$

with respect to a specified solid phase. This information allows one to ascertain permissible equilibrium solubility controls for dissolved constituents in that water. This water may be a surface or ground water, or a laboratory solution used for solubility or  $K_d$  measurements.

---

<sup>1</sup> Component (or basis) species are the “basis entities or building blocks from which all species in the system can be built” (Allison *et al.*, 1991). Examples include  $\text{Mg}^{2+}$ ,  $\text{UO}_2^{2+}$ ,  $\text{CO}_3^{2-}$ , and  $\text{SO}_4^{2-}$  for magnesium, hexavalent uranium [U(VI)], inorganic carbon, and oxidized sulfur [S(VI)], respectively. The set of components in MINTEQA2 is predefined. They are a set of linearly independent aqueous species in terms of which all aqueous speciation, redox, mineral, and gaseous solubility reactions in the MINTEQA2 thermodynamic database are written.

<sup>2</sup> Mineral solubility reactions in the MINTEQA2 database are written as formation (*i.e.*, precipitation) reactions. The solubility product,  $K_{sp,T}$ , (see Chapter 2), which is a commonly used term in the literature, refers to the equilibrium constant,  $K_{r,T}$ , for a mineral solubility reaction written as a dissolution reaction.

125

#### 5.2.4.1 Example of Modeling Study

Figure 5.2 shows the saturation indices calculated by Krupka *et al.* (1983)<sup>1</sup> for the mineral rutherfordine ( $\text{UO}_2\text{CO}_3$ ) for published analyses of solution samples taken from laboratory uranium solubility studies. The saturation index results demonstrate that these solution samples calculate to be at or very near equilibrium with respect to rutherfordine based on the available thermodynamic data for this mineral and U(VI) aqueous species included in the modeling calculations. Rutherfordine may have therefore precipitated during the course of the solubility studies reported in the cited literature.

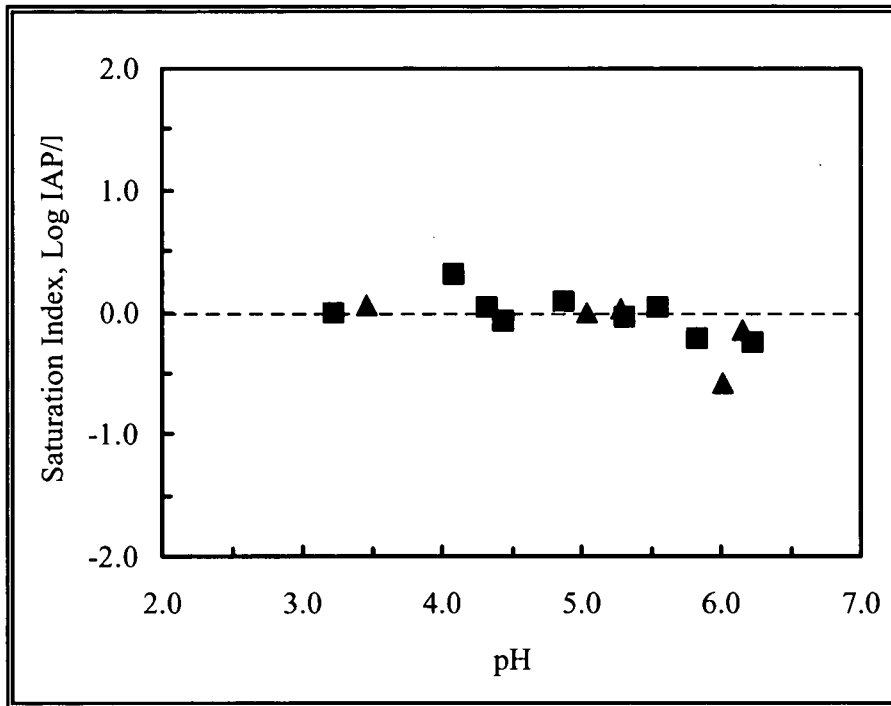


**Figure 5.2.** Saturation Indices calculated for rutherfordine ( $\text{UO}_2\text{CO}_3$ ) as a function of pH for solution analyses from Sergeyeva *et al.* (1972). [Adapted from WATEQ4 modeling results of Krupka *et al.* (1983). The filled square and triangle symbols refer, respectively, to solutions analyses from 25 and 50°C experiments by Sergeyeva *et al.* (1972)]

<sup>1</sup> Although Krupka *et al.* (1983) used the WATEQ4 chemical reaction code, their results are analogous to the types of saturation index calculations permitted with the MINTEQ2A code.

#### 5.2.4.2 Application to Evaluation of $K_d$ Values

Chemical reaction codes can be used to analyze the adequacy of laboratory measurements of  $K_d$  values for a particular soil-water system. As noted in Chapter 3, solubility limits have sometimes been exceeded during the process of making laboratory measurements of  $K_d$  values. This can result when the concentration of the contaminant spike introduced to the equilibration vessel is too great and/or when the initial chemical conditions, such as pH, vary greatly during the course of the measurements.

By modeling the aqueous speciation and saturation indices for the initial and final compositions of aqueous solutions present in the  $K_d$  experiments, the user can test if any solubility limits were exceeded during the measurements. In those cases where a contaminant-containing solid is precipitated, the determined  $K_d$  values are measurements of both solubility and adsorption processes and will result in an over-prediction of contaminant attenuation (via only adsorption processes) in the soil-water system.

Kaplan *et al.* (1998) conducted laboratory batch  $K_d$  experiments to study the effects of background geochemistry on the sorption of U(VI) on natural sediments. MINTEQA2 calculations indicated that dissolved U(VI) was present as essentially all aqueous anionic U(VI)-carbonate complexes. Waite *et al.* (1994) and others have shown that these complexes, due to their anionic nature, tend to sorb appreciably less to sediments than cationic U(VI) complexes present at lower pH values. However, the  $K_d$  values measured by Kaplan *et al.* (1998) increased from 1.07 to 2.22 ml/g as the pH increased from 8.17 to 9.31, and were  $>400$  ml/g at pH  $\approx$  10.3. Kaplan *et al.* (1998) used MINTEQA2 saturation index calculations to show that the apparent increase in U(VI)  $K_d$  values was due to the precipitation of uranium-containing solids and not to U(VI) adsorption to the sediment.

#### 5.2.5 Precipitation/Dissolution Submodel

The results from the solubility model are in turn used by the MINTEQA2 as input for the precipitation/dissolution submodel. Application of this submodel is optional. The user may select this submodel and its different options to predict the mass of a solid phase(s) that precipitates or dissolves in the modeled system. The mass transfer submodel determines the mass of a solid phase(s) (*e.g.*, a contaminant-containing solid or a mineral present in a soil) that precipitates from a ground water or dissolves from a soil-water system. If a given water composition calculates to be oversaturated,  $[\log (IAP/K_{r,T}) > 0]$ , with respect to a solid phase(s) considered in the modeling problem, the mass transfer model will decrease (*i.e.*, precipitate a solid phase) the masses of the appropriate dissolved constituents until the water composition is at equilibrium,  $[\log (IAP/K_{r,T}) = 0]$ , with respect to that solid phase(s). The MINTEQA2 output lists the mass of solid precipitated per a set volume of the system being modeled. If a given water composition calculates to be undersaturated,  $[\log (IAP/K_{r,T}) < 0]$ , with respect to a solid phase(s) selected in the modeling problem, the mass transfer model will increase (*i.e.*, dissolve a solid phase) the

masses of the appropriate dissolved constituents until the water composition is at equilibrium with respect to that solid phase(s) or until the user-specified finite mass of that solid has been completely dissolved. For those solids originally designated as having finite masses, the MINTEQA2 output gives the masses per set system volume of any of these solids remaining at final equilibrium.

#### 5.2.5.1 Example of Modeling Study

The solubility limits calculated by Krupka and Serne (1998) demonstrate one of several applications for a precipitation/dissolution submodel. Maximum concentration limits for dissolved americium, neptunium, nickel, plutonium, radium, strontium, thorium, and uranium were calculated using MINTEQA2 for 2 ground-water environments associated with a hypothetical LLW disposal system. The 2 limiting environments included: (1) a cement buffered system, wherein the leachate pH is controlled at values above 10 by the effective buffering capacity of the concrete, and (2) a ground-water buffered system, wherein the leachate pH and related solution parameters are dominated by the local ground-water system.

Figure 5.3 shows the maximum concentrations calculated by Krupka and Serne (1998) for total dissolved uranium as a function of pH. The predicted concentration limits are based on the equilibrium solubilities of schoepite [ $\text{UO}_2(\text{OH})_2 \cdot \text{H}_2\text{O}$ ] and uranophane [ $\text{Ca}(\text{H}_3\text{O})_2(\text{UO}_2)_2(\text{SiO}_4)_2 \cdot 3\text{H}_2\text{O}$ ]. These 2 solids were selected based on published phase-stability information and knowledge of the geochemistry of contaminant aqueous systems. Schoepite precipitates readily in short-duration laboratory experiments conducted at ambient temperatures. Because the concentration of dissolved uranium in equilibrium with schoepite is higher than the solubilities of other uranium solids that precipitate under these conditions or in nature, concentration limits based on schoepite are therefore expected to be highly conservative. The presence of alkali and/or alkaline earth ions at high pH conditions results in the precipitation of alkali/alkaline earth uranyl compounds that control the solubility of uranium at concentrations lower than those resulting from equilibrium with schoepite. Therefore, the solubility of uranophane may provide a more realistic solubility limit for dissolved uranium, especially at high pH conditions. Uranophane is known to exist in uranium-loaded cementitious mixtures and thus may be a realistic solubility control for dissolved uranium in cement dominated systems.

128

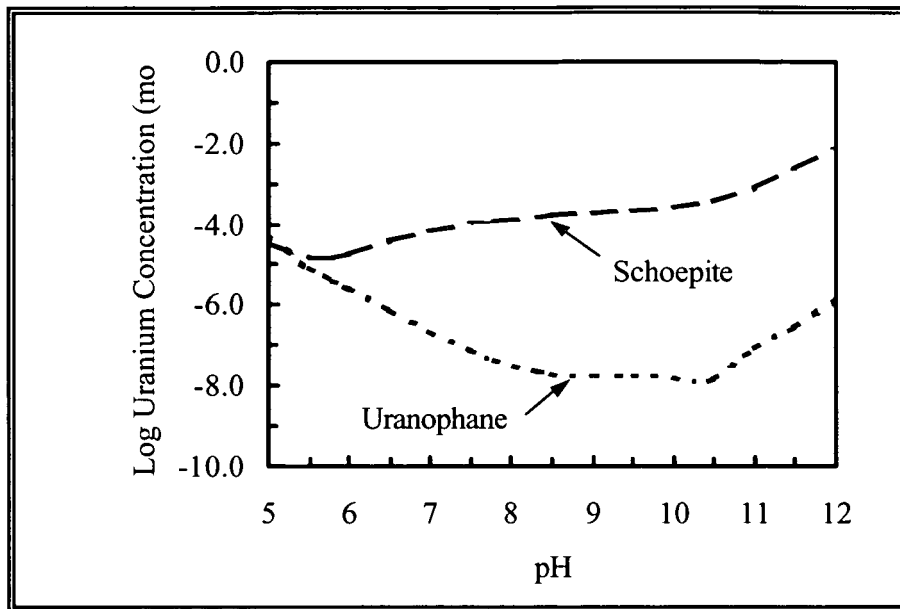


**Figure 5.3.** Maximum concentration limits calculated for total dissolved uranium as a function of pH based on the equilibrium solubilities of schoepite and uranophane.

#### 5.2.5.2 Application to Evaluation of $K_d$ Values

Chemical reaction codes can be used to calculate bounding, technically-defensible maximum concentration limits for dissolved contaminants as a function of key composition parameters (e.g., pH) of any specified soil-water system. The concentration of a dissolved contaminant predicted with default or site specific  $K_d$  values used in transport or risk assessment models may exceed the concentration limit based on solubility relationships. In these instances, the solubility-limited concentration may provide a more realistic bounding value than one based on a  $K_d$  value for the assessment calculation, and could have an important impact on the estimated level of risk. If a calculated concentration limit is based on the solubility of a mineral that is known to precipitate under analogous chemical conditions and over reasonable time frames, then the user knows that the dissolved concentrations of this contaminant in an actual, open soil-water system cannot exceed these values and will most likely be significantly less than these values due to adsorption and/or coprecipitation processes.

Moreover, as with the aqueous speciation calculations discussed in Section 5.2.3, mass transfer calculations can be rapidly and inexpensively repeated using a chemical reaction code to determine

their sensitivity to a wide range of chemical parameters for a soil-water systems. This includes easily measured parameters, such as pH, and analytical values that might have a wide range of uncertainty, such as the concentration of a dissolved complexant.

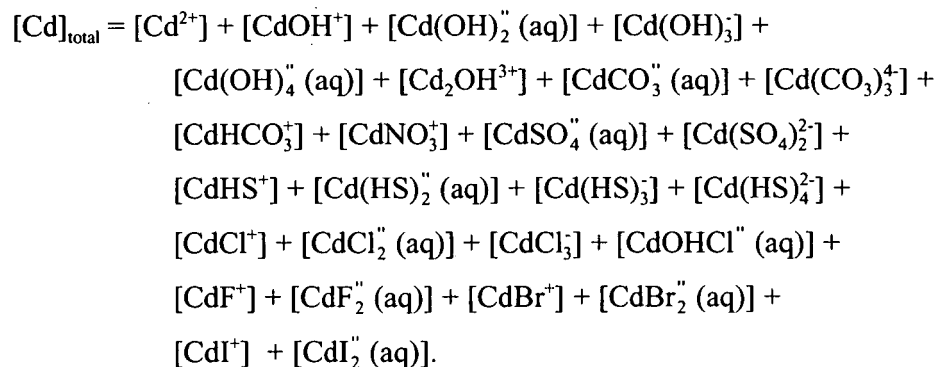
### 5.2.6 Adsorption Submodel

The MINTEQA2 also includes a submodel to calculate the adsorption of dissolved constituents onto the surfaces of solid phases that can be selected by the code user. The MINTEQA2 code includes 7 adsorption model options. These are:

- Non-electrostatic adsorption models
  - Activity partition coefficient ( $K_d^{\text{act}}$ ) model
  - Activity Langmuir model
  - Activity Freundlich model
  - Ion exchange model
  
- Electrostatic adsorption models
  - Constant capacitance model (CCM)
  - Diffuse layer model (DLM)
  - Triple layer models (TLM).

The equations and reactions that support these models, as coded in MINTEQA2, are described in greater detail in Section 3. These descriptions and associated equations are adapted from Allison *et al.* (1991).

The  $K_d^{\text{act}}$ , Langmuir, and Freundlich models in MINTEQA2 are formulated in terms of species activities, and not the more traditional approach of total concentrations of dissolved metal. In the latter case, the total concentrations of a dissolved metal M would equal the sum of the concentrations of all of its dissolved complexed and uncomplexed species. For example, using the species listed in the MINTEQA2 thermodynamic database, the total concentrations of dissolved cadmium,  $[\text{Cd}]_{\text{total}}$ , in the absence of any organic complexants in the water, could include the following species:



In the presence of organic complexants,  $[Cd]_{total}$  could also include, in addition to the cadmium species listed above, the concentrations of aqueous cadmium complexes containing citrate, acetate, EDTA, HEDTA, or other organic complexes.

A total concentration approach would therefore assume that all species of metal M adsorb with equal strength. Experimental data suggest, however, that only certain aqueous species react with the surfaces of a mineral [*e.g.*, Waite *et al.* (1994)]. Based on this assumption, these non-electrostatic models have been reformulated, as those coded in MINTEQA2, in terms of the activities of adsorbing species to provide activity-based models. The purpose of this approach is to reduce the dependency of the model parameters to effects from ionic strength and aqueous complexation of the adsorbing metal by effectively allowing the adsorption of only selected aqueous species of each metal.

Limitations remain, however, regarding these activity formulations of the  $K_d^{act}$ , Langmuir, and Freundlich models which restricts their range of applicability. These non-electrostatic adsorption models do not consider: charge balance on surface sites and adsorbed species, electrostatic forces between the adsorbing species and charge surface of the mineral, and reactions between the mineral and dissolved constituents other than the adsorbing metal. The effect of these processes changes with variations in the composition of an aqueous solution. These processes are, however, incorporated into the more robust, but more data intensive, electrostatic "surface complexation" adsorption model options in MINTEQA2.

The MINTEQA2 code includes the reaction components and formalisms necessary to enter the required adsorption data for any of the adsorption models. The code does not however have an adsorption database for these models. The user must provide the set of surface reactions and the associated equilibrium constants as part of the input data set. MINTEQA2 requires that this information be supplied relative to the adsorption of constituents onto specific mineral phases, such as amorphous ferric hydroxide  $[Fe(OH)_3 (am)]$ , and not a multi-mineral phase material, such as a soil or crushed rock. Examples of MINTEQA2 input files that include the adsorption modeling option are included in the data files distributed by EPA, and are also listed in Allison *et al.* (1991 Appendix D) and Peterson *et al.* (1987a). These examples demonstrate the major data requirements for some of the adsorption model options in MINTEQA2.

#### 5.2.6.1 Examples of Modeling Studies

Modeling studies by Peterson *et al.* (1986), Davis and Runnells (1987), Loux *et al.* (1989), and Turner *et al.* (1993) are examples of the use of MINTEQ adsorption model options. Peterson *et al.* (1986) and Davis and Runnells (1987) studied ground-water contamination associated with waste impoundments for uranium mill tailings using laboratory and computer modeling techniques. Peterson *et al.* (1986) modeled the adsorption of arsenic, chromium, lead, selenium, and zinc using the triple layer model (TLM) in MINTEQ. Their conceptual model was based on the assumption that adsorption of these metals occurred only on amorphous ferric hydroxide  $[Fe(OH)_3 (am)]$  that precipitated and dissolved during the course of their experiments.

Adsorption parameters for the TLM for amorphous ferric hydroxide were taken from published sources. The results of the adsorption calculations were in good agreement with some results from their laboratory experiments.

Davis and Runnels (1987) used MINTEQ to successfully model the behavior of zinc observed in laboratory column experiments. They assumed that the concentration of dissolved zinc measured in their solution samples was controlled by adsorption on amorphous ferric hydroxide [Fe(OH)<sub>3</sub> (am)] that precipitated as a result of pH changes occurring in their experiments. The adsorption of zinc on Fe(OH)<sub>3</sub> (am) was calculated using the TLM in MINTEQ. Davis and Runnels describe the selection of adsorption parameters used for the TLM.

Loux *et al.* (1989) used the MINTEQA2 code to model the pH-dependent partitioning of 8 cationic constituents by precipitation and/or adsorption on a sandy aquifer material in an oxidizing environment. The constituents of interest included barium, beryllium, cadmium, copper, nickel, lead, thallium, and zinc. Adsorption of these elements was based on amorphous iron oxide as the only reactive adsorption surface and calculated using the diffuse layer model (DLM). The adsorption parameters and associated reactions for the diffuse layer model were taken from Dzombak (1986). The modeling results were compared to laboratory data for the aquifer material spiked with the trace metals. The predicted concentrations based on the diffuse layer model for adsorption of lead, nickel, and zinc, provided a good description of the pH behavior observed for the spiked samples. The concentrations of the other trace metals were not adequately predicted by the model. These differences were attributed to limitations in the model and/or available thermochemical data.

Turner *et al.* (1993) used the TLM in MINTEQA2 code to model adsorption data for U(VI) on goethite [ $\alpha$ -FeO(OH)]. The FITEQL code was used for adsorption parameter optimization. Their study illustrates the extensive parameter-fitting process that the user must complete to use complex electrostatic adsorption models, such as the TLM.

#### 5.2.6.2 Application to Evaluation of $K_d$ Values

Chemical reaction models *cannot be used to predict a  $K_d$  value*. The user must supply the adsorption parameters when using any of the adsorption model options. Typically, the data required to derive the adsorption parameters needed as input for adsorption submodels in chemical reaction codes are more extensive than information reported in a laboratory batch  $K_d$  study. However, if the parameters have been determined for a particular constituent for a surface complexation model, a chemical reaction model, such as MINTEQA2, can be used to calculate the masses of a constituent that are dissolved or adsorbed and how changes in geochemical conditions, such as pH, affect its adsorption behavior. The user can then derive a  $K_d$  using the calculated dissolved and adsorbed masses of the constituent.

The EPA (EPA, 1992a, 1996) has used the MINTEQA2 model and this approach to estimate  $K_d$  values for several metals under a variety of geochemical conditions and metal concentrations to

support several waste disposal issues. The EPA in its "Soil Screening Guidance" determined MINTEQA2-estimated  $K_d$  values for barium, beryllium, cadmium, Cr(III), Hg(II), nickel, silver, and zinc as a function of pH assuming adsorption on a fixed mass of iron oxide (EPA, 1996; RTI 1994). The calculations assumed equilibrium conditions, and did not consider redox potential or metal competition for the adsorption sites. In addition to these constraints, EPA (1996) noted that this approach was limited by the potential sorbent surfaces that could be considered and availability of thermodynamic data. Their calculations were limited to metal adsorption on iron oxide, although sorption of these metals to other minerals, such as clays and carbonates, is well known.

The data needed to use surface complexation adsorption models are more extensive than those from  $K_d$  studies. More importantly, the data for surface complexation models are based on adsorption on pure mineral phases, such as  $\alpha$ - $\text{Al}_2\text{O}_3$ ,  $\beta$ - $\text{Al}_2\text{O}_3$ , böhmite, goethite, magnetite, lepidocrocite, ferrihydrite,  $\text{SiO}_2$ , biotite, or kaolinite. Natural soils are more complicated, commonly containing mixtures of more than 10 pure minerals and amorphous mineral coatings. Unless a user can technically defend the assumption that the adsorption of a specific contaminant is dominated in a specific soil-water system, for example, by goethite reactive surfaces, the user is still left with the challenge of extrapolating these modeling results for pure mineral substrates to complex heterogeneous soil-water systems. This issue has been and will continue to be the subject of intensive study, but is not likely to be resolved in the short term or impact contaminant migration and risk assessment modeling soon.

### 5.2.7 MINTEQA2 Databases

The MINTEQA2 model includes an extensive thermodynamic database that is integrated with the aqueous speciation, solubility, and precipitation/dissolution submodels. The content and equations governing the values stored in the thermodynamic database are described below. MINTEQA2 does not have per se an integrated adsorption submodel database. The adsorption reactions and associated model parameters are supplied by the user as part of each input file. However, as discussed below, the current MINTEQA2 software package is supplied with a limited data file for the diffuse layer model (DLM).

#### 5.2.7.1 Thermodynamic Database

The MINTEQA2 thermodynamic database is considered by many to be one of the most extensive databases for modeling the aqueous speciation and solubility of contaminants and geologically-significant constituents (*e.g.*, magnesium, silica, aluminum, *etc.*) in low-temperature, soil-water systems. To understand the fundamental data needs for a thermodynamic database of a chemical reaction code, the basic equations underlying the thermodynamic parameters stored in the MINTEQA2 thermodynamic database will be reviewed in the next section. The content of the MINTEQA2 thermodynamic database as distributed by EPA will be reviewed and then compared relative to the priority constituents considered in the scope of work for this project.

### 5.2.7.1.1 Basic Equations

Thermodynamic data used by MINTEQA2 are stored in the form of equilibrium constants ( $K_{r,298}^{\circ}$ ) and enthalpies (heats) of reaction ( $\Delta H_{r,298}^{\circ}$ ) for aqueous speciation, oxidation/reduction, mineral solubility, and gas solubility reactions. The reference temperature for the MINTEQA2 database, as with most geochemical models, is 298 K (25 °C). Equilibrium constants ( $\log K_{r,T}^{\circ}$ ) may be based on values that have been experimentally-determined or calculated from Gibbs free energies of reaction ( $\Delta G_{r,T}^{\circ}$ ) units of cal/mol according to the equation:

$$\log K_{r,T}^{\circ} = \frac{\Delta G_{r,T}^{\circ}}{2.303 R T} \quad (5.5)$$

where  $T$  = temperature in degrees Kelvin,  
 $R$  = gas constant (1.9872 cal/mol·K)

Values for  $\Delta G_{r,T}^{\circ}$  are calculated from published values for the Gibbs free energy of formation ( $\Delta G_{f,298}^{\circ}$ ) for each product and reactant in the aqueous speciation or solubility reaction by the equation:

$$\Delta G_{r,298}^{\circ} = \sum \Delta G_{f,298}^{\circ} (\text{products}) - \sum \Delta G_{f,298}^{\circ} (\text{reactants}) . \quad (5.6)$$

To calculate aqueous speciation and solubilities at temperatures other than 25°C, the equilibrium constants are recalculated by the MINTEQA2 code to the temperature  $T$  of interest using the van't Hoff relation:

$$\log K_{r,T}^{\circ} = \log K_{r,298}^{\circ} + \frac{\Delta H_{r,298}^{\circ}}{2.303 R} \left( \frac{1}{T} - \frac{1}{298} \right) . \quad (5.7)$$

Values for enthalpies of reaction are calculated from published enthalpy of formation values ( $\Delta H_{f,298}^{\circ}$ ) using the equation:

$$\Delta H_{r,298}^{\circ} = \sum \Delta H_{f,298}^{\circ} (\text{products}) - \sum \Delta H_{f,298}^{\circ} (\text{reactants}) . \quad (5.8)$$

Values for  $\Delta H_{r,298}^{\circ}$  cannot be calculated for some reactions, because  $\Delta H_{f,298}^{\circ}$  values have not been determined for 1 or more reaction products and/or reactants. In these cases, the MINTEQA2 code assumes that

$$\log K_{r,T}^{\circ} = \log K_{r,298}^{\circ} . \quad (5.9)$$

Because of the limitations in using the van't Hoff relation for extrapolations over a wide range of temperature, applications of the MINTEQA2 code are limited to temperatures less than 100°C.

### 5.2.7.1.2 Structure of Thermodynamic Database Files

Typically, each aqueous species, redox, mineral, and gas solubility reaction is represented by 2 fix-formatted lines in the thermodynamic database files supplied with MINTEQA2. A third line is sometimes included when the stoichiometry of a reaction is complex. The first file line includes the identification number, formula descriptor,  $\Delta H_{r,298}^{\circ}$  (if available),  $\log K_{r,298}^{\circ}$ , charge, and related data for each reaction. The second line includes the reaction stoichiometry information formulated in terms of the MINTEQA2 components. Each reaction is entered as a formation reaction; that is, the components react to form the "more complex" species, such as an aqueous complex or mineral phase. The hydrogen stoichiometric component of each reaction is balanced with the components  $H^+$  and  $H_2O$ . The hydroxyl species,  $OH^-$ , is not used as a component, but is "formed" in a separate reaction in MINTEQA2.

Based on the protocol used for the MINTEQA2 thermodynamic database, the formation reaction for the uranyl mixed hydroxide/carbonate aqueous species,  $(UO_2)_2CO_3(OH)_3^-$ , is



The corresponding entry in the MINTEQA2 database (in fixed format fields) for this reaction and its associated thermochemical data is

```
8931405 UO2)2CO3OH)3 -14.3940 -0.8969 0.000 0.000-1.00 4.00 0.00 651.0868
2.00 4 2.000 893 1.000 140 3.000 2 -3.000 330
```

For more detailed format information on the MINTEQA2 database files, the reader is referred to the documentation in Allison *et al.* (1991, Appendix A).

### 5.2.7.1.3 Database Components

The thermodynamic database in the original MINTEQ code (Felmy *et al.*, 1984) was taken from the WATEQ3 code (Ball *et al.*, 1981a). Therefore, many of the inorganic reactions and associated thermodynamic values in the MINTEQA2 database can be traced back to the database supplements and sources described in publications documenting the WATEQ series of chemical reactions codes (Ball *et al.*, 1981a, WATEQ2; Ball *et al.*, 1981b, WATEQ3; Plummer *et al.*, 1976, WATEQ; Truesdell and Jones, 1973, WATEQ; Truesdell and Jones 1974, WATEQ).

The thermodynamic database of the current version of MINTEQA2 includes the original MINTEQ database plus modifications and additions completed on contracts with EPA funding. Some of these supplements include, for example, those completed at PNNL, such as the addition of reactions for aqueous species, gases, and solids containing cyanide and antimony by Sehmel

(1989) and those containing chromium, mercury, selenium, and thallium by Deutsch and Krupka.<sup>1</sup> Documentation for these database supplements are not listed in Brown and Allison (1987, MINTEQA1) or Allison *et al.* (1991, MINTEQA2), and may not be publicly available.

The elements for which the MINTEQA2 thermodynamic database has aqueous speciation, mineral solubility, and/or gas solubility reactions are listed in Table 5.3. The second and third columns of this table list the component species used for these elements and the redox reactions, if any, included in MINTEQA2 for different valence states of a particular element. The reader should note that the database does not contain reactions and associated thermodynamic values for specific isotopes of a particular element. The calculated reactions for a soil-water system assumes the total mass of each element.

Although the list of elements in Table 5.3 is substantial, this table and/or a listing of the database files does not indicate if the database of a chemical reaction code, especially for key contaminants, is adequate (*i.e.*, completeness of reactions and quality of associated thermodynamic values) and up-to-date. The user essentially has this important responsibility. One should expect that, as the period of time between the publication of a code's documentation and its use in an application study increases, the thermodynamic database becomes dated and revisions may be warranted.

Table 5.4 lists the organic ligands for which the MINTEQA2 thermodynamic database has aqueous speciation reactions.<sup>2</sup> Because of the limited availability of thermodynamic data for metal-organic complexes important to contaminated soil-water systems, as compared to inorganic aqueous complexes, the MINTEQA2 database, as with all chemical reaction codes, is limited. It does not contain complexation reactions for all metals with each of the organic ligands listed in Table 5.4. The reader will need to do a computer search of the MINTEQA2 ASCII file containing these reactions to determine the extent of the organic complexation reactions for each metal.

#### 5.2.7.1.4 Status Relative to Project Scope

The contaminants chosen for study in this project include chromium, cadmium, cesium, tritium (<sup>3</sup>H), lead, plutonium, radon, strontium, thorium, and uranium. Because the MINTEQA2 thermodynamic database does not contain reactions for specific isotopes, an appraisal of the database content to aqueous speciation and solubility reactions containing tritium is not

---

<sup>1</sup> Deutsch, W. J., and K. M. Krupka. September 1985. MINTEQ Geochemical Code: Compilation of Thermodynamic Database for the Aqueous Species, Gases, and Solids Containing Chromium, Mercury, Selenium, and Thallium. Unpublished report prepared by Pacific Northwest Laboratory for the U.S. Environmental Protection Agency in Athens, Georgia.

<sup>2</sup> Although important to contaminant disposal and remediation activities (*i.e.*, "mixed wastes") in the United States, computer modeling of the complexation of contaminant metals with organic complexes was excluded from the scope of the current project due to funding limits.

appropriate. As will be discussed in Volume II of this report, the concentrations of dissolved tritium will be affected by exchange reactions involving hydrogen-containing species dissolved in the soil-water system.

Of the remaining elements, the MINTEQA2 thermodynamic database contains aqueous speciation and solubility reactions for chromium, including the valence states Cr(II), Cr(III), and Cr(VI); cadmium; lead; strontium; and uranium, including the valence states U(III), U(IV), U(V), and U(VI). Except for uranium, the adequacy of the database for these listed elements is not known. Data supplied by Deutsch and Krupka<sup>1</sup> in 1985 is the probable basis for the chromium reactions and associated thermodynamic data. The reactions for cadmium, lead, and strontium may be those taken from the WATEQ-series of codes and supplied with the original MINTEQ code by Felmy *et al.* (1984). It is not known if these have been revised or supplemented since that time.

The reactions and associated thermodynamic data for uranium aqueous species and solid phases were those supplied with the original MINTEQ code. They were taken from those added to WATEQ3 (Ball *et al.*, 1981a) and are based primarily on the compilation of uranium thermodynamic data by Langmuir (1978). Langmuir's review has been superseded by the comprehensive review and compilation of uranium thermodynamic data given in Wanner and Forrest (1992). This compilation represents a significant improvement and update to the values in Langmuir *et al.* (1978), including for U(VI) carbonate and hydrolysis species that are important in soil-water systems with pH values greater than 5.

Of the elements included in the project scope, the thermodynamic database distributed by EPA with MINTEQA2 does not contain reactions and associated thermodynamic data for aqueous species and solids containing cesium, plutonium, radon, and thorium. Published compilations of thermodynamic data for aqueous species, solids, and gases containing these elements are available, such as an Langmuir and Herman (1980), Lemire and Tremaine (1980), Peterson *et al.* (1987b), Phillips *et al.* (1988), Smith and Martell (1976 and more recent supplements), Smith *et al.* (1997), Wagman *et al.* (1982), and others. These sources can be used as good starting points for adding reactions for cesium, plutonium, radon, and thorium to the MINTEQA2 database. However, because these sources are becoming dated, additional reviews of the more recent thermodynamic literature would be needed to supplement them and generate more up-to-date compilations for these elements. Other compilations of thermodynamic data for these elements include databases compiled by geochemical modeling groups elsewhere in the United States and other countries. When documented, these databases are useful sources of information.

---

<sup>1</sup> Deutsch, W. J., and K. M. Krupka. September 1985. MINTEQ Geochemical Code: Compilation of Thermodynamic Database for the Aqueous Species, Gases, and Solids Containing Chromium, Mercury, Selenium, and Thallium. Unpublished report prepared by Pacific Northwest Laboratory for the U.S. Environmental Protection Agency in Athens, Georgia.

**Table 5.3.** Component species in MINTEQA2 thermodynamic database.

Element	Component Species	Valence States
Ag	Ag <sup>+</sup>	
Al	Al <sup>3+</sup>	
As	H <sub>3</sub> AsO <sub>3</sub> (aq), H <sub>3</sub> AsO <sub>4</sub> (aq)	As(III), As(V)
B	H <sub>3</sub> BO <sub>3</sub> (aq)	
Ba	Ba <sup>2+</sup>	
Br	Br <sup>-</sup>	
C	CO <sub>3</sub> <sup>2-</sup> , CN <sup>-</sup> , OCN <sup>-</sup>	
Ca	Ca <sup>2+</sup>	
Cd	Cd <sup>2+</sup>	
Cl	Cl <sup>-</sup>	
Cr	Cr <sup>2+</sup> , Cr(OH) <sub>2</sub> <sup>+</sup> , CrO <sub>4</sub> <sup>2-</sup>	Cr(II), Cr(III), Cr(VI)
Cu	Cu <sup>+</sup> , Cu <sup>2+</sup>	Cu(I), Cu(II)
F	F <sup>-</sup>	
Fe	Fe <sup>2+</sup> , Fe <sup>3+</sup>	Fe(II), Fe(III)
Electron	e <sup>-</sup>	
H	H <sup>+</sup> , H <sub>2</sub> O (l)	
Hg	Hg <sub>2</sub> <sup>2+</sup> , Hg(OH) <sub>2</sub> (aq)	Hg(I), Hg(II)
I	I <sup>-</sup>	
K	K <sup>+</sup>	
Li	Li <sup>+</sup>	
Mg	Mg <sup>2+</sup>	

Table 5.3. Continued.

Element	Component Species	Valence States
Mn	$\text{Mn}^{2+}$ , $\text{Mn}^{3+}$	Mn(II), Mn(III)
N	$\text{NH}_4^+$ , $\text{NO}_2^-$ , $\text{NO}_3^-$ , $\text{CN}^-$ , $\text{OCN}^-$	N(-III), N(III), N(V)
Na	$\text{Na}^+$	
Ni	$\text{Ni}^{2+}$	
P	$\text{PO}_4^{3-}$	
Pb	$\text{Pb}^{2+}$	
Rb	$\text{Rb}^{2+}$	
S	$\text{HS}^-$ , $\text{S}^0$ , $\text{SO}_4^{2-}$	S(-II), S(VI)
Sb	$\text{Sb}(\text{OH})_3$ (aq), $\text{Sb}(\text{OH})_6^-$	Sb(III), Sb(V)
Se	$\text{HSe}^-$ , $\text{HSeO}_3^-$ , $\text{SeO}_4^{2-}$	Se(-II), Se(IV), Se(VI)
Si	$\text{H}_4\text{SiO}_4$ (aq)	
Sr	$\text{Sr}^{2+}$	
Tl	$\text{Tl}^+$ , $\text{Tl}(\text{OH})_3$ (aq)	Tl(I), Tl(III)
U	$\text{U}^{3+}$ , $\text{U}^{4+}$ , $\text{UO}_2^+$ , $\text{UO}_2^{2+}$	U(III), U(IV), U(V), U(VI)
V	$\text{V}^{2+}$ , $\text{V}^{3+}$ , $\text{VO}^{2+}$ , $\text{VO}_2^+$	V(II), V(III), V(IV), V(V)
Zn	$\text{Zn}^{2+}$	

**Table 5.4.** Organic ligands in MINTEQA2 thermodynamic database.

Organic Constituents / Complexants	
acetate	methylamine
butyrate	2-methyl pyridine
iso-butyrate	3-methyl pyridine
citrate	4-methyl pyridine
diethylamine	n-butylamine
dimethylamine	nitrilotriacetate <sup>3-</sup>
EDTA <sup>4-</sup>	phthalate
ethylenediamine	propanoate
formate	salicylate
fulvate	tartrate
glutamate	tri-methylamine
glycine	tributylphosphate
hexylamine	valerate
humate	iso-valerate
iso-propylamine	
n-propylamine	

It should be noted that the thermodynamic database distributed with EPA's MINTEQA2 software package does not include reactions and thermodynamic data for aqueous species and solids containing americium, cobalt, neptunium, niobium, radium, and technetium. Although these radionuclides are not part of the scope of this project, they may be important with respect to contamination and remediation at some sites in the United States and/or performance assessments of proposed LLW and HLW disposal facilities or decommissioning sites. Except for niobium, published compilations of thermodynamic data for these elements, especially for americium (Silva *et al.*, 1995) and technetium (Rard, 1983), exist that can be used to supplement the MINTEQA2 database. The thermodynamic data for aqueous species and solids containing niobium are extremely limited which precludes adequate modeling of aqueous/solid phase equilibria for niobium in soil-water systems.

The thermodynamic database of MINTEQA2 was augmented by Krupka and Serne (1998) for aqueous species and solids containing several radionuclide elements of interest to NRC. These database modifications were based on data files provided by D. Turner<sup>1</sup> who had added these

---

<sup>1</sup> Center for Nuclear Waste Regulatory Analyses (CNWRA), Southwest Research Institute, San Antonio, Texas

reactions and thermodynamic data to his version of MINTEQA2. The database additions included MINTEQ-formatted reactions, associated thermodynamic data (*i.e.*,  $\log K_{r,298}^\circ$  and  $\Delta H_{r,298}^\circ$ ) and ancillary information (*e.g.*, identification number, formula, charge, mass, reaction stoichiometry) for aqueous species and solids containing americium, neptunium, plutonium, radium, technetium, thorium, and uranium. The database changes for uranium are based on the compilation by Wanner and Forest (1992), and supersede those listed in the MINTEQA2 database as obtained from EPA. Additional revisions to the thermodynamic data for these radionuclide elements were identified by Krupka and Serne (1998) and added to the MINTEQA2 files. These database modifications have not undergone an in depth examination relative to quality-assurance considerations.

#### 5.2.7.1.5 Issues Related to Database Modifications

Successful application of chemical reaction models to quantify contaminant release and transport in soil-water systems is dependent on the development of adequate and internally consistent thermodynamic databases. The thermodynamic databases of chemical reaction codes are typically revised or supplemented based on specific project needs and the availability of thermodynamic data for aqueous species, gases, and solids containing the constituents of interest.

Although an extensive number of tabulations and critical reviews [*e.g.*, see references in Serne *et al.* (1990, Table 3.2)] of thermodynamic data for inorganic complexes and solids have been published during the last 20 years, the selection of "best" values from these publications is a technically and logistically challenging effort. Some of the issues and problems associated with the selection of thermodynamic data are described in detail in Potter (1979), Nordstrom and Munoz (1985), and Smith and Martell (1995). The critical evaluation and selection of a thermodynamic database requires an understanding of general solution chemistry and the phase assemblages of minerals and related amorphous solids associated with a particular cationic and/or anionic constituent. The investigator developing the model's database must also be cognizant of the criteria initially used to review and select the original data for the published tabulations.

Because thermodynamic data tabulations usually contain an inadequate amount of reviewed thermodynamic data for aqueous species of trace metals, available tabulations are typically deficient for modeling contaminated soil-water systems. Researchers are thus faced with the difficult responsibility of assembling thermodynamic data from other possibly less-credible publications, borrowing values from extant chemical reaction models, and/or conducting their own reviews of published thermodynamic data. Because there is a growing reliance on thermodynamic review efforts completed by coworkers and other research organizations, documentation supporting these reviews and the rationale for selecting each datum that is "accepted" for a model's database are extremely important with respect to (1) defining the credibility of the database, (2) achieving an internally consistent database, (3) minimizing duplication in future review efforts, and (4) describing the selection criteria and calculation methods used in selecting the best values.

### 5.2.7.2 Sorption Database

The MINTEQA2 code is not designed to have a thermochemical database, analogous to the thermodynamic database, that is integrated with the adsorption submodel and its 7 model options. The adsorption reactions and associated model parameters need to be supplied by the user as part of each input file. This process and example input files are discussed in Allison *et al.* (1991).

However, the current MINTEQA2/PRODEFA2 software package is supplied with a limited adsorption data file for use with the diffuse layer adsorption model option. Data files are not supplied for any of the other adsorption model options. The data file, formatted in ASCII, is named *FEO-DLM.dbs*. It includes surface reactions and associated intrinsic conditional surface complexation constants applicable to the diffuse layer model for the adsorption of the trace metals  $\text{Ba}^{2+}$ ,  $\text{Be}^{2+}$ ,  $\text{Ca}^{2+}$ ,  $\text{Cd}^{2+}$ ,  $\text{Cu}^{2+}$ ,  $\text{Ni}^{2+}$ ,  $\text{Pb}^{2+}$ , and  $\text{Zn}^{2+}$ , and the ligands  $\text{H}_3\text{AsO}_3$  (aq),  $\text{H}_3\text{AsO}_4$  (aq),  $\text{H}_3\text{BO}_3$  (aq),  $\text{PO}_4^{3-}$ , and  $\text{SO}_4^{2-}$  onto 2 types of iron-oxide sites. The adsorption constants are based on data published by Dzombak (1986).<sup>1</sup>

#### 5.2.7.2.1 Status Relative to Project Scope

Of the elements chosen for study in this project, cadmium and lead are the only 2 elements included in the diffuse layer adsorption model data file supplied with MINTEQA2. As mentioned above, this file is restricted to adsorption onto 2 types of iron-oxide sites, and is therefore not applicable for the adsorption of these metals to other mineral reactive surfaces. None of the other contaminants, including chromium, cesium, plutonium, radon, strontium, thorium, or uranium, are supported by this data file.

The MINTEQA2/PRODEFA2 software package includes no adsorption database files for the activity partition coefficient ( $K_d^{\text{act}}$ ), activity Langmuir isotherm, activity Freundlich isotherm, ion exchange, constant capacitance, or triple layer adsorption models.

#### 5.2.7.2.2 Published Database Sources

No published compilations are known to exist for adsorption constants for the activity partition coefficient ( $K_d^{\text{act}}$ ), activity Langmuir isotherm, activity Freundlich isotherm, and ion exchange adsorption models used in MINTEQA2. Numerous individual data sets have been published for the adsorption of many individual contaminants on specific mineral substrates, such as  $\text{TiO}_2$  or goethite. Typically, these data are parameterized using 1 or more of the surface complexation models. Compilations and review of these studies was beyond the scope of this project.

Smith and Jenne (1988) (and related papers by Dzombak and Hayes, 1992, and Smith and Jenne, 1992) compiled and evaluated published values for triple layer model constants for the adsorption

---

<sup>1</sup> Personal communication from N. T. Loux at the U.S. Environmental Protection Agency in Athens, Georgia.

142

of numerous constituents on  $\alpha$ -FeO(OH), amorphous iron(III) hydrous oxide, and  $\alpha$ -MnO<sub>2</sub> solids. This study was conducted for the U.S. Environmental Protection Agency (Athens, Georgia) for use in modeling the migration of contaminants in ground-water systems. Their compilation included intrinsic constants and associated reaction stoichiometries for the adsorption of species containing the following constituents:

- For adsorption onto Fe(III) hydrous oxides: Ag, As(V), Ba, CO<sub>3</sub>, Ca, Cd, Co, Cr(VI), Cu(II), Fe(II), Hg(II), Mg, Mn(II), Np(V), Pb, Pu(IV), Sb(III), Sb(V), Se(VI), Se(IV), S, SO<sub>4</sub>, Th(I), U(VI), and Zn
- For adsorption onto  $\alpha$ -MnO<sub>2</sub>: Ag, Ba, Ca, Cd, Co, Cu(II), Fe(II), Hg(II), Mg, Mn(II), Pb, Th(I), and Zn.

Turner (1995) compiled and critically reviewed adsorption data reported in the literature for surface complexation models. He then used a uniform approach to parameterize these data using the diffuse layer, constant capacitance, and triple layer surface complexation models. His study was conducted in support of research funded by NRC to study the potential migration of radionuclides associated with the geologic disposal of commercial high level radioactive waste. Turner (1993) previously described the use of the MINTEQA2 chemical reaction code to model adsorption of radionuclides. Turner (1995) reported model constants for:

- Americium(III) on  $\alpha$ -Al<sub>2</sub>O<sub>3</sub>,  $\beta$ -Al<sub>2</sub>O<sub>3</sub>, and amorphous SiO<sub>2</sub>
- Neptunium(V) on  $\alpha$ -Al<sub>2</sub>O<sub>3</sub>,  $\beta$ -Al<sub>2</sub>O<sub>3</sub>, boehmite ( $\alpha$ -AlOOH), goethite [ $\alpha$ -FeO(OH)], magnetite (Fe<sub>3</sub>O<sub>4</sub>), lepidocrocite [ $\beta$ -FeO(OH)], ferrihydrite (5Fe<sub>2</sub>O<sub>3</sub> · 9H<sub>2</sub>O), amorphous SiO<sub>2</sub>, biotite mica [K(Mg,Fe)<sub>3</sub>(Al,Fe)Si<sub>3</sub>O<sub>10</sub>(OH,F)<sub>2</sub>], and kaolinite [Al<sub>2</sub>Si<sub>2</sub>O<sub>5</sub>(OH)<sub>4</sub>]
- Plutonium(IV) on goethite
- Plutonium(V) on  $\alpha$ -Al<sub>2</sub>O<sub>3</sub> and goethite
- Thorium on  $\alpha$ -Al<sub>2</sub>O<sub>3</sub> and amorphous SiO<sub>2</sub>
- Uranium(VI) on  $\alpha$ -Al<sub>2</sub>O<sub>3</sub>, magnetite, ferrihydrite, goethite, quartz (SiO<sub>2</sub>), and kaolinite
- Carbon on ferrihydrite.

We are not aware of any other major published compilations of adsorption thermochemical data for use with MINTEQA2. Moreover, it is very possible that individual investigators have compiled and parameterized their own databases of adsorption constants based on the needs of their individual research projects. General access, especially in these days of cost recovery, and quality assurance issues will likely prohibit the use of many such individual data files.

143

### 5.3 Adsorption Model Options in MINTEQA2

The MINTEQA2 chemical reaction code includes 7 adsorption model options. Each of these adsorption models and their associated equations and reactions are briefly described below. MINTEQA2 includes the following non-electrostatic adsorption models

- Activity partition coefficient ( $K_d^{act}$ ) model
- Activity Langmuir model
- Activity Freundlich model
- Ion exchange model

and electrostatic adsorption models

- Diffuse layer model
- Constant capacitance model
- Triple layer models.

The following descriptions and associated equations are adapted from the MINTEQA2 documentation by Allison *et al.* (1991). When using the adsorption model options, readers are cautioned to read the MINTEQA2 documentation carefully relative to correct entry and formulation of model reactions and associated constants.

It should be noted that the non-electrostatic models in MINTEQA2 are formulated in terms of species activities, and not the more traditional approach of total concentrations of dissolved metal. The purpose of this approach is to reduce the dependency of the model parameters to effects from ionic strength and aqueous complexation of the adsorbing metal.

Limitations remain, however, regarding these activity formulations which restricts the range of applicability of these non-electrostatic models. These non-electrostatic adsorption models do not consider: charge balance on surface sites and adsorbed species, electrostatic forces between the adsorbing species and charged surface of the mineral, and reactions between the mineral and dissolved constituents other than the adsorbing metal. The effect of these processes changes with variations in the composition of an aqueous solution. These processes are, however, incorporated into the more robust, but more data intensive, electrostatic "surface complexation" adsorption models. The following descriptions of the electrostatic adsorption models incorporated into MINTEQA2 are cursory. The reader is referred to sources, such as Westall and Hohl (1980), Morel *et al.* (1981), Barrow and Bowden (1987), and Davis and Kent (1990), for detailed descriptions, comparisons, and derivations of the relevant equations and reactions associated with these models.

### 5.3.1 Electrostatic Versus Non-Electrostatic Models

Hydrous oxides of iron, manganese, and aluminum and amorphous aluminosilicates that exist as discrete mineral grains or surface coatings on other minerals in soils are assumed to be primary adsorbents for trace metals ions. These solid phases have variable surface charges and exhibit amphoteric behavior. The solids have a net positive charge at pH values below their point of zero charge (PZC) and a net negative charge at pH values above the PZC (see Chapter 2).

These surface charges create electrostatic potentials extending into the surrounding solutions. Dissolved aqueous species that have a charge of the same polarity as the surface will be repelled, while aqueous species with a charge opposite to that of the surface will be attracted (adsorbed). The electrostatic potentials associated with charged surfaces may therefore affect the adsorption of dissolved species on these surfaces. Unlike the non-electrostatic adsorption models, the electrostatic models include a component that accounts for the electrostatic potentials at the charged surface. The mass action equations of electrostatic adsorption models include terms that modify the activities of adsorbing species approaching charged surfaces by the electrical work necessary to penetrate the zone of electrostatic potentials ( $\psi$ 's) associated with the mineral surface. The 3 electrostatic models in MINTEQA2 differ primarily in the types of surface species that are allowed within specific physical locations or layers extending away from the surface and in the parameters that each model uses.

The 3 electrostatic models in MINTEQA2 deal with adsorption as surface complexation reactions analogous to aqueous complexation reactions in solution. In the descriptions of the MINTEQA2 adsorption models that follow, surface sites are represented in the adsorption reactions and mass action expressions as SOH groups, where S refers to the mineral structure and adsorption site located at the solid-liquid interface. Some ions, such as  $H^+$ ,  $OH^-$ , and a variety of trace metal ions are assumed to be adsorbed by complexation with these surface sites.

In the triple layer model (TLM), the most complicated of the 3 electrostatic adsorption models in MINTEQA2, the space around the solid surface is represented in surface complexation adsorption models as 3 semi-infinite layers or zones between the solid surface and the solution (Figure 5.4). These zones are separated by the  $o$ ,  $\psi$ , and  $d$  planes. Starting at the mineral surface, The  $o$  plane represents the first interface between the solid surface and the aqueous phase. Generally, only the  $H^+$  and  $OH^-$  ions are allowed to penetrate the  $o$  layer to interact with the solid surface. Beyond the  $o$  plane, farther from the mineral surface, is the  $\psi$  plane which ends at the boundary of the diffuse zone, the  $d$  plane. Dissolved ions, such as macro constituents (*e.g.*,  $Na^+$ ,  $Ca^{2+}$ , and  $SO_4^{2-}$ ) and trace constituents ions that are adsorbing onto the solid surface are allowed into the  $\psi$  layer. The third layer is the diffuse zone where the ions are not influenced strongly by electrostatic charge on the solid surface. The ions in this region are considered to be counterions that neutralize any residual charge caused by the surface and adsorbed ions in the  $\psi$  layer. Continuing further from the mineral surface, the  $d$  layer blends into the bulk solution.

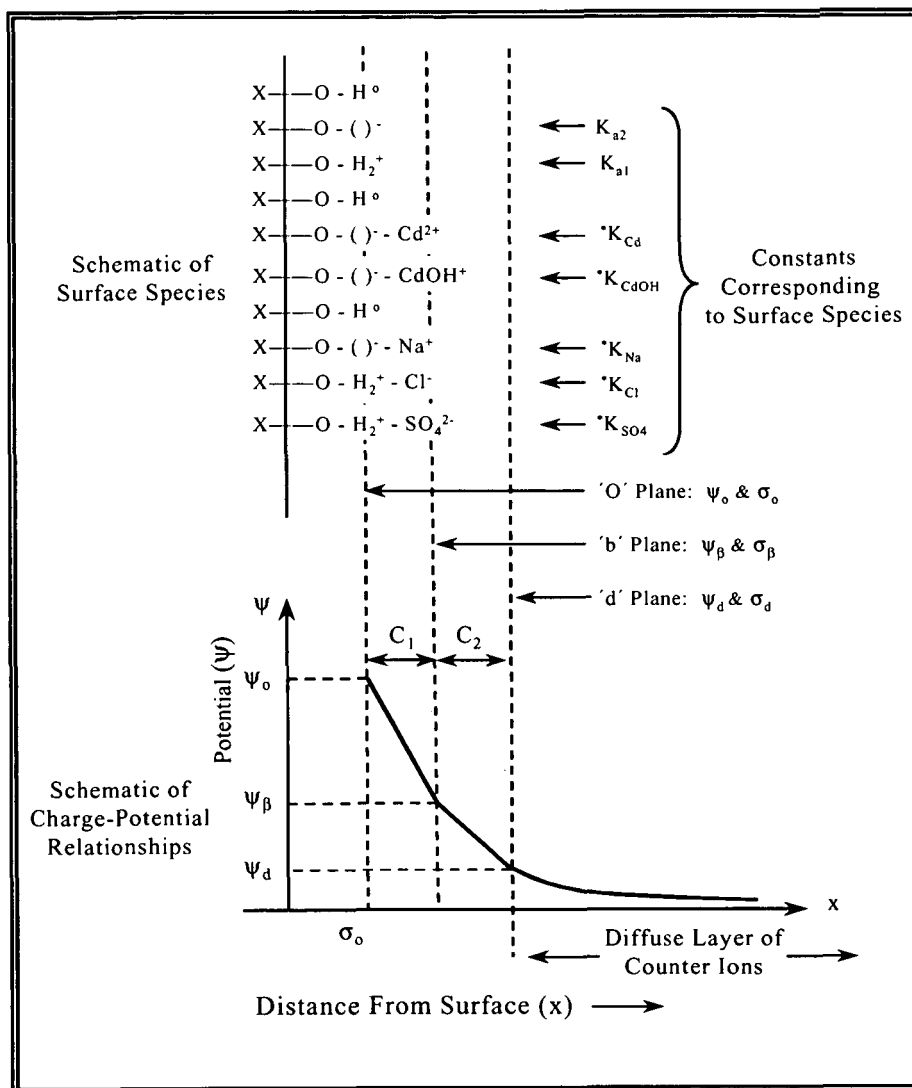


**Figure 5.4.** Schematic representation of the triple layer model showing surface species and surface charge-potential relationships. [Taken from Peterson *et al.* (1987a). Brackets in the o plane indicated deprotonated surface sites.]

The conceptual models for the constant capacitance (Figure 5.5) and diffuse layer models are simplified to only 2 zones separated by the *o* and *d* planes. The difference between these 2 adsorption models is in the function relating total surface charge,  $T_{\sigma}$ , to surface potential  $\psi_o$  (discussed in Sections 5.3.6 and 5.3.7). This function [ $\psi(x)$  in Figure 5.5)] is linear and exponential, respectively, in the constant capacitance and diffuse layer models. It should be noted that parameters subscripted with “*o*” in that 2-layer models are not equivalent to the *o* plane parameters defined for the triple layer model due to differences in the definition of the *o* plane.

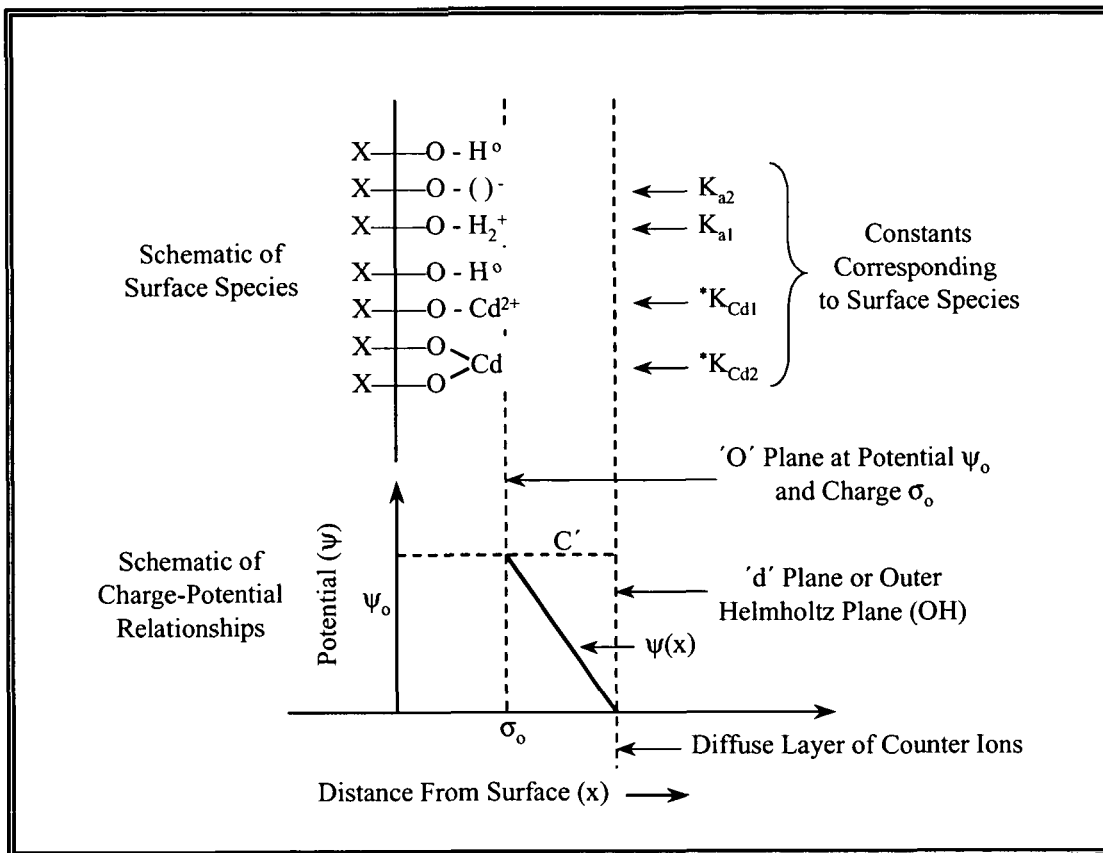


**Figure 5.5.** Schematic representation of the constant capacitance layer model showing surface species and surface charge-potential relationships. [Taken from Peterson *et al.* (1987a). Brackets in the *o* plane indicated deprotonated surface sites.]

147

In all 3 models, a charge,  $\sigma$ , associated with the surface is assumed to be balanced by a charge ( $\sigma_d$ ) associated with the diffuse layer  $d$  of counterions such that

$$\sigma = \sigma_d = 0 \quad (5.10)$$

In the constant capacitance and diffuse-layer models, all adsorbed ions contribute to the surface charge. However, the net charge  $\sigma$  due to adsorption in the triple layer model is the sum of the charges associated with 2 rather than 1 adsorbing plane. These include the innermost  $o$  plane and the  $\beta$  plane, which are characterized by charges  $\sigma_o$  and  $\sigma_\beta$ , respectively. Thus, for the triple layer model, the net surface charge is given by

$$\sigma = \sigma_o + \sigma_\beta \quad (5.11)$$

which is balanced by the charge in the diffuse layer such that

$$(\sigma_o + \sigma_\beta) = \sigma_d = 0 \quad (5.12)$$

Because the electrical potential gradients extending away from the mineral's surface result from the surface charge, the specifically adsorbed potential determining ions also govern distributions of counterions in the diffuse layer.

Activities of ions in solution and near the surface are influenced by the presence of electrostatic potentials arising from the surface charge. The activity difference between ions near the surface and those far away is the result of electrical work required to move them across the potential gradient between the charged surface and the bulk solution. The activity change between these zones is related to the ion charge,  $z$ , and the electrical potential,  $\psi$ , near the surface and can be expressed using the exponential Boltzmann expression,

$$\{X_s^z\} = \{X^z\} [e^{-\psi F/RT}]^z \quad (5.13)$$

- where  $z$  = charge of ion X,  
 $\{X_s^z\}$  = activity of an ion X of charge  $z$  near the surface,  
 $\{X^z\}$  = activity of ion X in bulk solution beyond the influence of the charged surface,  
 $e^{-\psi F/RT}$  = Boltzmann factor,  
 $F$  = Faraday constant,  
 $R$  = ideal gas constant, and  
 $T$  = absolute temperature in Kelvin.

The general algorithm is similar for all 3 electrostatic models in MINTEQA2. Each model is only briefly described below. The surface reactions for the electrostatic models in MINTEQA2 are written with the Boltzmann factor included as a reactant component with a stoichiometric factor appropriate for the reaction. Although these electrostatically-related components are included in the mass action equations, they are not analogous to the chemical components defined in

MINTEQA2 and have no analytical totals for their input values. Their total charges are determined from equations that are unique to each electrostatic model and potential. The activity coefficients for the Boltzmann factor components are set to unity in MINTEQA2.

Adsorption reactions are entered as part of MINTEQA2 input files. The MINTEQA2 code, as noted previously, has no integrated adsorption database. The adsorption reactions and associated equilibrium constants are written in terms of the neutral surface site, SOH. They are entered as formation reactions, analogous to the aqueous complexation and mineral solubility reactions included in the thermodynamic database. Published adsorption reactions and associated constants are, however, sometimes referenced to the protonated surface site  $\text{SOH}_2^+$  for adsorbing anions and the deprotonated site  $\text{SO}^-$  for adsorbing cations. In these cases, the user must modify the published reaction and equilibrium constant data in terms of MINTEQA2 components to use them in a MINTEQA2 input file.

### 5.3.2 Activity Partition Coefficient ( $K_d$ ) Model

The traditional partition coefficient,  $K_d$ , adsorption model (see Chapter 2) is defined as the ratio of the concentration of metal bound on the surface of the solid to the total concentration of metal dissolved in the liquid phase at equilibrium as in

$$K_d \square \frac{\text{Amount of element sorbed on solid} / \text{solid mass}}{\text{Amount of element dissolved in solution} / \text{solution volume}} \quad (5.14)$$

This process can be expressed as the surface adsorption reaction



where SOH = unreacted surface site,  
M = a dissolved metal M, and  
SOH·M = adsorption site occupied by a component or surface-bound metal M.

The convention used for symbols in the adsorption model equations discussed in this chapter follows that used by Allison *et al.* (1991). Although the basic adsorption equations are comparable to those listed in Chapter 2, the symbols may differ slightly.

The mass action expression for this reaction is

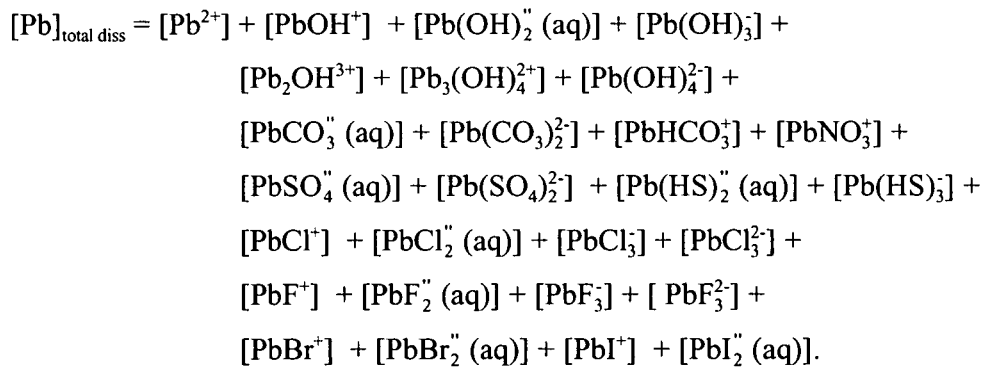
$$K_d \square \frac{[\text{SOH}\cdot\text{M}]}{[\text{M}]_{\text{total diss}}} \quad (5.16)$$

where  $[\text{SOH}\cdot\text{M}]$  = concentration of adsorption sites occupied by a component M or surface-bound metal per unit mass of adsorbing solid

$[M]_{\text{total diss}} = \text{total concentration of dissolved M at equilibrium.}$

Following common convention for thermodynamic nomenclature, reaction species indicated within [ ] refer to concentrations, and those indicated within { } refer to activities. Equation 5.16 assumes that the concentration of unreacted surface sites, SOH, are in great excess relative to the total concentration of dissolved metal and the activity of SOH is equal to 1.

As mentioned previously, the traditional  $K_d$  assumes that all species of metal M absorb with equal strength, and  $[M]_{\text{total diss}}$  includes all aqueous species containing metal M. For example, using the species listed in the MINTEQA2 thermodynamic database, the total concentrations of dissolved lead,  $[Pb]_{\text{total diss}}$ , in the absence of any organic complexants in the water, could include the following species:



In the presence of organic complexants,  $[Pb]_{\text{total diss}}$  would also include, in addition to the lead species listed above, the concentrations of aqueous lead citrate, acetate, EDTA, HEDTA, and other organic complexes.

Because experimental data suggest that only certain aqueous species react with the surface of a mineral, the traditional  $K_d$  model is reformulated in MINTEQA2 in terms of the activities of species to provide the activity  $K_d^{\text{act}}$  model.

In MINTEQA2, the mass action expression for the activity  $K_d^{\text{act}}$  model is

$$K_d^{\text{act}} = \frac{\{\text{SOH}\cdot\text{M}\}}{\{\text{M}\}} = \frac{[\text{SOH}\cdot\text{M}]}{\gamma_M[M]} \quad (5.17)$$

where  $\{\text{M}\} = \text{free activity of the uncomplexed "bare" cation of M in the equilibrium solution,}$   
 $\gamma_M = \text{activity coefficient of dissolved species M}$

The quantity  $\{\text{SOH}\cdot\text{M}\}$  is defined as equal to  $[\text{SOH}\cdot\text{M}]$ . This assumption is made because there is no generally accepted method for calculating activity coefficients for unreacted or reacted adsorption sites. The parameter  $K_d^{\text{act}}$  can be considered the equilibrium constant for the surface

reaction described in Equation 5.15. This model assumes that there is an unlimited supply of unreacted adsorption sites and the mineral surface cannot become saturated regardless of how much M adsorbs.

### 5.3.3 Activity Langmuir Model

The concentration-based Langmuir adsorption model has the constraint that the number of surface sites available for adsorption is limited. This is the only difference between the Langmuir and  $K_d$  adsorption models. The partition coefficient,  $K_d$ , model is linear with respect to the total concentration of a dissolved metal, whereas the Langmuir model is non-linear. The user must specify the concentration of available adsorption sites as part of the input file. The Langmuir equation for adsorption is defined by

$$[\text{SOH}\cdot\text{M}] = \frac{K_L [\text{SOH}]_{\text{total}} [\text{M}]_{\text{total diss}}}{1 + K_L [\text{M}]_{\text{total diss}}} \quad (5.18)$$

where  $K_L$  = Langmuir adsorption constant,  
 $[\text{SOH}\cdot\text{M}]$  = amount of adsorbed metal M per unit mass of adsorbing solid,  
 $[\text{SOH}]_{\text{total}}$  = total concentration of available surface adsorption sites, and  
 $[\text{M}]_{\text{total diss}}$  = total concentration of dissolved metal M at equilibrium.

The surface adsorption reaction used for the Langmuir model is identical to that for the  $K_d$  model



The equilibrium constant,  $K_L^{\text{act}}$ , for this reaction can be expressed in terms of activities as

$$K_L^{\text{act}} = \frac{\{\text{SOH}\cdot\text{M}\}}{\{\text{M}\}\{\text{SOH}\}} = \frac{a_{\text{SOH}\cdot\text{M}}}{a_{\text{M}} a_{\text{SOH}}} \quad (5.20)$$

As discussed previously, the activity coefficients pertaining to unreacted and reacted surface sites in this and the other adsorption models in MINTEQA2 are assigned values of unity.

Equation 5.20 can then be rewritten as

$$K_L^{\text{act}} = \frac{[\text{SOH}\cdot\text{M}]}{a_{\text{M}} [\text{M}] [\text{SOH}]} \quad (5.21)$$

The mass balance equation for the available surface sites is

$$[\text{SOH}]_{\text{total}} = [\text{SOH}\cdot\text{M}] + [\text{SOH}] \quad (5.22)$$

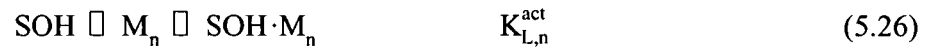
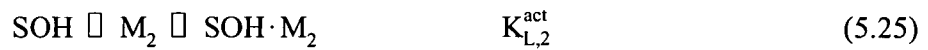
By combining Equations 5.21 and 5.22 in terms of  $[\text{SOH}]_{\text{total}}$  and  $[\text{SOH}\cdot\text{M}]$ , one obtains the Langmuir relationship in terms of activities

191

$$[\text{SOH} \cdot \text{M}] = \frac{K_L^{\text{act}} [\text{SOH}]_{\text{total}} \alpha_m [\text{M}]}{1 + K_L^{\text{act}} \alpha_m [\text{M}]} \quad (5.23)$$

By substituting  $K_L^{\text{act}}$  with  $K_L$  and setting  $\alpha_m$  to a value of 1, Equation 5.23 reduces to the concentration Langmuir model expressed in Equation 5.18.

To use MINTEQA2 to model competition between different metals for adsorption on the available surface sites, one must define the separate adsorption reactions on the surface. For the competitive Langmuir model for the competing metals  $M_1, M_2, \dots, M_n$ , separate reactions with associated mass balance expressions need to be formulated using Equations 5.19-5.21 such that



Geochemical modeling and plotting techniques may be used to derive constants for the activity Langmuir model from experimentally-measured, concentration-based  $K_L$  data. One must first determine if the concentration-based Langmuir model fits the experimental data by using the linear form of Equation 5.18

$$\frac{[\text{M}]_{\text{total diss}}}{[\text{SOH} \cdot \text{M}]} = \frac{1}{K_L [\text{SOH}]_{\text{total}}} + \frac{[\text{M}]_{\text{total diss}}}{[\text{SOH}]_{\text{total}}} \quad (5.27)$$

A plot of  $[\text{M}]_{\text{total diss}}/[\text{SOH} \cdot \text{M}]$  versus  $[\text{M}]_{\text{total diss}}$  will result in a straight line with the slope  $1/[\text{SOH}]_{\text{total}}$  and intercept  $1/K_L[\text{SOH}]_{\text{total}}$  if the data fit the Langmuir isotherm. The value for the concentration-based  $K_L$  is obtained by dividing this slope by the intercept. Geochemical modeling is then used to calculate the aqueous speciation of metal M for the composition of the aqueous solution in which the  $K_L$  data were determined. The  $K_L^{\text{act}}$  value can then be derived from an analogous plot in which the calculated activities  $\{M\}$  for metal M are plotted in place of the concentration term  $[M]$ .

### 5.3.4 Activity Freundlich Model

The concentration-based Freundlich equation for adsorption is defined by

$$[\text{SOH} \cdot \text{M}] = K_F [\text{M}]_{\text{total diss}}^{1/N} \quad (5.28)$$

where  $K_F$  = Freundlich adsorption constant,  
 $[\text{SOH} \cdot \text{M}]$  = amount of adsorbed metal M per unit mass of adsorbing solid,  
 $[\text{M}]_{\text{total diss}}$  = total concentration of dissolved metal M at equilibrium, and  
 $N$  = a constant.

The Freundlich equation is sometimes written with the exponent in Equation 5.28 being  $N$  instead of  $1/N$ . The Freundlich model assumes, like the  $K_d$  adsorption model, an unlimited supply of unreacted adsorption sites. For the special case where  $N$  equals 1, the mass action equations for the Freundlich and  $K_d$  models are identical.

The Freundlich model can be considered as a surface adsorption reaction where the stoichiometric coefficient for the adsorbed metal M equals  $1/N$  as in



The equilibrium constant,  $K_F^{\text{act}}$ , for this reaction can be expressed in terms of activities as

$$K_F^{\text{act}} = \frac{\{\text{SOH} \cdot \text{M}\}}{\{\text{M}\}^{1/N} \{\text{SOH}\}} \quad (5.30)$$

Like the activity  $K_d^{\text{act}}$  model, there is no mass balance on surface sites, and, assuming an excess of sites with respect to adsorbed metal M, the concentration,  $[\text{SOH}]$ , and activity  $\{\text{SOH}\}$ , of the unreacted surface sites are assumed equal and set to 1. Under these conditions and assuming  $\{\text{SOH} \cdot \text{M}\}$  equals  $[\text{SOH} \cdot \text{M}]$  as with the activity  $K_d^{\text{act}}$  and Langmuir models, Equation 5.30 becomes

$$K_F^{\text{act}} = \frac{[\text{SOH} \cdot \text{M}]}{\{\text{M}\}^{1/N}} \quad (5.31)$$

which is similar to the  $K_d^{\text{act}}$  model except that the stoichiometric coefficient  $1/N$  of the adsorbing species of metal M.

An approach using geochemical modeling and plotting techniques similar to that described for the activity Langmuir model may be used to calculate constants for the activity Freundlich model from experimentally-measured, concentration-based  $K_F$  data. One must first determine if the Freundlich model fits the experimental data by using the logarithmic form of the Freundlich mass action Equation 5.28

$$\log [\text{SOH} \cdot \text{M}] \approx \log K_F \approx \left( \frac{1}{N} \right) \log [\text{M}]_{\text{total diss}} \quad (5.32)$$

If the data fit the model, a plot of  $\log [\text{SOH} \cdot \text{M}]$  versus  $\log [\text{M}]_{\text{total diss}}$  will result in a straight line with the slope  $1/N$  and intercept  $\log K_F$ . Geochemical modeling is then used to calculate the aqueous speciation of metal  $M$  for the composition of the aqueous solution in which the  $K_F$  data were determined. The  $K_F^{\text{act}}$  value can then be derived by plotting the calculated activities  $\{M\}$  for the adsorbing species of metal  $M$  in place of the concentration term  $[\text{M}]_{\text{total diss}}$ .

### 5.3.5 Ion Exchange Model

Ion exchange sorption is defined as the process by which a dissolved ion  $M_2$  is exchanged for an ion  $M_1$  that already occupies a surface sorption site and ion  $M_1$  is in turn released back into solution. The ion exchange reaction can be expressed as



where  $M_1$  = the ion initially occupying the exchange site,  
 $M_2$  = the ion replacing  $M_1$  on the exchange site;  
 $\text{SOH} \cdot \text{M}_1$  = surface sites occupied by ion  $M_1$   
 $\text{SOH} \cdot \text{M}_2$  = surface sites occupied by ion  $M_2$ , and  
 $a$  and  $b$  = stoichiometric coefficients.

The equilibrium constant (selectivity coefficient),  $K_{\text{ex}}$ , for the exchange reaction expressed as

$$K_{\text{ex}} \approx \frac{\{M_1\}^a \{\text{SOH} \cdot \text{M}_2\}^b}{\{M_2\}^b \{\text{SOH} \cdot \text{M}_1\}^a} \approx \frac{\gamma_{M_1}^a [M_1]^a [\text{SOH} \cdot \text{M}_2]^b}{\gamma_{M_2}^b [M_2]^b [\text{SOH} \cdot \text{M}_1]^a} \quad (5.34)$$

The constant  $K_{\text{ex}}$  can be written in terms of concentrations by replacing activity of each species with the product of concentration and activity coefficient. The activity coefficients for the occupied sites,  $\text{SOH} \cdot \text{M}_n$ , are set equal to one as was assumed for the previous adsorption models in MINTEQA2.

### 5.3.6 Diffuse Layer Model

For the diffuse-layer model, the total charge,  $T_o$ , for plane  $o$  is calculated as

$$T_o \approx 0.1174 I^{1/2} \sinh(Z \approx_o F/2RT) \quad (5.35)$$

where  $Z$  = valency of the symmetrical electrolyte (which we take as unity),  
 $I$  = ionic strength, and

all other parameters are defined as in Equation 5.13.

Examples of surface reactions are listed below for protonation and deprotonation reactions as well as for a divalent cation  $M^{2+}$ . Boltzmann factors are represented in the mass action as components.

The surface reaction and corresponding mass action expression for the protonation reaction are, respectively,



and

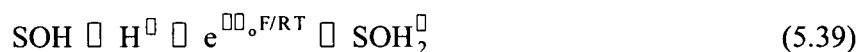
$$K \rightleftharpoons \frac{\{\text{SOH}_2^+\}}{\{\text{SOH}\} \{\text{H}_s^+\}} \quad (5.37)$$

where  $\text{H}_s^+$  denotes a hydronium ion near the surface.

The activity coefficients for the surface species  $\text{SOH}_2^+$  and  $\text{SOH}$  are assumed to be equal to unity. The activity of  $\text{H}_s^+$  must be corrected for the energy change required to move from the bulk solution to the charged surface. This activity change is represented by expressing  $\{\text{H}_s^+\}$  in terms of the activity of the bulk solution hydronium ion  $\{\text{H}^+\}$  and associated exponential Boltzmann expression for a charge  $z$  of 1 as

$$\{\text{H}_s^+\} \rightleftharpoons \{\text{H}^+\} e^{\frac{-F}{RT}} \quad (5.38)$$

Substituting this expression for  $\{\text{H}_s^+\}$  in Equations 5.36 and 5.37, one obtains the following surface reaction and mass action equation expressed in terms of the Boltzmann factor



and

$$K \rightleftharpoons \frac{\{\text{SOH}_2^+\}}{\{\text{SOH}\} \{\text{H}^+\} [e^{\frac{-F}{RT}}]} \quad (5.40)$$

The stoichiometry for the corresponding de-protonation reaction is



Substituting for  $\{\text{H}_s^+\}$  as above results in the following de-protonation surface reaction and mass action equation



and

$$K = \frac{\{SO^{\square}\} \{H^{\square}\} [e^{\square\square_o F/RT}]}{\{SOH\}} \quad (5.43)$$

The stoichiometry for a surface reaction involving a multivalent species, such as a divalent cation  $M^{2+}$ , is



The mass action expression for this type of adsorption reaction also includes the charge and stoichiometry for the adsorbing ion. Substituting for  $\{M_s^{2+}\}$  and for  $\{H_s^{\square}\}$  in Equation 5.44, one obtains the following mass action expressions

$$K = \frac{\{SO \cdot M^{\square}\} \{H_s^{\square}\}}{\{SOH\} \{M_s^{2\square}\}} = \frac{\{SO \cdot M^{\square}\} \{H^{\square}\} [e^{\square\square_o F/RT}]}{\{SOH\} \{M^{2\square}\} [e^{\square\square_o F/RT}]^2} \quad (5.45)$$

$$K = \frac{\{SO \cdot M^{\square}\} \{H^{\square}\}}{\{SOH\} \{M^{2\square}\} [e^{\square\square_o F/RT}]} \quad (5.46)$$

Mass action expressions for other surface reactions are formulated in a similar manner.

### 5.3.7 Constant Capacitance Model

The constant capacitance model is a special case of the diffuse layer model, applicable in theory only to systems at high, constant ionic strength. The constant capacitance model is similar to the diffuse layer model in that they both define specific adsorption of all ions on the  $o$  plane. Except for the values of the equilibrium constants, the mass action and charge balance equations are identical for these 2 adsorption models. Therefore, the surface reactions and mass action expressions described above for the diffuse layer model also apply to the constant capacitance model.

The difference in these 2 models is in the function relating total surface charge,  $T_o$ , to surface potential  $\psi_o$ . In the constant capacitance model, Equation 5.35 is approximated by

$$T_o = C \psi_o \quad (5.47)$$

where  $C$  is a constant capacitance term. Although the constant capacitance and diffuse layer models are implemented similarly, the capacitance term  $C$  is often treated as a fitting parameter rather than as a measured characteristic of the system.

### 5.3.8 Triple Layer Model

The triple layer model (Figure 5.4) includes 2 adsorbing planes instead of 1 plane as conceptualized in the diffuse layer and constant capacitances models. As implemented in MINTEQA2, the *o* plane, the inner most zone, only includes the protonation and deprotonation (*i.e.*, gain or loss of H<sup>+</sup>) reactions at the surface sites. The  $\square$  plane includes other specifically adsorbed ions with charge  $\square_0$  and potential  $\square_0$  in that zone. The diffuse layer or '*d*' plane, which is the outer most zone, includes non-specifically adsorbed ions affected by  $\square_d$  potentials. The capacitances between the *o* and  $\square$  planes and the  $\square$  and *d* planes are designated  $C_1$  and  $C_2$ , respectively. The user must provide values for both capacitance terms.

The total charges,  $T_{\square_0}$ ,  $T_{\square}$ , and  $T_{\square_d}$ , associated with *o*,  $\square$ , and *d* planes, respectively, in the triple-layer model are defined as

$$T_{\square_0} = C_1(\square_0 - \square_{\square}) \quad (5.48)$$

$$T_{\square} = C_1(\square_{\square} - \square_o) + C_2(\square_{\square} - \square_d) \quad (5.49)$$

$$T_{\square_d} = C_2(\square_d - \square_{\square}) \quad (5.50)$$

where  $\square_o$  = electrostatic potential at the *o* plane,  
 $\square_{\square}$  = electrostatic potential at the  $\square$  plane, and  
 $\square_d$  = electrostatic potential at the *d* plane.

Surface reactions as expressed in the triple layer model differ from those used for the diffuse layer and constant capacitance models only in that their mass action expressions include the proper stoichiometry for the electrostatic components representing the  $\square$  and *o* planes. The *d* plane, which has no specific adsorption, is therefore not a factor in the stoichiometry.

The surface protonation and deprotonation reactions for the triple layer model, except for their associated equilibrium constant values, are identical to those given above for the diffuse layer models. Examples of surface reactions and mass action expressions for the adsorption of a mono- and divalent cations and a monovalent anion adapted from Allison *et al.* (1991) are given below for the triple layer model. They show the stoichiometric coefficients for the electrostatic components representing the  $\square$  and *o* planes.

The surface reaction for the adsorption of the monovalent metal cation M<sup>+</sup> is



In the triple layer model,  $H_s^+$  and  $M_s^+$  occur in the  $o$  and  $\square$  planes, respectively. Therefore,

$$\{H_s^{\square}\} = \{H^{\square}\} [e^{\square o F/RT}] \quad (5.52)$$

and

$$\{M_s^{\square}\} = \{M^{\square}\} [e^{\square o F/RT}] . \quad (5.53)$$

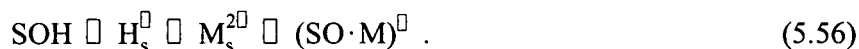
Substituting these expressions into Equation 5.51, the following MINTEQA2 reaction and mass action expression are obtained



and

$$K = \frac{\{SO \cdot M\} \{H^{\square}\} [e^{\square o F/RT}]}{\{SOH\} \{M^{\square}\} [e^{\square o F/RT}]} . \quad (5.55)$$

The surface reaction for the adsorption of the divalent metal cation  $M^{2+}$  is



For the divalent cation adsorbed in the  $\square$  plane,

$$\{M_s^{2\square}\} = \{M^{2\square}\} [e^{\square o F/RT}]^2 \quad (5.57)$$

Substituting this expression in the reaction above gives the following MINTEQA2 reaction and mass action expression



and

$$K = \frac{\{SO \cdot M^{\square}\} \{H^{\square}\} [e^{\square o F/RT}]}{\{SOH\} \{M^{2\square}\} [e^{\square o F/RT}]^2} . \quad (5.59)$$

The surface reaction for the adsorption of the monovalent anion  $A^-$  is

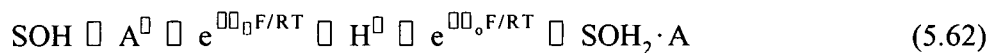


This reaction results in the formation of a neutral surface complex. For the anion adsorbed in the  $\square$  plane

158

$$\{A_s^{\ominus}\} = \{A^{\ominus}\} [e^{\ominus F/RT}] \quad (5.61)$$

Substituting this into the above anion adsorption reaction, one obtains the following MINTEQA2 reaction and mass action expression



and

$$K = \frac{\{\text{SOH}_2 \cdot A\} [e^{\ominus F/RT}]}{\{\text{SOH}\} \{A^{\ominus}\} \{\text{H}^{\oplus}\} [e^{\ominus F/RT}]} \quad (5.63)$$

The formulation of reactions and mass action expressions for other adsorbing cations and anions is similar to those examples given above.

#### 5.4 Summary

Chemical reaction models are valuable computational tools that may be used to analyze the macro-chemical processes (*e.g.*, aqueous complexation, redox, solubility, and adsorption equilibrium) affecting the composition of a soil-water system being studied in the laboratory, field lysimeter, or field site. They also be used to provide some bounding calculations for predicting the changes in chemistry that will result when 1 or more of these processes are imposed on a soil-water system.

Numerous chemical reaction models exist. The MINTEQA2 computer code was developed with EPA funding and is currently distributed by EPA in a form that executes on personal computers. MINTEQA2 includes aqueous speciation, solubility (*i.e.*, saturation indices), precipitation/dissolution, and adsorption submodels. MINTEQA2's adsorption submodel includes 4 non-electrostatic [activity partition coefficient ( $K_d^{\text{act}}$ ), activity Langmuir, activity Freundlich, and ion exchange] models and 3 electrostatic (diffuse layer, constant capacitance, and triple layer) adsorption model options.

MINTEQA2 and other similar chemical reaction models can be used in indirect ways to support evaluations of  $K_d$  values and related contaminant migration and risk assessment modeling. These applications include the following:

- Calculation of aqueous speciation to determine the ionic state and composition of the dominant species for a dissolved contaminant present in a soil-water system
- Calculation of bounding, technically-defensible maximum concentration limits for contaminants (based on solubility constraints) as a function of key composition parameters (*e.g.*, pH) of any specific soil-water system

- Analysis of data from laboratory measurements of  $K_d$  values to determine if any solubility limits were exceeded during the experiments.

Chemical reaction models, however, cannot be used to predict a  $K_d$  value. The user must supply the adsorption parameters when using any of the adsorption model options. However, MINTEQA2 may be used to predict the chemical changes that result in the aqueous phase from adsorption using any of 7 adsorption model options.

The MINTEQA2 model includes an extensive thermodynamic database that is integrated with the aqueous speciation, solubility, and precipitation/dissolution submodels. Of the elements included in the project scope, the thermodynamic database distributed by EPA with MINTEQA2 does not contain reactions and associated thermodynamic data for aqueous species and solids containing cesium, plutonium, radon, and thorium. Published compilations of thermodynamic data for aqueous species, solids, and gases containing these elements are available that can be used as starting points for upgrading the MINTEQA2 database to include cesium, plutonium, radon, and thorium aqueous species and solids. MINTEQA2 does not have per se an integrated adsorption submodel database. The adsorption reactions and associated model parameters must be supplied by the user as part of each input file.

160

## 6.0 REFERENCES

- Alberty, R. A. 1987. *Physical Chemistry*. Seventh Edition, John Wiley and Sons, New York, New York.
- Allison, J. D., D. S. Brown, and K. J. Novo-Gradac. 1991. *MINTEQA2/PRODEFA2, A Geochemical Assessment Model for Environmental Systems: Version 3.0 User's Manual*. EPA/600/3-91/021, U.S. Environmental Protection Agency, Athens, Georgia, March 1991.
- Ames, L. L., and J. E. McGarrah. 1980. *Basalt Radionuclide Distribution Coefficient Determinations, FY1979 Annual Report*. PNL-3146, Pacific Northwest Laboratory, Richland, Washington.
- Ames, L. L., J. E. McGarrah, B. A. Walker, and P. F. Salter. 1982. "Sorption of Uranium and Cesium by Hanford Basalts and Associated Secondary Smectite." *Chemical Geology*, 35:205-225.
- Ames, L. L., and D. Rai. 1978. *Radionuclide Interactions with Soil and Rock Media*. EPA 520/6-78-007, U.S. Environmental Protection Agency, Office of Radiation Programs, Las Vegas, Nevada.
- ASTM (American Society of Testing and Materials). 1987. "24-hour Batch-Type Measurement of Contaminant Sorption by Soils and Sediments." In *Annual Book of ASTM Standards, Water and Environmental Technology, Volume 11.04*, pp. 163-167, Philadelphia, Pennsylvania.
- ASTM (American Society of Testing and Materials). 1988. "Determining a Sorption Constant ( $K_o$ ) for an Organic Chemical in Soil and Sediments." In *Annual Book of ASTM Standards, Water and Environmental Technology, Volume 11.04*, pp. 731-737, Philadelphia, Pennsylvania.
- Atkinson, A. 1983. "Mathematical Modeling of Leaching From Porous Nuclear Waste-Forms." *Radioactive Waste Management and the Nuclear Fuel Cycle*, 3:371-386.
- Atkinson, A., K. Nelson, and T. M. Valentine. 1986. "Leach Test Characterization of Cement-Based Nuclear Waste Forms." *Nuclear and Chemical Waste Management*, 6:241-253.
- Atkinson, A., and A. K. Nickerson. 1988. "Diffusion and Sorption of Cesium, Strontium, and Iodine in Water-Saturated Cement." *Nuclear Technology*, 81:100-113.

161

- Backhus, D. A., J. N. Ryan, D. M. Groher, J. K. MacFarlane, and P. M. Gschwend. 1993. "Sampling Colloids and Colloid-Associated Contaminants in Ground Water." *Ground Water*, 31:466-479.
- Baetslé, L. H. 1967. "Migration of Radionuclides in Porous Media." In *Progress in Nuclear Energy, Series XII, Health Physics*, A.M.F. Duhamel (ed.), pp. 707-730, Pergamon Press, Elmsford, New York.
- Ball, J. W., E. A. Jenne, and M. W. Cantrell. 1981a. *WATEQ3: A Geochemical Model with Uranium Added*. Open-File Report 81-1183, U.S. Geological Survey, Menlo Park, California.
- Ball, J. W., and D. K. Nordstrom. 1998. "Critical Evaluation and Selection of Standard State Thermodynamic Properties for Chromium Metal and Its Aqueous Ions, Hydrolysis Species, Oxides, and Hydroxides." *Journal of Chemical and Engineering Data*, 43:895-918.
- Ball, J. W., D. K. Nordstrom, and E. A. Jenne. 1981b. *Additional and Revised Thermochemical Data and Computer Code for WATEQ2--A Computerized Chemical Model for Trace and Major Element Speciation and Mineral Equilibria of Natural Waters*. Water Resources Investigations WRI 78-116 (second printing), U.S. Geological Survey, Menlo Park, California.
- Ball, W. P., C. H. Buehler, T. C. Harmon, D. M. Mackay, and P. V. Roberts. 1990. "Characterization of a Sandy Aquifer Material at the Grain Scale." *Journal of Contaminant Hydrology*, 5:253-295.
- Barber, L. B., II., E. M. Thurman, and D. D. Runnells. 1992. "Geochemical Heterogeneity in a Sand and Gravel Aquifer: Effect of Sediment Mineralogy and Particle Size on the Sorption of Chlorobenzenes." *Journal of Contaminant Hydrology*, 9:35-54.
- Barrow, N. J., and J. W. Bowden. 1987. "A Comparison of Models for Describing the Adsorption of Anions on a Variable Charge Mineral Surface." *Journal of Colloid and Interface Science*, 119:236-250.
- Bates, R. L., and J. A. Jackson (eds.). 1980. *Glossary of Geology*. American Geological Institute, Falls Church, Virginia.
- Berry, J. A. 1992a. *A Review of Sorption of Radionuclides Under the Near- and Far-Field Conditions of an Underground Radioactive Waste Repository. Part I*. DoE/HMIP/RR/92/061 (Parts I). Harwell Laboratory, Oxfordshire, United Kingdom.

162

- Berry, J. A. 1992b. *A Review of Sorption of Radionuclides Under the Near- and Far-Field Conditions of an Underground Radioactive Waste Repository. Part II.* DoE/HMIP/RR/92/061 (Parts II). Harwell Laboratory, Oxfordshire, United Kingdom.
- Berry, J. A. 1992c. *A Review of Sorption of Radionuclides Under the Near- and Far-Field Conditions of an Underground Radioactive Waste Repository. Part III.* DoE/HMIP/RR/92/061 (Parts III). Harwell Laboratory, Oxfordshire, United Kingdom.
- Biggar, J. W., and D. R. Nielsen. 1962. "Miscible Displacement: II. Behavior of Tracers." *Soil Science Society of America Journal*, 26:125-128.
- Bolt, G. H., and M. G. M. Bruggenwert (eds.). 1978. *Soil Chemistry. A. Basic Elements.* Developments in Soil Science 5A, Elsevier Scientific Publishing Company, New York, New York.
- Bond, W. J., and P. J. Wierenga. 1990. "Immobile Water During Solute Transport in Unsaturated Sand Columns." *Water Resources Research*, 26:2475-2481.
- Bosma, W. J. P., and S. E. A. T. Van der Zee. 1993. "Transport of Reacting Solute in a One-dimensional Chemically Heterogeneous Porous Medium." *Water Resources Research*, 29:117-131.
- Bosma, W. J. P., S. E. A. T. Van der Zee, and C. J. Van Duijn. 1996. "Plume Development of a Nonlinearly Adsorbing Solute in Heterogeneous Porous Formations." *Water Resources Research*, 32:1569-1584.
- Bourcier, W. L. 1990. *Geochemical Modeling of Radionuclide Waste Glass Dissolution Using EQ3/6: Preliminary Results and Data Needs.* UCID-21869, Lawrence Livermore National Laboratory, Livermore, California.
- Bouwer, J. 1991. "Simple Derivation of the Retardation Equation and Application to Preferential Flow and Macrodispersion." *Ground Water*, 29:41-46.
- Box, G. E. P., and D. W. Behnken. 1960. "Some New Three Level Designs for the Study of Quantitative Variables." *Technometrics*, 2:455-475.
- Brown, P. L., A. Haworth, S. M. Sharland, and C. J. Tweed. 1991. *HARPHRQ: A Geochemical Speciation Program Based on PHREEQE.* Report NSS/R188, Harwell Laboratory, Harwell Laboratory, Oxfordshire, United Kingdom.
- Brown, D. S., and J. D. Allison. 1987. *MINTEQA1, an Equilibrium Metal Speciation Model: User's Manual.* EPA/600/3-87/012, U.S. Environmental Protection Agency, Athens, Georgia.

- Brusseau, M. L. 1994. "Transport of Reactive Contaminants in Heterogeneous Porous Media." *Reviews of Geophysics*, 32:285-313.
- Brusseau, M. L., and P. S. C. Rao. 1989. "Sorption Nonideality During Organic Contaminant Transport in Porous Media." *CRC Critical Reviews in Environmental Control*, 19:33-99.
- Brusseau, M. L., and J. M. Zachara. 1993. "Transport of  $\text{Co}^{2+}$  in a Physically and Chemically Heterogeneous Porous Media." *Environmental Science and Technology*, 27:1937-1939.
- Buck, J. W., G. Whelan, J. G. Droppo, Jr., D. L. Strenge, K. J. Castleton, J. P. McDonald, C. Sato, and G. P. Streile. 1995. *Multimedia Environmental Pollutant Assessment System (MEPAS): Application Guidance -- Guidelines for Evaluating MEPAS Input Parameters for Version 3.1*. PNL-10395, Pacific Northwest National Laboratory, Richland, Washington.
- Buddemeir, R. W., and J. R. Hunt. 1988. "Transport of Colloidal Contaminants in Groundwater: Radionuclide Migration at the Nevada Test Site." *Applied Geochemistry*, 3:535-548.
- Buffle, J., D. Perret, and M. Newman. 1992. "The Use of Filtration and Ultrafiltration for Size Fractionation of Aquatic Particles, Colloids, and Macromolecules." In *Environmental Particles. Part II. Sampling and Characterization of Particles of Aquatic Systems*, J. Buffle and H. Van Leeuwen (eds.), pp. 171-230, Lewis Publishers, Chelsea, Michigan.
- Burr, D. T., E. A. Sudicky, and R. L. Naff. 1994. "Nonreactive and Reactive Solute Transport in Three-dimensional Heterogeneous Porous Media: Mean Displacement, Plume Spreading, and Uncertainty." *Water Resources Research*, 30:791-815.
- Carter, S. L., M. M. Mortland, and W. D. Kemper. 1986. "Specific Surface." In *Methods of Soil Analysis -- Part 1: Physical and Mineralogical Methods*, A. Klute (ed.), Second Edition, pp. 413-422, Soil Science Society of America, Madison, Wisconsin.
- Carslaw, H. S., and J. C. Jaeger. 1959. *Conduction of Heat in Solids*. Oxford University Press, London, England.
- Chiou, Cary T., Susan E. McGroddy, and Daniel E. Kile. 1998. "Partition Characteristics of Polycyclic Aromatic Hydrocarbons on Soils and Sediments." *Environmental Science and Technology*, 32:264-269
- Cloninger, M. O., and C. R. Cole. 1981. *Reference Analysis on the Use of Engineered Barriers for Isolation of Spent Nuclear Fuel in Granite and Basalt*. PNL-3530, Pacific Northwest Laboratory, Richland, Washington.

- Cloninger, M. O., C. R. Cole, and J. F. Wahburn. 1980. *An Analysis on the Use of Engineered Barriers for Geologic Isolation of Spent Fuel in a Referenced Salt Repository*. PNL-3356, Pacific Northwest Laboratory, Richland, Washington.
- Coats, K. H., and B. D. Smith. 1964. "Dead-End Pore Volume and Dispersion in Porous Media." *Society of Petroleum Engineers Journal*, 4:73-84.
- Cochran, G. W., and G. M. Cox. 1957. *Experimental Design*. Second Edition, Wiley, New York, New York.
- Codell, R. B., K. T. Key, and G. Whelan. 1982. *A Collection of Mathematical Models for Dispersion in Surface Water and Groundwater*. NUREG-0868, U.S. Nuclear Regulatory Commission, Washington, DC.
- Cole, C. R., S. B. Yabusaki, and C. T. Kincaid. 1988. *CFEST-SC -- Coupled Fluid, Energy, and Solute Transport Code, SuperComputer Version*. Battelle, Pacific Northwest Laboratory, Richland, Washington.
- Corapcioglu, M. Y., and S. Kim. 1995. "Modeling Facilitated Contaminant Transport of Mobile Bacteria." *Water Resource Research*, 31:2639-2647.
- Cotton, F. A., and G. Wilkinson. 1972. *Advanced Inorganic Chemistry, A Comprehensive Test*. Third Edition. John Wiley and Sons, Inc., New York.
- Dagan, G. 1984. "Solute Transport in Heterogeneous Porous Formations." *Journal of Fluid Mechanics*, 145:151-177.
- Danielsson, L. G. 1982. "On the Use of Filters for Distinguishing Between Dissolved and Particulate Fractions in Natural Waters." *Water Research*, 16:179-182.
- Davies, O. L. 1954. *Design and Analysis of Industrial Experiments*. Hafner, New York, New York.
- Davis, J. A., and D. B. Kent. 1990. "Surface Complexation Modeling in Aqueous Geochemistry." In *Mineral-Water Interface Geochemistry*, M. F. Hochella, Jr. and A. F. White (eds.), pp. 177-260, Reviews in Mineralogy, Volume 23, Mineralogical Society of America, Washington, D.C.
- Davis, A., and D. D. Runnells. 1987. "Geochemical Interactions Between Acidic Tails Fluid and Bedrock: Use of the Computer Model MINTEQ." *Applied Geochemistry*, 2:231-241.

- Dayal, R., H. Arora, and N. Morcos. 1983. *Estimation of Cesium-137 Release from Waste/Cement Composites Using Data from Small-Scale Specimen*. NUREG/CR-3382, Nuclear Regulatory Commission, Washington, D.C.
- Dean, J. A. (ed.). 1973. *Lange's Handbook of Chemistry*. McGraw-Hill, New York, New York.
- Degueldre, C., G. Longworth, V. Mowlin, and P. Vilks. 1989. *Grimsel Colloid Exercise. An International Intercomparison Exercise on the Sampling and Characterization of Groundwater Colloids*. Technical Report 39, Paul Scherrer Institut-Bericht, Wurenlingen und Villigen, Switzerland.
- Delany, J. M. 1985. *Reaction of Topopah Spring Tuff with J-13 Water: A Geochemical Modeling Approach Using the EQ3/6 Reaction Path Code*. UCRL-53631 DE86 013226, Lawrence Livermore National Laboratory, Livermore, California.
- Delegard, C. H., and G. S. Barney. 1983. *Effects of Hanford High-Level Waste Compounds on Sorption of Cobalt, Strontium, Neptunium, Plutonium, and Americium of Hanford Sediments*. RHO-RE-ST-1 P, Rockwell Hanford Operations, Richland, Washington.
- Delegard, C. H., S. A. Gallagher, and R. B. Kasper. 1981. *Saturated Column Leach Studies: Hanford 216Z-Z-1A Sediment*. RHO-SA-210, Rockwell Hanford Operations, Richland, Washington.
- Douglas, L. A. 1989. "Vermiculites." In *Minerals in Soil Environments*, J. B. Dixon and S. B. Week (eds.), Second Edition. pp. 635-674, Soil Science Society of America, Madison, Wisconsin.
- Dragun, J. 1988. *Soil Chemistry of Hazardous Materials*. Hazardous Materials Control Research Institute, Silver Spring, Maryland.
- Dubinin, M. M., and L. V. Radushkevich. 1947. "Equation of the Characteristic Curve of Activated Charcoal." *Proceedings of the Academy of Sciences, Physical Chemistry Section, U.S.S.R.*, 55:331-333.
- Dzombak, D. A. 1986. *Toward a Uniform Model for the Sorption of Inorganic Ions on Hydrous Oxides*. Ph.D. Dissertation, Massachusetts Institute of Technology, Boston, Massachusetts.
- Dzombak, D. A., and K. F. Hayes. 1992. "Comment on "Recalculation, Evaluation, and Prediction of Surface Complexation Constants for Metal Adsorption on Iron and Manganese Oxides."" *Environmental Science and Technology*, 26:1251-1253.

1166

- Elabd, H., and W. A. Jury. 1986. "Spatial Variability of Pesticide Adsorption Parameters." *Environmental Science and Technology*, 20:256-260.
- EPA (U.S. Environmental Protection Agency). 1984. *Uncontrolled Hazardous Waste Site Ranking System, A User's Manual*. HW-10, U.S. Environmental Protection Agency, Washington, D.C.
- EPA (U.S. Environmental Protection Agency). 1988. *Superfund Exposure Assessment Manual*. EPA/540/1-88/001, U.S. Environmental Protection Agency, Washington, D.C.
- EPA (U.S. Environmental Protection Agency). 1989. *Transport and Fate of Contaminants in the Subsurface*. EPA/625/4-89/019, U.S. Environmental Protection Agency, Cincinnati, Ohio.
- EPA (U.S. Environmental Protection Agency). 1991. *Site Characterization for Subsurface Remediation*. EPA/625/4-91/026, Office of Research and Development, U.S. Environmental Protection Agency, Cincinnati, Ohio.
- EPA (U.S. Environmental Protection Agency). 1992a. *Background Document for Finite Source Methodology for Wastes Containing Metal*. HWEP-S0040, U.S. Environmental Protection Agency, Office of Solid Waste, Washington, D.C.
- EPA (U.S. Environmental Protection Agency). 1992b. "U.S. Environmental Protection Agency, 40 CFR 300, Appendix A, Uncontrolled Hazardous Waste Site Ranking System: A User's Manual." *Federal Register*, 47, No. 137, July 16, 1982.
- EPA (U.S. Environmental Protection Agency). 1993. "Environmental Characteristics of EPA, NRC, and DOE Sites Contaminated with Radioactive Substances." EPA 402-R-93-011, U.S. Environmental Protection Agency, Office of Radiation and Indoor Air (6603J), Office of Solid Waste and Emergency Response, Washington, D.C.
- EPA (U.S. Environmental Protection Agency). 1996. *Soil Screening Guidance: Technical Background Document*. EPA/540/R-96/018, U.S. Environmental Protection Agency, Washington, D.C.
- EPRI (Electric Power Research Institute). 1991. *Use of Batch and Column Methodologies to Assess Utility Waste Leaching and Subsurface Chemical Attenuation*. EPRI EN-7313, Electric Power Research Institute, Palo Alto, California.
- Erdal, B. R., Chairman. 1985. *Workshop on Fundamental Geochemistry Needs for Nuclear Waste Isolation*. US DOE CONF8406134, National Technical Information Service, Springfield, Virginia.

- Felmy, A. R., D. C. Girvin, and E. A. Jenne. 1984. *MINTEQ: A Computer Program for Calculating Aqueous Geochemical Equilibria*. EPA-600/3-84-032 (NTIS PB84-157148), Pacific Northwest Laboratory, Richland, Washington.
- Fischer, H. B., E. J. List, R. C.Y. Koh, J. Imberger, and N. H. Brooks. 1979. *Mixing in Inland and Coastal Waters*. Academic Press, New York, New York.
- Freeze, R. A., and J. A. Cherry. 1979. *Groundwater*. Prentice-Hall, Englewood Cliffs, New Jersey.
- Friedlander, G., J. W. Kennedy, and J. M. Miller. 1966. *Nuclear and Radiochemistry. Second Edition*. John Wiley and Sons, Inc., New York, New York.
- Freundlich, H. 1926. *Colloid and Capillary Chemistry*. Methuen, London, England.
- Gamerding, A. P., D. I. Kaplan, and C. T. Resch. 1998. *Uranium(VI) Sorption and Transport in Unsaturated, Subsurface Hanford Site Sediments – Effect of Moisture Content and Sediment Texture*. PNNL-11975, Pacific Northwest National Laboratory, Richland, Washington.
- Gamerding, A. P., and D. I. Kaplan. 1999. “Application of a Continuous-Flow Centrifugation Method and Determination of Heterogeneous Solute Transport in Disturbed, Unsaturated Sediments.” *Water Resources Research*, (in review).
- Garrels, R. M., and C. L. Christ. 1965. *Solutions, Minerals, and Equilibria*. Freeman, Cooper, and Company, San Francisco, California.
- Gaudet, J. P., H. Jegat, G. Vachaud, and P. J. Wierenga. 1977. “Solute Transfer, with Exchange Between Mobile and Stagnant Water, Through Unsaturated Sand.” *Soil Science Society of America Journal*, 41:665-671.
- Gee, G. W., and A. C. Campbell. 1980. *Monitoring and Physical Characterization of Unsaturated Zone Transport - Laboratory Analysis*. PNL-3304, Pacific Northwest Laboratory, Richland, Washington.
- Gee, G. W., A. C. Campbell, P. J. Wierenga, and T. L. Jones. 1981. *Unsaturated Moisture and Radionuclide Transport: Laboratory Analysis and Modeling*. PNL-3616, Pacific Northwest Laboratory, Richland, Washington.
- Gelhar, L. W., and C. L. Axness. 1983. “Three-Dimensional Stochastic Analysis of Macrodispersion in Aquifers.” *Water Resources Research*, 19:161-180.

- Giles, C. H., D. Smith, and A. Huitson. 1974. "A General Treatment and Classification of the Solute Adsorption Isotherm. I. Theoretical." *Journal of Colloid and Interface Science*, 47:755-765.
- Glasstone, S. 1972. *Thermodynamics for Chemists*. Robert E. Krieger Publishing Company, Huntington, New York.
- Goldberg, S. 1995. "Adsorption Models Incorporated into Chemical Equilibrium Models." In *Chemical Equilibrium and Reaction Models*, R. H. Loeppert, A. P. Schwab, and S. Goldberg (eds.), pp. 75-95, Special Publication Number 42, Soil Science Society of America, Inc., Madison, Wisconsin.
- Goltz, M. N., and P. V. Roberts. 1986. "Interpreting Organic Solute Transport Data from a Field Experiment Using Physical Nonequilibrium Models." *Journal of Contaminant Hydrology*, 1:77-93.
- Grim, R. E. 1968. *Clay Mineralogy*. McGraw-Hill Book Company, New York, New York.
- Gschwend, P. M., D. Backhus, J. K. MacFarlane, and A. L. Page. 1990. "Mobilization of Colloids in Groundwater Due to Infiltration of Water at Coal Ash Disposal Site." *Journal of Contaminant Hydrology*, 6:307-320.
- Gschwend, P. M., and M. C. Reynolds. 1987. "Monodispersed Ferrous Phosphate Colloids in an Anoxic Groundwater Plume." *Journal of Contaminant Hydrology*, 1:309-327.
- Gschwend, P. M. and S. Wu. 1985. "On the Constancy of Sediment-Water Partition Coefficients of Hydrophobic Organic Pollutants." *Environmental Science and Technology*, 19:90-96.
- Gu, B., and R. K. Schulz. 1991. *Anion Retention in Soil: Possible Application to Reduce Migration of Buried Technetium and Iodine*. NUREG/CR-5464, U.S. Nuclear Regulatory Commission, Washington, D.C.
- Haggerty, R., and S. M. Gorelick. 1995. "Multiple-Rate Mass Transfer for Modeling Diffusion and Surface Reactions in Media with Pore-scale Heterogeneity." *Water Resources Research*, 31:2383-2400.
- Hem, J. D. 1985. *Study and Interpretation of the Chemical Characteristics of Natural Water*. Water Supply Paper 2254, U. S. Geological Survey, Alexandria, Virginia.
- Higgins, G. H. 1959. "Evaluation of the Groundwater Contamination Hazard from Underground Nuclear Explosives." *Journal of Geophysical Research*, 64:1509-1519.
- Hillel, D. 1998. *Environmental Soil Physics*. Academic Press, San Diego, California.

- Ho, C. H., and N. H. Miller. 1986. "Formation of Uranium Oxide Sols in Bicarbonate Solutions." *Journal of Colloid and Interface Science*, 113:232-240.
- Hollander, M., and D.A. Wolfe. 1973. *Nonparametric Statistical Methods*. Wiley, New York, New York..
- Honeyman, B. D., and P. H. Santschi. 1988. "Metals in Aquatic Systems." *Environmental Science and Technology*, 22:862-871.
- Hopmans, J. W., H. Schukking, and P. J. J. F. Torfs. 1988. "Two-Dimensional Steady State Unsaturated Water Flow in Heterogeneous Soils with Autocorrelated Soil Hydraulic Properties." *Water Resources Research*, 24:2005-2017.
- INTERA (INTERA Environmental Consultants, Inc.). 1983. *Geochemical Models Suitable for Performance Assessment of Nuclear Waste Storage: Comparison of PHREEQE and EQ3/EQ6*. ONWI-473, INTERA Environmental Consultants, Inc., Houston, Texas.
- Ivanovich, M., A. G. Latham, G. Longworth, and M. Gascoyne. 1992. "Applications to Radioactive Waste Disposal Studies." In *Uranium-Series Disequilibrium. Applications to Earth, Marine, and Environmental Systems*, M. Ivanovich and R. S. Harmon (eds.), pp. 583-630, Oxford University Press, Oxford, England.
- Jackson, K. J., and W. L. Bourcier (technical organizers). 1986. *Proceedings of the Workshop on Geochemical Modeling*. CONF-8609134, National Technical Information Service, Springfield, Virginia.
- Jackson, R. E., and K. J. Inch. 1989. "The In-situ Absorption of Sr-90 in a Sand Aquifer at the Chalk River Nuclear Laboratories." *Journal of Contaminant Hydrology*, 4: 27-50.
- Jacobs, G. K., and S. K. Whatley (eds.). 1985. *Proceedings of the Conference on the Application of Geochemical Models to High-level Nuclear Waste Repository Assessment*. NUREG/CR-0062 (ORNL/TM-9585), Oak Ridge National Laboratory, Oak Ridge, Tennessee.
- James, R. V., and J. Rubin. 1986. "Transport of Chloride Ion in a Water-Unsaturated Soil Exhibiting Anion Exclusion." *Soil Science Society of America Journal*, 50:1142-1149.
- Jardine, P. M., G. K. Jacobs, and G. V. Wilson. 1993. "Unsaturated Transport Processes in Undisturbed Heterogeneous Porous Media: I. Inorganic Contaminants." *Soil Science Society of America Journal*, 57:945-953.

- Jenne, E. A. 1977. "Trace Element Sorption by Sediments and Soils - Sites and Processes." In *Symposium on Molybdenum in the Environment*, W. Chappel and K. Petersen (eds.), pp. 425-553, M. Dekker, Inc., New York, New York.
- Jenne, E. A. (ed.). 1979. *Chemical Modeling in Aqueous Systems. Speciation, Sorption, Solubility, and Kinetics*. Symposium Series 93, American Chemical Society, Washington, D.C.
- Jenne, E. A. 1981. *Geochemical Modeling: A Review*. PNL-3574, Pacific Northwest Laboratory, Richland, Washington.
- Jenne, E. A.. 1998a. "Adsorption of Metals by Geomedia: Data Analysis, Modeling, Controlling Factors, and Related Issues." In *Adsorption of Metals by Geomedia. Variables, Mechanisms, and Model Applications*, E. A. Jenne (ed.), p. 2-73, Academic Press, San Diego, California.
- Jenne, E. A. 1998b. "Priorities for Future Metal Adsorption Research." In *Adsorption of Metals by Geomedia. Variables, Mechanisms, and Model Applications*, E. A. Jenne (ed.), p. 549-560, Academic Press, San Diego, California.
- Johnson, W. H., S. M. Serkiz, L. M. Johnson, and S. B. Clark. 1995. "Uranium Partitioning Under Acidic Conditions in a Sandy Soil Aquifer." Paper presented at the Waste Management '95 Symposium, Tucson, Arizona, February 26 - March 2, 1995.
- Jury, W. A., H. Elabd, and M. Resketo. 1986. "Field Study of Napropamide Movement Through Unsaturated Soil." *Water Resources Research*, 22:749-755.
- Jury, W. A., W. R. Gardner, and W. H. Gardner. 1991. *Soil Physics*. John Wiley and Sons, Inc. New York, New York.
- Kaplan, D. I., P. M. Bertsch, and D. C. Adriano. 1995a. "Enhanced Transport of Contaminant Metals Through an Acidic Aquifer." *Ground Water*, 33:708-717.
- Kaplan, D. I., P. M. Bertsch, D. C. Adriano, and W. P. Miller. 1993. "Soil-Borne Mobile Colloids as Influenced by Water Flow and Organic Carbon." *Environmental Science and Technology*, 27:1193-1200.

171

- Kaplan, D. I., P. M. Bertsch, D. C. Adriano, and K. A. Orlandini. 1994a. "Actinide Association with Groundwater Colloids in a Coastal Plain Aquifer." *Radiochimica Acta*, 66/67:181-187.
- Kaplan, D. I., D. B. Hunter, P. M. Bertsch, S. Bajt, and D. C. Adriano. 1994b. "Application of Synchrotron X-Ray Fluorescence Spectroscopy and Energy Dispersive X-Ray Analysis to Identify Contaminant Metals on Groundwater Colloids." *Environmental Science & Technology*, 28:1186-1189.
- Kaplan, D. I., T. L. Gervais, and K. M. Krupka. 1998. "Uranium(VI) Sorption to Sediments Under High pH and Ionic Strength Conditions." *Radiochimica Acta*, 80:201-211.
- Kaplan, D. I., and R. J. Serne. 1995. *Distribution Coefficient Values Describing Iodine, Neptunium, Selenium, Technetium, and Uranium Sorption to Hanford Sediments*. PNL-10379, Supplement 1, Pacific Northwest Laboratory, Richland, Washington.
- Kaplan, D. I., R. J. Serne, and M. G. Piepho. 1995b. *Geochemical Factors Affecting Radionuclide Transport Through Near and Far Fields at a Low-Level Waste Disposal Site*. PNL-10379, Pacific Northwest National Laboratory, Richland, Washington.
- Kaplan, D. I., M. E. Sumner, P. M. Bertsch, and D. C. Adriano. 1996. "Chemical Conditions Conducive to the Release of Mobile Colloids from Ultisol Profiles." *Soil Science Society of America Journal*, 60:269-274.
- Karickhoff, S. W., D. S. Brown, and T. A. Scott. 1979. "Sorption of Hydrophobic Pollutants on Natural Sediments." *Water Research*, 13:231-248.
- Kim, J. J. 1986. "Chemical Behavior of Transuranic Elements in Aquatic Systems." In *Handbook on the Physics and Chemistry of the Actinides*, A. J. Freeman and C. Keller (eds.), pp. 413-455, Elsevier Science Publ., Amsterdam, Netherlands.
- Kincaid, C. T., J. R. Morrey, and J. E. Rogers. 1984. *Geohydrochemical Models for Solute Migration. Volume 1: Process Description and Computer Code Selection*. EPRI EA-3417, Volume 1, Battelle, Pacific Northwest Laboratories, Richland, Washington.
- Knoll, K. C. 1960. *Adsorption of Strontium by Soils Under Saturated and Unsaturated Flow Conditions*. HW-67830, General Electric Company, Hanford Atomic Products Operation, Richland, Washington.
- Koltermann, C. E., and S. M. Gorelick. 1996. "Heterogeneity in Sedimentary Deposits: A Review of Structure-Imitating, Process-Imitating, and Descriptive Approaches." *Water Resources Research*, 32:2617-2658.

- Krupka, K. M., E. A. Jenne, and W. J. Deutsch. 1983. *Validation of the WATEQ4 Geochemical Model for Uranium*. PNL-4333, Pacific Northwest Laboratory, Richland, Washington.
- Krupka, K. M. and J. R. Morrey. 1985. MINTEQ Geochemical Reaction Code: Status and Applications. In *Proceedings of the Conference on the Application of Geochemical Models to High-level Nuclear Waste Repository Assessment*, G. K. Jacobs and S. K. Whatley (eds.), pp. 46-53, NUREG/CR-0062 (ORNL/TM-9585), Oak Ridge National Laboratory, Oak Ridge, Tennessee.
- Krupka, K. M. and R. J. Serne. 1998. *Effects on Radionuclide Concentrations by Cement/Ground-Water Interactions in Support of Performance Assessment of Low-Level Radioactive Waste Disposal Facilities*. NUREG/CR-6377 (PNNL-11408), Pacific Northwest National Laboratory, Richland, Washington.
- LaGrega, M.D. 1994. *Hazardous Waste Management*. McGraw-Hill, Inc., New York, New York.
- Landström, O., C. E. Klockars, O. Persson, K. Andersson, B. Torstenfelt, B. Allard, S. Å. Larsson, and E. L. Tullborg. 1982. "A Comparison of In-situ Radionuclide Migration Studies in the Studsvik Area and Laboratory Measurements." In *Scientific Basis for Nuclear Waste Management V*, W. Lutze (ed.), pp. 697-706, Materials Research Society Symposia Proceedings, Volume 11, North Holland, New York, New York.
- Langmuir, D. 1978. "Uranium Solution-Mineral Equilibria at Low Temperatures with Applications to Sedimentary Ore Deposits." *Geochimica et Cosmochimica Acta*, 42:547-569.
- Langmuir, D. 1997. *Aqueous Environmental Geochemistry*. Prentice Hall, Upper Saddle River, New Jersey.
- Langmuir, D., and J. S. Herman. 1980. "The Mobility of Thorium in Natural Waters at Low Temperatures." *Geochimica Cosmochimica Acta* 44:1753-1766.
- Langmuir, I. 1918. "The Adsorption of Gases on Plane Surfaces of Glass, Mica, and Platinum." *Journal of the American Chemical Society*, 40:1361-1403.
- Lehninger, A. L. 1970. *Biochemistry*. Worth Publishers, Inc., New York, New York.
- Lemire, R. J., and P. R. Tremaine. 1980. "Uranium and Plutonium Equilibria in Aqueous Solutions to 200°C." *Journal of Chemical and Engineering Data*, 25:361-370.
- Lewis, G. N., and M. Randall. 1961. *Thermodynamics*. Revised by K. S. Pitzer and L. Brewer, McGraw-Hill Book Company, New York, New York.

- Lewis, R. E., T. T. Jarvis, M. R. Jarvis, and G. Whelan. 1994. *Eielson Air Force Base Operable Unit 2 Baseline Risk Assessment*. PNL-8752, Pacific Northwest Laboratory, Richland, Washington.
- Liang, L., J. F. McCarthy, L. W. Jolley, J. A. McNabb, and T. L. Mehlhorn. 1993. "Iron Dynamics: Observations of Transformation During Injection of Natural Organic Matter in a Sandy Aquifer." *Geochimica et Cosmochimica Acta*, 57:1987-1999.
- Lindenmeier, C. W., R. J. Serne, J. L. Conca, A. T. Owen, and M. I. Wood. 1995. *Solid Waste Leach Characteristics and Contaminant-Sediment Interactions Volume 2: Contaminant Transport Under Unsaturated Moisture Contents*. PNL-10722, Pacific Northwest Laboratory, Richland, Washington.
- Lindsay, W. L., 1979. *Chemical Equilibria in Soils*. John Wiley and Sons, New York, New York.
- Loeppert, R. H., A. P. Schwab, and S. Goldberg (eds.). 1995. *Chemical Equilibrium and Reaction Models*. Special Publication Number 42, Soil Science Society of America, Inc., Madison, Wisconsin.
- Loux, N. T., D. S. Brown, C. R. Chafin, J. D. Allison, and S. M. Hassan. 1989. "Chemical Speciation and Competitive Cationic Partitioning on a Sandy Aquifer Material." *Journal of Chemical Speciation and Bioavailability*, 1:111-125.
- Lyman, W. J., W. F. Reehl, and D. H. Rosenblatt. 1982. *Handbook of Chemical Property Estimation Methods -- Environmental Behavior of Organic Compounds*. McGraw-Hill, New York, New York.
- Mackay, D. M., W. P. Ball, and M. G. Durant. 1986. "Variability of Aquifer Sorption Properties in a Field Experiment on Groundwater Transport of Organic Solutes: Methods and Preliminary Results." *Journal of Contaminant Hydrology*, 1:119-132.
- McCarthy, J. F., and D. Degueudre. 1993. "Sampling and Characterization of Colloids and Particles in Groundwater for Studying their Role in Contaminant Transport." In *Environmental Particles*, J. Buffle and J. P. van Leeuwen (eds.), pp. 247-315. Lewis Publishers, Boca Raton, Florida.
- McDonald, M. G., and A. W. Harbaugh. 1988. *A Modular Three-Dimensional Finite-Difference Groundwater Flow Model*. U.S. Geological Survey Techniques of Water Resources Investigations, Book 6, Chapter A1, U.S. Geological Survey, Reston, Virginia.

174

- McKinley, I. G., and W. R. Alexander. 1993. "Assessment of Radionuclide Retardation: Uses and Abuses of Natural Analogue Studies." *Journal of Contaminant Hydrology*, 13:249-259.
- McKinley, J. P., and E. A. Jenne. 1991. "Experimental Investigation and Review of the "Solids Concentration" Effect in Adsorption Studies." *Environmental Science and Technology*, 25:2082-2087.
- McMahon, M. A., and J. W. Thomas. 1974. "Chloride and Tritiated Water Flow in Disturbed and Undisturbed Soils Cores." *Proceedings Soil Science Society of America*, 38:727-732.
- Meier, H., E. Zimmerhacki, G. Zeitler, P. Menge, and W. Hecker. 1987. "Influence of Liquid/Solid Ratios in Radionuclide Migration Studies." *Journal of Radioanalytical and Nuclear Chemistry*, 109:139-151.
- Melchior, D. C., and R. L. Bassett (eds.). 1990. *Chemical Modeling in Aqueous Systems II*. Symposium Series 416, American Chemical Society, Washington, D.C.
- Mercer, J. W., C. R. Faust, W. J. Miller, and F. J. Pearson, Jr. 1981. *Review of Simulation Techniques for Aquifer Thermal Energy Storage (ATES)*. PNL-3769, Pacific Northwest Laboratory, Richland, Washington.
- Mills, W. B., S. Liu, and F. K. Fong. 1991. "Literature Review and Model (COMET) for Colloid/Metals Transport in Porous Media." *Ground Water*, 29:199-208.
- Morel, F. M. M. 1983. *Principles of Aquatic Chemistry*. John Wiley and Sons, New York, New York.
- Morel, F. M. M., and J. G. Hering. 1993. *Principles and Applications of Aquatic Chemistry*. John Wiley and Sons, Inc., New York, New York.
- Morel, F. M. M., J. G. Yeasted, and J. C. Westall. 1981. "Adsorption Models: A Mathematical Analysis in the Framework of General Equilibrium Calculations." In *Adsorption of Inorganics at Solid-Liquid Interfaces*, M. A. Anderson and A. J. Rubin (eds.), pp. 263-294, Ann Arbor Science Publishers, Inc., Ann Arbor, Michigan.
- Morrey, J. R., C. T. Kincaid, and C. J. Hostetler. 1986. *Geohydrochemical Models for Solute Migration. Volume 3: Evaluation of Selected Computer Codes*. EPRI EA-3417, Volume 3, Battelle, Pacific Northwest Laboratories, Richland, Washington.
- Mucciardi, A. N., I. J. Booker, E. C. Orr, and D. Cleveland. 1979. "Statistical Investigation of the Mechanics Controlling Radionuclide Sorption, Part II." In *Second Contractor Information Meeting. Task 4*. R. J. Serne (ed.), Vol. 2, pp 333-425, PNL-SA-7352, Pacific Northwest Laboratory, Richland, Washington.

- Mucciardi, A. N., T. C. Johnson, and J. Saunier. 1980. "Statistical Investigation of the Mechanics Controlling Radionuclide Sorption, Part III." In *Third Contractor Information Meeting. Task 4*, J. F. Relyea (ed.), Vol. 1, pp. 1-75, PNL-SA-8571, Pacific Northwest Laboratory, Richland, Washington.
- Muller, A. B., D. Langmuir, and L. E. Duda. 1983. "The Formulation of an Integrated Physico-chemical-Hydrologic Model for Predicting Waste Nuclide Retardation in Geologic Media." In *Scientific Basis for Nuclear Waste Management VI*, D. G. Brookins (ed.), pp. 547-564, Materials Research Society Symposia Proceedings, Volume 15, North Holland, New York, New York.
- Nielsen, D. R., and J. W. Biggar. 1961. "Miscible Displacement in Soils: I. Experimental Information." *Soil Science Society of America Journal*, 25:1-5.
- Nielsen, D. R., and J. W. Biggar. 1962. "Miscible Displacement in Soils: II. Behavior of Tracers." *Proceedings Soil Science Society of America*, 26:125-128.
- Nielsen, D. R., J. W. Biggar, and K. T. Erh. 1973. "Spatial Variability of Field-Measured Soil-Water Properties." *Hilgardia*, 42:215-259.
- Nielsen, D. R., M. T. van Genuchten, and J. W. Biggar. 1986. "Water Flow and Solute Transport Processes in the Unsaturated Zone." *Water Resources Research*, 22:895-1085.
- Nordstrom, D. K., and J. W. Ball. 1984. "Chemical Models, Computer Programs and Metal Complexation in Natural Waters." In *Complexation of Trace Metals in Natural Waters*, C. J. M. Kramer and J. C. Duinker (eds.), pp. 149-169, Martinus Nijhoff/Dr. J. W. Junk Publishing Co., Netherlands.
- Nordstrom, D. K., and J. L. Munoz. 1985. *Geochemical Thermodynamics*. The Benjamin/Cummings Publishing Co., Inc., Menlo Park, California.
- Nordstrom, D. K., L. N. Plummer, T. M. L. Wigley, T. J. Woley, J. W. Ball, E. A. Jenne, R. L. Bassett, D. A. Crerar, T. M. Florence, B. Fritz, M. Hoffman, G. R. Holdren, Jr., G. M. Lafon, S. V. Mattigod, R. E. McDuff, F. Morel, M. M. Reddy, G. Sposito, and J. Thraikill. 1979. "Comparison of Computerized Chemical Models for Equilibrium Calculations in Aqueous Systems." In *Chemical Modeling in Aqueous Systems. Speciation, Sorption, Solubility, and Kinetics*, E. A. Jenne (ed.), pp. 857-892, American Chemical Society Symposium Series 93, Washington, D.C.

176

- O'Conner, D. J., and J. P. Connolly. 1980. "The Effect of Concentration of Adsorbing Solids on the Partition Coefficient." *Water Research*, 14:1517-1523.
- Oscarson, D. W., and H. B. Hume. 1998. "Effect of Solid:Liquid Ratio on the Sorption of  $\text{Sr}^{2+}$  and  $\text{Cs}^+$  on Bentonite." In *Adsorption of Metals by Geomedia. Variables, Mechanisms, and Model Applications*, E. A. Jenne (ed.), p. 277-289, Academic Press, San Diego, California.
- Papelis, C., K. F. Hayes, and J. O. Leckie. 1988. *HYDRAQL: A Program for the Computation of Chemical Equilibrium Composition of Aqueous Batch Systems Including Surface-Complexation Modeling of Ion Adsorption at the Oxide/Solution Interface*. Technical Report No. 306, Department of Civil Engineering, Stanford University, Stanford, California.
- Parsons, R. 1982. "Surface Properties of Oxides." *Journal of Electroanalytical Chemistry*, 118:2-18.
- Peck, A. J., R. J. Luxmoore, and J. L. Stolzy. 1977. "Effects of Spatial Variability of Soil Hydraulic Properties in Water Budget Modeling." *Water Resources Research*, 13:348-354.
- Penrose, W. R., W. L. Plozer, W. H. Essington, D. M. Nelson, and K. A. Orlandini. 1990. "Mobility of Pu and Am Through a Shallow Aquifer in a Semiarid Region." *Environmental Science & Technology*, 24:228-234.
- Petersen, L. W., P. Moldrup, O. H. Jacobsen, and D. E. Rolston. 1996. "Relations Between Specific Surface Area and Soil Physical and Chemical Properties." *Soil Science*, 161:9-21.
- Peterson, R. G., and L. D. Calvin. 1986. "Sampling." In *Methods of Soil Analysis, Part I. Physical and Mineralogical Methods*, A. Klute (ed.), American Society of Agronomy, Inc., Madison, Wisconsin.
- Peterson, S. R., C. J. Hostetler, W. J. Deutsch, and C. E. Cowan. 1987a. *MINTEQ User's Manual*. NUREG/CR-4808 (PNL-6106), Pacific Northwest Laboratory, Richland, Washington.
- Peterson, S. R., W. J. Martin, and R. J. Serne. 1986. *Predictive Geochemical Modeling of Contaminant Concentrations in Laboratory Columns and in Plumes Migrating from Uranium Mill Tailings Waste Impoundments*. NUREG/CR-4520 (PNL-5788), prepared by the Pacific Northwest Laboratory, Richland, Washington.
- Peterson, S. R., B. E. Opitz, M. J. Graham, and L. E. Eary. 1987b. *An Overview of the Geochemical Code MINTEQ: Application to Performance Assessment for Low-Level Wastes*. PNL-6112, Pacific Northwest Laboratory, Richland, Washington.

- Phillips, S. L., F. V. Hale, L. F. Silvester, and M. D. Siegel. 1988. *Thermodynamic Tables for Nuclear Waste Isolation. Aqueous Solutions Database*. NUREG/CR-4864 (LBL-22860), Volume 1, Lawrence Berkeley Laboratory, Lawrence, California.
- Pickens, J. F., R. E. Jackson, K. J. Inch, and W. F. Merritt. 1981. "Measurement of Distribution Coefficients Using a Radial Injection Dual-Tracer Test." *Water Resources Research*, 17:529-544.
- Pignatello, J. J. 1989. "Sorption Dynamics of Organic Compounds in Soils and Sediments." In *Reactions and Movement of Organic Chemicals in Soils*, B. L. Sawhney and K. Brown (eds.), pp. 45-80. SSSA Special Publication 22, Soil Science Society of America, Inc., Madison, Wisconsin.
- Plackett, R. L., and J. P. Burman. 1946. "The Design of Optimum Multifactorial Experiments." *Biometrika*, 33:305-325.
- Plummer, L. N., B. F. Jones, and A. H. Truesdell. 1976, *WATEQF - A FORTRAN IV Version of WATEQ, A Computer Program for Calculating Chemical Equilibrium of Natural Waters*. Water Resources Investigations WRI 76-13, U.S. Geological Survey, Reston, Virginia.
- Potter, R. W., III. 1979. "Computer Modeling in Low Temperature Geochemistry." *Reviews of Geophysics and Space Physics*, 17:850-860.
- Powell, R. M., and R. W. Puls. 1993. "Passive Sampling of Groundwater Monitoring Wells Without Purging: Multilevel Well Chemistry and Tracer Disappearance." *Journal of Contaminant Hydrology*, 12:51-77.
- Puls, R. W. 1990. "Colloidal Consideration in Groundwater Sampling and Contaminant Transport Predictions." *Nuclear Safety*, 31:58-65.
- Rai, D., A. R. Felmy, and J. L. Ryan. 1990. "Uranium(IV) Hydrolysis Constants and Solubility Product of  $\text{UO}_2 \cdot x\text{H}_2\text{O}(\text{am})$ ." *Inorganic Chemistry*, 29:260-254.
- Rai, D., and J. M. Zachara. 1984. *Chemical Attenuation Rates, Coefficients, and Constants in Leachate Migration. Volume 1: A Critical Review*. EPRI EA-3356, Volume 1, Electric Power Research Institute, Palo Alto, California.
- Rancon, D. 1973. "The Behavior in Underground Environments of Uranium and Thorium Discharged by the Nuclear Industry." In *Environmental Behavior of Radionuclides Released in the Nuclear Industry*. IAEA-SM-172/55, pp. 333-346, International Atomic Energy Agency, Vienna, Austria.

- Rard, J. A. 1983. *Critical Review of the Chemistry and Thermodynamics of Technetium and Some of its Inorganic Compounds and Aqueous Species*. UCRL-53440, Lawrence Livermore National Laboratory, Livermore, California.
- Read, D, P. J. Hooker, M. Ivanovich, and A. E. Milodowski. 1991. "A Natural Analogue Study of an Abandoned Uranium Mine in Cornwall, England." *Radiochimica Acta*, 52/53:349-356.
- Reichle, R., W. Kinzelbach, and H. Kinzelbach. 1998. "Effective Parameters in Heterogeneous and Homogeneous Transport Models with Kinetic Sorption." *Water Resources Research*, 34:583-594.
- Relyea, J. F. 1982. "Theoretical and Experimental Considerations for the Use of the Column Method for the Use of the Column Method for Determining Retardation Factors." *Radioactive Waste Management and the Nuclear Fuel Cycle*, 3(2):151-166.
- Ritger, P. D., and N. J. Rose. 1968. *Differential Equations with Applications*. McGraw Hill, New York, New York.
- Robin, M. J. L., E. A. Sudicky, R. W. Gillham, and R. G. Kachanoski. 1991. "Spatial Variability of Strontium Distribution Coefficients and Their Correlation with Hydraulic Conductivity in the Canadian Forces Base Borden Aquifer." *Water Resources Research*, 27:2619-2632.
- Routson, R. C., and R. J. Serne. 1972. *One-Dimensional Model of the Movement of Trace Radioactive Solute Through Soil Columns - The PERCEL Model*. BNWL-1718, Pacific Northwest Laboratory, Richland, Washington.
- Routson, R. C., G. S. Barney, R. H. Smith, C. H. Delegard, and L. Jensen. 1981. *Fission Product Sorption Parameters for Hanford 200-Area Sediment Types*. RHO-ST-35, Rockwell Hanford Operations, Richland, Washington.
- Roy, W. R., I. G. Drapac, S. F. J. Chou, and R. A. Griffin. 1991. *Batch-type Procedures for Estimating Soil Adsorption of Chemicals*. EPA/530-SW-87-006-F, Office of Solid Waste and Emergency Response, U.S. Environmental Protection Agency, Washington, D.C.
- RTI (Research Triangle Institute). 1994. *Chemical Properties for Soil Screening Levels. Draft Report*. Prepared for the Environmental Protection Agency, Office of Emergency and Remedial Response, Washington, D.C.
- Russo, D. 1989a. "Field-Scale Transport of Interacting Solutes Through the Unsaturated Zone 2. Analysis of the Spatial Variability of the Field Response." *Water Resources Research*, 25:2487-2495.

- Russo, D. 1989b. "Field-Scale Transport of Interacting Solutes Through the Unsaturated Zone 1. Analysis of the Spatial Variability of the Transport Properties." *Water Resources Research*, 25:2475-2485.
- Ryan, J. M., and P. M. Gschwend. 1990. "Colloid Mobilization in Two Atlantic Coastal Plain Aquifers: Field Studies." *Water Resources Research*, 26:307-322.
- Salter, P. F., L. L. Ames, and J. E. McGarragh. 1981a. *The Sorption Behavior of Selected Radionuclides on Columbia River Basalts*. RHO-BWI-LD-48, Rockwell Hanford Operations, Richland, Washington.
- Salter, P. F., L. L. Ames, and J. E. McGarragh. 1981b. *Sorption of Selected Radionuclides on Secondary Minerals Associated with the Columbia River Basalts*. RHO-BWI-LD-43, Rockwell Hanford Operations, Richland, Washington.
- Schindler, P. W., and G. Sposito. 1991. "Surface Complexation at (Hydro)oxide Surfaces." In *Interactions at the Soil Colloid-Soil Solution Interface*, G. H. Bolt, M. F. DeBoodt, M. H. B. Hayes, and M. B. Mc Bride (eds.), pp. 115-145, Kluwer Academic Press, New York, New York.
- Schwarzenbach, R. P., and J. Westall. 1981. "Transport of Nonpolar Organic Compounds from Surface Water to Groundwater. Laboratory Sorption Studies." *Environmental Science and Technology*, 15:1360-1367.
- Scott, H. D., R. E. Phillips, and R. F. Paetzold. 1974. "Diffusion of Herbicides in One Adsorbed Phase." *Proceedings Soil Science Society of America*, 38:558-562.
- Seaman, J. C., P. M. Bertsch, and W. P. Miller. 1995. "Ionic Tracer Movement Through Highly Weathered Sediments." *Journal of Contaminant Hydrology*, 20:127-143.
- Sehmel, G. A. 1989. *Cyanide and Antimony Thermodynamic Database for the Aqueous Species and Solids for the EPA-MINTEQ Geochemical Code*. PNL-6835, Pacific Northwest Laboratory, Richland, Washington.
- Sergeyeva, E. I., A. A. Nikitin, I. L. Khodakovskiy, and G. B. Naumov. 1972. "Experimental Investigation of Equilibria in the System  $\text{UO}_3\text{-CO}_2\text{-H}_2\text{O}$  in 25-200°C Temperature Interval." *Geochemistry International*, 9:900-910.
- Serkiz, S. M. And W. H. Johnson. 1994. *Uranium Geochemistry in Soil and Groundwater at the F and H Seepage Basins (U)*. EPD-SGS-94-307, Westinghouse Savannah River Company, Savannah River Site, Aiken, South Carolina.

- Serne, R. J., R. C. Arthur, and K. M. Krupka. 1990. *Review of Geochemical Processes and Codes for Assessment of Radionuclide Migration Potential at Commercial LLW Sites*. NUREG/CR-5548 (PNL-7285), Pacific Northwest Laboratory, Richland, Washington.
- Serne, R. J., and A. B. Muller. 1987. "A Perspective on Adsorption of Radionuclides onto Geologic Media." In *The Geological Disposal of High Level Radioactive Wastes*, D. G. Brookins (ed.), pp. 407-443, Theophrastus Publications, S.A., Athens, Greece.
- Serne, R. J., and J. F. Relyea. 1981. "The Status of Radionuclide Sorption-Desorption Studies Performed by the WRIT Program." In *The Technology of high-Level Nuclear Waste Disposal*, Volume 1, pp. 203-254, DOE/TIC-621, Technical Information Center, U.S. Department of Energy, Oak Ridge, Tennessee.
- Serne, R. J., R. C. Routson, and D. A. Cochran. 1973. *Experimental Methods for Obtaining PERCOL Model Input Verification Data*. BNWL-1721, Pacific Northwest Laboratory, Richland, Washington.
- Seth, Rajesh, Donald MacKay, and Jane Muncke. 1999. "Estimating the Organic Carbon Partition Coefficient and its Variability for Hydrophobic Chemicals." *Environmental Science and Technology*, 33:2390-2394.
- Sheppard, J. C., J. A. Kittrick, and T. L. Hart. 1976. *Determination of Distribution Ratios and Diffusion Coefficients of Neptunium, Americium, and Curium in Soil-Aquatic Environments*. RTO-221-T-12-2, Rockwell Hanford Operations, Richland, Washington.
- Sheppard, S. C., M. I. Sheppard, and W. G. Evenden. 1990. "A Novel Method Used to Examine Variation in Tc Sorption Among 34 Soils, Aerated and Anoxic." *Journal of Environmental Radioactivity*, 11:215.
- Silva, R. J., G. Bidoglio, M. H. Rand, P. B. Robourch, H. Wanner, and I. Puigdomenech. 1995. *Chemical Thermodynamics Series, Volume 2: Chemical Thermodynamics of Americium*. Elsevier Science, New York, New York.
- Smith, R. M., and A. E. Martell. 1976. *Critical Stability Constants. Volume 4: Inorganic Complexes*. Plenum Press, New York, New York.
- Smith, R. M., and A. E. Martell. 1995. "The Selection of Critical Stability Constants." In *Chemical Equilibrium and Reaction Models*, R. H. Loeppert, A. P. Schwab, and S. Goldberg (eds.), Special Publication Number 42, Soil Science Society of America, Inc., Madison, Wisconsin.
- Smith, R. M., A. E. Martell, and R. J. Motekaitis. 1997. *NIST Critically Selected Stability Constants of Metal Complexes Database. Version 4. Users Guide*. NIST Standard

(81)

- Reference Database 46, National Institute of Standards and Technology, Gaithersburg, Maryland.
- Smith, R. W., and E. A. Jenne. 1991. "Recalculation, Evaluation, and Prediction of Surface Complexation Constants for Metal Adsorption on Iron and Manganese Oxides." *Environmental Science and Technology*, 25:525-531.
- Smith, R. W. and E. A. Jenne. 1992. "Response to 'Comment on "Recalculation, Evaluation, and Prediction of Surface Complexation Constants for Metal Adsorption on Iron and Manganese Oxides."'" *Environmental Science and Technology*, 26:1253-1254.
- Smith, R. W. and E. A. Jenne. 1991. "Recalculation, Evaluation, and Prediction of Surface Complexation Constants for Metal Adsorption on Iron and Manganese Oxides." *Environmental Science and Technology*, 25:525-531.
- Smith, R. W. and E. A. Jenne. 1988. *Compilation, Evaluation, and Prediction of Trip-Layer Model Constants for Ions on Fe(III) and Mn(IV) Hydrated Oxides*. PNL-6754, Pacific Northwest Laboratory, Richland, Washington.
- Snedecor, G. W., and W. G. Cochran. 1967. *Statistical Methods*. Sixth Edition, Iowa State University Press, Ames, Iowa.
- Sposito, G. 1984. *The Surface Chemistry of Soils*. Oxford University Press, New York, New York.
- Sposito, G. 1989. *The Chemistry of Soils*. Oxford University Press, New York, New York.
- Sposito, G. 1994. *Chemical Equilibria and Kinetics in Soils*. Oxford University Press, New York, New York.
- Sposito, G., and J. Coves. 1988. *SOILCHEM: A Computer Program for the Calculation of Chemical Speciation in Soils*. Kearny Foundation for Soil Science, University of California, Riverside, California.
- SSSA (Soil Science Society of America). 1997. *Glossary of Soil Science Terms*. Soil Science Society of America, Madison, Wisconsin.
- Streng, D. L., and S. R. Peterson. 1989. *Chemical Data Bases for the Multimedia Environmental Pollutant Assessment System (MEPAS): Version 1*. PNL-7145, Pacific Northwest Laboratory, Richland, Washington.
- Stumm, W. (ed.). 1987. *Aquatic Surface Chemistry. Chemical Processes at the Particle-Water Interface*. John Wiley and Sons, New York, New York.

- Stumm, W., and J. J. Morgan. 1981. *Aquatic Chemistry. An Introduction Emphasizing Chemical Equilibria in Natural Waters*. John Wiley and Sons, New York, New York.
- Sudicky, E. A. 1986. "A Natural Gradient Experiment on Solute Transport in a Sand Aquifer: Spatial Variability of Hydraulic Conductivity and its Role in the Dispersion Process." *Water Resources Research*, 22:2069-2082.
- Sugita, F., R. W. Gillham, and C. Mase. 1995. "Pore Scale Variation in Retardation Factor as a Cause of Nonideal Reactive Breakthrough Curves. 2. pore Network Analysis." *Water Resources Research*, 31:113-119.
- Szecsody, J. E., A. Chilakapati, J. M. Zachara, and A. L. Garvin. 1998. "Influence of Iron Oxide Inclusion Shape on Co II/III EDTA Reactive Transport Through Spatially Heterogeneous Sediment." *Water Resources Research*, 34:2501-2514.
- Szecsody, J. E., J. M. Zachara, and P. L. Bruckhart. 1994. "Adsorption-dissolution Reactions Affecting the Distribution and Stability of Co (II) EDTA in Iron Oxide-Coated Sand." *Environmental Science and Technology*, 28(9):1706-1716.
- Szecsody, J. E., J. M. Zachara, A. Chilakapati, P. M. Jardine, and A. S. Ferreny. 1998. "Importance of Flow and Particle-Scale Heterogeneity on Co II/III EDTA Reactive Transport." *Journal of Hydrology*, 209:112-136.
- Tompson, A.F.B., A. L. Schafer, and R.W. Smith. 1996. "Impacts of Physical and Chemical Heterogeneity on Contaminant Transport in a Sandy Porous Medium." *Water Resources Research*, 32:801-818.
- Tompson, A. F. B. 1993. "Numerical Simulation of Chemical Migration in Physically and Chemically Heterogeneous Porous Media." *Water Resources Research*, 29:3709-3726.
- Tompson, A. F. B., and L. W. Gelhar. 1990. "Numerical Simulation of Solute Transport in Three-Dimensional Randomly Heterogeneous Porous Media." *Water Resources Research*, 26:2541-2562.
- Truesdell, A. H., and B. F. Jones. 1973. *WATEQ, A Computer Program for Calculating Chemical Equilibria of Natural Waters*. USGS-WRD-73-007, U.S. Geological Survey, Washington, D.C.
- Truesdell, A. H., and B. F. Jones. 1974. "WATEQ, A Computer Program for Calculating Chemical Equilibria of Natural Waters." *U.S. Geological Survey Journal of Research*, 2:233-248.

- Turner, D. R. 1991. *Sorption Modeling for High-level Waste Performance Assessment: A Literature Review*. CNWRA 91-011, Center for Nuclear Waste Regulatory Analysis, San Antonio, Texas.
- Turner, D. R. 1993. *Mechanistic Approaches to Radionuclide Sorption Modeling*. CNWRA 93-019, Center for Nuclear Waste Regulatory Analysis, San Antonio, Texas.
- Turner, D. R. 1995. *Uniform Approach to Surface Complexation Modeling of Radionuclide Sorption*. CNWRA 95-001, Center for Nuclear Waste Regulatory Analysis, San Antonio, Texas.
- Turner, D. R., T. Griffin, and T. B. Dietrich. 1993. "Radionuclide Sorption Modeling Using the MINTEQA2 Speciation Code." In *Scientific Basis for Nuclear Waste Management XVI*, C. G. Interrante and R. T. Pabalan (eds.), pp. 783-789, Materials Research Society Symposium Proceedings, Volume 294, Materials Research Society, Pittsburgh, Pennsylvania.
- van Genuchten, M. Th., and W. J. Alves. 1982. *Analytical Solutions of the One-Dimensional Convective-Dispersive Solute Transport Equation*. Technical Bulletin No. 1661, U.S. Department of Agriculture, Washington, D.C.
- van Genuchten, M. Th., and P. J. Wierenga. 1976. "Mass Transfer Studies in Sorbing Porous Media. I. Analytical Solutions." *Soil Science Society of America Journal*, 40:473-480.
- van Genuchten, M. Th., and P. J. Wierenga. 1986. "Solute Dispersion Coefficients and Retardation Factors." In *Methods of Soil Analysis -- Part 1: Physical and Mineralogical Methods*, A. Klute (ed.), Second Edition, Chapter 44, pp. 1025-1054, Soil Science Society of America, Madison, Wisconsin,
- Voice, T. C., C. P. Rice, and W. J. Weber. 1983. "Effect of Solids Concentration on the Sorptive Partitioning of Hydrophobic Pollutants in Aquatic Systems." *Environmental Science and Technology*, 17:513-518.
- Wagman, D. D., W. H. Evans, V. B. Parker, R. H. Shumm, I. Halow, S. M. Bailey, K. L. Churney, and R. L. Nuttall. 1982. "The NBS Tables of Chemical Thermodynamic Properties. Selected Values for Inorganic and C1 and C2 Organic Substances in SI Units." *Journal of Physical and Chemical Reference Data* 11(Supplement No. 2):1-392.
- Waite, T. D., J. A. Davis, T. E. Payne, G. A. Waychunas, and N. Xu. 1994. "Uranium(VI) Adsorption to Ferrihydrite: Application of a Surface Complexation Model." *Geochimica et Cosmochimica Acta*, 58(24):5465-5478.
- Wanner, H, and I. Forest (eds.). 1992. *Chemical Thermodynamics Series, Volume 1: Chemical Thermodynamics of Uranium*. (I. Grenthe, J. Fuger, R. J. M. Konings, R. J. Lemire, A. B.

- Muller, C. Nguyen-Trung, and H. Wanner, review team), North-Holland, Elsevier Science Publishing Company, Inc., New York, New York.
- Warrick, A. W., and A. Amoozegar-Fard. 1979. "Infiltration and Drainage Calculation Using Spatially Scaled Hydraulic Properties." *Water Resources Research*, 15:1116-1120.
- Warrick, A. W., and D. R. Nielsen. 1980. "Spatial Variability of Soil Physical Properties in the Field." In *Applications of Soil Physics*, D. Hillel (ed.), Chapter 13, pp. 319-345, Academic Press, New York, New York.
- Westall, J. C. 1986. "Reactions at the Oxide-Solution Interface: Chemical and Electrostatic Models." In *Geochemical Processes at Mineral Surfaces*, J. A. Davis and K. F. Hayes (eds.), pp. 54-78, ACS Symposium Series 323, American Chemical Society, Washington, D.C.
- Westall, J. C. 1994. "Modeling of the Association of Metal Ions With Heterogeneous Environmental Sorbents." In *Scientific Basis for Nuclear Waste Management Vol. XVIII. Part 2*, T. Murakami and R. C. Ewing (eds.), pp. 937-950, Materials Research Society Symposia Proceedings, Volume 353, Materials Research Society, Pittsburgh, Pennsylvania.
- Westall, J. C., and H. Hohl. 1980. "A Comparison of Electrostatic Models for the Oxide/Solution Interface." *Advances in Colloid and Interface Science*, 12:265-294.
- Westall, J. C., J. L. Zachary, and F. M. M. Morel. 1976. *MINEQL, A Computer Program for the Calculation of Chemical Equilibrium Composition of Aqueous Systems*. Technical Note 18, Department of Civil Engineering, Massachusetts Institute of Technology, Cambridge, Massachusetts.
- Whelan, G. 1996. *Use of Distribution Coefficients in Transport Modeling and Risk Assessments*. Letter Report, Pacific Northwest National Laboratory, Richland, Washington.
- Whelan, G., J. W. Buck, D. L. Streng, J. G. Droppo, Jr., B. L. Hoopes, and R. J. Aiken. 1992. "An Overview of the Multimedia Assessment Methodology MEPAS." *Hazardous Waste and Hazardous Materials*, 9(2):191-208.
- Whelan, G., J. P. McDonald, and C. Sato. 1996. *Multimedia Environmental Pollutant Assessment System (MEPAS): Groundwater Pathway Formulations*. PNNL-10907, Pacific Northwest National Laboratory, Richland, Washington.
- Whelan, G., D. L. Streng, J. G. Droppo, Jr., B. L. Steelman, and J. W. Buck. 1987. *The Remedial Action Priority System (RAPS): Mathematical Formulations*. PNL-6200, Pacific Northwest Laboratory, Richland, Washington.

Wildung, R. E., T. R. Garland and D. A. Cataldo. 1977. "Accumulation of Technetium by Plants." *Health Physics*, 32:314-317.

Wood, W. W., and J. Petratis. 1984. "Origin and Distribution of Carbon Dioxide in the Unsaturated Zone of the Southern High Plains of Texas." *Water Resources Research*, 20:1193-1208.

Yariv, S., and H. Cross. 1979. *Geochemistry of Colloid Systems*. Springer-Verlag, New York, New York.

Yeh, G. T., and Y. Tsai. 1976. "Analytical Three-Dimensional Transient Modeling of Effluent Discharges." *Water Resources Research*, 12:533-540.

Yeh, G. T. 1981. *AT123D: Analytical Transient One, Two, and Three Dimensional Simulation of Waste Transport in the Aquifer System*. ORNL-5602, Oak Ridge National Laboratory, Oak Ridge, Tennessee.

## **APPENDIX A**

### **Acronyms, Abbreviations, Symbols, and Notation**

## Appendix A

### Acronyms, Abbreviations, Symbols, and Notation

#### A.1.0 Acronyms And Abbreviations

AA	Atomic absorption
ASCII	American Standard Code for Information Interchange
ASTM	American Society for Testing and Materials
CCM	Constant capacitance (adsorption) model
CDTA	Trans-1,2-diaminocyclohexane tetra-acetic acid
CEAM	Center for Exposure Assessment Modeling at EPA's Environmental Research Laboratory in Athens, Georgia
CEC	Cation exchange capacity
CERCLA	Comprehensive Environmental Response, Compensation, and Liability Act
DLM	Diffuse (double) layer (adsorption) model
DDLm	Diffuse double layer (adsorption) model
DOE	U.S. Department of Energy
DTPA	Diethylenetriaminepentacetic acid
EDTA	Ethylenediaminetriacetic acid
EDX	Energy dispersive x-ray analysis
EPA	U.S. Environmental Protection Agency
EPRI	Electric Power Research Institute
HEDTA	N-(2-hydroxyethyl) ethylenedinitrilotriacetic acid
HLW	High level radioactive waste
IAEA	International Atomic Energy Agency
ICP	Inductively coupled plasma
ICP/MS	Inductively coupled plasma/mass spectroscopy
IEP (or iep)	Isoelectric point
LLNL	Lawrence Livermore National Laboratory, U.S. DOE
LLW	Low level radioactive waste
MCL	Maximum Contaminant Level
MEPAS	Multimedia Environmental Pollutant Assessment System
MS-DOS®	Microsoft® disk operating system (Microsoft and MS-DOS are registered trademarks of Microsoft Corporation.)
NPL	Superfund National Priorities List
NRC	U.S. Nuclear Regulatory Commission
NWWA	National Water Well Association
OERR	Office of Remedial and Emergency Response, U.S. EPA
ORIA	Office of Radiation and Indoor Air, U.S. EPA
OSWER	Office of Solid Waste and Emergency Response, U.S. EPA

PC	Personal computers operating under the MS-DOS® and Microsoft® Windows operating systems (Microsoft® Windows is a trademark of Microsoft Corporation.)
PNL	Pacific Northwest Laboratory. In 1995, DOE formally changed the name of the Pacific Northwest Laboratory to the Pacific Northwest National Laboratory.
PNNL	Pacific Northwest National Laboratory, U.S. DOE
PZC	Point of zero charge
RCRA	Resource Conservation and Recovery Act
SCM	Surface complexation model
SDMP	NRC's Site Decommissioning Management Plan
TDS	Total dissolved solids
TLM	Triple-layer adsorption model
UK	United Kingdom (UK)
UK DoE	United Kingdom Department of the Environment
UNSCEAR	United Nations Scientific Committee on the Effects of Atomic Radiation

## A.2.0 List of Symbols for the Elements and Corresponding Names

Symbol	Element	Symbol	Element	Symbol	Element
Ac	Actinium	Gd	Gadolinium	Po	Polonium
Ag	Silver	Ge	Germanium	Pr	Praseodymium
Al	Aluminum	H	Hydrogen	Pt	Platinum
Am	Americium	He	Helium	Pu	Plutonium
Ar	Argon	Hf	Hafnium	Ra	Radium
As	Arsenic	Hg	Mercury	Rb	Rubidium
At	Astatine	Ho	Holmium	Re	Rhenium
Au	Gold	I	Iodine	Rh	Rhodium
B	Boron	In	Indium	Rn	Radon
Ba	Barium	Ir	Iridium	Ru	Ruthenium
Be	Beryllium	K	Potassium	S	Sulfur
Bi	Bismuth	Kr	Krypton	Sb	Antimony
Bk	Berkelium	La	Lanthanum	Sc	Scandium
Br	Bromine	Li	Lithium	Se	Selenium
C	Carbon	Lu	Lutetium	Si	Silicon
Ca	Calcium	Lw	Lawrencium	Sm	Samarium
Cb	Columbium	Md	Mendelevium	Sn	Tin
Cd	Cadmium	Mg	Magnesium	Sr	Strontium
Ce	Cerium	Mn	Manganese	Ta	Tantalum
Cf	Californium	Mo	Molybdenum	Tb	Terbium
Cl	Chlorine	N	Nitrogen	Tc	Technetium
Cm	Curium	Na	Sodium	Te	Tellurium
Co	Cobalt	Nb	Niobium	Th	Thorium
Cr	Chromium	Nd	Neodymium	Ti	Titanium
Cs	Cesium	Ne	Neon	Tl	Thallium
Cu	Copper	Ni	Nickel	Tm	Thulium
Dy	Dysprosium	No	Nobelium	U	Uranium
Er	Erbium	Np	Neptunium	V	Vanadium
Es	Einsteinium	O	Oxygen	W	Tungsten
Eu	Europium	Os	Osmium	W	Wolfram
F	Fluorine	P	Phosphorus	Xe	Xenon
Fe	Iron	Pa	Protactinium	Y	Yttrium
Fm	Fermium	Pb	Lead	Yb	Ytterbium
Fr	Francium	Pd	Palladium	Zn	Zinc
Ga	Gallium	Pm	Promethium	Zr	Zirconium

190

### A.3.0 List of Symbols and Notation

$\alpha$	Dispersivity in the x, y, or z direction
$\alpha$	Capacity factor or ratio of the moles per unit volume of water-saturated solid, $C_s$ , to the moles per unit volume of liquid, $C_l$
$\alpha$	Activity coefficient
$\alpha$	Constrictivity of the porous media
$\alpha'$	Mass-related constant
$\alpha$	Parameter in Dubinin-Radushkevich isotherm model equal to "RT ln (1 + 1/ $C_l$ )"
$\alpha$	First-order degradation/decay coefficient
$\alpha$	Volumetric water content
$\alpha_m$	Volume fraction of water associated with the mobile domain
$\alpha_v$	Total water content
$\alpha_{vz}$	Moisture content in the vadose zone
$\mu$	Mobility
$\rho_b$	Bulk density
$\rho_{particle}$	Particle density
$\rho$	Net charge associated with the surface of adsorbing mineral as conceptualized in electrostatic adsorption models
$\rho_d$	Charge associated with the diffuse layer d of counterions as conceptualized in electrostatic adsorption models
$\rho_o$	Charge associated with the o layer as conceptualized in electrostatic adsorption models
$\rho_o$	Charge associated with the o layer as conceptualized in electrostatic adsorption models
$\rho_s$	Surface charge at the Stern layer
$\rho_{sd}$	Standard deviation associated with the Gaussian solution
$\tau$	Tortuosity of the porous media
$v_x$	Pore velocity in direction x
$\nu$	Porosity
$\nu_o$	Effective porosity
$\nu_m$	Mobile water fraction as defined by the ratio of the volume fraction of water associated with the mobile domain, $\alpha_m$ , to the total water content, $\alpha_v$
$\psi$	Electrical potential
$\psi_d$	Potential at the diffuse layer
$\psi_o$	Potential at the surface (plane o)
$\psi_s$	Potential at the Stern layer
A	Concentration of free or unoccupied surface absorption site on a solid phase
ads	Adsorption
$A_i$	Concentration of adsorbate (or species) I on the solid phase at equilibrium
$A_m$	Adsorption capacity of adsorbent per unit mass
am	Amorphous

aq	Aqueous
C	Radioactivity of tracer on sediment
C	Constant capacitance term
CEC	Cation exchange capacity
$C_i$	Concentration of adsorbate (or species) I in solution at equilibrium
$C_l$	Moles per unit volume of liquid
$C_{om}$	Concentration of organic material
$C_s$	Moles per unit volume of water-saturated solid
$C_T$	Total mass at the site per total site volume
$C_{Tp}$	Total mass at the site per dry weight of soil
D	Proportionality constant or diffusion coefficient
$D^*$	Dispersion coefficient in the x, y, and z directions adjusted for retardation with the retardation factor
$D_a$	Apparent diffusion coefficient
$D_e$	Effective diffusion coefficient
$D_i$	Intrinsic diffusion coefficient
$D_{mech}$	Mechanical dispersion
$D_{mol}$	Molecular diffusion coefficient
$D_p$	Diffusion coefficient for a species within a porous media
$D_x$	Dispersion coefficient in direction x
$e^-$	Free electron
$e^{-0F/RT}$	Boltzmann factor
Eh	Redox potential of an aqueous system relative to the standard hydrogen electrode
F	Faraday constant, 23,060.9 cal/V·mol
$f_{oc}$	Fraction (w/w) of organic material in soil
$\Delta G_{f,298}^\circ$	Gibbs free energy of formation at 298 K
$\Delta G_{f,T}^\circ$	Gibbs free energy of formation at temperature T
$\Delta G_{r,298}^\circ$	Gibbs free energy of reaction at 298 K
$\Delta G_{r,T}^\circ$	Gibbs free energy of reaction at temperature T
$^3H$	Tritium
$H_1$	Thickness of the vadose zone
$h_m$	Mixing-zone thickness
$\Delta H_{f,298}^\circ$	Enthalpy (or heat) of formation at 298 K
$\Delta H_{f,T}^\circ$	Enthalpy (or heat) of formation at temperature T
$\Delta H_{r,298}^\circ$	Enthalpy (or heat) of reaction at 298 K
$\Delta H_{r,T}^\circ$	Enthalpy (or heat) of reaction at temperature T
I	Ionic strength
IAP	Ion activity product
$J_{ix}$	Flux of species I in direction x
K	A constant in the Langmuir, Freundlich and Dubinin-Radushkevich isotherm models
$K_{DR}$	Concentration-based, conditional equilibrium constant calculated from Dubinin-Radushkevich adsorption isotherm

$K_d$	Concentration-based partition (or distribution) coefficient
$K_d^{\text{act}}$	Activity-based partition coefficient
$K_{\text{dis}}$	Dissolution equilibrium constant
$K_{\text{ex}}$	Exchange reaction constant
$K_F$	Concentration-based, conditional equilibrium constant calculated from Freundlich adsorption isotherm
$K_F^{\text{act}}$	Activity-based, conditional equilibrium constant calculated from Freundlich adsorption isotherm
$K_L$	Concentration-based, conditional equilibrium constant calculated from Langmuir adsorption isotherm
$K_L^{\text{act}}$	Activity-based, conditional equilibrium constant calculated from Langmuir adsorption isotherm
$K_{\text{oc}}$	Organic-carbon partition coefficient
$K_{\text{om}}$	Organic-matter partition coefficient
$K_{r,298}$	Equilibrium constant at 298 K
$K_{r,T}$	Equilibrium constant at temperature T
$K_{\text{sp},T}$	Solubility product
l	Liter
M	Generic term for metal or radionuclide constituent
m	Meter
$M_A$	Instantaneous mass released per unit area
$M_{\text{ads}}$	Mass of constituent I associated with the adsorbed phase in the vadose zone
$M_{\text{aq}}$	Mass of constituent I associated with the aqueous phase in the vadose zone
$M_{\text{rel}}$	Released mass
$M_{\text{saturated}}$	Total mass of constituent I associated with the saturated zone
$M_{\text{sed}}$	Sediment mass
$M_{\text{Total}}$	Total combined mass of constituent I in the vadose and saturated zones
$M_{\text{vadose}}$	Total mass of constituent I associated with the vadose zone
ml	Milliliter
mol	Mole
mV	Millivolt
N	Constant in the Freundlich isotherm model
n	Total porosity
$n_e$	Effective porosity
pE	Negative common logarithm of the free-electron activity
pH	Negative logarithm of the hydrogen ion activity
$\text{pH}_{\text{zpc}}$	pH for zero point of charge
R	Ideal gas constant, 1.9872 cal/mol·K
$R_f$	Retardation factor
s	Solid phase species
SI	Saturation index, as defined by $\log(IAP/K_{r,T})$
SOH	Unreacted surface site occupied by a hydroxyl group

SOH·M	Used in the non-electrostatic adsorption models for an adsorption site occupied by component M or surface-bound metal
SO·M	Used in the electrostatic adsorption models for an adsorption site occupied by component M or surface-bound metal
T	Absolute temperature, usually in Kelvin unless otherwise specified
$T_0$	Total surface charge for plane $o$
$t$	Time
$t_{max}$	End of the break-through curve during a column experiment
$t_{min}$	Beginning of the break-through curve during a column experiment
$t_{pulse}$	Mean residence time of a solute during a column experiment for a pulse release
$t_T$	Total advective travel time of the contaminant
$t_{ss}$	Mean residence time of a solute during a column experiment for a steady-state release
$t_{step}$	Mean residence time for a step input/release
TDS	Total dissolved solids
$V_{source}$	Volume associated with the contaminated source
$V_w$	Volume of water (or adsorbate solution)
$v^*$	Contaminant velocity
$v_c$	Contaminant velocity
$v_d$	Darcy velocity
$v_p$	Pore-water velocity
$X_{Gf}$ , $Y_{Gf}$ , $Z_{Gf}$	Green's functions (which are orthogonal) in the x, y, and z directions, respectively
$x$	Distance in the x direction
$y$	Off-centerline distance
$Z$	Valence state
$z$	Charge of ion
{ }	Activity
[ ]	Concentration

194

## Appendix B

### Definitions

**Absorption** - partitioning of a dissolved species into a solid phase.

**Adsorption** - partitioning of a dissolved species onto a solid surface.

**Adsorption Edge** - the pH range where solute adsorption sharply changes from ~10% to ~90%.

**Actinon** - name occasionally used, especially in older documents, to refer to  $^{219}\text{Rn}$  which forms from the decay of actinium.

**Activity** - the effective concentration on an ion that determines its behavior to other ions with which it might react. An activity of ion is equal to its concentration only in infinitely dilute solutions. The activity of an ion is related to its analytical concentration by an activity coefficient,  $\gamma$ .

**Alkali Metals** - elements in the 1A Group in the periodic chart. These elements include lithium, sodium, potassium, rubidium, cesium, and francium.

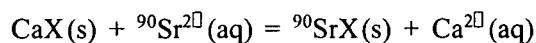
**Alpha Particle** - particle emitted from nucleus of atom during one type of radioactive decay. Particle is positively charged and has two protons and two neutrons. Particle is physically identical to the nucleus of the  $^4\text{He}$  atom (Bates and Jackson 1980).

**Alpha Recoil** - displacement of an atom from its structural position, as in a mineral, resulting from radioactive decay of the release an alpha particle from its parent isotope (*e.g.*, alpha decay of  $^{222}\text{Rn}$  from  $^{226}\text{Ra}$ ).

**Amphoteric Behavior** - the ability of the aqueous complex or solid material to have a negative, neutral, or positive charge.

**Basis Species** - see component species.

**Cation Exchange** - reversible adsorption reaction in which an aqueous species exchanges with an adsorbed species. Cation exchange reactions are approximately stoichiometric and can be written, for example, as



where X designates an exchange surface site.

**Cation Exchange Capacity (CEC)** - the sum total of exchangeable cations that a sediment can adsorb.

**Code Verification** - test of the accuracy with which the subroutines of the computer code perform the numerical calculations.

**Colloid** - any fine-grained material, sometimes limited to the particle-size range of  $<0.00024$  mm (*i.e.*, smaller than clay size), that can be easily suspended (Bates and Jackson 1979). In its original sense, the definition of a colloid included any fine-grained material that does not occur in crystalline form.

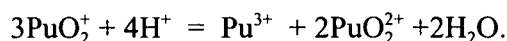
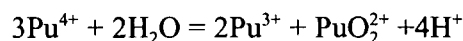
**Complexation (Complex Formation)** - any combination of dissolved cations with molecules or anions containing free pairs of electrons.

**Component Species** - "basis entities or building blocks from which all species in the system can be built" (Allison et al. 1991). They are a set of linearly independent aqueous species in terms of which all aqueous speciation, redox, mineral, and gaseous solubility reactions in the MINTEQA2 thermodynamic database are written.

**Detrital Mineral** - "any mineral grain resulting from mechanical disintegration of parent rock" (Bates and Jackson 1979).

**Deuterium (D)** - stable isotopes  $^2\text{H}$  of hydrogen.

**Disproportionation** - is a chemical reaction in which a single compound serves as both oxidizing and reducing agent and is thereby converted into more oxidized and a more reduced derivatives (Sax and Lewis 1987). For the reaction to occur, conditions in the system must be temporarily changed to favor this reaction (specifically, the primary energy barrier to the reaction must be lowered). This is accomplished by a number of ways, such as adding heat or microbes, or by radiolysis occurring. Examples of plutonium disproportionation reactions are:



**Electron Activity** - unity for the standard hydrogen electrode.

**Far Field** - the portion of a contaminant plume that is far from the point source and whose chemical composition is not significantly different from that of the uncontaminated portion of the aquifer.

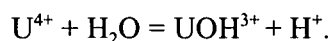
**Fulvic Acids** - breakdown products of cellulose from vascular plants (also see humic acids). Fulvic acids are the alkaline-soluble portion which remains in solution at low pH and is of

lower molecular weight (Gascoyne 1982).

**Humic Acids** - breakdown products of cellulose from vascular plants (also see fulvic acids).

Humic acids are defined as the alkaline-soluble portion of the organic material (humus) which precipitates from solution at low pH and are generally of high molecular weight (Gascoyne 1982).

**Hydrolysis** - a chemical reaction in which water reacts with another substance to form two or more new substances. For example, the first hydrolysis reaction of  $U^{4+}$  can be written as



**Hydrolytic Species** - an aqueous species formed from a hydrolysis reaction.

**Ionic Potential** - ratio ( $z/r$ ) of the formal charge ( $z$ ) to the ionic radius ( $r$ ) of an ion.

**Isoelectric Point (iep)** - pH at which a mineral's surface has a net surface charge of zero. More precisely, it is the pH at which the particle is electrokinetically uncharged.

**Lignite** - a coal that is intermediate in coalification between peat and subbituminous coal.

**Marl** - an earthy substance containing 35-65% clay and 65-35% carbonate formed under marine or freshwater conditions

**Mass Transfer** - transfer of mass between two or more phases that includes an aqueous solution, such as the mass change resulting from the precipitation of a mineral or adsorption of a metal on a mineral surface.

**Mass Transport** - time-dependent movement of one or more solutes during fluid flow.

**Mire** - a small piece of marshy, swampy, or boggy ground.

**Model Validation** - integrated test of the accuracy with which a geochemical model and its thermodynamic database simulate actual chemical processes.

**Monomeric Species** - an aqueous species containing only one center cation (as compared to a polymeric species).

**Near Field** - the portion of a contaminant plume that is near the point source and whose chemical composition is significantly different from that of the uncontaminated portion of the aquifer.

**Peat** - an unconsolidated deposit of semicarbonized plant remains in a water saturated environment.

**Polynuclear Species** - an aqueous species containing more than one central cation moiety, *e.g.*,  $(\text{UO}_2)_2\text{CO}_3(\text{OH})_3$  and  $\text{Pb}_4(\text{OH})_4^{4+}$ .

**Protium (H)** - stable isotope  $^1\text{H}$  of hydrogen.

**Retrograde Solubility** - solubility that decreases with increasing temperature, such as those of calcite ( $\text{CaCO}_3$ ) and radon. The solubility of most compounds (*e.g.*, salt,  $\text{NaCl}$ ) increases with increasing temperature.

**Species** - actual form in which a dissolved molecule or ion is present in solution.

**Specific Adsorption** - surface complexation via a strong bond to a mineral surface. For example, several transition metals and actinides are specifically adsorbed to aluminum- and iron-oxide minerals.

**Sol** - a homogeneous suspension or dispersion of colloidal matter in a fluid.

**Solid-Solution Phase** - a solid material in which a minor element is substituted for a major element in a mineral structure.

**Thoron** - name occasionally used, especially in older documents, to refer to  $^{220}\text{Rn}$  which forms from the decay of thorium.

**Tritium (T)** - radioactive isotope  $^3\text{H}$  of hydrogen.

**Tritium Units** - units sometimes used to report tritium concentrations. A tritium unit (TU) is equivalent to 1 atom of  $^3\text{H}$  (tritium) per  $10^{18}$  atoms of  $^1\text{H}$  (protium). In natural water that produces  $7.2 \times 10^{-3}$  disintegrations per minute per milliliter (dpm/ml) of tritium, 1 TU is approximately equal to 3.2 picocuries/milliliter (pCi/ml).

**APPENDIX C**

**Standard Method Used At  
Pacific Northwest National Laboratory  
For Measuring Laboratory Batch  $K_d$  Values**

## Appendix C

### Standard Method Used At Pacific Northwest National Laboratory For Measuring Laboratory Batch $K_d$ Values

*The standard method reproduced below is used by the authors of this report and their coworkers at the Pacific Northwest National Laboratory in Richland, Washington for the measurement of  $K_d$  values. It is adapted from the procedure described in Relyea et al. (1980).<sup>1</sup>*

#### 1.0 Applicability

This procedure describes the method for measuring radionuclide distribution coefficients ( $K_d$ 's) of geologic material. This procedure includes descriptions for analyses of unconsolidated, loosely consolidated, consolidated porous, and intact, impermeable geological materials.

#### 2.0 Definitions

- Cold wash: Contact of solid sample with nonradioactive groundwater for purposes of establishing chemical equilibrium with nontracer aqueous constituents.
- Tracer: Radioactive element added to groundwater solution to indicate migration and retardation events.
- Spiked groundwater: Groundwater with tracer.
- Blank tube: Centrifuge tube containing spiked groundwater but no solids.
- Radiation Work Procedure (RWP): This is a set of instructions for safe handling of radioactive material in the laboratory. The RWP covers a number of topics and shall be read and understood before performing any work in the laboratory.

#### 3.0 Responsible Staff

- Task leader
- Cognizant staff

---

<sup>1</sup> Relyea, J. F., R. J. Serne, and D. Rai. 1980. *Methods for Determining Radionuclide Retardation Factors: Status Report*. Pacific Northwest Laboratory, Richland, Washington

## 4.0 Procedure

### 4.1 Materials

pH meter  
pH combination electrode 0-14 pH  
Magnetic stirrer  
Stir bars  
Scintillation vials  
pH buffers  
Groundwater  
No. 18 stainless steel sieve (1 mm)  
No. 50 sieve (0.3 mm)  
Mortar and pestle  
Analytical balance (accuracy within  $\pm 0.01$  g) - Refer to operation manual specific to balance for use instructions.  
50 ml polycarbonate centrifuge tubes with screw caps  
Teflon tape  
Groundwater  
Orbit shaker  
Centrifuge  
Vacuum pipets  
0.45-micrometer polycarbonate membrane filters  
Radioactive tracer  
Plastic bags

### 4.2 Safety Precautions

In using radioactive substances and/or solutions protective clothing should be used to reduce the possibility of contamination. Each laboratory is supplied with a radiation work procedure (RWP) which outlines the types and quantities of radionuclides permitted with instructions for handling. Record the number of the RWP in the laboratory record book.

### 4.3 Sample Characterization

Before the  $K_d$  study perform the following analyses to characterize solid and groundwater samples (perform groundwater analysis within one month prior to study). Include the following:

202

#### 4.3.1 For groundwater

- pH
- bulk chemistry (Ca, Mg, Na, K, Cl, NO<sub>3</sub>, SO<sub>4</sub>, CO<sub>3</sub>, HCO<sub>3</sub>)

#### 4.3.2 For solids

- Mineralogy
- Surface area
- Cation exchange capacity
- Moisture content
- Particle size analysis

Procedures which may be used to determine the above parameters are referenced at the end of this document. Record all results.

### 4.4 Sample Preparation

#### 4.4.1 Groundwater

- 4.4.1.1 Filter groundwater through a 0.45- $\mu$ m polycarbonate membrane before it is used in a batch  $K_d$  measurement.
- 4.4.1.2 If retardation parameters (such as pH, ionic strength, and complexing ligand concentration) are to be studied, chemically analyze the synthetic or altered groundwater after preparation and filtration and record results.

#### 4.4.2 Solid

- 4.4.2.1 Unconsolidated Material. To remove particles greater than one millimeter ( $>1.0$  mm), the sample shall be wet-sieved with groundwater by passing the sample through a No. 18 stainless steel sieve. If tests with the material are to be conducted in an inert atmosphere or in a controlled atmosphere, rock samples are to be prepared under those same atmospheric conditions. This requires minimum contact of the rock with air from the time it is removed from the earth until the time the experiment is concluded. This condition holds for Sections 4.5.2.2 and 4.5.2.3. The particle size shall be determined and reported with results from Section 4.3.
- 4.4.2.2 Loosely Consolidated Material. The sample shall be disaggregated by an ultrasonic method or by hand with a mortar and pestle. A portion of the intact material shall be preserved for dynamic testing. Disaggregation

shall proceed no farther than that required to reduce the sample to its natural grain size. Fresh surfaces will be exposed to weathering, but this procedure should reduce fracturing of particles to a minimum. Remove particles >1.0 mm as in Section 4.5.2.1. The particle size distribution after disaggregation shall be reported with results in Section 4.3.

- 4.4.2.3 Consolidated Porous Material (and intact, impermeable rock). A portion of the intact sample shall be preserved (and maintained under conditions that simulate those in situ) for dynamic testing. The remaining sample is to be crushed to pass through a No. 18 sieve (<1 mm). Crushing must be accomplished by means that minimize the introduction of extraneous material, such as metal filings, into the sample. The sample should then be wet sieved through a No. 50 sieve (0.30 mm) to obtain particle sizes between 0.30 mm and 1.00 mm.
- 4.4.2.4 After samples have been sized (Sections 4.5.2.1, 4.5.2.2 or 4.5.2.3), they must be homogenized to insure that the same particle size distribution is obtained for each subsample to be studied.

#### 4.4.3 Equilibrium

- 4.4.3.1 Prepare 50 ml polycarbonate centrifuge tubes with screw caps by obtaining and recording tare weights and assigning identifications which are unique to each sample tube.
- 4.4.3.2 After homogenizing, 1-g ( $1.0 \text{ g} \pm 0.01 \text{ g}$ ) samples are to be weighed (and weights recorded) into centrifuge tubes. Wrap centrifuge tube threads with Teflon tape to prevent leaks.
- 4.4.3.3 Thirty-milliliters of filtered, nonspiked (no radioactive tracer) groundwater is added to each tube, including blanks with no soil, for a "cold" wash. The tube caps are to be replaced before the tubes are placed on a shaker for a gentle overnight agitation (about one oscillation per second).
- 4.4.3.4 Next centrifuge the tubes to separate solids and liquids. Remove the solutions with a vacuum pipettes to prevent removal of the rock sample (some liquid will remain in the tube).
- 4.4.3.5 Repeat the wash procedure twice more for a total of three cold (nonradioactive) washes. Before the centrifuge step on the third wash, measure and record the pH of the solid-solution. If the pH has changed from its natural equilibrium value as measured in the field, the rock

sample and groundwater have not yet re-established equilibrium. Continue to wash until the pH is stable. A change in pH is most likely to occur with samples of crushed rock (Section 4.4.2.3) because fresh surfaces (either rock or cementing agents) have been exposed.

- 4.4.4 After removal of the third wash solution, each tube must be reweighed and the weight must be recorded to determine the volume of excess solution left in each sample. Secure the cap of each tube to prevent evaporation, which would result in an increased salt concentration in the remaining solution. The excess solution volume is found by dividing the excess solution weight by the solution density.

#### 4.5 Addition of Tracer

- 4.5.1 The adding of tracer to a solution represents a critical step in the execution of radionuclide migration studies. Two items must be carefully considered: (1) the total amount of tracer added must be soluble in the volume of solution used and (2) the chemical composition of the groundwater or synthetic groundwater must remain unchanged, except for the addition of the radionuclide(s) to be studied.
- 4.5.2 Dry the tracers so that excess acid or base in the stock solution is removed. Do not dry volatile tracers in acid media or they will be lost. The chemical produced by drying must be soluble in the solutions used in experimentation. (An incorrect procedure would be to dry plutonium basic media that would produce an insoluble  $\text{PuO}_2$  or  $\text{Pu}[\text{OH}]_4$  precipitate.)
- 4.5.3 Exception to the dry-addition rule must be made in some cases for radionuclides that have multiple oxidation states. When drying might change the tracer stock solution's oxidation state--such as Pu(VI) to Pu(IV)--tracer should be added to solution in as small a volume as possible with as little excess salt and acid or base as possible. Otherwise, a dry, soluble, salt-free tracer shall be added to groundwater.
- 4.5.4 Allow the tracer solution to sit for at least one week under conditions to be used in the experiment (in equilibrium with air if the aquifer is in equilibrium with air, or under controlled atmosphere conditions if the aquifer is not in equilibrium with air). Make any necessary adjustments to pH during the equilibration time. Solution is to be filtered ( $0.45 \mu\text{m}$ ) after equilibration prior to contact with the geologic material.
- 4.5.5 Calculate and record the amount of tracer (mol/l) present in the groundwater just prior to contact with the geologic material. Additionally, report any carrier isotope of the element added with the tracer and any natural occurrence of the element in groundwater.

#### 4.6 Rock and Groundwater Contact

- 4.6.1 Thirty milliliters (30 ml) of filtered groundwater containing the radioactive tracer is added to each sample tube containing one gram (1 g) of solid. In addition, 30 ml of spiked groundwater is placed in each of three empty (blank) centrifuge tubes (prewashed as in Section 4.4.3). The blank tubes are needed to detect sorption of tracer by centrifuge tube walls.
- 4.6.2 After replacing the tube caps, the tubes are placed in plastic bags (5 to 20 tubes per bag) to contain any contamination caused by leaky tubes. Next, the tubes are placed on a shaker (for linear reciprocating shaker, place tubes horizontally) so that the solid-solution mixture makes maximum contact. Set the shaking speed to 0.8 to 1.2 oscillations per second to ensure mixing of solid and liquid but to reduce grinding of particles.
- 4.6.3 If time is not a parameter being studied, then contact between solid and liquid is to be seven days (7 days). Record the actual contact time allowed. The samples are then removed from the shaker and the tubes are visually checked for leaks (decontaminate if necessary and discard leaky tubes).
- 4.6.4 The blank and sample tubes are centrifuged for twenty minutes (20 min) at 10,000 g ( $g = 980 \text{ cm/sec}^2$ ) or more, and fifteen milliliters (15 ml) of effluent is filtered through a pre-washed  $0.45 \mu\text{m}$  polycarbonate-membrane-type filter. (Pre-wash with groundwater from Section 2.2 to remove foreign particles and soluble impurities). Analyze filtered effluent samples for tracer activity. Next, the effluent is decanted from the blanks into cleanly washed tubes and the empty blank tubes are analyzed for tracer activity adsorbed on tube walls. If tracer activity on blank tube walls is greater than 10 percent of the total blank activity (determined in Section 4.7.3), do not use the blank influent activity for  $K_d$  calculation. If the activity sorbed on blank walls is significantly greater than 10 percent (using a one-tailed "t" test and combined counting error and statistical variation between blanks), directly count the activity of the sample. Methods for both cases follow.

#### 5.0 Batch $K_d$ Calculations

##### 5.1 When tracer is not sorbed by blank tube wall

- 5.1.1 Data needed for  $K_d$  calculation are: (1) excess solution volume,  $V_{\text{excess}}$  (ml) left from the third cold wash (weight of excess solution divided by solution density); (2) mass of solid aquifer material,  $M_{\text{sed}}$  (g); (3) volume of groundwater with radioactive tracer added,  $V_{\text{spike}}$  (ml); (4) activity or concentration of tracer in the

206

effluent solution,  $C_{\text{effluent}}$  (dpm/ml); and (5) the tracer activity or concentration in the influent blank,  $C_{\text{blank}}$  (dpm/ml).

5.1.2 The tracer concentration on the solid phase,  $A_i$  (or  $q_i$ ), is:

$$A_i \text{ or } q_i = \frac{(C_{\text{blank}} \times V_{\text{spike}}) + C_{\text{effluent}} (V_{\text{spike}} + V_{\text{excess}})}{M_{\text{sed}}} \quad (1)$$

The  $K_d$  is then given by:

$$K_d = \frac{(C_{\text{blank}} \times V_{\text{spike}}) + C_{\text{effluent}} (V_{\text{spike}} + V_{\text{excess}})}{C_{\text{effluent}} \times M_{\text{sed}}} \quad (2)$$

5.2 When tracer is sorbed by blank tube wall (Gamma or X-ray Emitting Isotopes)

5.2.1 If the radioactive tracer is adsorbed on the walls of blank tubes, determine the tracer adsorbed by the solid by direct measurement. Use a traceable standard made with the same type of geologic material as used in the test.

5.2.2 For this procedure, after the sediment and traced groundwater have contacted for at least 7 days, the samples are centrifuged to separate solids from liquids, then the liquid effluent is decanted from the sample tube using a vacuum pipette, and the sample is weighed to determine the excess effluent solution volume ( $V_{\text{excess}}$ ). The solid sample is then dried (it should be "air dried" in the same manner as when originally weighed, either in air or in a controlled atmosphere) and transferred to a clean polycarbonate centrifuge tube. The weight of the dry sample  $M_{\text{sed}}$  (g) is then determined and radiocounting of the dry sample is performed for tracer activity,  $C$  (dpm), using the same detector, sample position, and radioanalytical techniques as used for the attenuation standard prepared in Section 5.2.1.

5.2.3 Determine the effluent tracer activity,  $C_{\text{effluent}}$  (dpm/ml), in geometries that are traceable to a standard. The  $K_d$  can then be calculated from:

$$K_d = \frac{C - (C_{\text{effluent}} \times V_{\text{excess}})}{C_{\text{effluent}} \times M_{\text{sed}}} \quad (3)$$

### 5.3 When tracer is sorbed by blank tube wall ( $\alpha$ - or $\beta$ -Emitting Isotopes)

5.3.1 If the radioactive tracer is adsorbed by sample container walls, only the effluent activity can be determined simply and directly. Two options are available for determination of the activity adsorbed by the rock sample. One method is to remove both the solid sample and effluent from the original container and to strip the isotope from the container wall by some means. Mass balance will allow calculation of the  $K_d$  if one knows the amount of radionuclide in the effluent on the tube wall and the total radionuclide initially added. A second method is to chemically remove the radionuclide from the rock sample and count it.

Problems with the first method include the possibility that some of the solid may adhere to the wall and raise the apparent activity of the nuclide adsorbed by the container. Removal of the solid sample may also cause leaching of the container wall and result in an apparent low activity for nuclides adsorbed by the container. This can be minimized by using tubes made of material most appropriate to your sample; consider Teflon, glass, or various plastics to minimize adherence.

The second method is subject to incomplete removal of the nuclide from the solid or loss of material during any additional steps required for extraction, or both.

## 6.0 Reporting Results from Radionuclide Migration Experiments

6.1 The following generic  $K_d$  coding form (Table 1) includes the information to be obtained. (The different data categories and abbreviations are described in Section 6.2.)

### 6.2 Explanation of $K_d$ Coding Form

#### 6.2.1 Category I. Reference

- A. *Name* of the person who performed experiments
- B. *Date* that the experiment was started.
- C. *Comments* regarding deviations from procedure, anomalies that occurred during the process, other pertinent information.

208

Table 1. Generic  $K_d$  coding form.

Reference	Experimental Details	Geologic Media	Aqueous Phase	Nuclide	Adsorption Function
A. Name	A. Method	A. Name	A. BEG	A. ISO	A. $K_d$
B. Date Started	B. State	B. Origin	B. Macro	B. CONC	B. Units
C. Comments	C. Ratio	C. Total	C. Trace	C. SPE	C. Direction
	D. Time	D. Mineral	D. END	D. ADD	D. NUM
	E. Temperature	E. $CO_3$		E. Loading	
	F. ATM	F. OX			
	G. SEP	G. CEC			
	H. Analyze	H. AEC			
	I. RAD	I. SA			

### 6.2.2 Category II. Experimental Details

- A. *Method* refers to batch, axial filter, column, intact core, channel chromatography, and so forth. For batch method, add more detail as to whether cold washes and blank corrections were used. For example, use mnemonics such as

“BATCH (3W, BC) = batch, three cold washes, with blank tube sorption correction”

“BATCH (OW) = batch, zero cold washes and no correction.”

- B. *State* of geologic media such as crushed 40  $\mu\text{m}$ ; intact core 2.5 cm dia x 5 cm; tablet 1 cm x 0.5 cm; crushed 30-80  $\mu\text{m}$ , etc.
- C. *Ratio* of solids to solution for batch  $K_d$ ; for columns include pore velocity or column velocity (for example, 1 PV = 1 cm/hr, CV = 0.5 cm/hr) and porosity and column bulk density; PR = porosity, BD = bulk density.
- D. *Time* of contact such as shaking time for batch system or residence time in flow through columns (h) = hours, (d) = days.

- E. *Temp* is the temperature of the experiment in  $^{\circ}\text{C}$ .
- F. *ATM* is the equilibrating atmosphere air,  $\text{N}_2$ , Ar, 10 percent  $\text{CO}_2$  - 90 percent Ar, and so forth.
- G. *SEP* stands for separation technique; did you use filters (give median pore size) or centrifugation (include approximate g's)?
- “FIL(.4) = filter 0.4  $\mu\text{m}$ ”
- “CEN(50) = centrifuged at 50 g's where  $g = 980 \text{ cm/sec}^2$  units.”
- H. *Analyze* states whether the  $K_d$  is determined by analyzing (or counting) liquids only or solid and liquid:
- “L/L = liquids only”
- “S/L = solid and liquid”
- I. *RAD* is a list of all radioisotopes that were run simultaneously in the experiment. Example: “Sr, Cs, Tc” means these isotopes were run together.

### 6.2.3 Category III. Geologic Media

- A. *Name*. Use the generic name of the rock or mineral, e.g., basalt, granite, montmorillonite.
- B. *Origin*. Include a geographic description and some formation information, e.g., Eleana shale, Sentinel Gap basalt, Argillaceous Shale Wards #404561.
- C. *Total*. Identify the chemical composition as oxides ( $\text{SiO}_2$ ,  $\text{Al}_2\text{O}_3$ ,  $\text{TiO}_2$ ,  $\text{FeO}$ ,  $\text{Fe}_2\text{O}_3$ ,  $\text{MnO}$ ,  $\text{CaO}$ ,  $\text{MgO}$ ,  $\text{K}_2\text{O}$ ,  $\text{Na}_2\text{O}$ ,  $\text{P}_2\text{O}_5$  in percent.
- D. *Minerals*. Identify the minerals present in the rock sample, listing the major ones first, the minor ones last, in the order of the composition percentages in which they appear (largest first). If there are quantitative estimates, add this information as percent and tr = 5 percent.
- E.  $\text{CO}_3$  = carbonate content of rock.
- F. *OX* = hydrous Fe, Mn, Al oxides content of rock.

- G. *CEC* = cation exchange content of material; units = meq/100g. Specify pH of system (typically pH = 7).
- H. *AEC* = anion exchange content of material; units = meq/100g. Specify pH of system.
- I. *SA* = surface area; use "EG" for ethylene glycol, "BET" for gas adsorption, use units m<sup>2</sup>/g, for example: EG(1.3).

#### 6.2.4 Category IV. Aqueous Phase

A. *BEG* signifies measurements made prior to tracer adsorption.

B. *Macro* constituents include:

- pH
- Eh (units vs. S.H.E.)
- Na<sup>+</sup>
- Ca<sup>2+</sup>
- K<sup>+</sup>
- Mg<sup>2+</sup>
- Cl<sup>-</sup>
- HCO<sub>3</sub><sup>-</sup>; CO<sub>3</sub><sup>2-</sup>
- SO<sub>4</sub><sup>2-</sup>
- SiO<sub>4</sub>

C. *Trace* constituents include:

- NO<sub>3</sub>, ppm
- Organic carbon
- B
- Trace metals or anything else measured.

D. *END* signifies measurements (if performed) taken at the same time as K<sub>d</sub> determined.

#### 6.2.5 Category V. Nuclide

A. *ISO*. Isotope used such as <sup>237</sup>Pu, <sup>95m</sup>Tc.

B. *CONC*. Concentration added to groundwater in M = molarity. Include any carrier if present.

- C. *SPE*. Species or valence state added, if known. Also state whether the valence state distribution was determined after equilibration state, e.g., "Pu(VI) BEG; Pu(IV) 15 percent, Pu(V) 50 percent, Pu(VI) 10 percent END" (which means that the original spike was 100 percent Pu(VI), and after shaking the final distribution was as shown).
- D. *ADD* describes how the tracer was added to the groundwater; DRY means evaporated to dryness and groundwater added; WET/PH/3DFO.4 means a small aliquot of liquid tracer was added to the groundwater, the pH of the system was re-adjusted to the appropriate value and shaken for 3 days to filtration through 0.4  $\mu\text{m}$  filters before usage.
- "DRY/1DC50" means the dried spike was brought back into solution equilibrated for one day, and centrifuged at 50 g's before usage.
- E. *Loading* describes (a) the percent of total exchange capacity of the adsorbent filled with the nuclide of interest or (b) the mass of nuclide adsorbed/mass of adsorbent at the condition when the  $K_d$  measurement is performed. This value can be calculated from knowledge of the cation or anion exchange capacity in case (a) and from mass balance considerations. One must know the original mass of the nuclide used in each experiment.

#### 6.2.6 Category VI. Adsorption Function

- A.  $K_d$ . Place the value for  $K_d$ . If a retardation factor is determined in a flow-through column as a function of water velocity, designate by the symbol RF.

Where several measurements were made, also give the standard deviation, such as

" $75 \pm 12 = a K_d$ "

"(RF)  $60 \pm 30 =$  retardation factor"

- B. *Units*. ml/g or ml/m<sup>2</sup>.
- C. *Direction*.  
 ADS = adsorption direction  
 DES = desorption direction  
 ADS-DES = A spike addition to a column.
- D. *NUM* = number of observations used to derive data point, for example:  
 3 = triplicate samples.

212 | 212